NON-ANTHROPOGENIC SOURCES OF CARBON DIOXIDE IN THE GLOWWORM CAVE, WAITOMO

A thesis
submitted in partial fulfilment
of the requirements for the degree of

MASTER OF SCIENCE

in Earth and Ocean Sciences and Chemistry

at

The University of Waikato

by

NATALIE MARGARET MIEDEMA

THE UNIVERSITY OF
WAIKATO
Te Whare Wānanga o Waikato

UNIVERSITY OF WAIKATO

2009

Abstract

The Waitomo Caves attract approximately 500 000 tourists each year. A requirement of tourist cave management is that the partial pressure of carbon dioxide (P_{CO_2}) is kept below levels that are: hazardous to the health of visitors, hazardous to the glowworms and other natural inhabitants, or potentially corrosive to speleothems. For the Glowworm Cave at Waitomo, the maximum permissible P_{CO_2} level is 2400 ppm. When exceeded, the tourist operators are required to close the cave. Ten years of monitoring data at the Glowworm Cave was analysed. Most of the variation in P_{CO_2} could be attributed to CO_2 respired by tourists, and the mixing of cave air with lower P_{CO_2} outside air. Occasionally, there were periods with high P_{CO_2} levels while the cave was closed to tourists. The main objective of this study was to investigate the potential role of the Waitomo Stream in contributing CO_2 to the Glowworm Cave atmosphere.

Analysis of ten years of Glowworm Cave monitoring data showed that the 2400 ppm P_{CO_2} limit was, on average, exceeded five times each year, with a total of 48 events between 1998 and 2007. Of the P_{CO_2} limit exceedences, approximately 31% of events were largely driven by high tourist numbers; 27% of P_{CO_2} limit exceedences were mainly driven by increased discharge, rainfall, and/or a low temperature gradient between the cave and outside air, whilst 29% of the P_{CO_2} limit exceedences were due to a combination of tourists and increased discharge, rainfall, and/or a low temperature gradient. The remaining 13% of exceedences were unexplained by tourists or the factors investigated. It may be that the unexplained exceedences were due to the night time closure of the cave door, restricting air exchange.

The P_{CO_2} of the Waitomo Stream was measured by equilibrating air with the streamwater within a closed loop. The air was passed continuously through an infrared gas analyser (IRGA). The streamwater P_{CO_2} typically ranged between 600 – 1200 ppm. Fluctuations in the P_{CO_2} of the Waitomo Stream coincided with P_{CO_2} fluctuations in the Glowworm Cave air, and under most conditions, the stream probably acted as a sink for cave air CO_2. However, following rainfall events, the stream P_{CO_2} increased, exceeding cave air P_{CO_2}, thus acting as a source of CO_2 to the cave air. High stream P_{CO_2} often occurred at times when air flow through the cave was restricted, e.g. when the temperature gradient between the cave air and outside air was low, or stream levels were high, thus limiting air movement. The combination of high stream P_{CO_2} and a low temperature gradient increased the likelihood of high cave air P_{CO_2}.

Dripwater was measured to determine whether an increase in dripwater P_{CO_2} occurred in response to rainfall events. When rainfall events resulted in increased discharge, the dripwater P_{CO_2} sometimes increased (occasionally exceeding 5000 ppm), however the pattern was not consistent.

The chemistry of the Waitomo and Okohua (Ruakuri) Streams was monitored with daily samples collected and analysed for major ions: HCO_3^-, Ca^{2+}, Na^+, Mg^{2+}, and $\delta^{13}C$ stable isotope. The HCO_3^-, Ca^{2+}, Na^+ and Mg^{2+} concentrations in the streamwater decreased with increased discharge, presumably due to dilution. Increased discharge following rainfall events correlated with increasing P_{CO_2} in the Waitomo Stream, suggesting that soil atmosphere CO_2 dissolved in soil waters, and carried to the stream by saturated flow, was responsible for the streamwater P_{CO_2} increase. Ca in the stream showed both an increase and a decrease with respect to rainfall. Increased Ca in the stream occurred at times when the discharged waters were coming from the phreatic zone, and thus sufficient time had lapsed for CO_2 in the discharge waters to react with the limestone (carbonate dissolution reaction). Decreased Ca occurred when the infiltration and percolation of rainwater was rapid, and thus the streamwater was characterised by a higher P_{CO_2} and a lower Ca concentration, as insufficient time had lapsed for the discharge waters to equilibrate with the limestone.

Increased negativity in the $\delta^{13}C$ of the Waitomo and Ruakuri Streams coincided with increased discharge. During summer low flow, the $\delta^{13}C$ of Waitomo Stream waters was -11.3 ‰, whereas during high stream discharge events, the $\delta^{13}C$ dropped to -12 – -14 ‰. The $\delta^{13}C$ of limestone is 0 ‰, the atmosphere is -7 ‰, and the soil atmosphere is reported to be about -24 ‰, thus the decrease in $\delta^{13}C$ during high flow events supports the contention that soil atmosphere CO_2 is a likely source of the increased CO_2 in flood waters.

Acknowledgements

Associate Professor Chris Hendy, thank you so much for your theories and ideas, for your knowledge and guidance and most of all for your unwavering confidence in both me and the project. No question or task was ever too big for you. I have really appreciated your supervision throughout this thesis, thank you!

Dr. Megan Balks, thank you for guiding me through the write-up of this thesis. The meetings, the questions and the endless pen-covered drafts have been incredibly valuable in my learning over the past year. Thank you so much.

Travis Cross: honestly, what can I say?! This thesis would have been near impossible without you! You have been so giving of your time to this project. Organising the collection of water samples, bi-weekly data downloads, spontaneous visits, countless question-filled e-mails, organising equipment purchases, your amazing log book, the list could add another 40 000 words to this thesis! Thank you so much! I am truly grateful for all you have done!

Thank you to Shelley Katea (for the organising of) and THL for funding this project, as well as to the University of Waikato Masters Scholarship and the Alumni Scholarship for the financial support through the duration of this work.

A huge thank you must also go out to all of the following people:
Suus Rutledge, Barend van Maanen and Paul Mudge: thank you so much for the countless hours you put in, trying to help me figure out MATLAB. I have really appreciated all of the time and effort you put into helping me out, thank you; Craig Hosking (for all of your technical support; not to mention the baking!); Peter Jarman and Steve Hardy, thank you for letting me base myself in your office for a while – perhaps one day I will officially apply for an apprenticeship with you guys! In particular, thanks to Peter for all of your help; testing my methods, setting up my gear, trouble-shooting and problem solving, your assistance in the

field – thank you so much; thank you Steve Cameron (ICP-MS analyses) and Steve Cooke (isotope work); Glen Balks, thank you so much for your timely help with the tourist number data! Thank you Brian Clark and Chris Sistern in the workshop for all of the bits and pieces you made, fixed and loaned to me over the year; Stewart Finlay and the Physics Department for lending me the GLX; Margaret Bellingham and Brian Smith (NIWA) for your help in providing me with Glowworm Cave and Waitomo Stream data; Doug Stewart and many others at Environment Waikato for your assistance in providing Waitomo Stream discharge and other Waitomo Catchment data; Annie Barker, for letting me share your lab and office, and for all of your help; Ray Littler, for your help with my predictive model; Brett Loper, for your not-so-rudimentary help with all questions computer and printing related and for your assistance with finding the perfect words! Thank you to the members of the Waitomo EAG for teaching me so much about caves and for your useful feedback on my work; Angus Stubbs and the GWC and BWR guides for the water samples you collected for me each day; thanks too to Dave Campbell, Karin Bryan, Ivan Bell, Jacinta Parenzee, Louis Schipper, Sydney Wright and Jacqui MacKenzie for all of your help. Thank you Lisa Pearson for your help and support throughout the year and especially for providing me with that crucial number when I was ready to give up, or at least ignore the problem! Thanks to all the other Earth Science MSc students who have contributed to making the Masters experience what it has been!

Bryna, thank you for your support, words of encouragement, advice, inspiration (your five-month A-grade MSc effort was incredibly amazing and awe-inspiring!), for all of your proof-reading, and for being the awesome friend and flatmate you are.

Finally, a huge thank you to my families. Mr and Mrs Niemand, thank you so much for being my ‘other’ parents. You have been so amazing to me over the last five years, welcoming me into your home and treating me like a third daughter. I really appreciate your love, support and genuine interest in all that I do. Thank you both so much for all that you have done for me.

Thank you so much Rafi, Belinda, Aaliyah and Savanah, Annemarie and Hayden, Kirk, Scott and Gina, and Jolie. Thanks for being so understanding of my lack of communication and my 'absence' on so many levels, and for always being there to remind me what really is important in life.

To Poppa and Gran, thank you for always being proud of me and my achievements. It really means a lot to me!

Thank you Pake and Beppe ... for always being so supportive, loving, encouraging and interested! I miss you both so much and think of you often! You were always so interested in what any of us were doing and I know you would have loved to hear about my work in the caves. Thank you for being the roots of our family!

Mum and Dad … where do I start?! Thank you so much for your unfailing support, your constant love, and the ongoing encouragement you have given me throughout my years at university. The visits, catch-ups over coffee (and cake!), meals, texts and phone calls have all been hugely appreciated! Thank you for instilling in me the knowledge that with hard work, faith and determination anything can be achieved. You are both amazing, I love you so much.

And Clarisse! What a crazy, fun-filled, laughter-filled, enjoyable adventure this has been! Thank you for making the last four and a bit years what they have been and thank you so much for everything you have done in getting this thesis to the point of bound beauty. For the countless trips to Waitomo, helping me manually enter all those bicarbonate numbers, the diagrams, the data analysis suggestions, the proof-reading, for your company during long nights in the labs, for encouraging me when I really needed it – you really have been amazing! Thank you so much! I could not imagine the MSc experience without you!

Table of Contents

List of Figures

Chapter One:

Chapter Two:

Chapter Three:

Chapter Four:

Chapter Five:

Chapter Six:

Chapter Seven:

Appendix A.2:

List of Tables

Appendix A.3:

Appendix A.4:

List of Equations

1.0 Chapter One: Introduction

1.1 Background on caves and karst processes

Caves are fascinating underground environments developed by the dissolution of rock. Rainwater dissolves carbon dioxide (CO_2) from the atmosphere forming a weak solution of carbonic acid (H_2CO_3). The soil is an ultimate source of CO_2 due to microbial and plant root respiration in the O and A horizons (White, 1988). As rainwater percolates through the soil, it increases in acidity. Soil pore spaces give way to fissures in the underlying bedrock which continue to provide the percolating rainwater with a flow path. Upon contact with limestone, the CO_2 enriched water reacts with the relatively insoluble $CaCO_3$, which is transformed into calcium bicarbonate ($Ca(HCO_3)_2$, an intermediate phase that does not exist as an independent entity) (Williams, 2004), and subsequently dissolves the limestone; e.g.

$$CaCO_3 + H_2O + CO_{2(aq)} = Ca^{2+}{}_{(aq)} + 2HCO_3^{-}{}_{(aq)} \qquad \text{(Equation 1.1)}$$

Over time, the dissolution (or chemical erosion) of limestone continues and fissures in the limestone are enlarged, forming caves. Whilst dissolution is the primary mechanism of cave formation, physical erosion also occurs where weakened sections of rock collapse; for example, Hollow Hill at Waitomo, New Zealand's largest cave, endured physical erosion via a roof collapse, after which flowing streams removed the debris (Williams, 2004).

The dissolution process responsible for the development of cave systems, along with condensation and evaporation, are fundamental in developing cave formations. Cave formations include a range of both speleothem and speleogen features. Speleothems are depositional features in caves including stalactites and stalagmites (Moore, 1952), formed by saturated solutions of calcite ($CaCO_3$) dripping into the cave. The water in the solutions evaporates, leaving a deposit of calcite (Figure 1.1). Speleogens are erosion features, such as scallops, ceiling and floor channels, as well as bedrock projections and protrusions (Culver & White, 2005).

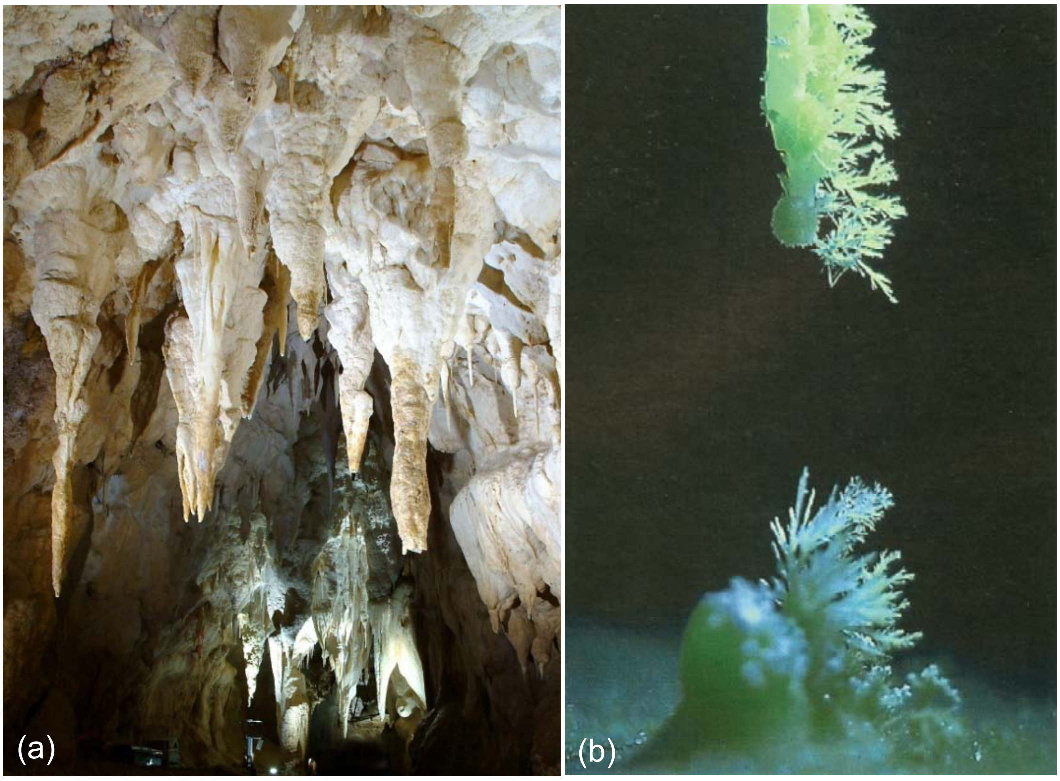

Figure 1.1. Speleothems: (a) stalactites in Ruakuri Cave, Waitomo (photo: THL); (b) aragonite frostwork, Cupp-Coutunn Cave, Turkmenistan (photo: Valdimir Matlsev) (Hill & Forti, 1997).

Caves and their decorative formations are fragile systems, and are influenced by a unique combination of both natural variables and anthropogenic inputs. The natural variables include climate (e.g. CO_2, temperature, precipitation), soil and rock chemistry, and hydrogeological setting (e.g. lithology, thickness of soluble rocks and degree of fractionation) (White, 1988). Alterations to the natural variables can lead to cave degradation. Furthermore, caves are popular tourist attractions around the world, with estimates indicating that more than 150 million people visit tourist caves each year (Cigna & Burri, 2000). Tourism significantly alters the balance of natural variables within cave systems; for example, by increasing the CO_2 levels through respiration, increasing cave temperature through body heat and lighting, and modifying airflow and cave hydrology.

The Waitomo Caves, located in the central North Island, are the most visited caves in New Zealand, with more than 500 000 visitors annually (four times more tourists each year than any other show cave in either New Zealand or Australia) (de Freitas & Schmekal, 2003). Cave tourism in Waitomo began in 1889 with the opening of the Glowworm Cave as a show cave (tourist cave) (Figure 1.2). The display of glowworms in the Glowworm Cave makes this the most visited cave in the Waitomo region. The Glowworm Cave is, therefore, an important attraction with both aesthetic and ecological significance (de Freitas & Schmekal, 2003).

Figure 1.2. A tour underway in the Grotto at the Glowworm Cave, Waitomo (photo: THL).

The Glowworm Cave is operated by Tourism Holdings Ltd. (THL) under a licence that specifies that CO_2 levels in the cave must be measured continuously. In the event of CO_2 exceeding 2400 parts per million (ppm), tour operations must cease. Periodically, the CO_2 levels are exceeded within the Glowworm Cave, and whilst there is a known correlation between visitor numbers and cave CO_2, it appears that there may be another variable/s impacting on the cave air CO_2 levels.

1.2 The effect of high CO_2 in caves

CO_2 is an essential component in many biological processes, including plant photosynthesis and root and microbial respiration. CO_2 is also a by-product of human respiration, occurring in human breath at a concentration of approximately 4% (40000 ppm) (de Freitas & Banbury, 1999; Baldini *et al*., 2006). CO_2 is soluble and, when dissolved, increases the acidity of water (by forming carbonic acid), thereby making the water corrosive to carbonate rocks such as limestone. The air expelled by tourists is warm (usually at a temperature much higher than that of the cave atmosphere), saturated with water vapour, and contains elevated CO_2 (de Freitas & Schmekal, 2003). As the warm, moisture-laden, acidic air cools, it condenses against the cooler cave walls and cave formations. The acidic condensation leads to the corrosion of speleothems (de Freitas & Schmekal, 2003), a process known as condensation corrosion (Ford & Williams, 1989).

The earth's atmospheric CO_2 is constantly rising but has been cited at approximately 0.03% in recent years (377.38 parts per million (Keeling & Whorf, 2005)), and is relatively constant worldwide. The CO_2 in caves, however, can vary from 0.03% to more than 6%) over a range of spatial and temporal scales (Batiot-Guilhe *et al*., 2007. For some time, tourists were thought to be the primary source of cave CO_2, however, more recent work has shown that in some show caves more CO_2 is produced by natural processes (e.g. the oxidation of organic matter in the soil which subsequently enters caves via percolation waters) than is produced by tourists within caves (Cigna, 2005 after Bourges *et al.*, 1998). A number of natural sources of cave CO_2 have been identified, including: the atmosphere (typically low concentrations) and draughts, such as those created by fast-moving underground streams; the soil, where CO_2 from microbial and plant root respiration accumulates and is dissolved and transported into the cave system through groundwater; oxidation of organic matter; and, deep gas diffusion or transport (Batiot-Guilhe *et al*., 2007).

1.3 Objectives and hypotheses

In light of the findings of Batiot-Guilhe *et al*. (2007), the role of the Waitomo Stream and stalactite dripwater as natural sources of CO_2 in the cave air were investigated in two Waitomo caves: the Glowworm Cave and the Ruakuri Cave. The stream is a prominent feature in both caves; to the best of my knowledge no previous studies have been undertaken on the relationships between high cave air CO_2, stream discharge and streamwater CO_2 concentrations.

The objectives of this thesis were to:

- analyse historic Glowworm Cave air CO_2 records to determine if peaks, unexplained by tourist numbers, were linked with increased streamflow;
- determine if there was a correlation between the CO_2 levels in the Glowworm and Ruakuri Cave atmospheres and the Waitomo Stream CO_2;
- investigate possible sources of CO_2 in streamwater; and,
- investigate alternative factors (including temperature, rainfall and stream water level) that may influence cave air CO_2 levels.

The hypotheses investigated in this thesis were that:

- anomalous increases in the partial pressure of carbon dioxide (P_{CO_2}) in the Glowworm Cave air were associated with increases in the Waitomo Stream P_{CO_2} – *addressed in Chapter Five*;
- the P_{CO_2} of the Waitomo Stream increased in response to rainfall events – *addressed in Chapter Five*;
- the additional P_{CO_2} in the Waitomo Stream during events of increased discharge was derived from the soil – *addressed in Chapter Six*;
- historic P_{CO_2} limit exceedences in the Glowworm Cave air data, which could not be explained by tourist numbers, could be related to events of increased Waitomo Stream discharge – *addressed in Chapter Seven*.

2.0 Chapter Two: Literature review

2.1 Karst landscapes and cave systems

A cave is 'a natural cavity in a rock which acts (or has at some stage acted) as a conduit for water flow between input points (i.e. streamsinks), and output points (i.e. springs or seeps)' (Gillieson, 1996 after White, 1984, p.1). Caves can vary greatly, particularly in the way that they are formed. For example, mechanical processes, such as rock falls, will form tectonic caves, whilst sea caves and aeolian caves are the product of erosion and scour (White & Culver, 2005). The focus of this thesis was on solution caves. Solution caves are formed by the dissolution of rock as water passes through, and are a common feature of karst landscapes. Karst landscapes are characterised by caves and undergroundwater systems developed in soluble rocks such as limestone, marble, dolomite and sandstones (Gillieson, 1996; Ford & Williams, 2007). Karst landscapes have a distinctive subsurface hydrology which arises as a result of 'high rock solubility and well developed secondary porosity' (Ford & Williams, 2007, p.2). Along with the subsurface hydrology, other characteristic features of karstic terrains include closed depressions, sinking streams, fluted rock outcrops, large springs, and caves (Ford & Williams, 2007).

2.1.1 Formation of caves in limestone

Solution caves are formed by the dissolution of any soluble rock, however for the purposes of this thesis, only the formation of caves in limestone will be discussed. The process of cave and speleothem formation has been well studied (e.g. Adams & Swinnerton, 1937; Jennings, 1985; White, 1988; Hill & Forti, 1997). The following paragraphs describe the processes of karst dissolution and subsequent cave formation. For more detailed descriptions of the processes of karst dissolution refer to Gillieson (1996), or Ford and Williams (2007).

Water becomes acidified by dissolving carbon dioxide (CO_2) from the atmosphere and the soil air (Equation 2.1), forming an aqueous solution of hydrogen (H^+) and bicarbonate (HCO_3^+) ions. The acidified water then percolates down through fractured limestone ($CaCO_3$). When the acidic H^+ ions come into contact with the limestone, the Ca^{2+} and CO_3^{2-} ions are dissolved (Equation 2.2). The continuation of this reaction results in an equilibrium being reached. Equation 2.3 shows the balancing process of $CaCO_3$ dissolution (Adams & Swinnerton, 1937; Hendy, 1971).

$$CO_2 + H_2O \rightleftharpoons H^+ + HCO_3^- \qquad \text{(Equation 2.1)}$$

$$H^+ + CaCO_3 \rightleftharpoons Ca^{2+} + HCO_3^- \qquad \text{(Equation 2.2)}$$

$$CO_2 + H_2O + CaCO_3 \rightleftharpoons Ca^{2+} + 2HCO_3^- \qquad \text{(Equation 2.3)}$$

A simplified description of the limestone dissolution process was given by Gillieson (1996). CO_2 slowly diffuses from air into water (Equation 2.4) before becoming hydrated and forming carbonic acid (Equation 2.5). Equation 2.6 shows the rapid dissociation of carbonic acid into hydrogen and hydrogen carbonate ions. The $CaCO_3$ or calcite crystal lattice is then dissociated into Ca^{2+} and CO_3^{2-} ions (Equation 2.7). Carbonate ions are associated with hydrogen ions to form hydrogen carbonate (Equation 2.8). In reverse, the removal of CO_3^{2-} ions in Equation 2.8 disturbs the balance of Equation 2.7 so that more carbonate must be dissociated for the balance to be restored. In addition, the association of H^+ and

CO_3^{2-} ions disturb the equilibrium of Equation 2.6, and further dissociation is promoted. This alters the equilibrium of Equation 2.5 and, essentially, more CO_2 from the gas phase is required for the reactions to proceed to equilibrium. These reactions will continue until the forward and reverse reactions are in equilibrium, and the solution is saturated with respect to calcite.

$$CO_{2(\mathrm{air})} \rightleftharpoons CO_{2(\mathrm{aq})} \quad \text{(Equation 2.4)}$$

$$CO_{2(\mathrm{aq})} + H_2O \rightleftharpoons H_2CO_3 \quad \text{(Equation 2.5)}$$

$$H_2CO_3 \rightleftharpoons H^+ + HCO_3^- \quad \text{(Equation 2.6)}$$

$$CaCO_3 \rightleftharpoons Ca^{2+} + CO_3^{2-} \quad \text{(Equation 2.7)}$$

$$H^+ + CO_3^{2-} \rightleftharpoons + HCO_3^- \quad \text{(Equation 2.8)}$$

The formation of caves, via the process described by Equations 2.4 – 2.8, occurs as the calcite-saturated water (that flows through cracks and fractures in the limestone) is replaced with water that has not yet reached calcite saturation. Water conduits (or channels) become active zones of calcite dissolution and are constantly widened in the process (Figure 2.1). Whilst the form of caves is typically linked to the angle of the bedding planes, this is not always the case. For example, in Waitomo, the bedding planes are horizontal, however, the passages tend to be vertical. This is because the joints within the limestone, and not the bedding planes themselves, are the dominant conduits.

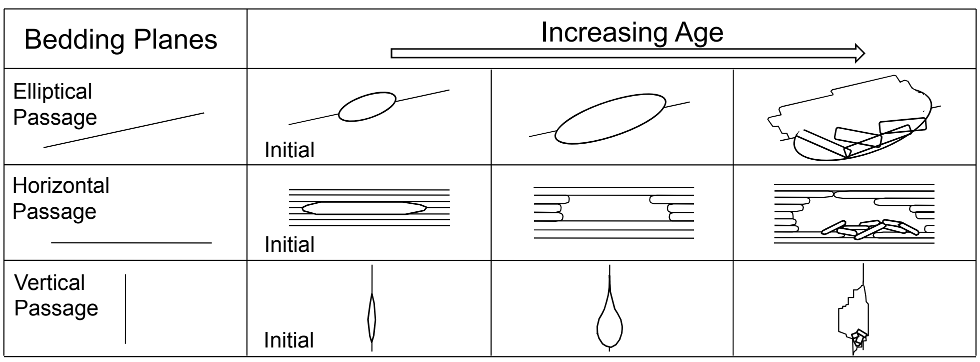

Figure 2.1. Cave development along three varied bedding planes (adapted from Gillieson, 1996).

2.1.2 Open and closed systems

Karst systems can be defined as either open or closed systems based on the interaction of solid, liquid, and gas CO_2 phases. In open systems all three phases freely interact at any given time; for example, in an open-air pool of water on a limestone surface. The aqueous H^+ and H_2CO_3 are converted into bicarbonate by reacting with solid $CaCO_3$. For the reaction to reach equilibrium, more CO_2 is required, which can be readily dissolved across the water-air interface to replenish the aqueous CO_2 and H_2CO_3 (Hendy, 1971; Ford & Williams, 2007). This can similarly be represented by a karst system where the soil layer is minimal or nonexistent (see Figure 2.2a), or where the soil pores are air-filled rather than water-filled, and thus can readily exchange $CO_{2(g)}$ with the acidified water as calcite is being dissolved (Hendy, 1971; McCabe, 1977).

In closed systems, the calcite dissolution process occurs in isolation from the atmosphere (Figure 2.2b). Initially, water will absorb gaseous CO_2 from the air until the water is saturated and the CO_2 is at equilibrium with H_2CO_3 and HCO_3^-. The water will then flow until it is no longer in contact with air before it begins to react with carbonates. At Waitomo, thick, carbonate-free soils overlying limestone, create a buffer that inhibits the exchange of CO_2 with the aqueous solution, creating a closed system. The Waitomo karst has uncharacteristically thick soils as a result of many successive layers of volcanic ash deposits.

In reality, many systems are likely to be partially open and partially closed (Ford & Williams, 2007). Where soils have a low air volume or low temperatures, they act as closed systems, as the rate of CO_2 dissolution exceeds the supply of gaseous CO_2. The nature of the system (i.e. whether it is open or closed) effects how long it takes for CO_2 to reach the underlying limestone, the rate of speleothem growth, the quantity of CO_2 in the cave atmosphere (C. Hendy, pers. comm., 2008), and the isotopic composition of the calcite precipitated on speleothems (Hendy, 1971).

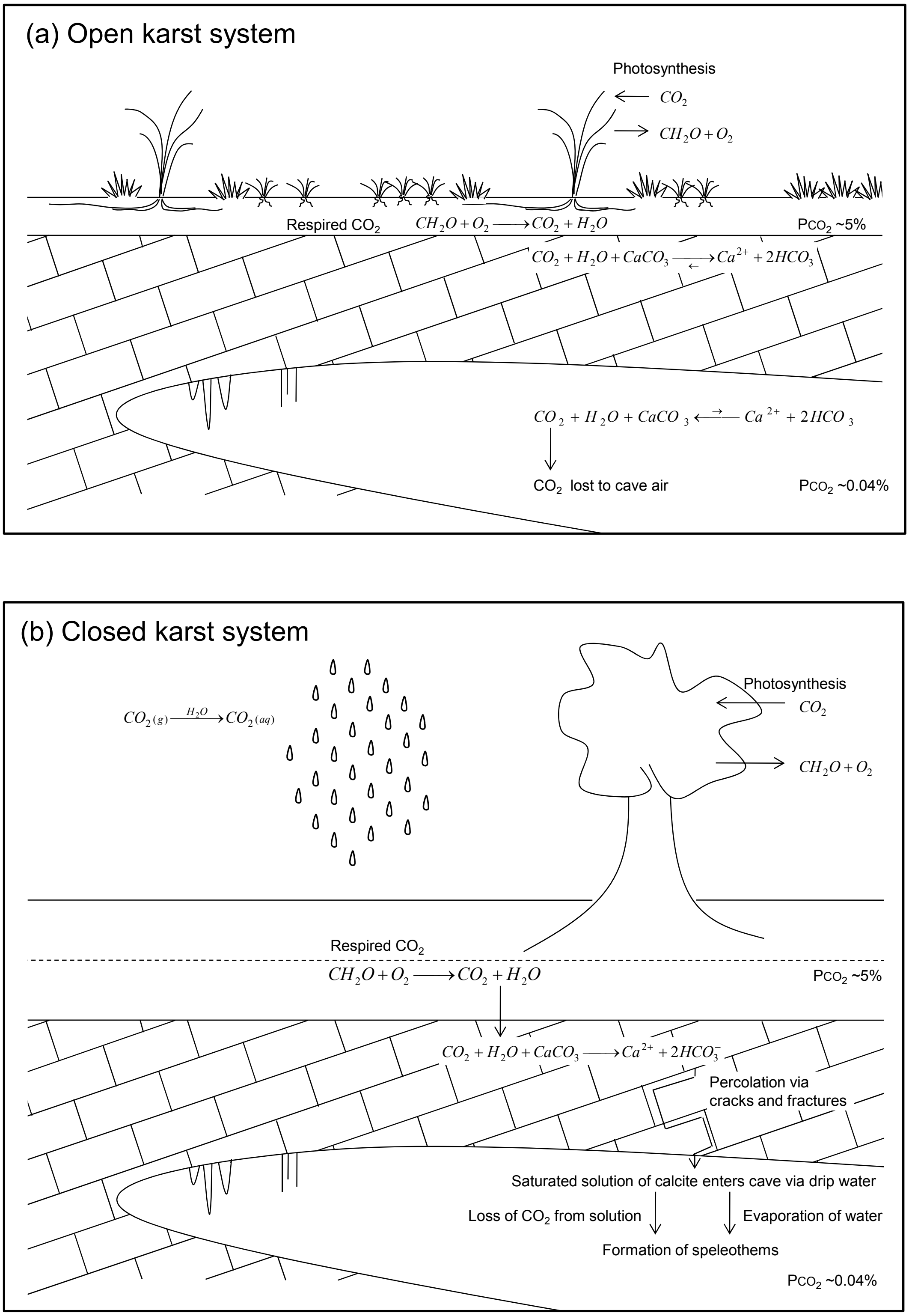

Figure 2.2. Systems in karst landscapes; (a) an open system; and (b) a closed system (adapted from Hendy, 1971).

2.1.3 Formation of speleothems

'Speleothem' is a collective term used to describe cave decorations such as stalactites, stalagmites, straws and columns; the awe-inspiring natural features that make caves so appealing to tourists (Figure 2.3).

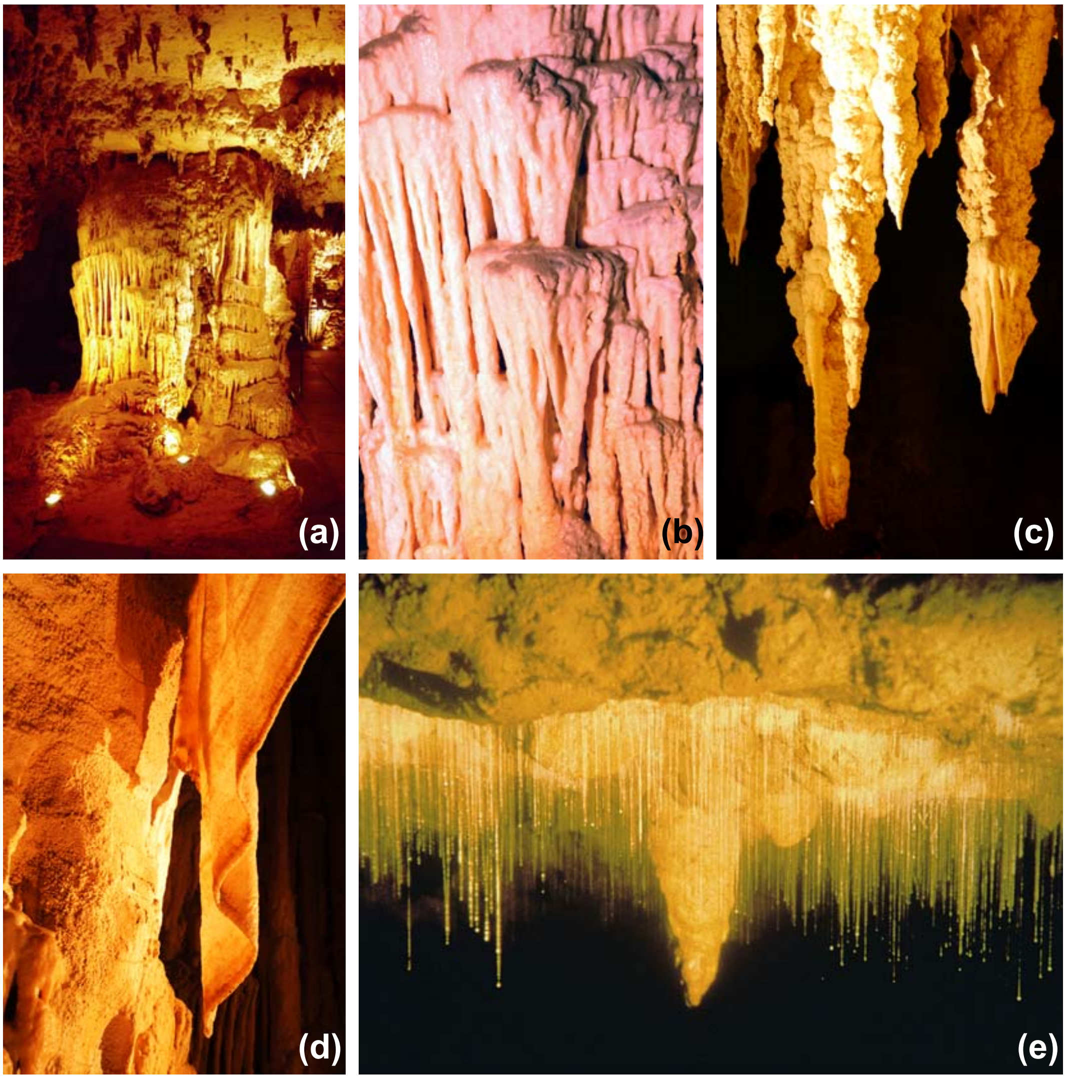

Figure 2.3. Speleothems in the Waitomo Caves; (a) a column of flowstone in the Organ Loft; (b) close-up of the smooth surface of calcite flowstone; (c) stalactites; (d) shawl of calcite in the Ruakuri Cave; and (e) hundreds of straws surrounding a stalactite (photos: THL).

Speleothems form by a similar process to caves, through the displacement of calcite during dissolution processes. Carbon dioxide, the most soluble of the common atmospheric gases, has a solubility that is proportional to its partial pressure (Henry's Law), and is inversely proportional to temperature (Garrels & Christ, 1965). Partial pressure can be defined as part of the total pressure exerted by a mixture of gases that is attributable to the gas of interest. For the dissolution of CO_2 in water, Henry's Law may be written as:

$$CO_{2(\text{aq})} = C_{ab} \times PCO_2 \times 1.963 \quad \text{(Equation 2.9)}$$

where CO_2 is in g.L^{-1}, C_{ab} is the temperature-dependent absorption coefficient (e.g. when the temperature of the solution is 0, 10, 20 and 30°C, C_{ab} is 1.713, 1.194, 0.878 and 0.665, respectively); P_{CO_2} is the partial pressure of CO_2; and 1.963 is the weight of 1 L of CO_2, in grams, at one atmosphere and at 20°C. In the standard atmosphere, P_{CO_2} at sea level has a modern global mean value of approximately 0.038% or 0.00038 atmosphere (380 ppm). With an increase in altitude, P_{CO_2} decreases slightly. In the soil, however, atmospheric CO_2 can entirely replace O_2, increasing the P_{CO_2} of the rooting zone in the soil up to 21%, making soil P_{CO_2} a much more significant factor in the process of limestone dissolution (Ford & Williams, 2007).

When CO_2 is dissolved in water, the water is acidified and thus dissolves calcite as it percolates down through the overlying limestone. The percolation waters, typically rich in dissolved CO_2 and saturated with respect to calcite, enter cave conduits as dripwater (Gillieson, 1996). From here speleothems can form by either:

(a) CO_2 outgassing; or

(b) evaporation of water.

Compared to the soil atmosphere, caves are relatively depleted in CO_2. The low P_{CO_2} in cave air promotes the outgassing of CO_2 as the dripwaters equilibrate with the cave atmosphere. Calcite will only deposit in a cave environment when the P_{CO_2} of the cave atmosphere is less than the P_{CO_2} of dripwater (Hendy, 1971). With the decreasing partial pressure of CO_2 in solution, the saturation levels of the solution with respect to calcite are increased (i.e. less $CaCO_3$ is needed for the solution to be saturated, see Figure 2.4), thus creating the necessary preconditions for calcite precipitation (Gillieson, 1996). Outgassing of CO_2 from dripwaters is considered to be the primary mechanism of carbonate deposition (Gillieson, 1996), and the resulting calcite formations are typically dense crystalline structures such as straws, stalactites and flowstone (Figure 2.3). Differences between speleothem formations are generally the result of variations in the rate of the dripwater feeding, and the growth rate of, each formation (White, 1988).

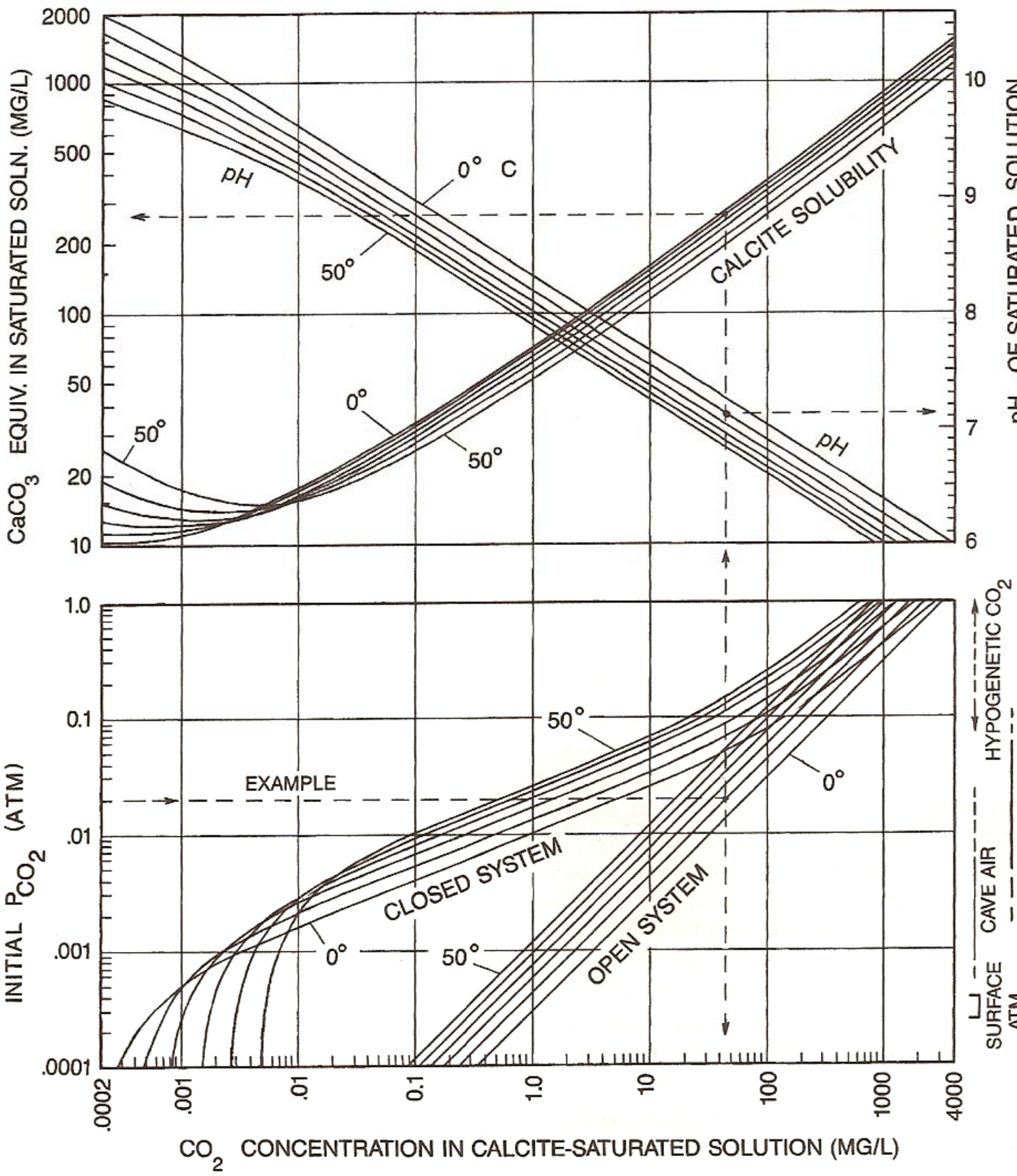

Figure 2.4. Comparison of the concentration of CO_2 in solutions for closed and open systems at given initial P_{CO_2} levels, and the corresponding calcite saturation levels (Ford & Williams, 2007).

The formation of evaporite deposits in caves occurs predominately near cave entrances or in draughty or dry caves (relative humidity 75 – 90% (White, 1988)). The rapid deposition of calcite, encouraged by evaporation, leads to separate crystallites forming. Evaporite formations are typically soft and porous with an earthy texture and are often pasty to touch (Ford & Williams, 2007). Evaporite deposits include cave coral, calcite popcorn (Figure 2.5) and aerosols (Hill & Forti, 1997). Gypsm ($CaSO_4.2H_2O$) is also commonly formed by evaporation.

Figure 2.5. Cave popcorn in the Józef-hegy Cave, Budapest, Hungary (photo: Istvan Czajlik, Hill & Forti, 1997).

2.1.4 Caves and their importance

Caves have played a significant part in human life for millennia. People have used caves for many purposes: from dwellings and shelters, to a place of worship; for water supply and the generation of hydroelectricity to the mining of cave formations and guano (Gillieson, 1996); from munitions factories to burial grounds; and from desirable recreation and tourist destinations to niches for scientific research (White & Culver, 2005). This study will focus primarily on the use, importance, and problems associated with caves used as tourist attractions.

2.2 Tourist caves

A tourist (or 'show') cave is a cave system that has been developed to enable tourists to comfortably enjoy the beauty of natural cave systems. Although a clear definition of a tourist cave has not been established, a tourist cave usually fulfils the following conditions: trails have been constructed on the floor, some form of lighting (typically electric) exists, guided tours are available, an entrance fee is required, and regular opening and closing hours are typically adhered to.

The oldest record of a cave tour dates back to 1213 in the Postojna Cave, Slovenia, however no record of tour by admission fee exists prior to 1633, when the Count Benvenut Petac allowed paying tourists into the Vilenica Cave, Slovenia (Cigna, 2005). Since these early days of cave tourism, hundreds more caves have been developed into tourist caves. Ford and Williams (2007) estimated that there are roughly 650 tourist caves worldwide, and approximated the gross annual income from tourist caves to be US$2.5 billion. Zhang and Jin (1996) estimated that there were about 800 tourist caves in the world (cited in Cigna & Burri, 2000), whilst a frequently updated website dedicated to tourist caves and cave statistics, suggested that there are 1127 tourist caves, from 121 countries (Showcaves, 2008). According to the showcaves website, the United States of America has the highest number of tourist caves at 155, followed by France at 110. Australia is reported to have 58 tourist caves, whilst New Zealand has a total of nine tourist caves.

Cigna and Burri (2000) conducted an evaluation of tourist caves and, based on data from 150 of the tourist caves worldwide (19% of all tourist caves using the reported number of 800 tourist caves globally from Zhang and Jin (1996)), 150 million people visit tourist caves each year. Tourists annually spend an estimated US$2.3 billion on cave attractions. Thus, tourist caves are important to the economy, on both a local and national scale.

2.2.1 Caves in New Zealand

There are four significant karst regions in New Zealand: Takaka Valley in northwest Nelson; Punakaiki, south of Westport; Te Anau, southwest of Queenstown (all of which are situated along the South Islands west coast); and the King Country in the central-west North Island (Figure 2.6). The Waitomo Caves are situated in the King Country karst, and were the focus of this thesis.

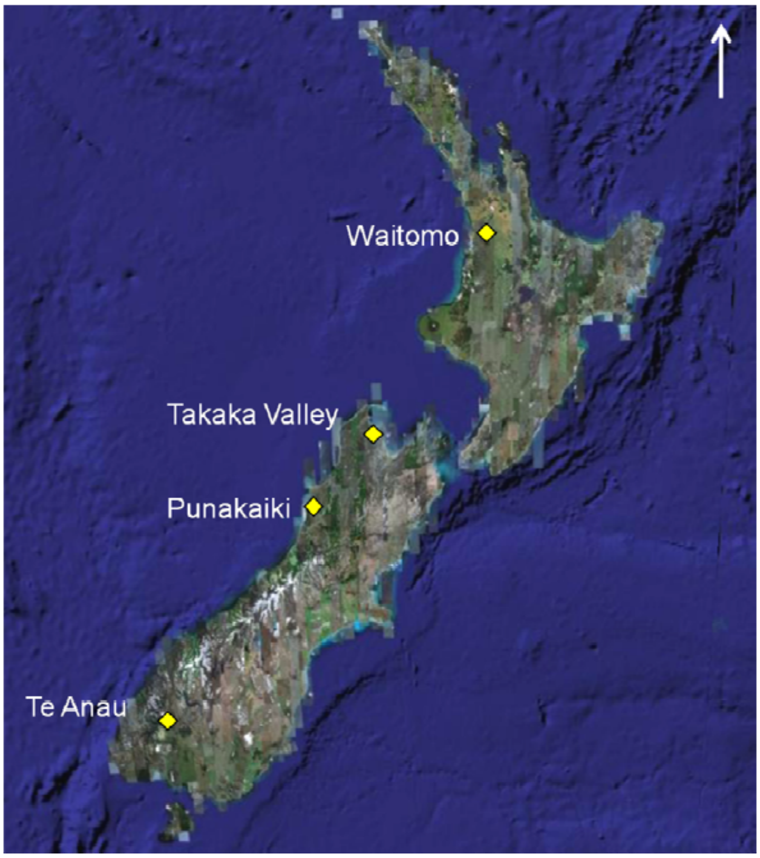

Figure 2.6. Map indicating the location of the four significant regions of karst in New Zealand (Source: adapted from Google Earth).

2.2.2 The Waitomo Caves

The caves of the Waitomo region were known to the local Maori people decades, and possibly even centuries, before Europeans discovered the caves. Evidence of this includes a burial site in the Ruakuri Cave, a sacred site (wahitapu), from where people are prohibited. The Waitomo area was named by the local Maori of the time with Waitomo translating into 'water entering a hole in the ground' (Doorne, 1999). The karst and cave systems of the region are valued for their association with the Maori people, their uniqueness and attributes of natural heritage, their importance in natural history research, and their role in supplying water. The Waitomo karst region is also renowned for its recreational and tourism opportunities (Department of Conservation, 1999).

The first written account of cave exploration in Waitomo was recorded in 1849, when Dr. A. Roberts wrote of a Moa bone collecting expedition (Wilde, 1986). Cave tourism in the region began at the end of the 19^{th} century, and since then, the reputation of the Waitomo Caves as a tourist destination has flourished.

Today the Waitomo area hosts approximately 500 000 visitors per annum, which includes visitors to the Waitomo Glowworm Cave (Figure 2.7), Ruakuri, Aranui, and Black Water Rafting, as well as to other tourist activities operated in the area. Only 10 – 20% of the visitors comprise domestic tourists (S. Katae, pers. comm., 2008). Cave tourism is categorised by Tourism New Zealand as nature tourism (which also includes many other tourist activities, including beaches, scenic boat cruises, bush walks and geothermal attractions). New Zealand tourism research shows that of a possible 75 nature tourism activities, visits to glowworm caves is ranked 11^{th}, with 289 000 international visitors to glowworm caves throughout New Zealand in 2006. Comparatively, the domestic market ranked visits to glowworm caves 25^{th} out of the 75 listed activities, with only 64 000 domestic tourists visiting glowworm caves in 2006 (Ministry of Tourism Research, 2008). The Waitomo Glowworm Cave is, by far, the most popular tourist cave in New Zealand (S. Katae, pers. comm., 2008).

Figure 2.7. The Cathedral in the Glowworm Cave, Waitomo (photo: THL).

The Waitomo region comprises solution caves. Solution cave development, discussed in Section 2.1.1, is made possible by the underlying geology of a region. The King Country karst system extends in a patchy distribution from Kawhia, in the north, to Awakino, in the south, and from approximately 8 km east of Te Kuiti to the west coast (Figure 2.8) (Kermode, 1974). This karst system consists of Oligocene aged Orahiri Limestone and the younger, Miocene aged Otorohanga Limestone. Together, these limestones make up the Upper Te Kuiti Group (Figure 2.9). Both the Orahiri and the Otorohanga limestone formations are pure and crystalline, with > 90% calcium carbonate (Williams, 2004). The Te Kuiti Group comprises flaggy limestone layers, roughly 100 m thick, overlying calcareous siltstones and sandstones. The Waitomo Caves are part of a larger karst system in the King Country that has formed within the Te Kuiti Group limestones. The Te Kuiti Group is a transgressive sequence, typically between 100 – 300 m thick, that was formed by gradual marine inundation during a period of sediment starvation (Nelson, 1973). The Te Kuiti Group sequence in the area is made up of the basal unit Aotea sandstone, overlain by Orahiri limestone, overlain by Waitomo sandstone, followed by the Otorohanga limestone (Figure 2.9) (White & Waterhouse, 1993).

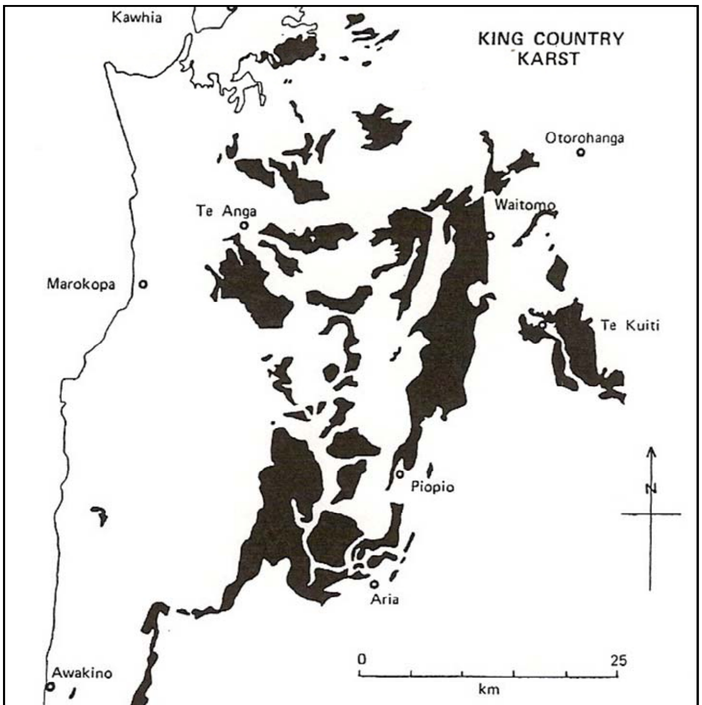

Figure 2.8. The extent of the Waitomo/King Country karst system (from Kermode, 1974).

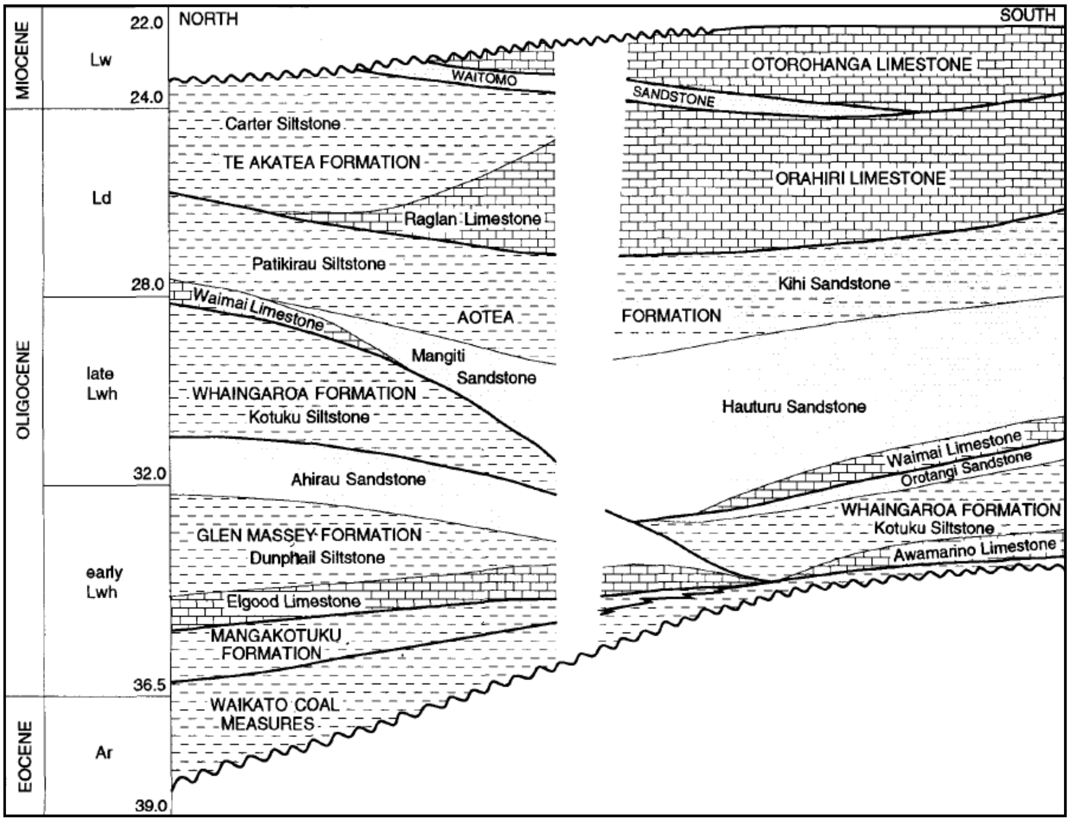

Figure 2.9. A simplified schematic section through the Te Kuiti Group from near Onewhero in the north to Mahoenui in the south, showing the general distribution and relationships of the formations (White & Waterhouse, 1993).

2.2.2.1 The Glowworm Cave

The Glowworm Cave was first explored by Fred Mace, a government surveyor, and Tane Tinorau, a local Maori Chief, in 1887 (Wilde, 1986). In 1889, the same year the Glowworm Cave opened as a tourist cave, a chief surveyor from Auckland, Thomas Humphreys, surveyed and photographed the Waitomo Glowworm Cave as part of the preparation of an “official” report (Wilde, 1986). Early on, the cave suffered under the hand of vandals which led to both the Glowworm Cave and the Ruakuri Reserve becoming protected under the Scenery Preservation Act, 1908. By 1910, a chief guide had been appointed, and the Glowworm Cave was well established as a tourist destination. In 1926, electric lighting was installed in the Glowworm Cave (Wilde, 1986).

Today the Glowworm Cave is one of New Zealand’s premier tourist attractions, as well as being the most visited cave in Australasia (de Freitas, 1998; Schmekal & de Freitas, 2001). Just under half a million people visit Waitomo’s Glowworm

Cave each year, with an influx of visitors during the summer months (November – April). During the peak summer season, visitor numbers can rise to more than 2000 people per day, with the bulk of the visitors passing through the cave between 11 a.m. and 2 p.m. daily (Doorne, 1999; de Freitas & Banbury, 1999; Schmekal & de Freitas, 2001). Whilst the cave decorations of the Glowworm Cave are beautiful, it is the stunning display of the unique glowworms that make this cave so popular.

Glowworms (*Arachnocampa luminsosa*) are essential to the tourism and promotion of the Glowworm Cave. They are unique to Australia and New Zealand, giving an awe-inspiring night sky appearance. However, glowworms are sensitive to environmental changes. Increased temperature gradients (i.e. the difference between inside cave temperatures and outside temperatures), increased airflow, and higher evaporation rates, particularly if prolonged, induce physiological stress on glowworms (de Freitas, 1998). In 1979, stress, possibly caused by the intensified tourism, led to only 4% of the glowworms displaying their lights, and prompted the closure of the Glowworm Cave for three months. Given the popularity of glowworms, and the importance of the Glowworm Cave to the New Zealand tourism industry, the cost to the region of such a closure is significant. The cave closure highlighted the need for environmental monitoring in the Glowworm Cave (de Freitas, 1998).

2.2.2.2 Ruakuri Cave

Ruakuri is the most stunning and undamaged tourist cave in New Zealand. Ruakuri (two (‘rua’) dogs (‘kuri’), or ‘den of dogs’ as it translates into the English language), was known to Maori some 400 or 500 years ago. The Maori people had used the cave entrance above the stream as a burial site for the deceased. James Holden explored the cave in the early 1900’s and began guided tours through the cave in 1904 (Wilde, 1986). Subsequently, tourism activities were taken over by the Tourist Hotel Corporation (THC). In 1987, New Zealand cave tourism began to diversify, with the first black water rafting tours taking place in Ruakuri (Duckeck, 2008). Black water rafting involves tourists float down the cave river on a tractor tyre inner-tube in the dark.

Tourism in Ruakuri ceased in 1988 due to a dispute between the Holden family and THC. Following the purchase of Black Water Rafting by Tourism Holdings Ltd. (THL), an intense upgrade of the cave entrance, paths, and lighting occurred. The design and engineering that occurred in the development of Ruakuri includes: suspended walkways, carefully developed air-lock chambers to avoid altering the natural microclimate of the system, and artistically designed lighting to create a magical atmosphere. In 2005, Ruakuri was reopened with daily guided tours.

Tourist caves such as the Glowworm and Ruakuri Caves are precious natural and economic commodities. The wellbeing of tourist caves is vital to the survival of New Zealand's tourism industry, and careful management is required to maintain the beauty and 'health' of the caves. Thus, any factor that may negatively impact the cave environment must be mitigated. Before the factors can be mitigated, it is essential to identify the problematic factors (and their sources).

2.3 Impacts of visitors and infrastructure on caves

2.3.1 Introduction

Caves are typically characterised by muddy passages with uneven floors and, in the case of more recently formed passages, the cave floor is often an active conduit, making exploration impossible without getting wet feet (e.g. Waipuna cave, Waitomo). Similarly, non-tourist or 'wild' caves, may be impossible to enter and explore without technical equipment and expertise. Whilst the challenges of caving contribute to the 'love of the sport' for passionate recreational cavers, the average tourist would much prefer to see the beauty of a cave whilst remaining clean, dry, and out of harm's way. To meet the needs of tourists, 'wild' caves have been modified to enable easy access and an enjoyable experience. Even though such modifications are essential from a tourism perspective, they can have some serious impacts on cave environments.

The impacts of tourism on caves can be divided into two general categories: immediately visible (direct) impacts; and less obvious (indirect) impacts, which take longer to become apparent (Russell & MacLean, 2008).

2.3.2 Direct impacts

The direct impacts of tourism in tourist caves are always visually obvious, and often degrade the aesthetic appeal of the cave. Direct impacts include modification of entrance ways, introduction of lighting, construction of walkways, and the addition of cave dust to caves, as well as vandalism to cave formations.

2.3.2.1 Entrance ways

Caves are often difficult to access with narrow entrances that are awkward to navigate. Natural entrances are either widened (e.g. the upper entrance at the Glowworm Cave), or new entrances are created (e.g. the new drum passage at Ruakuri) to improve tourist access to caves. In single-entrance caves, a second entrance is often created to avoid backtracking by tour groups which would double the impact to the cave environment (Russell & MacLean, 2008). A second entrance is also beneficial for the tourist experience as separate groups are less likely to pass each other during a tour. However, the construction of additional entrances can alter the natural airflow through a cave.

2.3.2.2 Lighting

Permanent lighting in tourist caves is problematic for speleothems. Orange lighting (or broad spectrum emission lights) (Figure 2.10) heat up and dry the surrounding air, inhibiting speleothem growth. Moreover, the presence of broad spectrum emission light has resulted in the growth of 'lampenflora', or opportunistic algae and mosses, on speleothems and cave walls (Cigna, 2005). The use of narrow spectrum (or 'cool') lights can reduce lampenflora growth (Ford & Williams, 2007).

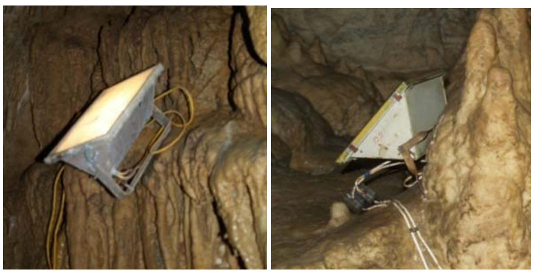

Figure 2.10. Old broad spectrum lights, typical of the original lighting used in tourist caves at Waitomo (photo: Travis Cross).

2.3.2.3 Walkways

Navigation through a cave system is often difficult, due to muddy, slippery or uneven surfaces. Walkways are generally constructed to improve access, as well as safety, throughout tourist caves. In many instances, walkways are beneficial to the cave system, as they confine tourists to a path, enabling cave operators to restrict access to delicate areas. In the early years of cave development, walkways and associated handrails were often constructed using timber, and the damp cave environment meant that much maintenance was required. Many historic pathways have since been abandoned, but often the remains of such pathways are still present in tourist caves (e.g. in Ruakuri). New pathways and infrastructure within caves are typically constructed using inert materials (e.g. concrete, some plastics, and stainless steel) (Cigna, 2005).

2.3.2.4 Cave dust

Cave dust is comprised of lint from clothes, hair, and flakes of dry skin. Cave dust can accumulate in tourist cave systems and cause the slow degradation to the aesthetic value of tourist caves (Figure 2.11) (Michie, 1999). Cave dust can also act as a food source for cave organisms, and can therefore increase microbial activity in tourist caves.

Figure 2.11. Accumulation of cave dust on meshing in a tourist cave (photo: Travis Cross).

2.3.2.5 Vandalism

Caves and karst systems are vulnerable due to the stable nature of the environment and the slow growth of speleothems. In the early days of cave tourism, vandalism, through the breaking of stalactites and stalagmites, was common, as speleothems were desirable souvenirs for tourists. Speleothems are easily degraded, and even touching will affect cave formations (as the oil, mud, or dirt on fingertips will become trapped under subsequent layers of calcite), discolouring the speleothems. Educating people about the vulnerability of cave environments has been identified as the key to reduce cave vandalism (Department of Conservation, 1999). Whilst an awareness of the delicate nature of cave systems is actively raised at Waitomo through various avenues (e.g. the school, museum, and tour guides), an attack of vandalism occurred even as recently as 2005. Vandals forced entry into the cave and splashed litres of paint across cave walls and formations (Figure 2.12).

Figure 2.12. Clean-up in the Glowworm Cave, Waitomo, following a vandalism attack, whereby paint was thrown around the cave and speleothems (photo: Travis Cross).

2.3.3 Indirect impacts

Throughout the history of tourist cave development, direct and indirect impacts have been closely linked. Indirect impacts are generally less obvious than direct impacts and result when the natural energy balance of a cave system is disturbed. Whilst direct impacts refer to the physical alteration of a cave system, indirect impacts are often the result of such physical alterations. For example, the enlargement or addition of entrance ways (direct impact) alters the airflow of a cave and thus affects the cave temperature and humidity, as well as rates of condensation and evaporation (indirect impacts) (Russell & MacLean, 2008). Similarly, abandoned wooden walkways and the accumulation of cave dust (direct impacts) provide food sources for microorganisms, resulting in more decomposition and increased cave air CO_2 (indirect impact) (Cigna, 2005; Russell & MacLean, 2008).

Caves are typically stable environments with small energy fluxes (de Freitas, 1998), and constant temperatures (Cigna, 1993); therefore an influx of people into a cave system (along with the physical alterations associated with tourist cave development), can easily disrupt the natural balance and modify the environment. Two key impacts that tourists have on caves are microclimate modification (where microclimate refers to all atmospheric environmental processes that occur within a cave (de Freitas & Schmekal, 2003)), and impacts on the CO_2 level in the cave atmosphere. The following three sections (2.3.3.1 – 2.3.3.3) describe the impact tourists have on cave microclimate. As CO_2 is the focus of this thesis, the impact of tourists (and other sources) on cave air CO_2 levels, will be discussed in detail in Section 2.4.

2.3.3.1 Temperature

Changes in cave air temperature are largely associated with tourists emitting body heat, and the heat output from lights (Villar *et al*., 1984; Gillieson, 1996; Cigna & Burri, 2000; Russell & MacLean, 2008). The thermal contribution from one person walking through the cave is reported to be 170 W (where 1 W=1 $J.s^{-1}$) (Villar *et al*., 1984). Likewise, cave lighting that has not been upgraded to ‘high efficiency’ lamps, can impact the temperature of cave systems (Cigna, 2005). For example, Cigna and Burri (2000 after Forti, 1980) described one instance in the Castellana Caves in Italy where a 1 kW bulb, placed 50 cm from a rock wall, resulted in an increase of more than 10 °C in the temperature of the wall, within a matter of seconds. Increased air temperature directly affects airflow, condensation, and evaporation in caves.

2.3.3.2 Humidity

Caves are typically damp environments with high relative humidity. Changes in cave air humidity are largely driven by three factors: the temperature and specific humidity of outside air, sensible and latent heat fluxes between the cave air and cave surfaces, and vapour fluxes between the cave air and cave surfaces (de Freitas & Littlejohn, 1987). Reductions in the relative humidity of cave air alter condensation and evaporation processes, which ultimately affect the development of speleothems. The development of tourist caves typically leads to a reduction in cave air humidity through a number of mechanisms including: increased air flow when entrances are enlarged or created (de Freitas, 1998; Russell & MacLean, 2008), and increased cave temperature, through lighting and tourist body heat (Cigna, 1993). For example, increased air flow in the Glowworm Cave, Waitomo, resulted in a reduction in relative humidity of the cave air, and thus increased evaporation, adversely impacting the glowworms (de Freitas, 1998). In the Castellana Caves in Italy, the installation of lights in the cave lead to a significant increase in rock temperature, which resulted in a decrease in relative humidity from between 95 – 100% to between 55 – 60%, and created a strong upward draught (Cigna & Burri, 2000 after Forti, 1980).

2.3.3.3 Condensation and evaporation

Condensation of moisture-laden cave air onto cave walls and speleothems and the subsequent evaporation, is a function of the vapour gradient between rock surfaces and the cave (de Freitas & Schmekal, 2003). The vapour gradient is altered by the exchange of air between the cave and the outside environment, which either increases or decreases condensation/evaporation rates. Experimental evidence showed that the gradient between outside and cave rock temperatures is the key indicator of condensation (de Freitas & Schmekal, 2003). As rock temperature shows little variation, condensation is primarily a function of air temperature (de Freitas & Schmekal, 2003), with condensation maxima occurring seasonally during the summer, as well as diurnally during the middle of the day (10.00 a.m. – 4.00 p.m.) (Dublyansky & Dublyansky, 1998). Conversely, evaporation maxima occur during the winter and at night time (when the rock temperature is warmer than that of the cave air) (de Freitas & Schmekal, 2003).

As condensation (and evaporation) is primarily a function of air temperature, changes to air temperature will alter condensation and evaporation rates. Warming of the cave air by tourists and cave lighting will increase condensation rates. Increased air flow (i.e. due to the modification of a tourist cave entrance, or the facilitating of ventilation to flush the cave) results in a greater temperature gradient between the air and rock, thus altering the rate of condensation and evaporation. For example, when the Glowworm Cave is ventilated during the summer months, warmer outside air will enter the cave, resulting in a greater temperature gradient between the cave rock and cave air, thus inducing condensation (de Freitas & Schmekal, 2003). When the cave is ventilated during the night, when outside air temperature is colder than the cave rock, evaporation is induced.

2.4 CO_2 in the cave atmosphere

2.4.1 Introduction

CO_2 rich waters are responsible for dissolving carbonate rock to form caves, and precipitating calcite results in the formation of speleothems, thus making CO_2 a crucial component of cave development (Section 2.1.1). In the same way that CO_2 in solution forms and decorates caves, CO_2 rich waters can also dissolve and destroy speleothems. As cave air CO_2 is substantially higher in tourist caves compared to wild caves, the following section provides a detailed overview of CO_2 in tourist caves, including sources of cave air CO_2 and the effects elevated CO_2 can have on cave systems.

2.4.2 Effects of elevated CO_2 in caves

2.4.2.1 Human health and safety

Carbon dioxide is a significant issue in tourist caves as it affects both the comfort of tourists and the state (or 'health') of speleothems. When exposed to excessive levels of CO_2, humans respond with symptoms such as increased respiration rate, sweating or shivering, headaches and drowsiness (de Freitas & Banbury, 1999). Whilst permissible levels vary greatly depending on the desired objective (i.e. with regard to ventilation, air quality or health, safety and physiological well-being), the New Zealand Occupational Safety and Health Service have set two workplace limits on CO_2 levels based on exposure time (New Zealand Department of Labour, 1994). The first limit is 5000 ppm, which is the '8-hour time-weighted average exposure standard designed to protect (people) from the effects of long term exposure' (New Zealand Department of Labour, 1994, p.11). The second limit is 30 000 ppm and is known as the short-term exposure limit, which applies to any 15 minute period during a day. Five thousand parts per million is typically cited as being the level that should not be exceeded in tourist caves with the comfort of tourists and guides in mind (Dragovich & Grose, 1990; de Freitas & Banbury, 1999; Doorne, 1999). Toxic levels of approximately 5% (50 000 ppm) are extremely rare.

2.4.2.2 Condensation corrosion

Condensation corrosion is a process of chemical weathering, whereby CO_2 enriched water vapour, that is under-saturated with respect to calcite, condenses on a soluble calcite surface (i.e. cave wall, speleothem), enabling the potential for dissolution to occur (de Freitas & Schmekal, 2003; James, 2004a after Fairbridge, 1968). Whilst condensation corrosion occurs naturally in wild caves, the occurrence of condensation corrosion is substantially magnified in tourist caves. Humans exhale air that is rich in CO_2, saturated with water vapour, and at a temperature usually much higher than that of the ambient cave air temperature (de Freitas & Schemekal, 2006). The thermal gradient between the warm air respired by tourists compared to the colder walls of the cave, results in condensation forming on the rock walls and speleothems. The condensate is invariably under-saturated (with respect to calcite) and has a high P_{CO_2} compared to the cave surfaces, thus making the condensate aggressive, triggering dissolution and thus corrosion (Tarhule-Lips & Ford, 1998; de Freitas & Schemekal, 2006).

The severity of condensation corrosion can be increased when given conditions prevail. Firstly, the corrosive nature of condensation is considerably increased as the amount of dissolved CO_2 increases (de Freitas & Schmekal, 2003), as more calcite must be dissolved before equilibrium is reached. Secondly, the effects of condensation corrosion are magnified in caves where the speleothems are inactive. Inactive speleothems are dry and thus lack the protection of a calcite saturated solution which would act as a buffer, reducing the effect of CO_2 enriched condensation waters (James, 2004b).

When the aggressive condensation waters evaporate, and CO_2 degasses from the solution, the calcite is re-precipitated and a different type of calcite feature is formed. The depositional features formed as the condensate evaporates, are typically flaky deposits of soft, microcrystalline calcite, or small pits, bell holes, and cave coral (Figure 2.13) (James, 2004a). The cycle of condensation followed by evaporation is believed to enhance the condensation corrosion process (Tarhule-Lips & Ford, 1998; de Freitas & Schemekal, 2006).

Figure 2.13. Brittle appearance of the effect of condensation-evaporation processes on typically smooth calcite formations, Glowworm Cave, Waitomo (photo: Bruce Mercer)

McCabe (1977) analysed dripwaters collected from Waipuna Cave in Waitomo, and found that dripwater from straw stalactites was aggressive when it exceeded 2500 – 3000 ppm. From this research, it was suggested that a (perhaps conservative) threshold for the (nearby) Glowworm Cave atmosphere P_{CO_2} should be set at 2400 ppm (Kermode, 1978). The 2400 ppm limit is the current P_{CO_2} threshold stated in the licence agreement under which the Glowworm Cave operates.

2.4.3 Anthropogenic-induced sources of cave CO_2

There are two main anthropogenic sources of CO_2 in tourist cave environments (Amar, 2004 after James, 1977; James & Dyson, 1981; de Freitas & Banbury, 1999). These sources are:

1. respiration of people in the caves; and,
2. microbial activity in the sediment breaking down organic matter and respiring CO_2.

2.4.3.1 Human respiration

Carbon dioxide is exhaled as a by-product of respiration, with human breath containing 4% CO_2 by volume (de Freitas & Banbury, 1999; Baldini *et al*., 2006). Therefore, when a cave is opened to tourists, the CO_2 levels of the cave air increase (de Freitas & Banbury, 1999; Russell & MacLean, 2008). Whilst CO_2 is denser than air, respired air is warm and well-mixed and, therefore, does not separate. CO_2 diffuses rapidly through air, and as warm air rises, the dominant direction of diffusion is upwards through a cave system (de Freitas & Banbury, 1999; James, 2004b).

Respired CO_2 in caves is directly correlated with the number of visitors to the cave, with a single visitor contributing an estimated 17 $l.h^{-1}$ CO_2 to the cave atmosphere (de Freitas & Banbury, 1999 after Marion, 1979). As human respiration is considered the major source of CO_2 to cave environments, it is not surprising that the CO_2 concentrations in caves follow seasonal and diurnal patterns that reflect tourist numbers. Seasonal patterns generally include a summer maxima and winter minima in cave air CO_2, as tourist numbers are generally higher during the summer holiday period (Troester & White, 1984; Ek & Gewelt, 1985; Cigna, 1993; Faimon *et al*., 2006). Diurnal patterns of high day time CO_2 concentrations (during cave tourist operation hours) and low night time CO_2 concentrations have also been directly attributed to tourists visiting caves (Dragovich & Grose, 1990; Cigna, 1993; Pulido-Bosch *et al*., 1997; Song *et al*., 2000; Fernandez-Cortes *et al*., 2006). An 'Easter Effect' has also been reported in many Australian caves, with the CO_2 markedly increasing over the Easter holiday period due to increased tourist numbers (James, 1994).

2.4.3.2 Microbial activity

Microorganisms contribute CO_2 to cave environments via oxidation and degradation of organic matter, as well as through microbial respiration. In many wild caves, microbial activity is restricted due to limited food sources. Microbial activity is enhanced by the presence of people in caves, as people contribute cave dust (lint, hair, and flakes of skin), and sediment and organic matter (attached to footwear), to the cave. Cave dust and organic inputs contribute to the energy pool of the cave system, acting as a food source for microorganisms.

Another factor that contributes to the food source (and thus CO_2 contribution) of microorganisms, is sediment brought into caves during floods. Whilst sediment input is not necessarily specific to tourist caves, at times, people have either modified the course of the river or stream upstream of, or within, the cave. Such alterations can be for agricultural purposes, flood prevention, or for the ease of operating boat tours through the caves. River or stream alterations can enhance the amount of sediment deposited during floods, which is subsequently decomposed by microorganisms. A study in the Bungonia Cave in New South Wales, Australia, found that, following a flood event, the contribution of CO_2 from microorganisms increased to more than 5% of the total cave P_{CO_2} (Gillieson, 1996 after James, 1977).

2.4.4 Non-anthropogenic sources of cave CO_2

Anthropogenic sources of CO_2 have been well studied and are recognised as being the main sources of CO_2 in tourist caves, however, non-anthropogenic CO_2 sources are often overlooked within tourist caves. Three main non-anthropogenic sources of CO_2 have been identified in caves (Amar, 2004 after James, 1977; James & Dyson, 1981; Baldini *et al*., 2006). These sources are:

1. diffusion of soil gas through soil and rock;
2. degassing from dripwater entering the cave; and,
3. degassing from streams (or water bodies) within the cave.

It is acknowledged that a fourth non-anthropogenic source of CO_2 exists in some cave environments; that is, CO_2 seepage from porous reservoirs usually of an igneous origin (Baldini *et al*., 2006). However, as igneous sources are relatively rare and irrelevant for the Waitomo Caves, no further discussion on igneous sources of CO_2 has been included.

2.4.4.1 Gaseous diffusion through soil and rock

The production of CO_2 is concentrated in the upper O and A horizons of the soil, and is derived from biological processes including photosynthesis, respiration, microbial activity, and the decomposition of organic matter (Adams & Swinnerton, 1937 after Smith & Brown, 1933). Plants act as pumps, drawing CO_2 out of the air for photosynthesis and then transpiring CO_2 into the soil atmosphere. The contribution of CO_2 from microbes (e.g. bacteria, actinomycetes, and fungi), however, is greater than the CO_2 contribution of plants. Plant and microbe productivity increase with temperature and soil moisture; therefore, warm, wet conditions are typically associated with high soil CO_2 in the rooting zone. Soil CO_2 also varies with soil type.

As CO_2 is a heavy gas that easily diffuses through air, the CO_2 produced in the soil is capable of draining down through soil pore spaces and bedrock fissures into underlying caves (Ford & Williams, 2007). In the unsaturated (vadose) zone, below the soil profile, a pool of organic matter exists, sourced from the soil and washed or leached into the microfissural network (Atkinson, 1977). The degradation of the organic matter where ventilation (and thus oxygen) is limited, results in the air becoming more CO_2 enriched. Organic degradation can be a significant source of CO_2 in caves, particularly where there is little or no air movement, with CO_2 reaching lethal levels (> 5%) in some instances (Ford & Williams, 2007). Bourges *et al*. (2001) found that in non-visited, deep parts of the Aven d'Orgnac (France), the CO_2 concentrations ranged from 2 – 5% by volume, with $\delta^{13}C$ values of -19 ‰. The $\delta^{13}C$ value of -19 ‰ is consistent with a biogenic origin. Whilst some of the CO_2 was a component of diphasic (a combination of water and air) infiltration, CO_2 enriched air samples from the microfissural network in the rock indicate that air draining downwards from the soil zone is also a probable source of the CO_2 enriched cave air (Bourges *et al*., 2001). Baldini *et al*. (2006) recorded higher cave air P_{CO_2} in roof fissures, joints, and at locations adjacent to walls and suggested that such locations were sheltered from advection, allowing the localised accumulation of P_{CO_2}.

Higher CO_2 concentrations occurred during the summer than the winter, positively correlating with outside air temperature (Bourges *et al*., 2001). The higher summer CO_2 concentrations is consistent with both soil and unsaturated zone CO_2 production, where respiration is positively correlated with temperature.

2.4.4.2 Dripwater

Dripwater typically has elevated P_{CO_2} compared to the atmosphere, and is often supersaturated with respect to calcite (Thrailkill & Robl, 1981). Degassing (or outgassing) of CO_2 from dripwater is a rapid process (Thrailkill & Robl, 1981) controlled by a number of factors, including: the P_{CO_2} gradient between the cave air and the dripwater, and the depth of the dripwater layer (i.e. the thinner the layer of flowing or dripping water, the quicker the rate of CO_2 degassing).

Dripwater is derived from the saturated (phreatic) zone. Rainwater percolates down through the soil and through the vadose zone before reaching the water table and recharging the phreatic zone. Rainwater typically contains a P_{CO_2} level equal to that of the atmosphere (~ 380 ppm), and becomes CO_2 enriched as it percolates through the soil. As the CO_2 enriched (acidic) solution comes into contact with the limestone, dissolution occurs, and the water tends towards calcite saturation. The dissolution process is slow, with some groundwater taking years (i.e. in the order of 1000 years) to achieve equilibrium with the rock (Adams & Swinnerton, 1937; McCabe, 1977 after Plummer & Wigley, 1976). Reactions within carbonate solutions are also slow, with 'response times' in the order of one hour (McCabe, 1977 after Roques, 1969). Thus, it is evident that the kinetics involved in the reaction at the solid-liquid interface, limit the rate of limestone dissolution (McCabe, 1977). In addition, factors such as pH, temperature, P_{CO_2}, flow rate, and trace elements will influence the rate of dissolution.

CO_2 outgassing forces dripwater to a high degree of supersaturation with respect to calcite. When the solution reaches approximately five times supersaturation, calcite will begin to precipitate.

2.4.4.3 Stream

Carbon dioxide in streams is either produced *in situ* via in-stream biological activity, where CO_2 enters streamwaters from external sources including groundwater seepage (which consists primarily of soil-derived, biologically produced CO_2), or CO_2 will diffuse into the stream across the air-water interface. Streams typically have elevated partial pressures of CO_2 relative to the atmosphere (Hoffer-French & Herman, 1989; Rebsdorf *et al.*, 1991). As stream CO_2 is largely derived from the soil, with dissolved CO_2 entering the stream through groundwater seepage, some of the factors that control the streamwater P_{CO_2} are synonymous to the controls on the P_{CO_2} of the soil. Soil P_{CO_2} (and thus stream P_{CO_2}) levels are influenced by several factors (Rebsdorf *et al.*, 1991), including:

- soil texture (e.g. clay particles swell and thus inhibit the exchange of CO_2 in the soil during wet weather (Mitoke, 1974));

- soil temperature and moisture (e.g. the karstlands in China which contained soil P_{CO_2} ~ 500 ppm during the dry, cool season, and 26000 – 40000 ppm in the warm, monsoon season (Ford & Williams, 2007 after Yuan, 2001);
- vegetation (e.g. soil CO_2 is higher under forests compared to bare rock catchments or in soils disturbed by cultivation (Adams & Swinnerton, 1937);
- catchment aspect (e.g. south facing slopes (in the Northern Hemisphere) become warmer during the day compared to north facing slopes, and thus resulted in an increase in both soil microbial respiration and plant growth. This, in turn, resulted in an increase in soil (and thus stream) P_{CO_2} (Pentecost, 1992);
- organic matter content (e.g. the higher the content of organic matter in the soil, the greater the microbial activity and decomposition, thus increasing the CO_2 concentration of the soil).

Additionally, stream P_{CO_2} will vary based on:

- the flowpath and residence time of groundwater within the aquifer, which can result in seasonal variability in the P_{CO_2} of streamwater (Mayer, 1999). Low flow seepage water has a longer residence time in the unsaturated soil and vadose zones, than high flow waters. This gives the soil water more time to achieve equilibrium with the soil P_{CO_2}. In turn, the CO_2 enriched water, which percolates more slowly through the limestone (compared to high flow percolation rates), is more aggressive towards the calcite, and thus the seepage water entering streams is characteristically higher in CO_2 and more saturated with respect to calcite, than streamwater in the winter (Hoffer-French & Herman, 1989). In contrast, during high flow conditions on a broad seasonal scale, stream P_{CO_2} levels are lower due to faster seepage rates (as soil is already saturated). The lower stream P_{CO_2} under high flow conditions is representative of dilution. Further studies have investigated stream P_{CO_2} following rainfall (storm events) (e.g. Liu *et al*., 2004; 2007). The fractured nature of karst aquifers mean that during high flow conditions, percolation, and thus streamflow response, can be exceptionally rapid (Groves & Meiman, 2005). During storm events, stream P_{CO_2} has been reported to both increase and decrease (over a 200 km spatial scale) (Liu *et al*., 2007). Decreases in stream P_{CO_2} during storm events are the result of dilution. Increases in stream P_{CO_2} during storm events are associated with infiltrating rainwater dissolving CO_2, before seeping into streamwaters (soil CO_2 effect) (Liu *et al*., 2004; 2007).

- the mixing of different water masses (Mayer, 1999). For example, during a flood event in the karst complex 'Grotte di Frasassi-Grotta Grande del Vento' in Italy, the flow direction of the Sentino River was reversed. Cold 'external' waters flowed up-stream, mixing with the warmer waters of the karst system. The two water masses, with different temperatures and different CO_2 concentrations, mixed, resulting in a solution that was under-saturated (with respect to carbonates). As the water cooled, an increase in the CO_2 concentration occurred, and subsequently the aggressiveness of the solution increased (Dragoni & Verdacchi, 1993).

- in-stream biological activity, which can also be influenced by catchment use. For example, in exposed streams, such as in farmland areas, an abundance of macrophyte and algal growth is common. Therefore, the pronounced diurnal variation of CO_2 and O_2 reflects photosynthetic and respiratory processes (Rebsdorf *et al*., 1991). In small, low-order, shaded streams, diurnal variation in P_{CO_2} has also been reported (Guasch *et al*., 1998).

- water temperature. For example, a decrease in water temperature leads to an increase in the solubility of CO_2 and thus less CO_2 outgassing will occur. Hoffer-French and Herman (1989) reported that it is virtually impossible to determine whether the diurnal variation is the result of biological activity or temperature fluctuations.

- the P_{CO_2} disequilibrium between the stream and atmosphere being the driving force for CO_2 outgassing (Hoffer-French & Herman, 1989). As streams typically contain higher P_{CO_2} levels than the atmosphere (Hoffer-French & Herman, 1989; Rebsdorf *et al*., 1991), CO_2 dissolved in streamwater readily degasses across the air-water boundary in an attempt to obtain equilibrium with the atmosphere. Therefore, if the atmospheric P_{CO_2} level is elevated compared to the stream (e.g. as occurs in tourist caves), then the P_{CO_2} concentration gradient is reversed, and thus, the stream could potentially act as a CO_2 sink.
- acid rain inputs. In some areas in the Northern Hemisphere, stream chemistry can also be influenced by acid rain, which lowers the pH of the stream, resulting in stream P_{CO_2} levels that are almost eight times higher than the P_{CO_2} levels of streamwater that is in equilibrium with air (Rebsdorf *et al*., 1991).

2.5 Summary and conclusion

Caves are unique and complex environments that are formed and destroyed by dissolution processes. As CO_2 in solution is the primary chemical driving force in cave formation, and because caves are typically confined environments with limited airflow, elevated levels of CO_2 in caves (with respect to the outside environment) are common. However, when the P_{CO_2} of the cave atmosphere increases over and above the natural levels, as is common within tourist caves, the result can be destructive on caves and their features (through the process of condensation corrosion).

Tourist caves are often important tourism destinations, particularly in small townships such as Waitomo, where the local economy is often reliant on, and driven by tourists. As the problem of condensation corrosion in caves is magnified by high CO_2 levels, a good knowledge of CO_2 sources, sinks and their respective contributions is important for effective cave management. A substantial amount of research has been done on the effects of tourism on cave air P_{CO_2} (as well as temperature), however non-anthropogenic sources of CO_2 in caves are less well studied. Gaseous diffusion, dripwater degassing and streamwater degassing have been identified as key potential sources of CO_2 to caves. Regardless of the differing mechanisms by which gaseous CO_2 enters the cave (i.e. diffusion through rock and degassing from karst waters), the CO_2 is primarily biogenic in origin, and comes from the soil air.

Of the non-anthropogenic CO_2 sources identified (gaseous diffusion, dripwater degassing, and streamwater degassing), stream and dripwater sources are likely to be the dominant sources at Waitomo. Therefore, the remainder of this thesis will investigate the possibility of the stream and dripwater contributing CO_2 to the Glowworm Cave environment.

3.0 Chapter Three: Site description and methods

3.1 Introduction

In order to better understand the effect of non-anthropogenic sources of CO_2 on cave environments, three related studies were undertaken. First, historical records of P_{CO_2}, temperature, rainfall and streamflow data from the Glowworm Cave were analysed. Next, measured stream P_{CO_2} (Glowworm and Ruakuri Caves) and dripwater P_{CO_2} (Glowworm Cave) were evaluated to investigate the patterns associated with stream and dripwater P_{CO_2}. Finally, the stream and dripwater chemistry were examined in an attempt to quantify the origin of the stream and dripwater P_{CO_2}.

Chapter Three provides a description of the monitoring programme and sampling locations within the Glowworm and Ruakuri Caves, and an explanation of the methods used in the data acquisition and analysis. For raw data files refer to discs at the back of this thesis.

3.2 Location and climate of Waitomo

The Glowworm and Ruakuri Caves are located in the Waitomo district, 55 km southwest of Hamilton City in the North Island, of New Zealand (38°15' S, 175°06' E) (Figure 3.1).

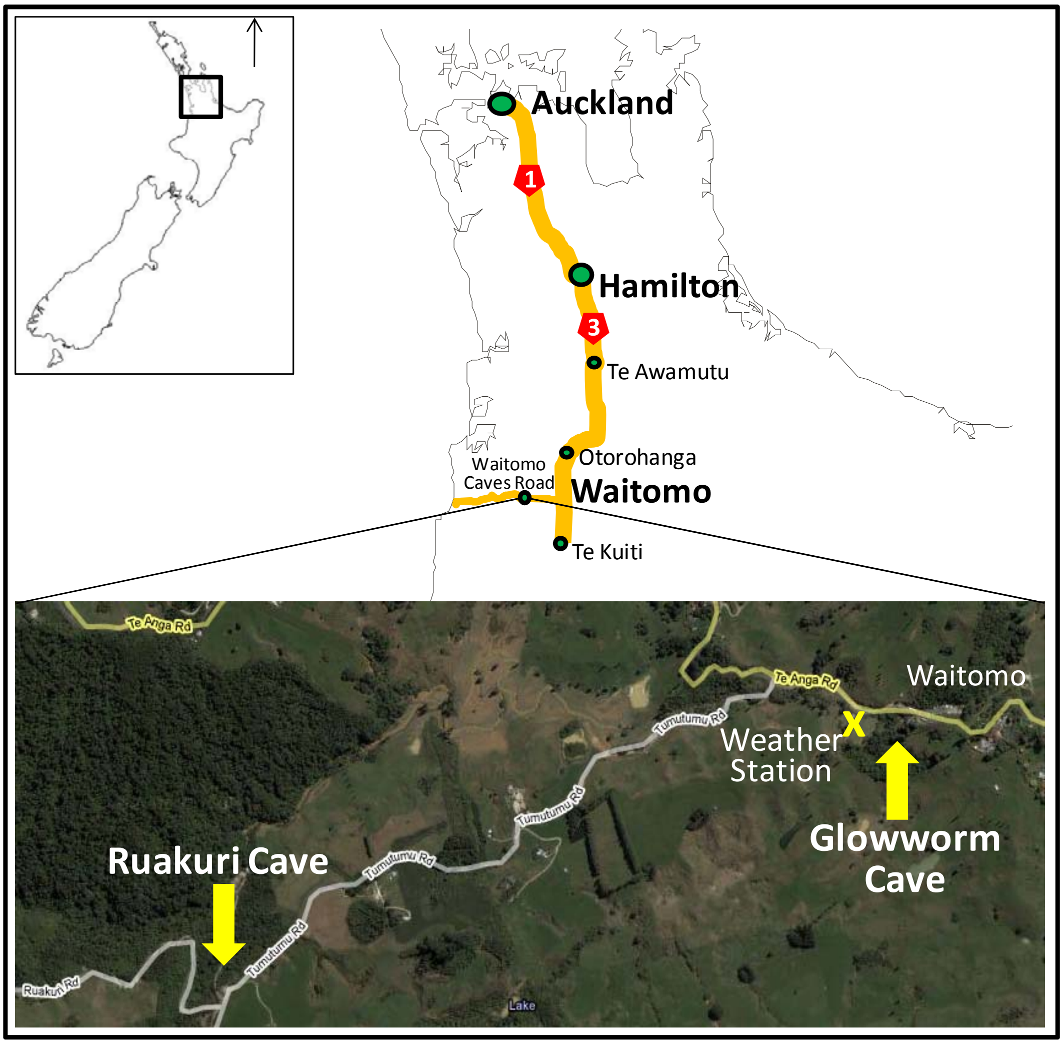

Figure 3.1. Location of the Waitomo study site including the Glowworm and Ruakuri Caves (source: googlemaps.com).

The Waitomo region has a mild, sub-temperate climate. Mean daily temperature maxima and minima for the warmest month (January) are 24.1 °C and 12.6 °C, while, for the coldest month (July) mean daily temperature maxima and minima are 13.1 °C and 3.3 °C. Rainfall is typically frequent throughout the year, although winter is generally wetter with more frequent flooding than summer. The mean annual precipitation is 1530 mm (de Freitas & Schmekal, 2003).

The year 2008 was unique in that the summer period (December 2007 – March 2008) was particularly dry, whilst the winter period was wetter than usual, with a total rainfall from July – September of 965 mm.

3.3 Morphology of the Glowworm Cave

The Glowworm Cave has two entrances: the Upper Entrance, from which two passages (the main passage and the Blanket Chamber Passage) extend; and the Lower Entrance, located slightly northwest of, and 14 m below, the Upper Entrance (Figure 3.2).

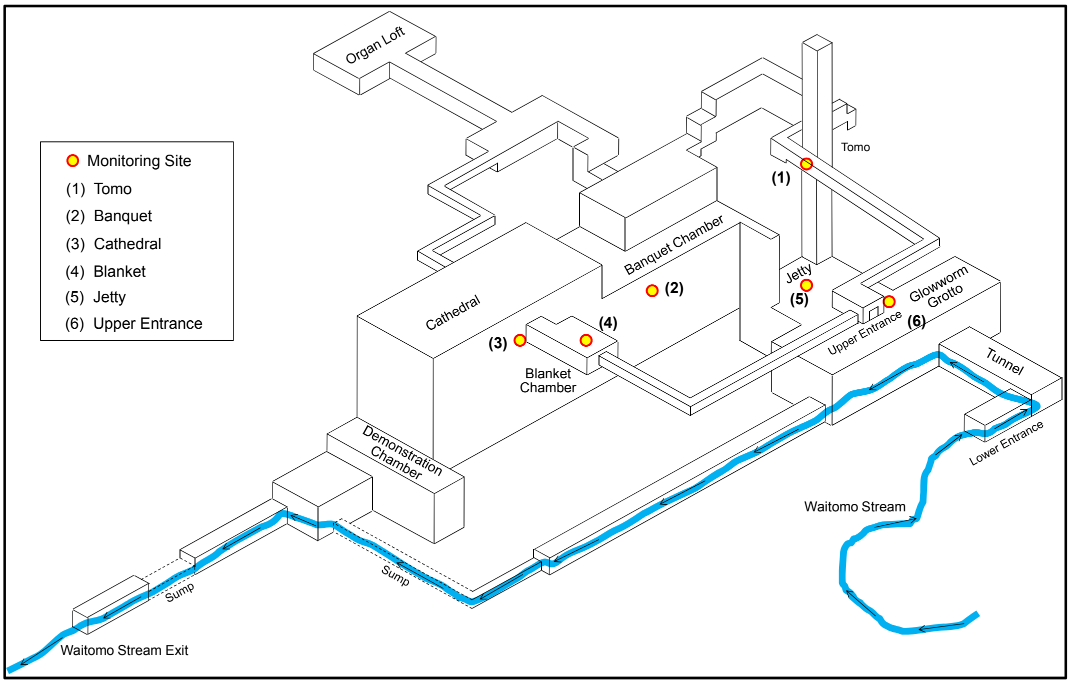

Figure 3.2. Schematic of the Glowworm Cave at Waitomo indicating the location of the monitoring sites (adapted from de Freitas *et al*., 1982).

There are two distinct levels within the Glowworm Cave: the upper level, which comprises the Main Passage, the Blanket Chamber and the Organ Loft; and the lower level, consisting of the Banquet Chamber, the Cathedral, the Demonstration Chamber, and the Glowworm Grotto. The Blanket Chamber Passage extends horizontally for 40 m and varies in diameter between 1 – 4.5 m. There are a number of active straws present in the Blanket Chamber. The Organ Loft, a 40 m long, beautifully decorated cul-de-sac passage, is situated on the opposite side of the cave to the Blanket Chamber. The main passage is 39 m long and passes alongside the Tomo, a 13 m vertical shaft that connects the Main Passage with the Glowworm Grotto, before stepping down to the Banquet Chamber. The largest chamber in the Glowworm Cave is the Cathedral, a 40 m long, 11 m wide and 13 m high chamber that links all sections of the cave. The Glowworm Grotto is comprised of a water filled chamber, approximately 30 m long, 10 m wide and 5 m high. It is the ceiling of the Glowworm Grotto that houses the large display of glowworms, the caves' most prestigious feature (de Freitas & Banbury, 1999). The Waitomo Stream flows through the lower entrance, along a 40 m tunnel, and into the Glowworm Grotto. From the Grotto, the Waitomo Stream enters a submerged passage way (sumps) for a short distance, and then emerges in the Demonstration Chamber, a section of the cave that is joined to the Cathedral. The Waitomo Stream sumps again down-river of the Demonstration Chamber, before emerging outside the cave (Figure 3.2).

3.4 Morphology of Ruakuri Cave

Ruakuri Cave is characterised by an active stream and is essentially horizontal in form (Figure 3.3). The main passage of Ruakuri is the Stream Passage, which is up to 20 m high and 5 m wide in some places (Williams *et al*., 1999a). Whilst Ruakuri has a number of entrances (including the stream passage entrances and the 'Tapu' entrance), the key access point for tourist parties (excluding Black Water Rafting groups) is the newly developed Drum Entrance. The Drum Entrance is a large (approximately 10 m in diameter) spiral entrance that was excavated in 2003/2004. A cylindrical passage with air-lock doors joins this spiral entrance way with the Drum Passage. The Drum Passage gradually slopes downwards, eventually joining up with the Stream Passage (Figure 3.3).

The tourist route follows the Stream Passage for another ~ 50 m, before veering upwards away from the stream to the Mirror Pool. Holden's Cavern is a large chamber that separates the Mirror Pool chamber from the Ghost Walk. Prior to the upgrade of Ruakuri in 2003/2004, a rockfall prevented access between the Mirror Pool and Holden's Cavern (Figure 3.3).

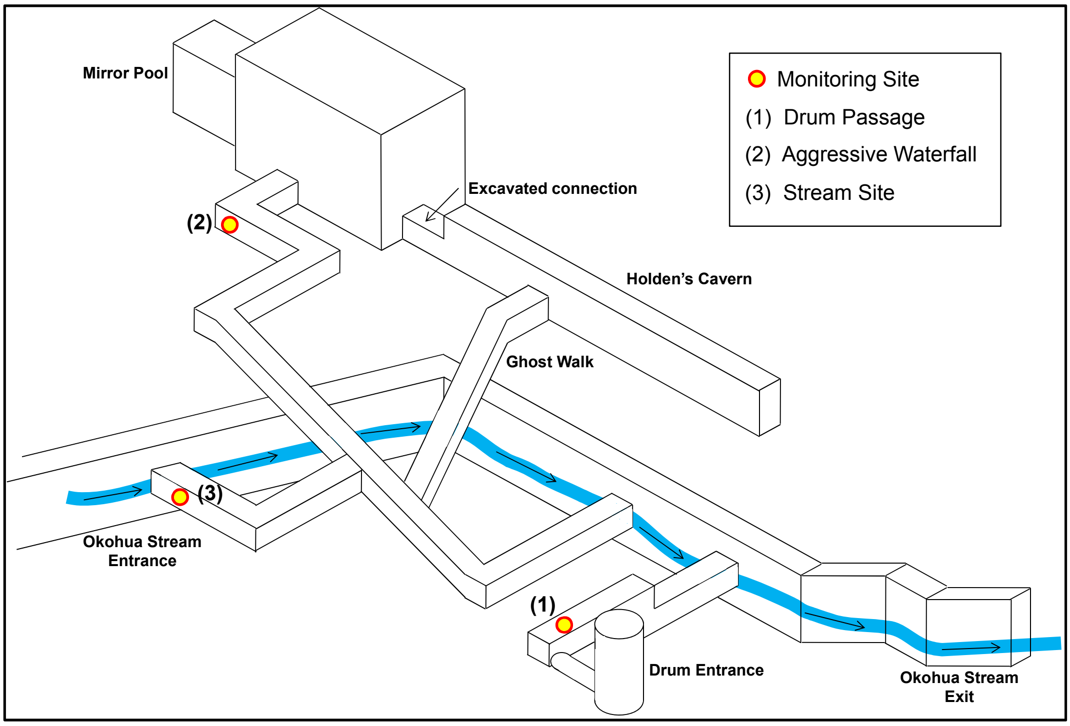

Figure 3.3. Schematic of the Ruakuri Cave at Waitomo indicating the location of the monitoring sites (adapted from Crossley, 1998).

3.5 Data collection

Following the recommendations of de Freitas (1998), a long term monitoring programme was established for the Glowworm Cave. The monitoring programme is currently maintained by the tourism operators, THL, and involves ongoing collection of climate data (both within and outside the Glowworm Cave), and comprises a 10 year historic dataset. Following the 2003/2004 development and re-opening of the Ruakuri Cave, a monitoring programme similar to that of the Glowworm Cave, was established within the Ruakuri Cave. The long term measurements included: cave air P_{CO_2} (partial pressure of CO_2), temperature, rainfall (collected by THL), and streamflow (collected by Environment Waikato). For the year 2008, the long term measurements continued, however additional data was collected specifically for this research. The additional short term measurements included stream and dripwater P_{CO_2}. The majority of the data for both the historic and the 2008 collection periods were recorded using CR10X data loggers. Tourist number data for the Glowworm Cave, obtained through admission sales records, were also available for the entire period (1998 – 2008).

3.5.1 Cave air CO_2

CO_2 was measured from 1998 – 2008 using Vaisala GMP222 (0 – 5000 ppm) sensors (Figure 3.4). The Vaisala GMP222 sensor operates based on the nondispersive infrared (NDIR) single-beam dual-wavelength principal (or infrared gas analyser (IRGA)) (Vaisala, 2004). Air was passed into a sample chamber, where an infrared light was directed towards an optical filter. The optical filter eliminated all light except the wavelength absorbed by CO_2 molecules, thus detecting and measuring CO_2. The Vaisala GMP222 has an accuracy of ± [75 ppm CO_2 + 2% of the reading] (Vaisala, 2004). The CO_2 measurement was not affected by water vapour (or dust) as the sensor can operate in conditions of 100% (non-condensing) relative humidity, thus making the Vaisala GMP222 sensor ideal for the cave environment (Vaisala, 2004). Measurements were taken every 60 seconds and a mean of the data was recorded every ten minutes.

Figure 3.4. Vaisala GMP222 CO_2 sensor (source: www.vaisala.com).

CO_2 was measured at two locations in the Glowworm Cave: in the Cathedral, and the Organ Loft (Figure 3.5). The Cathedral sensor was located high on the wall, just below the opening into the Blanket Chamber. The Organ Loft sensor was located on the hand rail at the end of the Organ Loft Chamber. Both CO_2 sensors were situated in the upper reaches of the Glowworm Cave. Even though CO_2 is a heavy gas, additional heat and air currents throughout the cave, resulting from high visitation numbers, ensures that the air within the Glowworm Cave is well mixed. The Cathedral CO_2 sensor provided a better average CO_2 dataset compared to the Organ Loft sensor, which was particularly sensitive due to its 'cul-de-sac' location. Only CO_2 data from the Cathedral site was used for this research.

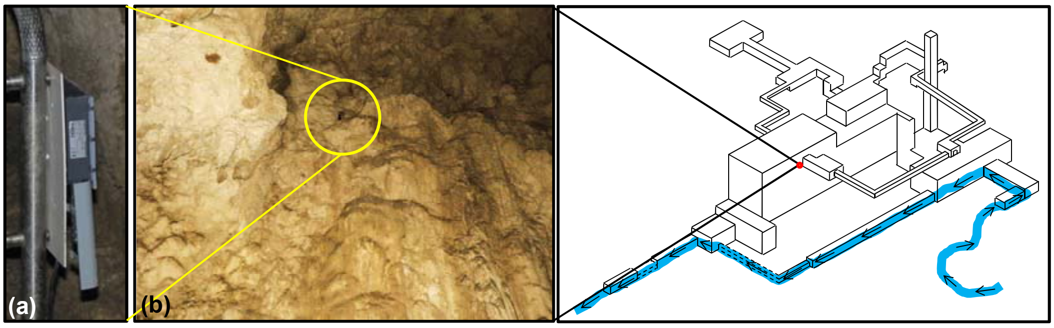

Figure 3.5. Location of the CO_2 sensors in the Glowworm Cave. (a) A close up image of the CO_2 sensor in the Organ Loft; and (b) the CO_2 sensor on the wall of the Cathedral.

Carbon dioxide was also measured at two locations within Ruakuri Cave; in the Drum Passage and at the Aggressive Waterfall (Figure 3.6).

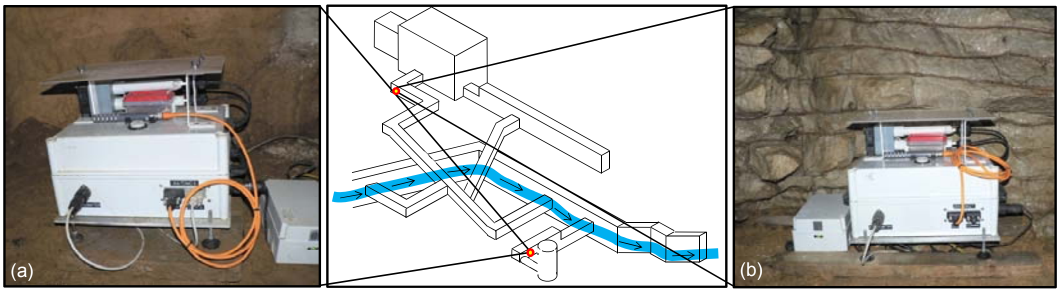

Figure 3.6. Monitoring stations within Ruakuri Cave; (a) the Drum Passage and (b) Aggressive Waterfall (CO_2 sensor is attached to the orange cord; temperature sensors are the white tube-shaped sensors behind the CO_2 sensors).

3.5.2 Temperature

Campbell Scientific 107 temperature probes were used to measure air temperature both inside and outside the caves. The 107 probes used a BetaTherm 100K6A1 thermistor which measured temperature ranging between -35 °C and +50 °C and had a precision of ≤ ±0.01 °C over -35 °C – +50 °C (Campbell Scientific, 2008a). The temperature sensors located outside the cave were housed in radiation shields to ensure data were representative of the ambient air temperature. Data were recorded every 30 minutes and were available from 1998 – 2008 inside and outside the Glowworm Cave, as well as at the weather station. Data were also recorded every 30 minutes in the Ruakuri Cave for the year 2008.

Cave air temperature was measured at three locations within the Glowworm Cave: the Tomo, the Banquet Chamber, and the Jetty (Figure 3.7). Stream temperature was also recorded at the Jetty site (data obtained from NIWA). Similarly, cave air temperature was recorded at two locations within Ruakuri Cave: the Drum Passage, and the Aggressive Waterfall. At each site, the temperature probes were located 1 – 2 m above the cave floor and positioned 0.1 – 0.3 m from the cave wall. Outside air temperature was measured at the weather station, as well as at the upper entrance of the Glowworm Cave.

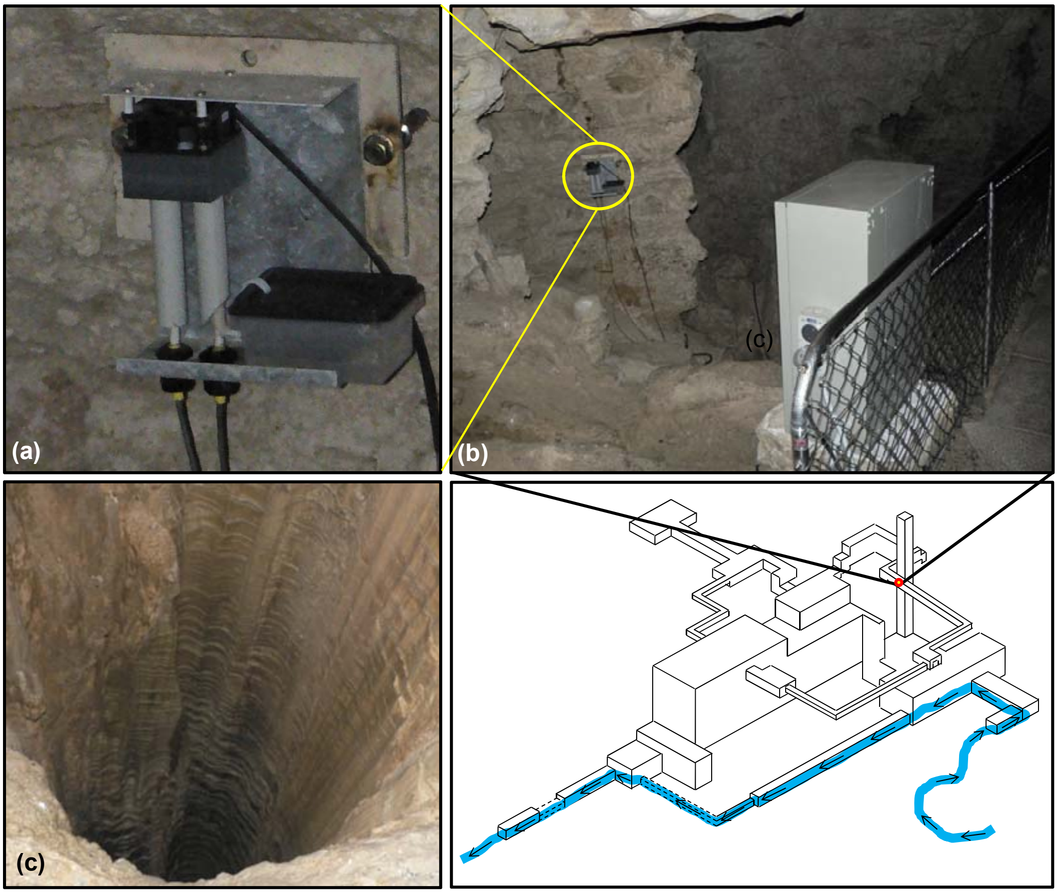

Figure 3.7. Temperature monitoring set-up used in the Glowworm and Ruakuri Caves. (a) The temperature probe set-up, and (b) the Master data logger at (c) the Tomo site.

Glowworm Cave measurements of Waitomo Stream temperature and stream P_{CO_2} are incomplete for 2008. Ruakuri Cave stream temperature and P_{CO_2} data for 2008 were even more incomplete than the Waitomo Stream data and, therefore, have not been presented. High water levels and associated sediment build-up subsequently burying sensors, as well as boats damaging the temperature probes, contributed to the gaps in the stream data.

3.5.3 Rainfall

Rainfall was measured using a Hydrological Services tipping bucket rain gauge (Figure 3.8). The specifications of the rain gauge are as follows: a diameter of 20 cm, a precision better than ± 2% (between 25 – 500 $mm.hr^{-1}$), and a 0.254 mm resolution (Campbell Scientific, 2008b). Measurements were recorded at 30 minute intervals at the Waitomo weather station, located next to the Waitomo Water Treatment Plant on Te Anga Road (Figure 3.8), and were available from 1998 – 2008.

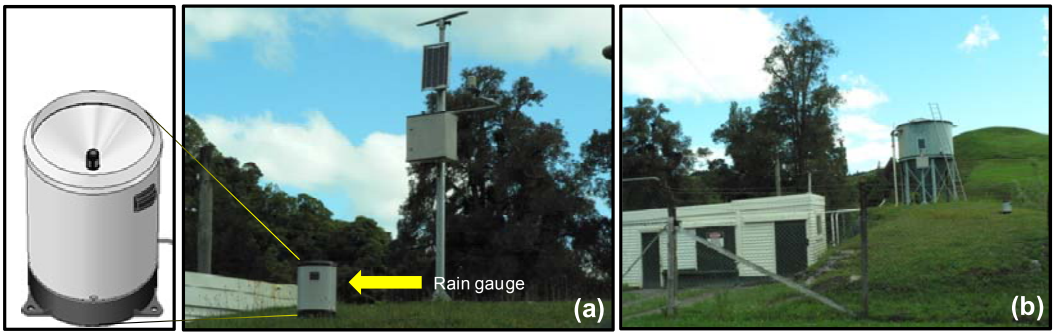

Figure 3.8. The Waitomo weather station where local rainfall and air temperature data are recorded. (a) Tipping bucket rain gauge, and (b) the weather station, located between the Glowworm and Ruakuri Caves.

3.5.4 Streamflow

Waitomo Stream flow data was measured by Environment Waikato. Streamflow data were available from 1998 – 2008. The data were obtained from an automated recorder located at the Ruakuri Cave exit, just upstream of the Okohua Stream and Waitomo Stream confluence (near the Ruakuri Reserve Car Park) (Figure 3.9). The Okohua Stream is a tributary of the Waitomo Stream.

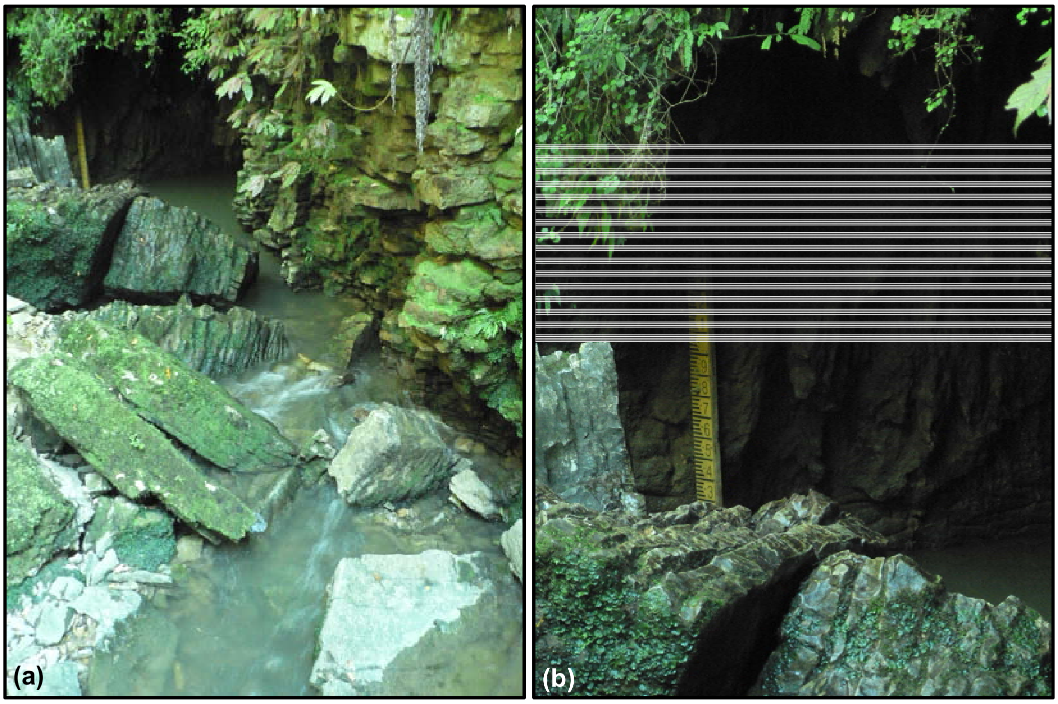

Figure 3.9. Waitomo streamflow recorder site. (a) The staff gauge, and (b) the location that the Okohua Stream exits the Ruakuri Cave, marking the site where streamflow data is recorded (data collected by Environment Waikato).

3.5.5 Stream P_{CO_2}

Stream P_{CO_2} was recorded at the Jetty in the Glowworm Cave (Waitomo Stream) (Figure 3.2 and Figure 3.10a) and at the Stream Site in Ruakuri Cave (Okohua Stream, a tributary of the Waitomo Stream) (Figure 3.3 and Figure 3.10b). Waitomo Stream P_{CO_2} data were obtained for the periods 9th July – 13th Septemper 2008 and 25th October 2008 – 10th January 2009. Okohua Stream (hereafter referred to as Ruakuri Stream) P_{CO_2} data were obtained for the period 14th October 2008 – 10th January 2009, however due to difficulties at the Ruakuri Stream site, I was not confident in the data and therefore the Ruakuri Stream P_{CO_2} data were not presented.

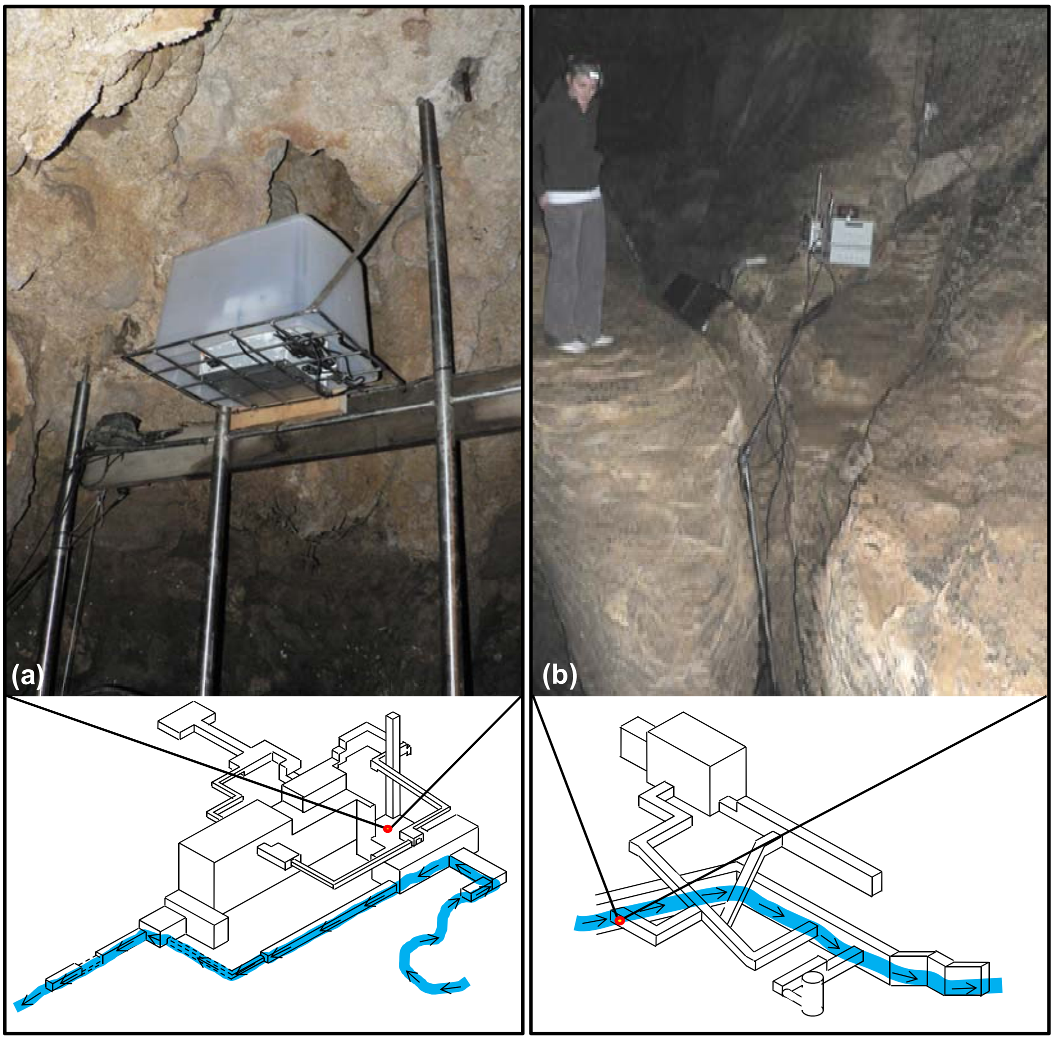

Figure 3.10. Location of stream CO_2 data collection sites in (a) the Glowworm Cave, and (b) Ruakuri (photo: Travis Cross).

Few studies have attempted to directly measure free CO_2 in streamwater. Typically, studies of CO_2 in water have used alkalinity measurements to calculate the amount of CO_2 present (e.g. Hoffer-French & Herman, 1989; Rebsdorf *et al*., 1991; Liu *et al*., 2004; 2007). However, as it is difficult to measure pH accurately, especially when the sample has a low ionic strength, calculating CO_2 from alkalinity measurements is inadequate for measuring free CO_2 (Neal & Thomas, 1985). The possibility of using a headspace analysis technique, using the equilibrium that is reached between CO_2 in air and water, was investigated by Hope *et al*. (1995). Following collection, the headspace gas was analysed using an IRGA, a simple and sensitive method for measuring dissolved free CO_2 in streamwater (Hope *et al.*, 1995). An adaption of the methods outlined by Hope *et al*. (1995) was used to acquire continuous measurements of stream CO_2.

A Vaisala GMP222 (0 – 5000 ppm) sensor (identical to those used to measure cave air PCO_2) was used to measure stream CO_2. The sensor was installed into a closed-path system (Figure 3.11).

The system also comprised an AquaOne pump (set on 'high') which pumped air through copper tubing down through the stream where the copper tubing emerged at the base of a stainless steel pipe. Air was bubbled up through the column of water within the stainless steel pipe, where CO_2 was exchanged with the water. The air was passed through a water trap (which prevented condensing water vapour from being passed into the sensor) and then to the Vaisala CO_2 IRGA. The air was then recycled back though the system as part of a closed loop. Measurements were taken once every minute and the average was recorded every 10 minutes using a CR10X data logger. Where stainless steel pipes or copper tubing were impractical to use, gas-impervious silicon tubing was used instead.

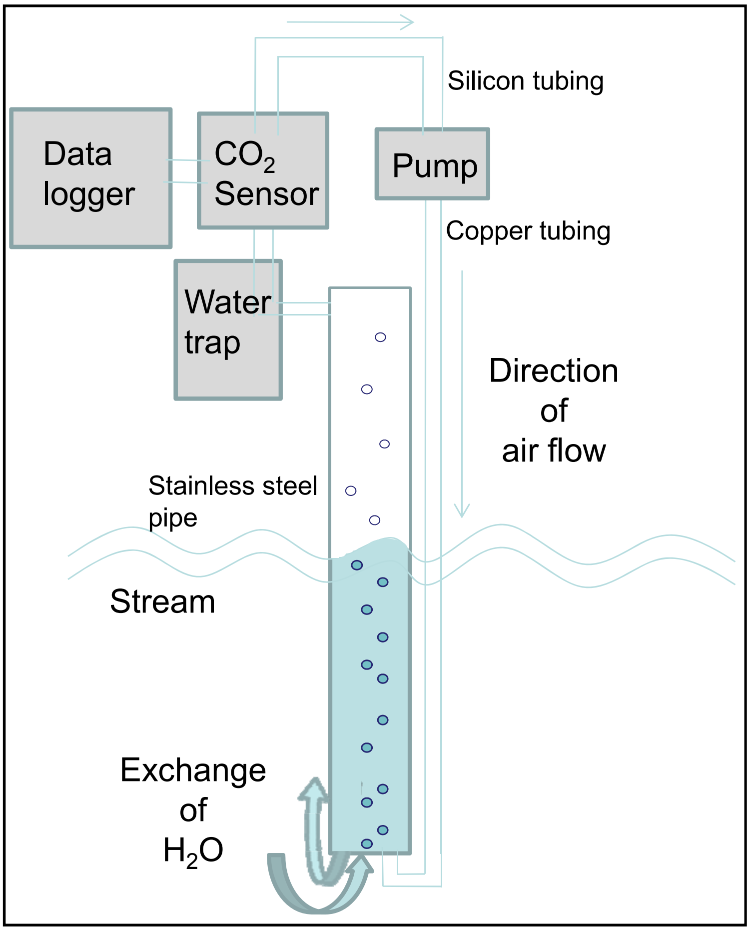

Figure 3.11. The closed path bubbling system used to measure stream CO_2.

3.5.6 Dripwater CO_2

The P_{CO_2} of dripwater from a straw located in the Blanket Chamber of the Glowworm Cave was measured using a closed path system (Figure 3.12). A length of silicon tubing was attached to an active straw at one end and to a rubber bung at the other end, which was used to seal a conical flask. The dripwater was collected in the conical flask and the dripwater reached equilibrium with the air in the headspace. Three additional holes were made in the rubber bung. Two of the holes were used to complete the closed path loop. For example, silicon and stainless steel tubing connected one of the holes in the rubber bung to the water trap, which was connected to the CO_2 sensor, which was then connected to the pump. The pump was then connected to the second hole in the rubber bung. The purpose of the pump was to continually circulate the air throughout the closed path system, so that frequent measurements of the dripwater P_{CO_2} (through the air-water equilibrium) were obtained. The third hole in the rubber bung acted as an overflow outlet, enabling the dripwater to siphon out periodically.

The CO_2 sensor used to measure the dripwater CO_2 was also a Vaisala GMP222 sensor, however this sensor covered a broader range (0 – 10000 ppm CO_2) than the sensors used to measure the stream and air CO_2 in other parts of the caves. The Vaisala GMP222 sensor operated with the same level of precision of ± [75 ppm CO_2 + 2% of the reading] and was designed with a similar built-in mechanism to cope with water vapour, as the other sensors used in this study. Thus, gaseous water molecules did not affect the CO_2 measurement. Dripwater P_{CO_2} measurements, using the 0 – 10000 ppm P_{CO_2} sensor, were obtained between 17^{th} November 2008 – 11^{th} January 2009. Preliminary dripwater P_{CO_2} measurements were recorded from the 12^{th} July – 18^{th} August, using a CO_2 sensor with a 0 – 5000 ppm range, however the data indicated that this range was too low to encapsulate the true P_{CO_2} of the dripwater (e.g. see Figure 6.1).

Figure 3.12. Closed path system used to measure dripwater CO_2 in the Blanket Chamber, Glowworm Cave.

3.5.7 Stream P_{CO_2} method validation

In an attempt to validate the closed path bubbling technique used to collect the stream and dripwater P_{CO_2} data, a trial was set up in the laboratory to determine two factors: (i) that water was being exchanged between the ‘stream’ and the column of water in the exchange tube, and (ii) to roughly determine how quickly changes in the P_{CO_2} were detected by the air bubbles in the exchange column (and thus the CO_2 sensor).

The set-up illustrated in Figure 3.11 was simulated in the laboratory (Figure 3.13a and b). A large (0.8 m (height) × 0.14 m (diameter)), clear Perspex column was partially filled with water (up to 0.6 m) to simulate the stream. Initially, a test was run to identify whether enough circulation was occurring for the water in the exchange column to interact and exchange with the water in the ‘stream’. The pump was turned on so that air was bubbling into the bottom of the exchange column and circulating through the closed path system. Several drops of rhodamine dye were added to the water. The dye dispersed through the water column. Upon reaching the bottom of the exchange tube, the turbulent action of the bubbles being released into the exchange column (from the closed path system) caused the dye to be sucked up into the exchange tube. This proved that exchange was taking place between the ‘stream’ and the exchange column.

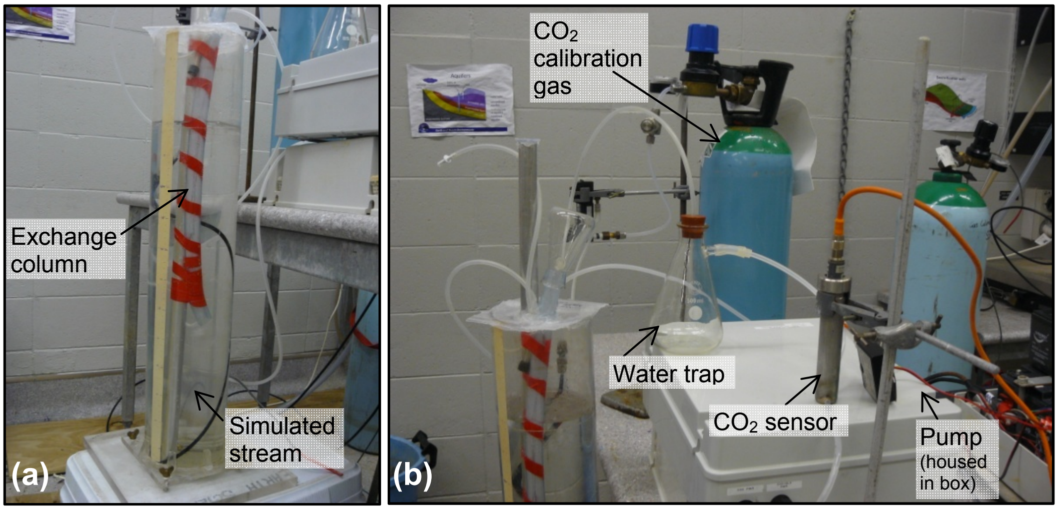

Figure 3.13. A simulation of the PCO_2 closed path bubbling system used to obtain continuous measurements of the PCO_2 of water. (a) The column of water used to simulate the stream and the exchange column, in which the air bubbles exchanged with the water, ultimately enabling the PCO_2 of the water to be measured. (b) The closed path bubbling system set-up with the water trap, CO_2 sensor and pump connected in series.

The top of the Perspex column was then sealed using a plastic sheet and silicon sealant to limit the loss of CO_2 to the atmosphere. CO_2 calibration gas (5000 ppm) was pumped into the water column (at a rate of 1 l.min^{-1}) at various times and for various durations over a two day period (7th – 8th October 2008). Although the PCO_2 of the 'stream' responded immediately to the 5000 ppm PCO_2 gas being pumped into the 'stream' water (reaching a maxima within 2 – 3 minutes), the PCO_2 of the 'stream' did not exceed 2000 ppm (Figure 3.14).

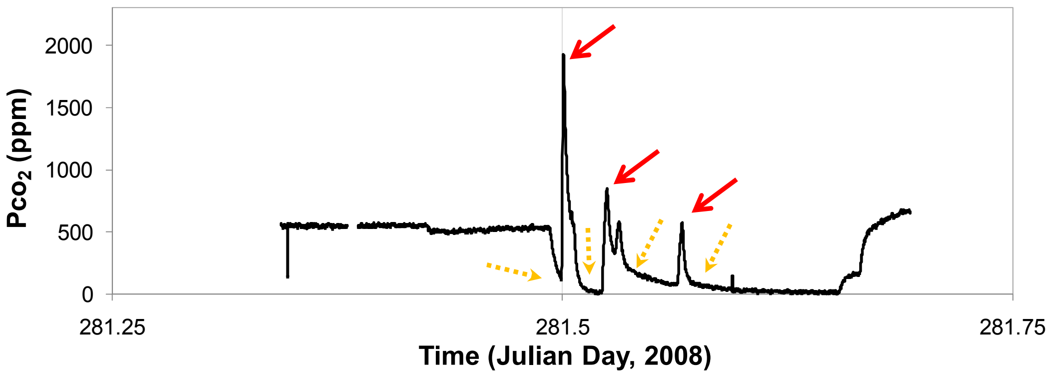

Figure 3.14. PCO_2 data for the simulated 'stream' during the lab trial on day 281 (7th October 2008). Red arrows indicate an immediate response in the PCO_2 of the water when CO_2 was pumped into the water. The yellow dotted arrows show decreases in the 'stream' PCO_2 associated with times when N_2 gas was pumped into the 'stream' instead of CO_2 gas.

A subsequent trial was carried out to test the possibility of the 'stream' acting as a sink for atmospheric CO_2. CO_2 with a concentration of 5000 ppm was pumped into the air space above the 'stream'. Within minutes, the 'stream' PCO_2 started to increase (Figure 3.15). The increase showed the potential for water bodies to act as a CO_2 sink, within poorly ventilated environments like caves.

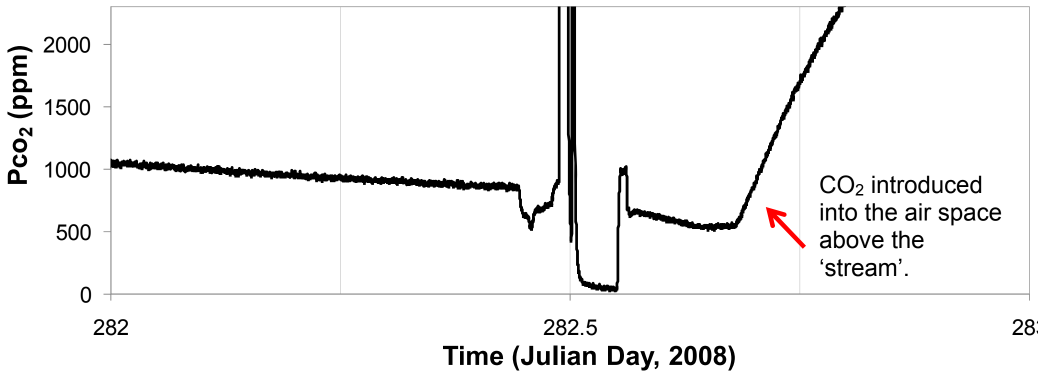

Figure 3.15. PCO_2 data for the simulated 'stream' during the lab trial on day 282 (8th October 2008). The red arrow indicates the period when the 'stream' acted as a CO_2 sink, absorbing CO_2 that had been pumped into the air space above the water.

3.6 Water chemistry programme

During 2008, dripwater and streamwater samples were collected and analysed to investigate the chemistry of karst waters. For raw data, refer to Appendix A.1.

3.6.1 Water sample collection

Streamwater samples were collected daily by the Glowworm Cave and Black Water Rafting guides within the Glowworm and Ruakuri Caves. Sampling from the Waitomo Stream occurred at the Jetty in the Grotto of the Glowworm Cave. The Ruakuri Stream samples were collected where the stream emerges from the Ruakuri Cave at the Ruakuri Reserve. Sampling at the Waitomo Stream began on the 21st of January 2008 (Julian day 21) and sampling at Ruakuri Stream commenced on the 3rd March 2008 (day 63). Samples were collected in 50 mL Falcon tubes and stored in a dark place at room temperature until it was possible collect them from the guides (typically once every three weeks). For a period of three months, samples were collected in triplicate on alternate days from each site.

Nine dripwater samples were collected from a stalactite in the Blanket Chamber (Glowworm Cave) between the 17th June and 5th September. Two series of dripwater samples were obtained using an autosampler which enabled a high frequency record of water samples to be obtained. The first series of autosampler water sampling occurred on the 9th and 10th of September (days 253 and 254). Sampling commenced at 9.00 a.m. and occurred at one hour intervals for 24 hours. The second autosampler run occurred from the 6th – 8th of October (days 280 – 282). The second autosampler run occurred at two hour intervals.

All samples were analysed for sodium (Na) and calcium (Ca). Streamwater samples were also analysed for bicarbonate (HCO_3^-) and ^{13}C isotope ($\delta^{13}C$).

3.6.2 Sample preparation and analysis

Each stream and dripwater sample was centrifuged for 10 minutes on 4000 rpm. Using an automatic pipette (10 mL), each streamwater sample was then divided into three separately labelled 15 mL Falcon tubes. The samples were subsequently prepared for ^{13}C isotope and inductively coupled plasma-mass spectrometer (ICP-MS) analysis. The sample for bicarbonate analysis required no further preparation. Dripwater samples were only analysed by ICP-MS, thus only a single 10 mL dripwater sample was pipetted into a 15 mL Falcon tube for further analysis.

3.6.2.1 Isotope

In order to prepare the isotope samples for analysis, barium hydroxide ($Ba(OH)_2$) was required for the precipitation of carbonates out of solution. A saturated solution of $Ba(OH)_2$ was made up and left to stand overnight to allow the precipitate to settle. One millilitre of $Ba(OH)_2$ was added to each sample and the samples were immediately sealed using screw top lids. Each sample was inverted and then left over night, during which time a precipitate usually formed. The following day, samples were centrifuged for 20 minutes at 4000 rpm. The supernatant was then discarded and the sample was rinsed with ~ 10 mL of distilled water before being centrifuged again. This process was repeated twice to ensure that the $Ba(OH)_2$ was displaced. Samples were then placed in a desiccator with silica gel and left for several days, until dry. Samples were then analysed for $\delta^{13}C$ by acidification with 100% H_3PO_4 using a CAPs automatic carbonate reactor attached to a GEO 20-20 isotope ratio mass spectrometer.

3.6.2.2 ICP-MS

The elemental composition of each water sample was analysed using the ICP-MS unit at the University of Waikato. A bulk sample of tap water was set aside at the start of the study and several tap water samples were analysed with each batch of karst water samples as a quality control measure. Each sample was acidified by adding 200 µL (0.2 mL) concentrated nitric acid (HNO_3). Following acidification, the samples were ready for ICP-MS analysis.

3.6.2.3 Bicarbonate

Samples used to obtain bicarbonate results did not need any prior preparation. Each sample was analysed to determine the bicarbonate concentration using a 702 SM Titrino automatic titrator. The pH was measured by the Titrino titrator and hydrochloric acid (HCL) was added dropwise to the sample until two specified end points (pH 5.5 and 3.5) were reached. A 'print-out' was obtained from the Titrino titrator. Using the values from the print-out, a calibration curve was calculated using Excel (see Appendix A.2).

3.7 Data analysis

3.7.1 Data quality and filtering

Initial plotting of the historic data showed that the data contained spikes (Figure 3.16). Typically, the spikes were obvious and consistent, occurring at either -6999 or -1750 ('hard' spikes). The 'hard' spikes depicted periods when the CO_2 sensor failed, or when the CO_2 level was outside the sensor's detection range, and thus were removed from the time series. Additional spikes also occurred at random within the dataset, where numbers appeared in the sequence that were obviously erroneous ('soft' spikes) (e.g. Table 3.1). The 'soft' spikes were also deleted from the dataset.

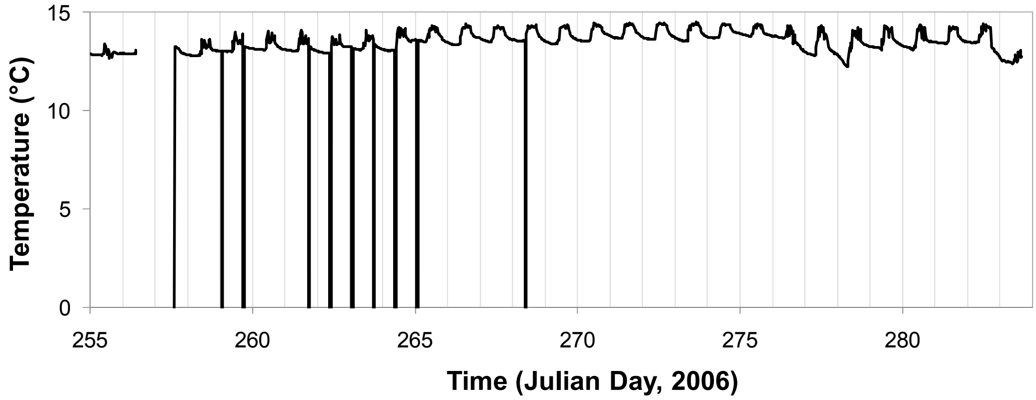

Figure 3.16. Air temperature in the Glowworm Cave for days 255 – 283 (12th September – 11th October 2006) showing 'hard' spikes in the data (vertical lines indicating a value of -6999).

Table 3.1. Air temperature data for the Glowworm Cave showing an example of a 'soft' spike (shaded area) in the raw data.

Year	Julian Day	Time	Banquet Chamber Air Temp.
2000	30	300	16.12
2000	30	330	16.12
2000	30	400	16.11
2000	30	430	1.982
2000	30	500	1.983
2000	30	530	15.87
2000	30	600	15.84
2000	30	630	15.83
2000	30	700	15.82
2000	30	730	15.83

3.7.2 Missing data

Gaps occurred frequently between 1998 and 2007 in all of the data measured. The duration of the missing data varied. At times, several measurement points were missing (e.g. on the 14th July 2000 two hours of air temperature data for the Banquet Chamber were missing between 12.30 p.m. and 2.30 p.m.), whilst on other occasions several days of data were missing (e.g. Glowworm Cave air P_{CO_2} data between 27th – 30th November 2006). Short-term periods of missing data (i.e. hours to days) within the Glowworm Cave microclimate record could be attributed to temporary sensor malfunctioning, manual downloads interrupting the recording of data, data loggers running out of storage space, thus over writing earlier data, or power outages affecting the recording of data.

At times throughout the 1998 – 2007 period, large portions of data were missing (e.g. three months, January – March, 2006, of Glowworm Cave air temperature and air P_{CO_2} data). This was likely the result of a failure to download the data loggers, or incorrect archiving of the data, resulting in the loss of record. Similarly, between 19th April 2006 – 9th May 2006 and 26th June 2006 – 15th July 2006 data was identical to the 2005 data for the same periods. Data for 2006 had been replaced by 2005 data, and thus resulting in a loss of 2006 data. This error is likely to be associated with the archival of the data.

Missing data in the Environment Waikato streamflow record (e.g. 20th February 2004 – 2nd March 2004) were associated with a major flood event. Gaps in the tourist number data (e.g. 21st June 2004; 7th – 13th December 2005) were the result of human error. The predominant cause for missing water chemistry data was human error, whereby the collection of a daily sample was forgotten. However, many of the gaps in the $\delta^{13}C$ record were associated with insufficient carbonate in the samples, resulting in a limited amount of precipitate forming, and thus no result could be obtained.

3.7.3 Data analysis methods

Temperature, P_{CO_2}, rainfall, streamflow and water chemistry data were predominantly plotted in time series in their highest frequency form. This was to enable trends and relationships to be identified over time between the various climatic factors. Microsoft Excel was primarily used for data analysis and plotting. Where duplicate water samples were available the mean of the data was plotted.

The analysis of seasonal and annual trends involved the plotting of daily means. In some instances (e.g. historic P_{CO_2} data), seven-day running means were calculated to eliminate noise from the data and clarify the trends.

4.0 Chapter Four: Pattern of tourists, temperature and P_{CO_2} in the Glowworm Cave

4.1 Introduction

Chapter Four presents a general description of the microclimate of the Glowworm Cave using ten years of historic data (1998 – 2007). An analysis of time series data was also carried out to establish seasonal trends in temperature, cave air P_{CO_2}, and tourist numbers. Glowworm Cave air temperature data throughout this thesis refers to recordings from the Banquet Chamber. The Banquet Chamber was the least influenced by external temperatures and thus was the most stable and reflective of the majority of the cave. The Banquet Chamber was also the closest site to the Cathedral, where the P_{CO_2} sensor was located. In addition, temperature was recorded at two other sites within the Glowworm Cave: at the Jetty, and near the top entrance of the Tomo; however external air temperature influences both of these sites.

Data from two contrasting months, January (mid-summer) and July (mid-winter), were chosen across a subset of the ten years, between 1998 and 2007, to highlight the difference in daily patterns of P_{CO_2}. The events of particular concern were when the cave air P_{CO_2} exceeded 2400 ppm, as the cave must be closed to tourists during these events. The high P_{CO_2} events, hereafter described as P_{CO_2} limit exceedences, were reported.

4.2 Patterns of temperature, P_{CO_2} and tourist numbers

4.2.1 Temperature

The mean air temperature between 1998 and 2007 in the Glowworm Cave was 14.73 °C. The mean external air temperature was 13.28 °C (Figure 4.1a and 4.1b). Cave air temperature was more consistent than external air temperature, with a mean annual range of 5.1 °C. External air temperature had a mean annual range of 27.5 °C.

The mean annual temperatures within the Glowworm Cave from 1998 – 2001 were somewhat (up to 1.5 °C) warmer than the years 2004 – 2007. The cooler result for 2006 compared to the other years was most likely due to the effect of missing data from January to March. Only 209 days of available data were available in 2006, compared to between 327 and 365 days of available data for the years 1999 to 2005 and 2007 (Refer to Appendix A.3). The year 1998 had 289 days of available cave temperature data.

4.2.2 Partial pressure of CO_2

Mean annual P_{CO_2} varied between 687 ppm (in 2005) and 1002 ppm (in 2007) (Figure 4.1c). Annual minimum P_{CO_2} values ranged between 195 ppm (in 2000) and 454 ppm (in 2007) over the ten years, whilst annual maximum P_{CO_2} was more variable (e.g. extending between 2525 ppm (1999) and 3946 ppm (2003)) (Figure 4.1c). As atmospheric CO_2 is approximately 380 ppm, it is likely that the minimum P_{CO_2} of 195 ppm, recorded in the Glowworm Cave in 2000, is erroneous and possibly the result of poor logger calibration.

4.2.3 Tourists

Between 1998 and 2007, the number of tourists visiting the Glowworm Cave varied from a minimum of 300 000 (1998) to a maximum of 400 000 (2002). (Figure 4.1d). Between 1998 and 2002, the number of tourists steadily increased, whilst after 2002 tourist numbers decreased.

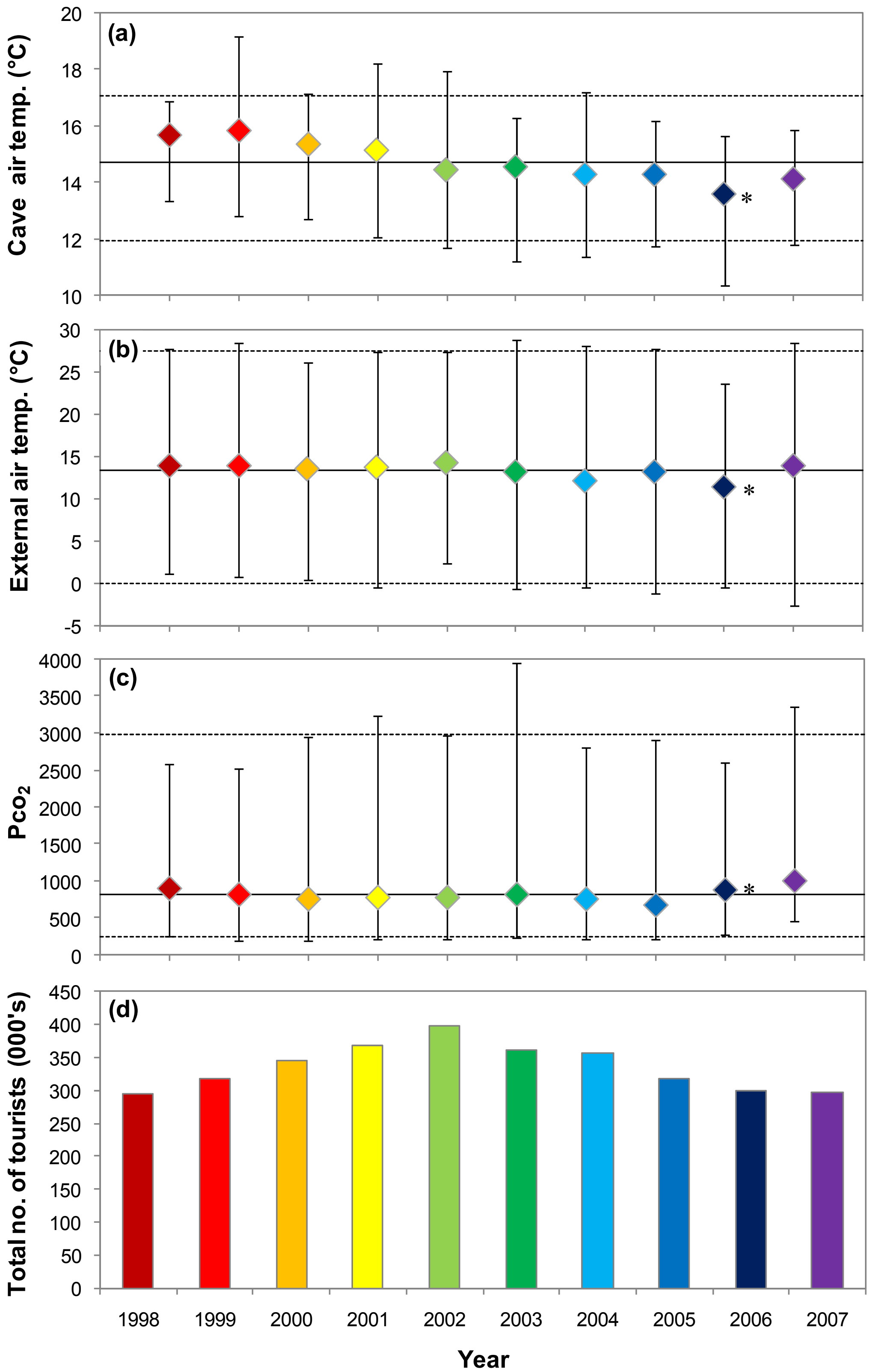

Figure 4.1. Temperatures, P_{CO_2} and tourist numbers for the Glowworm Cave, from 1998 – 2007. (a) Mean annual temperature in the Glowworm Cave, (b) mean annual air temperature outside the cave, (c) mean daily cave air P_{CO_2}, (d) annual total tourist numbers. Error bars indicate annual maxima and minima. The solid line and respective dotted lines in each plot represent the mean, mean maxima and mean minima across the ten years (1998 – 2007). *Mean in 2006 is influenced by missing data from January – March.

4.3 Variations in temperature, cave air P_{CO_2} and tourists

There was a distinct seasonal pattern in the temperature, cave air P_{CO_2}, and daily number of visitors in the Glowworm Cave (Figure 4.2). Generally, the P_{CO_2}, internal and external temperatures, and number of tourists per day were highest during the “summer” months of November through to April and lowest in the “winter” months of May to October (Figure 4.2).

The mean summer temperature inside the cave over the ten year period (1998 – 2007) was 15.50 °C and outside the cave was 16.33 °C. Comparatively, the mean winter temperature inside the cave was 14.06 °C and outside the cave was 10.68 °C. There were also, on average, 450 more visitors per day to the Glowworm Cave during the summer compared to the winter. The daily mean P_{CO_2} was higher in summer (882 ppm) than in winter (761 ppm). The daily maximum P_{CO_2} was higher during the summer (1476 ppm) than the winter (1219 ppm).

The CO_2 levels in the Glowworm Cave peaked twice during the year: once around day 100 (mid-April), and again on day 270 (at the end of September/beginning of October) (Figure 4.2a). Whilst on both occasions the number of tourists markedly increased, there were fewer tourists during these periods compared to January and December (Figure 4.2b). If P_{CO_2} was influenced by tourists alone, then cave air CO_2 would have peaked when tourist numbers were highest, however, cave air CO_2 was, at times, higher than usual in the presence of very little or even in the absence of tourists in the caves.

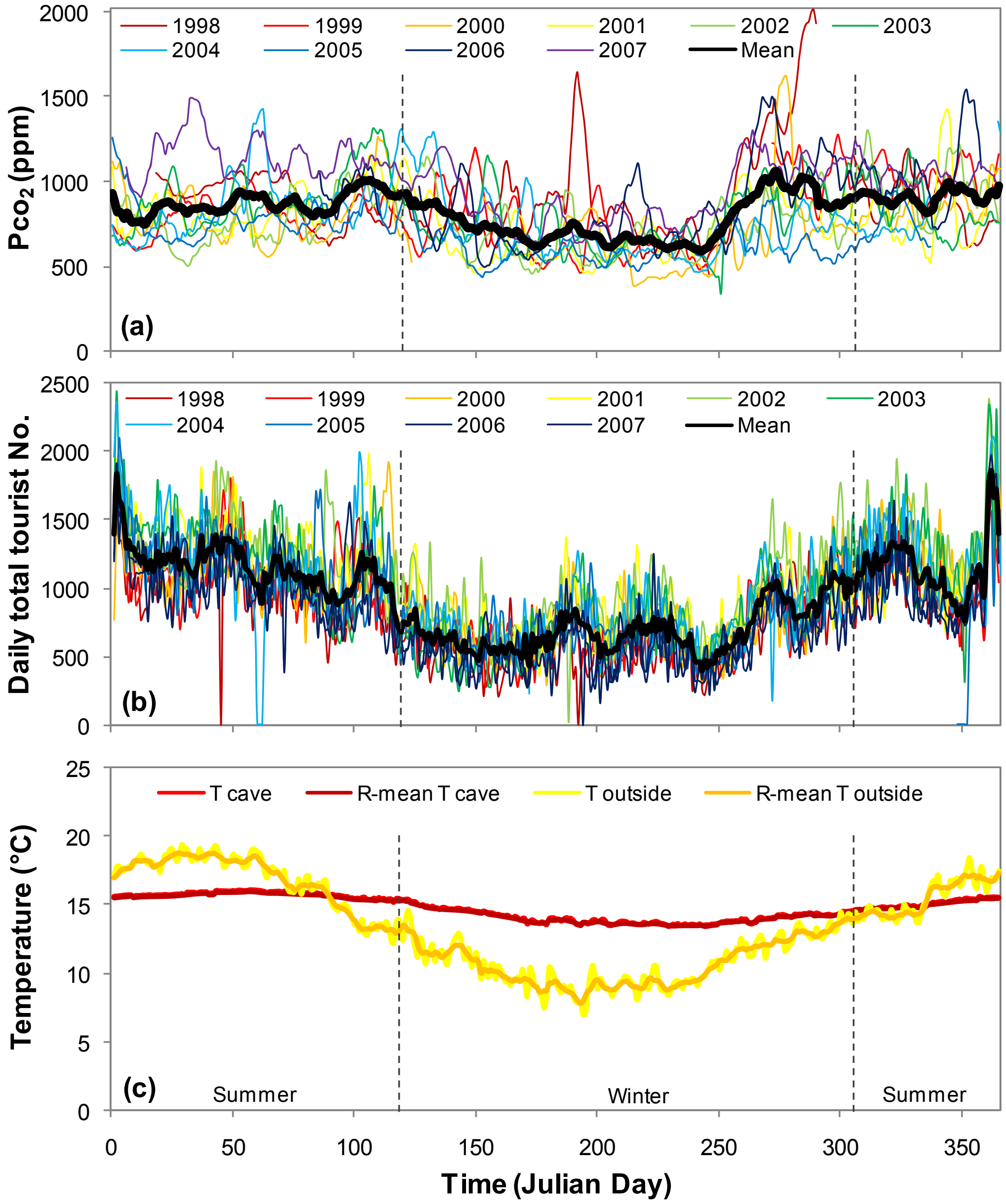

Figure 4.2. Annual variation of P_{CO_2}, tourist numbers and temperature for the Glowworm Cave from 1998 – 2007. (a) Seven-day running means of P_{CO_2} for each year between 1998 – 2007 (coloured lines), with the mean across the ten years plotted in black. (b) Daily total tourist numbers for the years 1998 – 2007 (coloured lines) and the ten-year mean (black line). (c) Daily mean internal and external temperatures for the Glowworm Cave and a seven-day running mean of the daily temperatures. The dashed vertical lines at day 121 (1st May) and 305 (1st November) indicate the beginning of the "winter" and "summer" periods, used throughout this thesis.

When the April and September/October P_{CO_2} peaks (Figure 4.2a) were compared to the temperature data (Figure 4.2c), it was apparent that the peaks coincided with times when mean daily outside temperatures had decreased, intersecting the more stable mean daily temperatures within the cave. At the point of intersection between the mean daily cave and external air temperatures (i.e. spring and autumn) (Figure 4.2c), the temperature gradient (difference between cave air and outside air temperatures) is zero. The temperature gradient between the Glowworm Cave air and the outside air can be used as a substitute for density differences between internal and external air masses (de Freitas *et al*., 1982). There are a number of factors that contribute to air flow within caves (e.g. number of entrances, elevation differences between entrances, entrainment of air by flowing water, and the frequency and duration of cave entrance/air flow route restrictions (de Freitas *et al*., 1982)). However, thermally induced disequilibrium in air density is a key factor in the amount of air exchange that occurs. As air flow is strongly dependent on temperature, seasonal differences in the direction of airflow are common (Figure 4.3). Therefore, when the temperature gradient is low, air exchange is limited, and thus natural flushing of the Glowworm Cave is restricted. This seasonal transition is, therefore, likely to contribute to the increase in CO_2 within the Glowworm Cave in autumn and late spring.

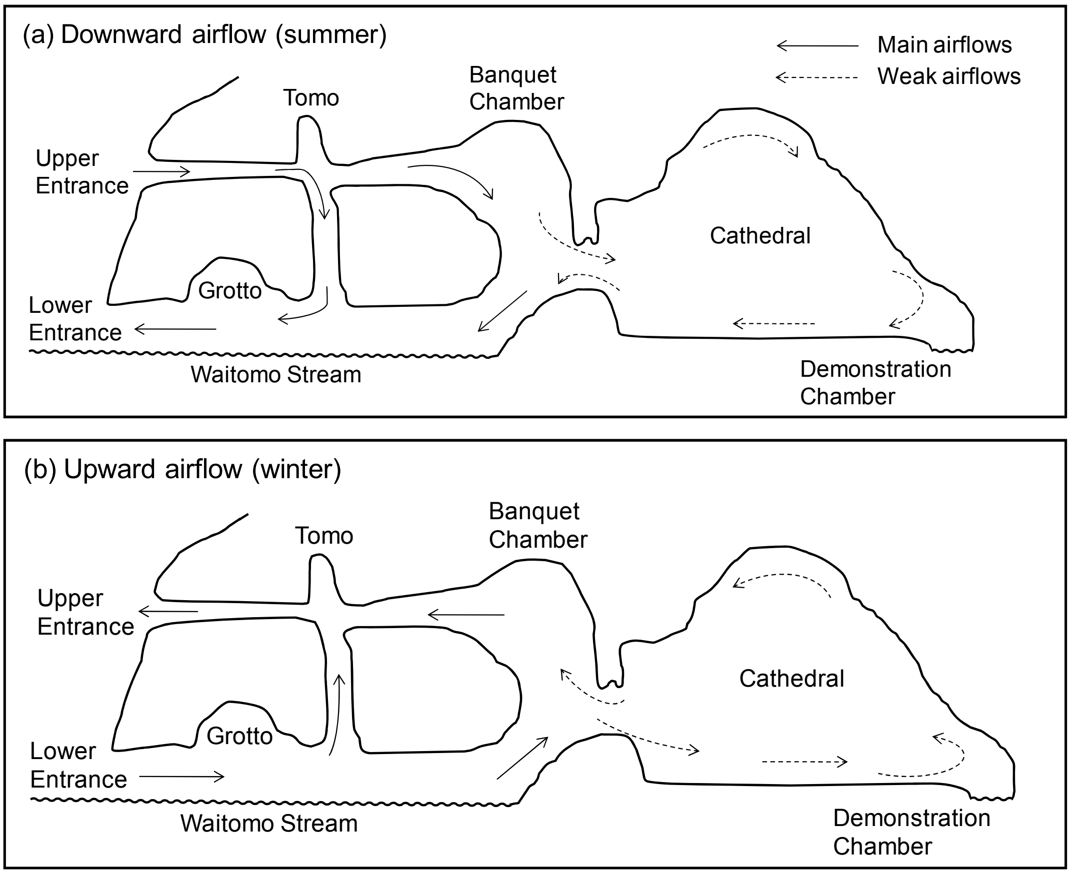

Figure 4.3. Cross-sectional view of the airflow patterns in the Glowworm Cave showing: (a) downward airflow, and (b) upward airflow (adapted from de Freitas *et al*., 1982).

Monthly analyses indicated that during the last ten years, January was the busiest month, with 1280 tourists visiting the Glowworm Cave on average each day (Figure 4.4a). This was more than double that of June, the least busy month, where the daily mean number of tourists was 570. The partial pressure of carbon dioxide in the Glowworm Cave was lowest during August and highest during April (Figure 4.4b). Mean daily rainfall for the Waitomo region between 1998 and 2007 was lowest during March and April, with approximately 3.5 $mm.day^{-1}$. Rainfall peaked during July, with a mean daily total of 6.95 $mm.day^{-1}$ (Figure 4.4c). Mean temperature within the Glowworm Cave was highest in late summer (March – April) at about 16 °C, and lowest during the winter (July – August), averaging 13.8 °C. Mean external air temperatures were much more variable than the cave temperatures, peaking during February (18 °C) and decreasing to about 9 °C in July (Figure 4.4d). The mean temperature gradient between the Glowworm cave and outside air was highest in the winter (July) and lowest in spring – early summer (October – November).

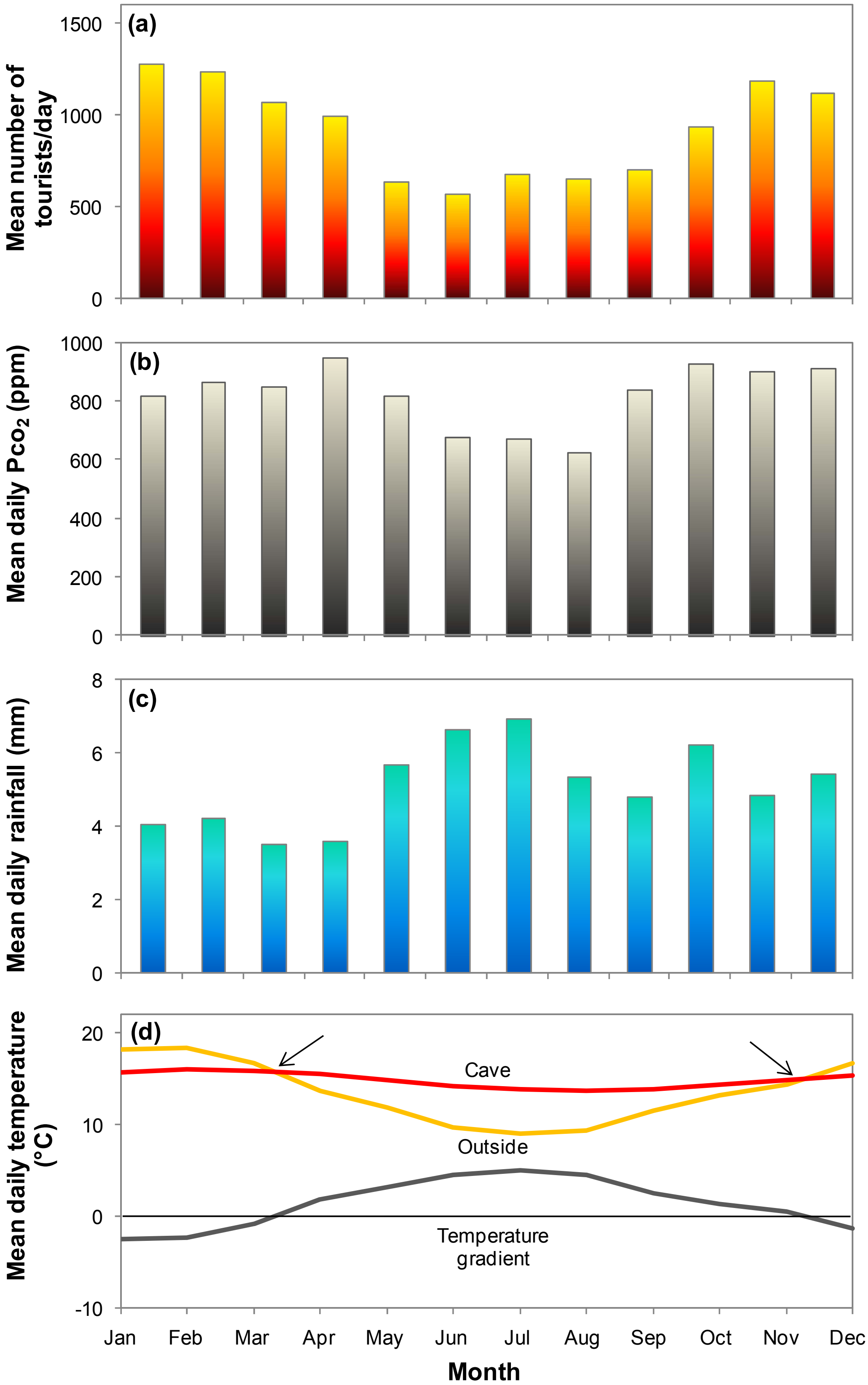

Figure 4.4. Mean monthly tourist numbers, $P\text{CO}_2$ and cave and external air temperatures for the Glowworm Cave, and mean monthly rainfall for Waitomo, for 1998 – 2007. (a) Mean number of tourists per day, (b) mean daily $P\text{CO}_2$, (c) mean rainfall per day, and (d) mean daily temperature and absolute daily temperature gradient between the Glowworm Cave and outside air. Arrows in (d) indicate the point of intersection between the mean daily temperatures within and outside the Glowworm Cave, where the theoretical temperature gradient is zero.

4.4 Seasonal comparisons of the diurnal cycle

Cave air temperature was very stable, with a mean of 15.5 °C during the summer and 14.06 °C during the winter. The mean daily range in temperature recorded in the Banquet Chamber was 0.80 °C, calculated from daily ranges for five randomly selected years (1998, 1999, 2000, 2003 and 2005). The range for the summer months was 0.58 °C, while in winter, the range was 1.03 °C. Outside temperatures fluctuated diurnally, with maximum temperatures occurring during the day, typically around mid-afternoon, and daily minimum temperatures occurring just before dawn (Figure 4.5).

A comparison of January and July data across five of the ten years between 1998 and 2007 highlighted the difference in daily patterns of P_{CO_2} between the summer and winter. There was a strong diurnal pattern in cave air P_{CO_2} (Figure 4.5). In the summer (represented by January), maximum P_{CO_2} typically occurred during the day, between 12.30 p.m. and 1.00 p.m., while minima occurred around 8.00 a.m. This emphasised the presence of tourists in the cave during the day, with the morning being the busiest time (Figure 4.5). The Glowworm Cave attracts the most visitors during the summer months and this is reflected in the cave air P_{CO_2} concentrations, where the highest measurements were recorded in the summer. The daily maximum P_{CO_2} was approximately 100 ppm higher in January than July. Similarly, the daily minimum P_{CO_2} was roughly 150 ppm higher in January than July (Figure 4.5). There was a slight increase in P_{CO_2} between 8.00 p.m. and 9.00 p.m. in January (Figure 4.5a). It is likely that this is associated with a Glowworm Cave tour occurring at 8.00 p.m. between 26th December and 28th February each year, to accommodate tourist demand during the peak season.

The diurnal cycle of external temperature (Figure 4.5) showed a peak during the day, with the coolest temperatures occurring at night. The cave air temperature was stable, with little diurnal variation for both summer and winter.

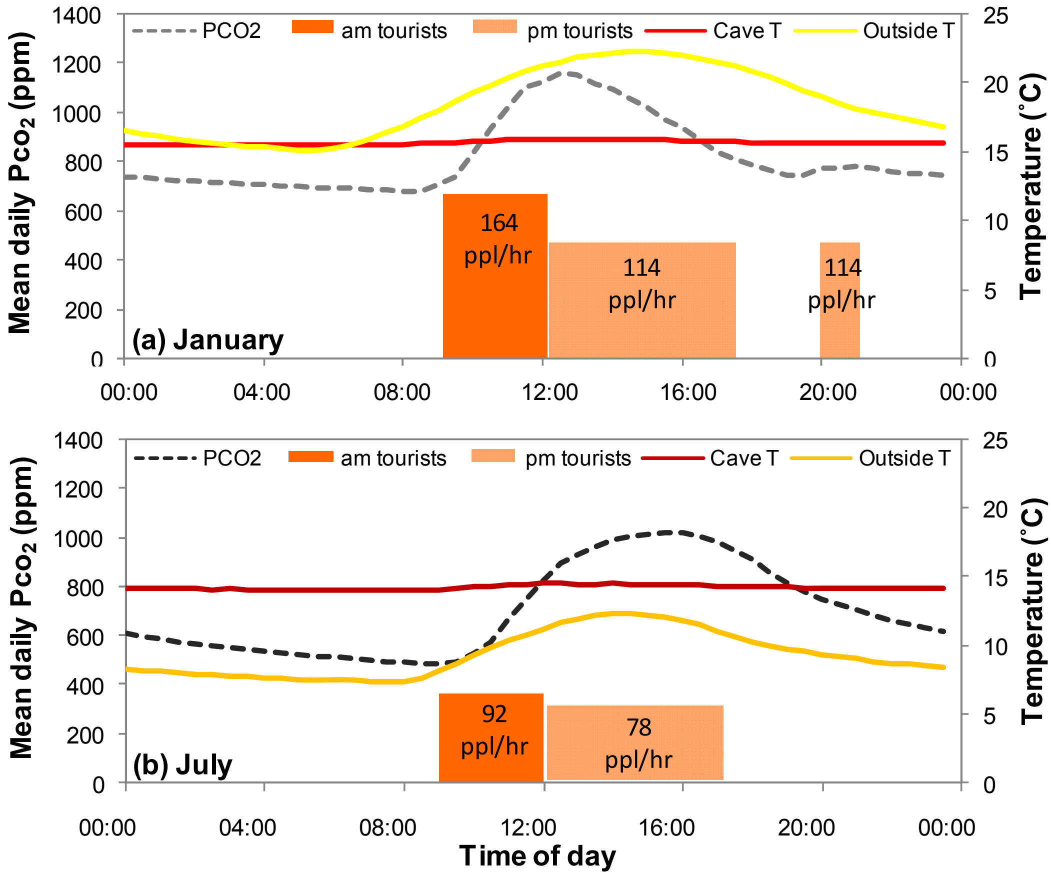

Figure 4.5. Average daily cycle of P_{CO_2}, cave and outside air temperatures, and tourist numbers for (a) January and (b) July. Data presented are a mean of five randomly selected years (1998, 1999, 2000, 2003, 2005). Summer = 9.5 hours of tours; (9.00 a.m. – 5.30 p.m., and 8.00 p.m. – 9.00 p.m.) Winter = 8 hours (9.00 a.m. – 5.00 p.m.).

The diurnal pattern of the temperature gradient differed between January and July. In January (summer), the average temperature gradient was low during the night (approximately 2 °C) and at a maximum during mid-afternoon. In July (winter), the temperature gradient was reversed, with the minimum occurring during mid-afternoon and the maximum at approximately 8.00 a.m. (Figure 4.6). As the midday P_{CO_2} maxima are unavoidably high in summer (due to daily tours and visitors making the most of summer holidays), it is appropriate that the mean temperature gradient also peaked at mid-afternoon during summer. The stronger temperature gradient and, therefore, the potential for flushing, may explain why the P_{CO_2} in January typically falls more rapidly than during July, which normally shows a more gradual decline following the daily closure of the Glowworm Cave (Figure 4.5 and Figure 4.7).

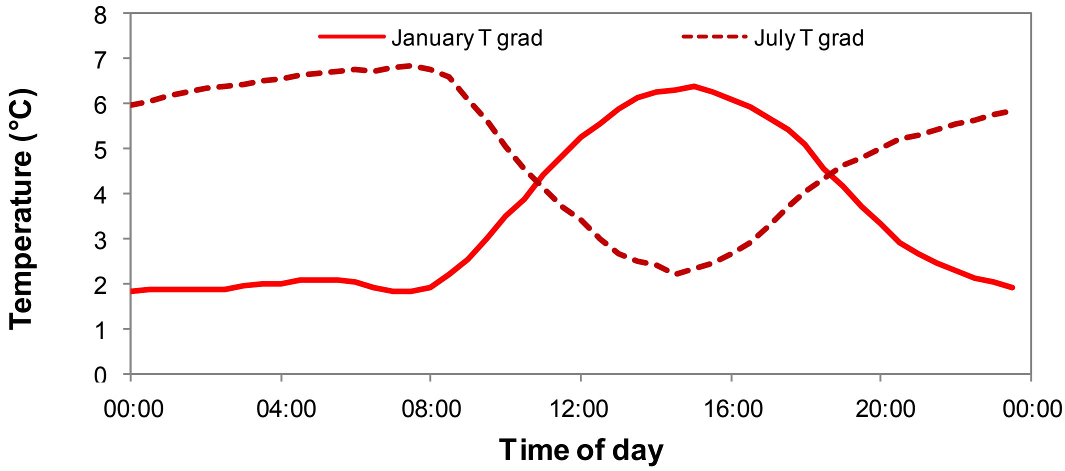

Figure 4.6. Absolute temperature gradient between the Glowworm Cave air and external air in January and July. (Data presented is a mean of five randomly selected years (1998, 1999, 2000, 2003, 2005)).

Figure 4.7 shows the pattern of P_{CO_2} during January and July. January (Figure 4.7a) had more pronounced peaks compared to July (Figure 4.7b). In January, there was also evidence of a decrease in the rate of P_{CO_2} decline in the evening, (e.g. in the earlier part of the month, Julian day 4 – 6) and often even an increase in P_{CO_2} at night, with a secondary peak occurring around midnight (e.g. Julian day 13 through to the end of the month). It is possible that the evening tour (which occurs from 8.00 p.m. – 9.00 p.m. during January and February) is responsible for the secondary P_{CO_2} peak that is evident during January (Figure 4.7a, also Figure 4.5). July showed smooth daily P_{CO_2} increases and decreases with no secondary peaks at night. There was also a difference in the mean daily minimum P_{CO_2} between January and July. January had a higher mean daily minimum P_{CO_2} (517 ppm) than July (449 ppm). Similarly, there was a difference in the mean daily maximums between January and July, with January having a higher mean daily maximum of 1353 ppm, than July (1134 ppm) (Figure 4.7).

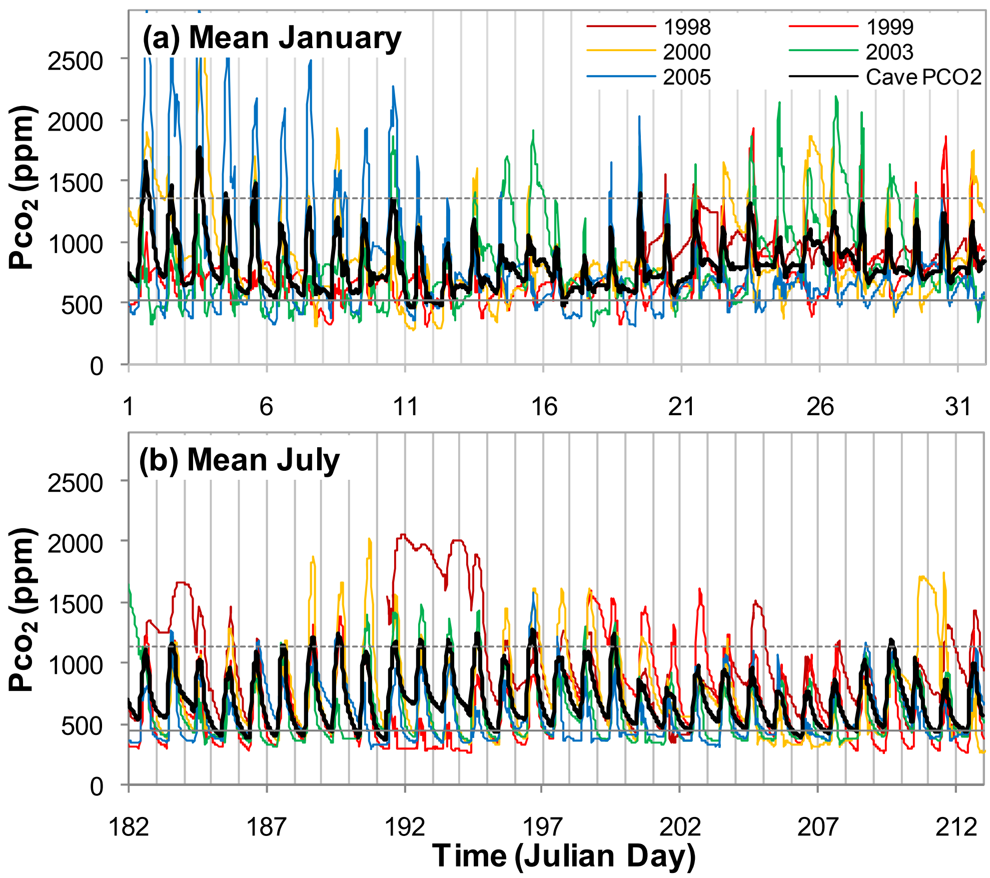

Figure 4.7. Glowworm Cave PCO_2 for a summer (January) and winter (July) month between 1998 and 2007. Half hourly averaged data for five randomly selected years: 1998, 1999, 2000, 2003 and 2005 (coloured lines); and the mean across the five randomly selected years (black line), are presented. (a) January and (b) July.

4.5 Daily PCO_2 limit exceedences

Whilst the typical PCO_2 pattern is strongly diurnal with a day time peak approximately 500 ppm higher than the daily minimum, there were several occasions each year when the PCO_2 pattern differed from the norm.

As the Glowworm Cave is operated under a licence that specifies PCO_2 must not exceed 2400 ppm, it is when the CO_2 goes above this level that it becomes problematic for the cave operators. Whilst anomalies below the 2400 ppm level may be interesting, to reduce the data processing requirements, only events where the PCO_2 exceeded 2400 ppm were investigated. Between 1998 and 2007, the PCO_2 of the cave air exceeded the 2400 ppm limit 48 times (Table 4.1), resulting in the temporary closure of the Glowworm Cave. Given that the current admission charge is $35 per adult to tour the Glowworm Cave, and that on average 920 tourists visit the Glowworm Cave each day, if the cave is closed for just one day the total revenue directly lost, as a result of admission cancellations, would be $32 000. If this is multiplied by 4.8 (the mean number of times the cave air exceeds 2400 ppm CO_2 every year), the revenue lost by Tourism Holdings Ltd. due to high CO_2 would be just under $155 000 per year. It is unlikely that on every occasion when the CO_2 exceeds 2400 ppm entry would be prohibited for the entire day, however, even closure of the cave for part of a day comes at a substantial cost. The effects of such a loss could potentially become permanent as operators of organised tours may source alternative attractions to avoid the chance of disappointing tourists when high CO_2 levels prevent entry into the Glowworm Cave.

Table 4.1. Events where Glowworm Cave PCO_2 exceeded 2400 ppm, and associated cave conditions between 1998 and 2007.

Event	Date	Time[1]	Event Duration (h)	Max. CO_2 (ppm)	Mean Discharge[2] ($m^3.s^{-1}$)	No. of Tourists	Mean T cave[3] (°C)	Mean T out[4] (°C)	Mean T grad.[5]
1	27/09/98	15:00	1	2428	3.62	1097	15.67	16.13	-0.46
2	03/10/98	15:00	3	2551	1.38	948	15.49	16.39	-0.90
3	10/10/98	12:00	2	2591	4.08	913	15.73	16.38	-0.65
4	14/10/98	15:30	6	2549	5.69	1271	15.98	17.99	2.71
5	17/02/99	13:00	0.5	2438	0.41	1455	16.66	23.22	-6.56
6	11/11/99	14:00	4	2525	6.13	1228	15.94	17.88	-1.94
7	03/01/00	14:00	5	2689	1.01	1684	16.08	16.37	-0.21
8	21/04/00	14:00	10	2802	0.69	1704	16.42	16.16	0.26
9	22/04/00	0:00	6.5	2864	0.62	1699	16.44	16.54	-0.11
10	02/10/00	14:00	10	2841	30.11	801	15.26	14.24	1.02
11	03/10/00	0:00	23	2945	14.30	663	15.31	12.05	3.26
12	04/10/00	0:00	2.5	2782	7.81	804	15.09	11.52	3.56
13	29/12/00	13:30	10.5	2954	9.28	1287	16.33	18.27	-1.94
14	30/12/00	0:00	4.5	2628	5.13	1822	16.20	16.32	-0.12
15	02/01/01	17:00	0.5	2439	2.44	1937	16.26	16.28	-0.02
16	23/02/01	13:00	3	3250	4.96	1204	17.68	16.99	0.70
17	07/12/01	20:30	3.5	3043	8.20	773	15.17	18.22	-3.04
18	08/12/01	0:00	10.5	2846	7.09	1195	15.19	17.27	-2.09
19	09/12/01	15:30	8.5	2586	11.13	677	15.09	18.68	-3.59
20	10/12/01	12:30	3	2815	6.39	952	15.43	18.49	-3.06
21	28/12/01	14:30	1.5	2606	1.36	1919	15.43	18.84	-3.41
22	18/03/02	14:00	3.5	2754	1.70	1259	15.90	16.92	-1.02
23	29/09/02	15:30	6.5	2718	4.04	1650	14.41	17.02	-2.61
24	09/11/02	17:30	0.5	2410	1.69	1425	14.69	17.57	-2.88
25	11/11/02	16:00	2	2470	2.00	1365	14.77	16.06	-1.29
26	13/12/02	20:30	0.5	2403	1.81	1131	15.12	14.50	0.62
27	26/12/02	14:30	3.5	2982	3.03	1999	15.54	16.09	-0.55
28	27/12/02	14:00	6.5	2982	1.51	2387	15.29	17.21	-1.77
29	23/11/03	12:00	8.5	3946	4.52	1831	15.26	14.68	0.58
30	29/12/03	12:30	0.5	2424	3.30	1072	15.78	14.51	1.27
31	15/11/04	13:30	1.5	2809	3.60	1536	15.38	14.26	1.11
32	01/01/05	15:00	4.5	2893	3.74	1588	15.19	15.90	-0.71
33	02/01/05	13:00	2.5	2844	3.02	1588	15.64	18.14	-2.49
34	03/01/05	12:30	3.5	2911	2.45	2086	15.43	19.03	-3.60
35	04/01/05	13:00	3.5	2799	2.10	1940	15.24	18.64	-3.40
36	07/01/05	13:30	1	2492	4.15	1585	15.36	17.73	-2.37
37	18/12/06	13:30	4.5	2603	0.95	1017	14.53	17.94	-3.40
38	20/12/06	15:30	5.5	2484	1.27	1173	14.46	14.16	0.29
39	21/01/07	13:00	0.5	2401	0.54	1406	14.97	21.19	-6.22
40	04/02/07	15:00	1	2429	0.45	1122	15.08	18.19	-3.12
41	05/02/07	11:00	5	2567	0.48	936	15.11	21.32	-6.21
42	11/02/07	12:30	1.5	2506	0.41	1253	15.40	23.43	-8.03
43	12/02/07	11:30	2	2582	0.41	1014	15.22	18.29	-3.07
44	08/04/07	14:00	0.5	2488	0.41	1624	15.36	19.61	-4.25
45	29/09/07	16:00	2	2517	1.13	1002	14.16	15.32	-1.17
46	30/09/07	13:30	2.5	2709	1.09	1181	14.35	16.56	-2.22
47	05/11/07	15:30	6.5	2658	6.30	775	14.38	14.27	0.11
48	07/11/07	12:30	1.5	3358	2.41	1281	14.80	17.60	-2.80

[1] Time of first instance that PCO_2 exceeded 2400 ppm on the given day.
[2] Mean discharge for the duration of the event.
[3,4,5] Mean temperature in the cave, temperature outside, and temperature gradient for the duration of the event.

4.5.1 Cave conditions surrounding the PCO_2 limit exceedences

It is well known that human respiration is the predominant cause of CO_2 elevations within tourist caves (Dragovich & Grose, 1990; Pulido-Bosch *et al.*, 1997). However, this study did not find a strong relationship between tourist numbers and maximum PCO_2 (R^2= 0.22) (Figure 4.8). Few studies have looked at natural sources of CO_2 within tourist caves. If tourists were the sole CO_2 source in caves, then it is expected that events of anomalous CO_2 would be reflected by unusual patterns in cave visitation. To investigate this further, tourist numbers during the PCO_2 limit exceedences in the Glowworm Cave between, 1998 and 2007, were investigated.

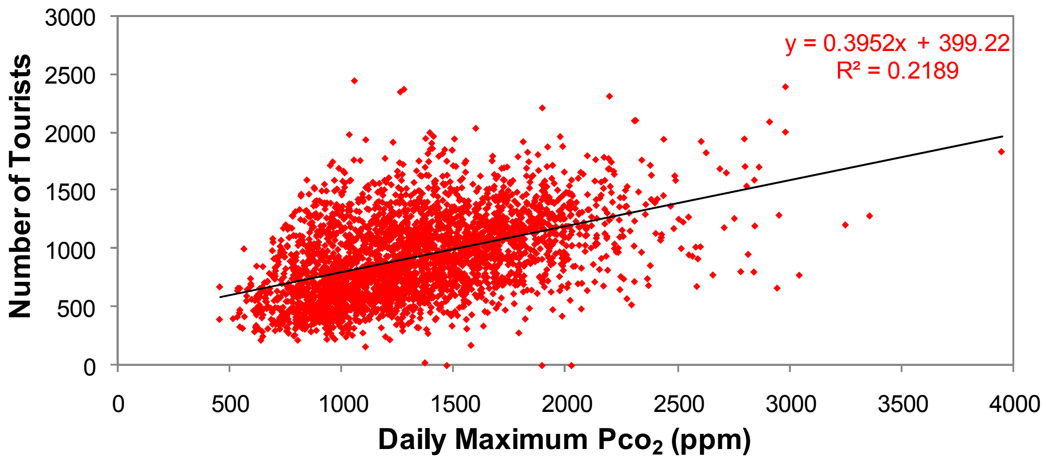

Figure 4.8. The correlation between daily maximum PCO_2 and the total daily number of tourists to visit the Glowworm Cave between 1998 and 2007.

Thirty eight of the PCO_2 limit exceedences occurred during the summer, the busiest season for the Glowworm Cave, and ten events occurred during the winter. During 32 of the PCO_2 limit exceedences, the number of tourists visiting the caves was less than 1500 and tourist numbers were less than 1000 during ten of PCO_2 limit exceedences. Of the 48 PCO_2 limit exceedences which occurred in the Glowworm Cave between 1998 and 2007, the maximum PCO_2 was 3946 ppm (which occurred in November 2003), whilst the mean maximum PCO_2 was 2715 ppm.

Of the winter events, one event had fewer tourists than the ten year winter mean of 696 people (with 677 visitors). Of the summer PCO_2 limit exceedences, ten events had fewer tourists than the ten year summer average of 1147 people. Such P_{CO_2} limit exceedences show that there must be other factors (i.e. not just tourists) contributing to cave air P_{CO_2}.

4.5.2 Summary of three P_{CO_2} limit exceedences

Whilst this Chapter has examined all of the P_{CO_2} limit exceedences that occurred between 1998 and 2007, 'anomalous' P_{CO_2} events (a term used throughout the remainder of this thesis) refer to occasions when the P_{CO_2} increased during the night or when night time P_{CO_2} was higher than the base level, as well as events when P_{CO_2} was higher than normal during the day. Three examples of P_{CO_2} limit exceedences that occurred between 1998 and 2007, which also featured an anomalous pattern of cave air P_{CO_2}, have been presented along with the number of tourists to visit the cave on each day (Figure 4.9). Each example provided a few days of the 'normal' pattern of CO_2 within the Glowworm Cave prior to the P_{CO_2} limit exceedence, followed by a return to the normal CO_2 pattern. In all three examples, the CO_2 maintained a day time peak with the exception of day 37 (6th February 2007) in Figure 4.9c, when the daily CO_2 maxima occurred just before midnight. In all three examples, CO_2 levels did not recover to base level during the night (Figure 4.9).

On days 270 – 273 of 2000 (26th – 29th September; Figure 4.9a), the daily maximum P_{CO_2} ranged between 900 and 1300 ppm, with tourist numbers of between 800 and 1000. Every night, the base level returned to approximately 400 ppm reflecting the typical diurnal trend in cave air P_{CO_2}. On day 274 (30th September 2000), CO_2 within the Glowworm Cave peaked at 2000 ppm with less than 1000 visitors. During the night of day 274 to day 275, CO_2 decreased to a minimum of 1500 ppm, over 1000 ppm higher than the typical base level for winter months within the Glowworm Cave. The two following days and nights showed a similar pattern, with day time CO_2 continuing to rise over and above the elevated night time CO_2, reaching higher maximums each day, despite the tourist numbers being well below 1000. In the early hours of day 278 (4th October 2000), CO_2 rapidly decreased to approximately 900 ppm before rising again in response to the daily activity of tours. From day 279 the pattern of CO_2 within the

Glowworm Cave largely returned to normal, although day 281 – 283 also showed higher night time CO_2 compared to the 'normal base level' (of approximately 350 – 400 ppm). The elevated night time CO_2 observed from days 281 – 283, however, was less than the night time CO_2 observed from days 274 – 277.

In the second P_{CO_2} limit exceedence, a sharp increase in P_{CO_2} occurred on day 341. Compared to the previous day, there were 250 fewer people in the Glowworm Cave on day 341, yet the maximum CO_2 increased by more than 2300 ppm (Figure 4.9b). The third example, Figure 4.9c, followed much the same pattern with base level CO_2 not being reached during the night following day 35 (4th February 2007), and day 42 (11th February 2007). Figure 4.9 indicated that CO_2 in the Glowworm Cave is not exclusively driven by tourists.

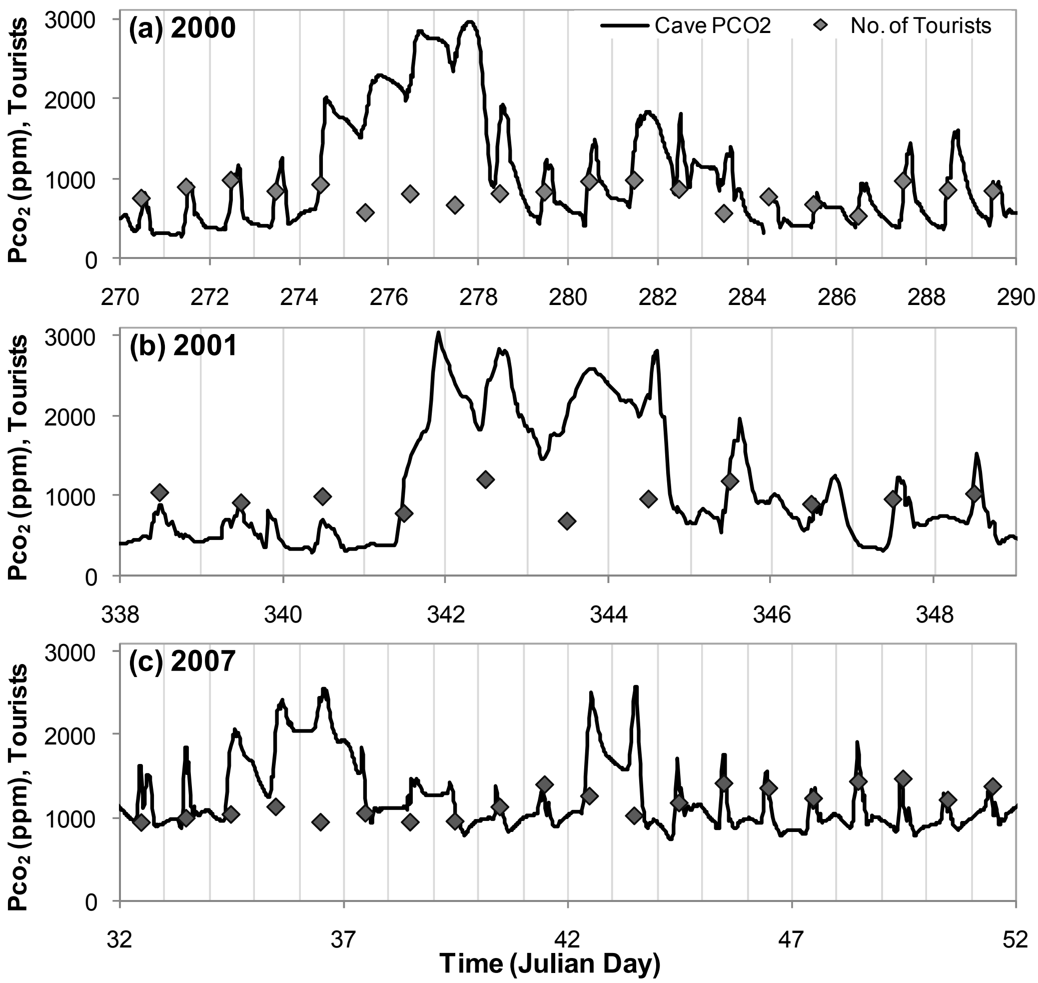

Figure 4.9. Three examples of P_{CO_2} limit exceedences, during which the pattern of cave air P_{CO_2} was also anomalous, that occurred between 2000 and 2007. (a) 26th September – 15th October 2000, (b) 4th – 14th December 2001, (c) 1st – 21st February 2007. Vertical gridlines represent midnight of a 24 hour period.

4.6 Box model

The amount of CO_2 in the Glowworm Cave air is a function of the rate at which CO_2 enters or is released within the cave (a combination of all sources) compared to the rate of removal (sinks) (de Freitas & Banbury, 1999; Figure 4.10). Aside from tourists, karst and cave research has identified several other (non-anthropogenic) sources of CO_2 including: microbial activity inside the cave, geothermal activity or the release of volcanic gases, and soil derived CO_2 entering caves via gaseous diffusion through the overlying soil and rock (Amar, 2004 after James, 1977; James & Dyson, 1981) or through percolation waters (Cigna, 2005 after Bourges *et al.*, 1998). In the Glowworm Cave, geothermal and volcanic activity was absent and, therefore, cannot be contributing CO_2 to the cave air. As the P_{CO_2} of the Glowworm Cave air rises rapidly (e.g. ~ 1000 ppm over two hours), it was clear that a proportion of the CO_2 within the Glowworm Cave was unexplained by any of the currently known sources. A simple box model was constructed to describe the amount of P_{CO_2} in the Glowworm Cave atmosphere using the relative contributions of CO_2 from several sources and sinks (Figure 4.10).

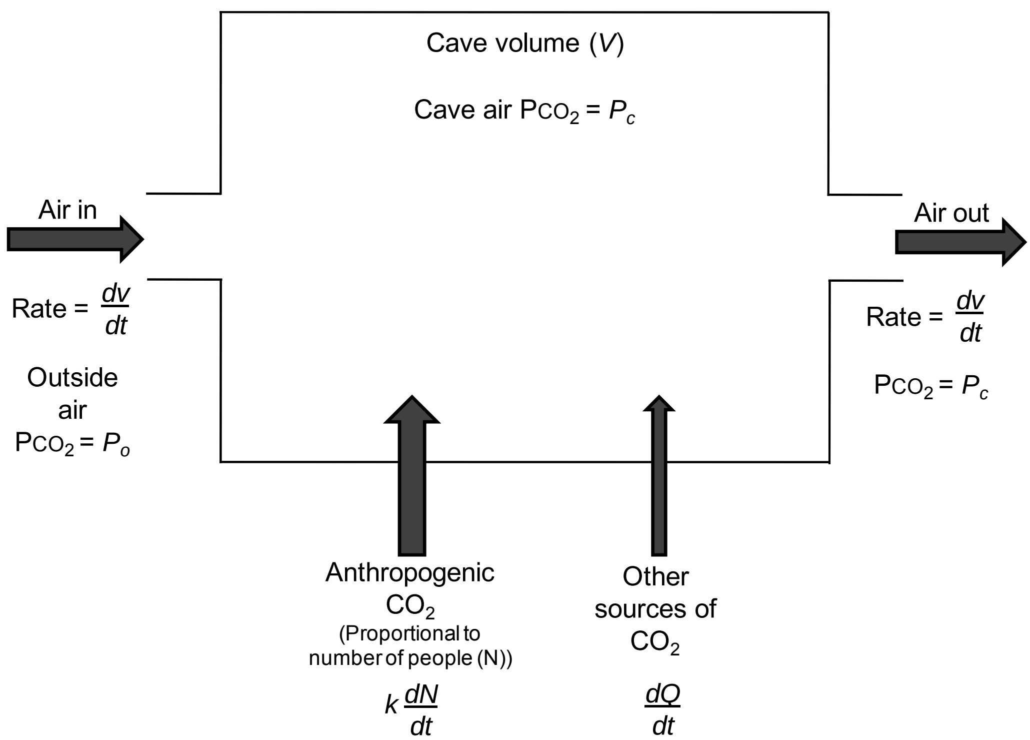

Figure 4.10. Box model showing sources and sinks of CO_2 in the Glowworm Cave.

The total amount of CO_2 entering the cave is described by:

$$\frac{dv}{dt}P_o + k\frac{dN}{dt} + \frac{dQ}{dt} \qquad \text{(Equation 4.1)}$$

where *dv/dt* is the rate at which air, described as a volume (*v*) enters the cave over time (*t*), with a concentration of CO_2 (P_o) equal to the P_{CO_2} of the external atmosphere. *dN/dt* is the rate of tourists (*N*) entering the cave over time (*t*), (assuming anthropogenic CO_2 is proportional to the number of people in the cave) where *k* is the 'proportionality constant' (equal to the mean rate at which tourists generate CO_2). *dQ/dt* describes the rate at which all other sources of CO_2 (*Q*) enter the cave over time (*t*), which could include CO_2 from stream and dripwaters, microbial respiration and other unidentified sources.

The total amount of CO_2 to exit the cave is described by:

$$\frac{dv}{dt}P_c \qquad \text{(Equation 4.2)}$$

where *dv/dt* is the rate at which air, described as volume (*v*), exits the cave, and (*t*) is time in seconds. The air mass has a CO_2 concentration (P_c) equal to the P_{CO_2} of the cave air.

The rate of change in cave air P_{CO_2} is therefore:

$$\frac{dP_c}{dt} = \frac{1}{V}\left(k\frac{dN}{dt} + \frac{dv}{dt}(P_o - P_c) + \frac{dQ}{dt}\right) \qquad \text{(Equation 4.3)}$$

where:

P_c is the partial pressure of CO_2 in the cave air, so that

dP_c/dt is the rate of change in cave air CO_2 over time (*t*);

V is the total volume of cave air (which, for the Glowworm Cave, is approximately 4000 m^3 (de Freitas & Schmekal, 2003));

N is the number of tourists; and,

k is a constant value, so that

kdN/dt is the rate of tourists (*dN*) entering the cave over time (*t*) with the constant (*k*) representing the contribution each tourist makes to cave P_{CO_2} (e.g. 17 $l.h^{-1}$ (de Freitas & Banbury, 1999 after Marion, 1979));

P_o is the partial pressure of CO_2 of the outside air;

P_c is the partial pressure of CO_2 of the cave air; so

$dv/dt(P_o - P_c)$ is the rate of change in the partial pressure of the cave air based on the amount of air flow (*dv/dt*) and the difference between P_o and P_c; and

dQ/dt is the rate of CO_2 contributed to the cave environment from all other sources (e.g. dripwaters, stream and microbial activity)

In developing the box model two assumptions were made: (i) that the volume of the cave air (*V*) remains constant, and (ii) that the air pressure remains constant.

Of the sources of CO_2 within the Glowworm Cave, we can estimate the contribution of CO_2 from tourists to be 17 $l.h^{-1}$ (de Freitas & Banbury, 1999 after Marion, 1979). The P_{CO_2} of dripwater within caves at Waitomo has also been investigated (e.g. in Waipuna Cave, (McCabe, 1977)), as well as concentrations and variability of CO_2 within the volcanic ash soils in Waitomo (Gunn & Trudgill, 1982). Other potential sources of CO_2 into the Glowworm Cave (e.g. geothermal or microbial respiration) are likely to be small and have not been further investigated in this research.

4.7 Discussion

4.7.1 Seasonal variation in Glowworm Cave climate conditions

The Glowworm Cave P_{CO_2} exhibited pronounced seasonality, with minima occurring during the winter and P_{CO_2} maxima occuring in the summer. P_{CO_2} maxima, however, occurred twice during the year; once in April, and again in late September/early October. The P_{CO_2} maxima roughly coincided with autumn and spring periods, when the outside air temperature was changing. Between March and April (autumn), the mean outside air temperature dropped below the mean cave temperature. Conversely, between October and November (spring), the outside air temperature increased relative to the cave air temperature. During the autumn and the spring periods the temperature gradient between the Glowworm Cave and the outside air was at a minimum. The temperature gradient can be used as a proxy for cave ventilation (de Freitas *et al*., 1982), with a low temperature gradient signifying reduced air flow. It is therefore probable that the autumn and spring P_{CO_2} maxima were, at least in part, a result of reduced ventilation. Similar correlations between P_{CO_2} maxima and temperature gradient minima were observed in Císařská Cave, Czech Republic (Faimon *et al*., 2006).

The high summer/low winter P_{CO_2} also coincided with the trend in tourist numbers in the Glowworm Cave. During the summer, tourist numbers were higher than in winter, primarily because of the summer holiday season. Tourist numbers also increased for a short period during April due to the Easter holidays. During the April/Easter period, CO_2 in the cave air increased and this has been described as the 'Easter effect' (James, 1994). The Easter effect was identified in two Australian tourist caves, the Gaden-Coral Cave and the Jenolan Caves (James, 1994).

Another factor that is likely contributing to the high summer/low winter P_{CO_2} trend in the Glowworm Cave, is the concentration of CO_2 in the overlying soil (Troester & White, 1984). Soil air P_{CO_2} fluctuates seasonally (Atkinson, 1977), with minima occurring in the winter and maxima occurring in the spring to early summer at Waitomo (Gunn & Trudgill, 1982). Soil moisture and temperature have important roles in regulating soil air P_{CO_2} levels (Parfitt *et al*., 1997), which, in turn, influence plant growth and microbial activity. A greater amount of plant biomass and increased litter production also contribute to soil CO_2 levels (e.g. Gunn and Trudgill (1982) reported that soil under forest cover had higher P_{CO_2} than nearby pasture-covered soils). CO_2 from the soil air is capable of reaching the cave environment either by migrating downward through cracks and fissures in the bedrock (possibly because CO_2 is heavier than oxygen) (Ek & Gewelt, 1985) or by becoming dissolved in water (for example dripwater), and then degassing into the cave air, until an equilibrium is established.

4.7.2 Diurnal variation in Glowworm Cave climate conditions

A clear diurnal trend is evident in Glowworm Cave P_{CO_2}. P_{CO_2} minima occur at approximately 9.00 a.m., just before daily tours commenced, whilst daily P_{CO_2} maxima typically occurred between midday and mid-afternoon at the Glowworm Cave. The relationship between tourists and day time peaks in cave air P_{CO_2} has been well established (Dragovich & Grose, 1990; Pulido-Bosch *et al.*, 1997; de Freitas & Banbury, 1999; Song *et al.*, 2000, Faimon *et al.*, 2006). A comparison of the summer and winter diurnal P_{CO_2} cycle highlighted several trends: firstly, the summer P_{CO_2} levels were higher than winter P_{CO_2} levels by approximately 100 ppm; secondly, the summer daily P_{CO_2} maxima typically occurred at midday, whilst winter P_{CO_2} maxima occurred between 3.00 p.m. and 4.00 p.m.; and thirdly, the summer P_{CO_2} pattern had a secondary peak between 8.00 p.m. and 9.00 p.m. Higher summer P_{CO_2} concentrations, the timing of P_{CO_2} maxima and the secondary P_{CO_2} peak that occurred in the summer can all be attributed to the number of visitors to the Glowworm Cave. Another trend evident in the daily P_{CO_2} data is that after the P_{CO_2} maxima was reached, the CO_2 level decreased more rapidly in the summer than in the winter. The rate at which the P_{CO_2} concentration decreased following daily maxima is largely a function of ventilation (de Freitas & Banbury, 1999).

Cave ventilation (due to increased temperature gradient) is a likely explanation for the P_{CO_2} peaking at different times depending on the season. In the summer, the greatest temperature gradient occurred during the middle of the day when outside air temperature was high (mean summer maximum approximately 22 °C, based on January data), compared to temperature inside the Glowworm Cave (roughly 15.8 °C). In the winter (represented by July), the temperature gradient was smallest in the middle of the day (~ 3 °C). The low winter day time temperature gradient reduced the flushing of the cave, and therefore, the CO_2 level in the cave remained high for a longer period during the afternoon. A management tool that can be used in the Glowworm Cave in an attempt to reduce CO_2 is opening and closing the entrances to induce a draught. As summer is the busiest season, it is probable that the door was opened more frequently during the summer compared to the winter, and that may have contributed to the more rapid decline in P_{CO_2} during the summer, compared to winter.

4.7.3 P_{CO_2} limit exceedences in the Glowworm Cave air

A positive relationship has been reported between daily maximum P_{CO_2} levels and the number of tourists in the Glowworm Cave (this study, Figure 4.8) as well as in other caves (Dragovich & Grose, 1990). However, there were a number of occasions between 1998 and 2007 when the P_{CO_2} in the Glowworm Cave was high, whilst tourist numbers were normal, low, or even absent. In instances when the elevated P_{CO_2} could not be explained by tourist numbers, and the cave air P_{CO_2} remained elevated during the night time, the events were considered to be 'anomalous'. The presence of such anomalous events suggested that there was a source other than the tourists that was contributing to the P_{CO_2} of the Glowworm Cave air. A box model was constructed to differentiate between the known and the unknown sources and sinks of CO_2 within the Glowworm Cave (Figure 4.10). The remaining challenge was to identify and determine what the unknown source(s) of P_{CO_2} in the Glowworm Cave air were, in order to better understand the dynamics of CO_2 within the Glowworm Cave.

4.8 Conclusion

- Glowworm Cave air P_{CO_2} typically followed the pattern of tourist numbers with highs during the summer, and in the day time, and lows during the winter and at night time. Daily minimum P_{CO_2} occurred just before cave tours commence at 9.00 a.m.

- Overlying both the diurnal and seasonal CO_2 trends were variations in airflow, which were largely driven by temperature differences between the cave and external atmospheres. When the temperature gradient was high, airflow through the cave was enhanced, whilst a small temperature gradient resulted in restricted airflow, and thus flushing of the cave air was limited.

- In spring and autumn, when the temperature gradient between the cave and outside air was low, P_{CO_2} tended to be higher than at other times of the year.

- Ten years of Glowworm Cave air P_{CO_2} data highlighted the presence of P_{CO_2} limit exceedences that were not directly caused by high tourist numbers. The occurrence of P_{CO_2} limit exceedences, independent of high tourist numbers, indicated that an additional source(s) existed.

5.0 Chapter Five: Stream P_{CO_2}

5.1 Introduction

Until now, fluxes in Glowworm Cave P_{CO_2} have largely been attributed to tourists. However, by investigating ten years of time series data (Chapter Four), it has been possible to demonstrate that there are other sources contributing CO_2 to the cave environment. Water percolating through soil dissolves CO_2 and thus, has been shown to elevate CO_2 levels in receiving stream systems (Jones & Mulholland, 1998). Stream systems have been shown to have elevated CO_2 concentrations, as percolating water dissolves soil CO_2 (Jones & Mulholland, 1998). Knowledge of stream CO_2 prompted the suggestion that the Waitomo Stream may also be a source (and possibly a sink) of CO_2 to the Glowworm Cave.

The Waitomo Stream is a prominent feature of the Glowworm Cave, and enters the cave through the lower entrance before flowing 40 m through a tunnel into the Glowworm Grotto. The Glowworm Grotto is a 30 m long chamber, 10 m wide and 5 m high. The stream continues along another passage (approximately 50 m long), then sumps, emerging at the Demonstration Chamber. The Waitomo Stream sumps one more time within the Glowworm Cave before emerging outside the cave (de Freitas *et al*., 1982).

5.2 Hypotheses and chapter objectives

The objective of this chapter was to test the hypotheses that:

- **anomalous increases in Glowworm Cave air PCO_2 were associated with increases in the Waitomo Stream PCO_2; and**
- **the PCO_2 of the Waitomo Stream increased following rainfall events.**

Continuous stream PCO_2 data were collected between June and December 2008 for the Waitomo Stream, along with rainfall records for the Waitomo district, Waitomo Stream discharge, cave air PCO_2 and temperature data. A second dataset including Ruakuri Cave air PCO_2 and temperature, external air temperature and the temperature gradient between the cave and outside atmospheres were also obtained to highlight the consistency of the patterns within a second, nearby cave. However, stream PCO_2 data for Ruakuri are incomplete due to sensor malfunction. Data are presented at three time scales. Firstly, annual summaries of the cave (climatic) and stream (physical and chemical) parameters are presented to highlight seasonal variation. A more detailed plot of two months of data to illustrate typical and anomalous stream PCO_2 patterns is shown and changes within the diurnal pattern associated with stream PCO_2 anomalies are described.

5.3 Relationship of stream PCO_2 to the box model

Given the hypothesis that variations in Glowworm Cave air PCO_2 are associated with variations in the Waitomo Stream PCO_2, the box model (described in section 4.6) can be modified to include the stream as an independent source of CO_2 to the cave atmosphere (Figure 5.1).

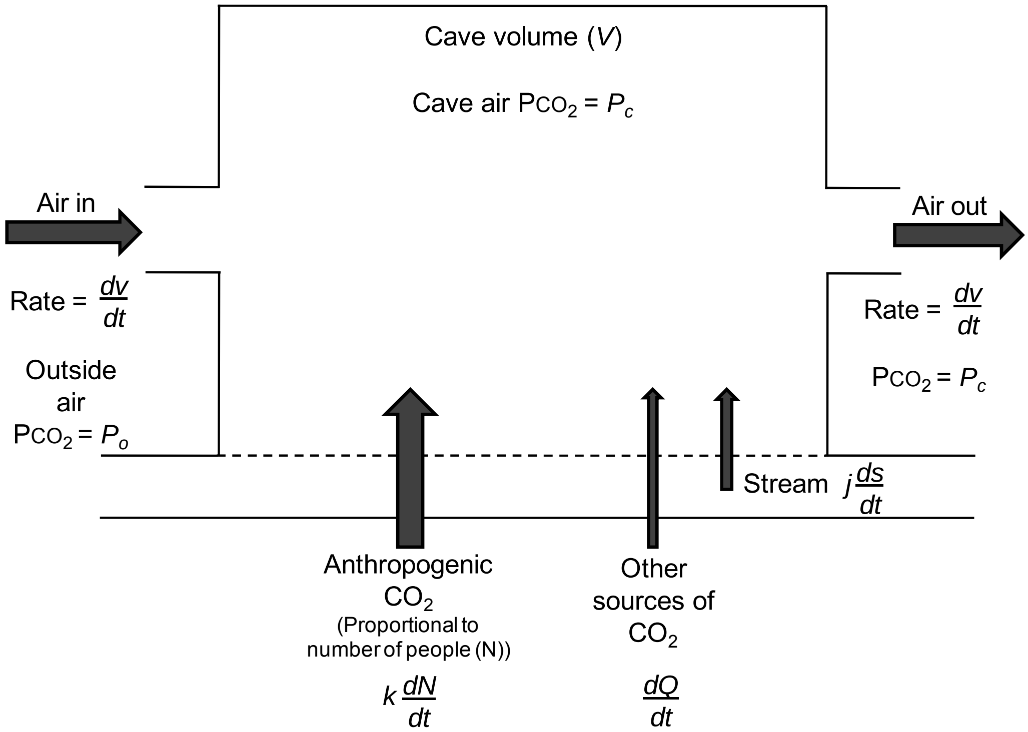

Figure 5.1. Modified box model (see Figure 4.10), to include the stream as a separate source contributing CO_2 to the cave.

The CO_2 contribution from the stream can be defined as:

$$j\frac{ds}{dt} \qquad \text{(Equation 5.1)}$$

where ds/dt is the volume of streamflow, (t) is time, and j is a constant determined using Henry's Law (which allows calculation of the amount of CO_2 coming out of the water in relation to its partial pressure).

Therefore the contribution of P_{CO_2} from the stream into the cave air is:

$$\frac{ds}{dt}j(P_s - P_c) \qquad \text{(Equation 5.2)}$$

where P_s - P_c is the difference in P_{CO_2} between the stream and cave air.

The rate of change in cave air P_{CO_2}, with the addition of the stream component, is therefore:

$$\frac{dP_c}{dt} = \frac{1}{V}\left(k\frac{dN}{dt} + \frac{dv}{dt}(P_o - P_c) + \left(\frac{dQ}{dt} - \frac{ds}{dt} j(Ps - P_c) \right) \right) \qquad \text{(Equation 5.3)}$$

where:

P_c is the partial pressure of CO_2 in the cave air, so that

dP_c/dt is the rate of change in cave air CO_2 and (t) is time;

V is the total volume of cave air;

N is the number of tourists, and

k is a constant value, so that

kdN/dt is the rate of tourists (dN) entering the cave and (t) is time, with the constant (k) representing the contribution each tourist makes to cave PCO_2;

P_o is the partial pressure of CO_2 of the outside air;

P_c is the partial pressure of CO_2 of the cave air; so

$dv/dt(P_o - P_c)$ is the rate of change in the partial pressure of the cave air based on the rate of air flow (dv/dt) and the difference between P_o and P_c;

dQ/dt is the rate of CO_2 contributed to the cave environment from all other sources (e.g. dripwaters, stream, microbial activity, etc.);

ds/dt is the volume change in streamflow and (t) is time;

j is a constant value (based on Henry's Law); and

P_s - P_c is the difference in PCO_2 between the stream and cave air.

Under typical conditions the stream component ($j(ds/dt)$) is very small, however, if the number of tourists (dkN/dt), or the air flow component ($dv/dt(P_o$ - P_c)), decreases substantially, then the stream ($ds/dt(P_o$ - P_c)) (and other sources Q) become an important component of the equation. While the tourist component is typically substantial, when tourist numbers are greatly reduced (or become zero, which can occur during times of high water or high CO_2 levels), then the tourist component, as a source of CO_2 to the cave air, becomes negligible. Similarly, the air flow component ($dv/dt(P_o$ - P_c)) can be greatly reduced when the stream level rises (i.e. during times of flood) blocking off the entrance, or when the cave-to-outside air temperature gradient becomes small, preventing air flow. The stream-input component of the equation ($ds/dt(P_o$ - P_c)) can increase if the difference between P_s and P_c is large, or if the flow rate of the stream increases, then the magnitude of $ds/dt(P_o$ - P_c) will increase.

Stream parameters (e.g. PCO_2 and discharge), external parameters (e.g. temperature and rainfall), and cave parameters (e.g. temperature and temperature gradient (pertaining as a proxy for air flow)) for the Glowworm and Ruakuri Caves, were examined in relation to cave air PCO_2, to determine if any relationships existed between the cave air PCO_2 and any of the monitored parameters. Emphasis was placed on the relationship between the Glowworm Cave air and the Waitomo Stream to test the hypothesis that increases in Glowworm Cave air PCO_2 are associated with increases in the Waitomo Stream PCO_2. The further hypothesis, that decreases in Glowworm Cave air PCO_2 are associated with decreases in the Waitomo Stream PCO_2, was also considered, highlighting the potential of the Waitomo Stream as a CO_2 sink.

5.4 Seasonal trends for the Glowworm and Ruakuri Caves

Glowworm and Ruakuri Cave air PCO_2 was highly variable throughout the measurement period, with the cave air generally having higher PCO_2 in summer than in winter (Figure 5.2a and Figure 5.3a). Ruakuri showed a stronger seasonal trend, with less variability over short time steps, than the Glowworm Cave. The Ruakuri Cave is larger with more entrances, and therefore, has a cave microclimate that is less susceptible to the effects of high numbers of tourists (de Freitas & Littlejohn, 1987) (and probably less responsive to short term variability in stream conditions). In spite of the summer-high, winter-low seasonal trend, the highest daily mean cave air PCO_2 for the Glowworm Cave in 2008 occurred on day 216 (3rd August), which was preceded by several events of high CO_2. The peaks in cave air CO_2 in 2008 (between days 195 and 220) matched similar peaks in the daily mean stream PCO_2 (Figure 5.2b). The peaks in cave air CO_2 also coincided with peaks in discharge (Figure 5.2d).

Waitomo Stream PCO_2 (Figure 5.2b) showed a similar seasonal trend (summer-high, winter-low), with the daily mean PCO_2 ranging between 500 and 1900 ppm. The winter base level was approximately 500 ppm. During the summer months, base level CO_2 increased to approximately 1000 ppm. The PCO_2 in the stream was between 1.3 – 5 times higher than atmospheric CO_2. Stream PCO_2 was more variable during the winter, with a series of large peaks occurring between July and September. Conclusive seasonal trends could not be made due to insufficient long term data.

Rainfall in Waitomo was most prevalent during the winter (Figure 5.2c and Figure 5.3b) and this was matched by higher discharge measured in the Waitomo Stream during the winter months (Figure 5.2d and Figure 5.3c).

Seasonal air temperature of the Ruakuri Cave (measured in the Drum Passage) was more stable than the Glowworm Cave, with a range of only 0.8 °C (compared to over 4.5 °C for the Glowworm Cave) (Figure 5.2f, g; Figure 5.3e, f). The difference in temperature gradient between summer and winter for each cave was roughly the same, with absolute averages of about 5 °C and maxima of approximately 10 °C. The direction of the gradient was reversed between summer and winter. During the summer, the gradient was typically negative (due to higher outside air temperatures), whilst winter months were generally accompanied by a positive gradient trend (due to lower outside air temperatures). The temperature gradient is an important component in the cave environment, as it drives airflow, and thus air exchange, between the cave and the outside environment due to density differences in air masses (de Freitas *et al*. 1982).

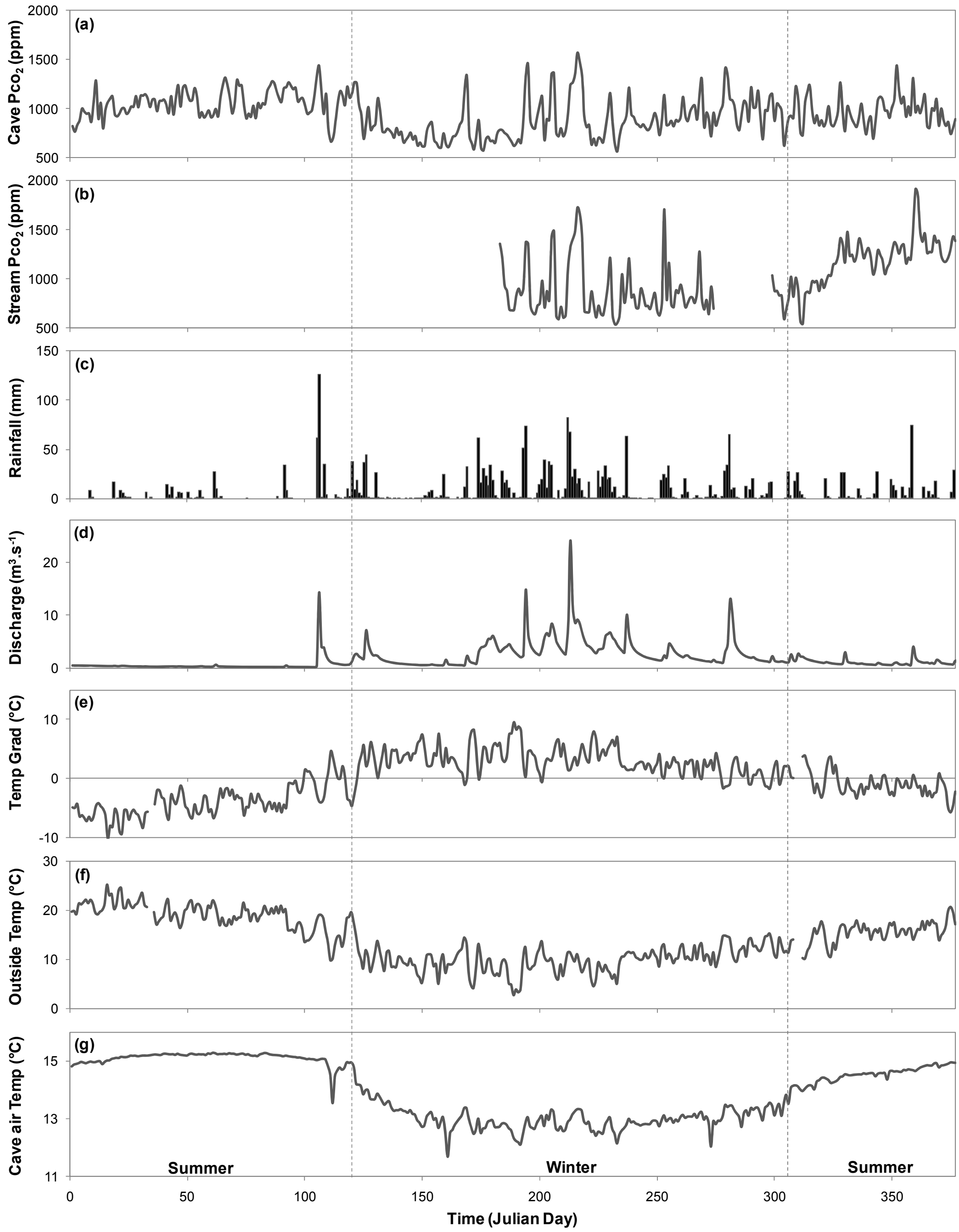

Figure 5.2. Glowworm Cave and Waitomo Stream monitoring data for 2008. (a) Mean daily cave air P_{CO_2}; (b) mean daily stream P_{CO_2}; (c) daily total rainfall; (d) mean daily discharge; (e) mean daily temperature gradient between the Glowworm Cave and outside air temperature; (f) mean daily external air temperature; and (g) mean daily cave air temperature. Dotted lines indicate "winter" (1st May – 31st October) and "summer" (1st November – 30th April).

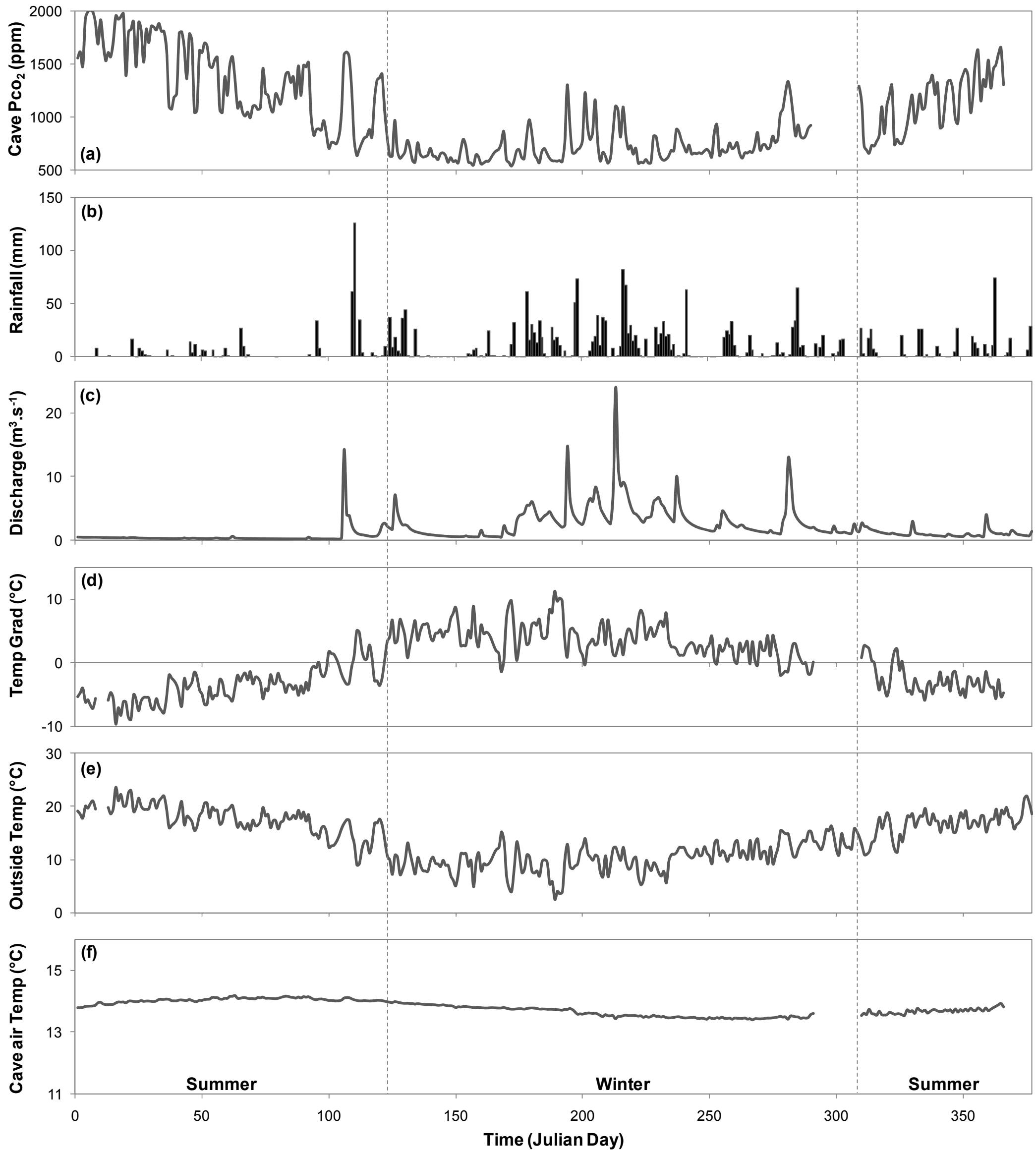

Figure 5.3. Ruakuri Cave and stream monitoring data for 2008. (a) Mean daily cave air P_{CO_2} (measured in the Drum Passage); (b) daily total rainfall; (c) mean daily discharge; (d) mean daily temperature gradient between the Ruakuri Cave and outside air temperature; (e) mean daily external air temperature (measured at the Waitomo weather station); and (f) mean daily cave air temperature. Dotted lines indicate "winter" (1st May – 31st October) and "summer" (1st November – 30th April).

5.5 Cave air P_{CO_2} anomalies and Waitomo Stream dynamics

Stream P_{CO_2}, Waitomo Stream discharge, rainfall and cave temperature were plotted alongside Glowworm Cave air P_{CO_2} for days 191 – 257 of 2008 (9th July – 13th September) (Figure 5.4). Despite having no stream P_{CO_2} data available for the Ruakuri Cave, cave microclimate parameters for the same time periods were plotted (Figure 5.5) to determine if the trends observed in the Glowworm Cave were also apparent in the Ruakuri Cave. The more detailed data clearly showed the presence of diurnal variation within the P_{CO_2} of the cave and stream, as well as the temperature, with peaks usually occurring during the day.

On several occasions throughout July and August, cave air CO_2 differed from the norm, with CO_2 failing to return to base level (anomalous events). The anomalous events were investigated in both the Glowworm and Ruakuri Caves to determine which parameters (other than tourists), were driving the anomalies (Figure 5.6 – Figure 5.13). The cave air P_{CO_2} during the anomalous events displayed a strong relationship with stream P_{CO_2} with identical patterns, typically of a similar magnitude, observed in stream P_{CO_2}, compared to cave air P_{CO_2}. For every anomalous cave air (thus anomalous stream P_{CO_2}) event that occurred in the Glowworm Cave, the presence of both rainfall and a considerable peak in discharge from the Waitomo Stream were evident (Figure 5.4b, c and d). With the onset of increasing stream discharge, the stream P_{CO_2} increased and remained elevated (compared to base level) for a period of at least 24 hours (Figure 5.6a, Figure 5.8a, Figure 5.10a and Figure 5.12a). As the storm peak in the hydrograph (discharge) subsided, the CO_2 in both the stream and cave air within the Glowworm Cave returned to a normal diurnal pattern.

Ruakuri Cave air CO_2 has a similar relationship of elevated CO_2 with rainfall (thus increased discharge) (Figure 5.7a, Figure 5.9a, Figure 5.11a, and Figure 5.13a) for the same events as presented for the Glowworm Cave. Where the Drum Passage P_{CO_2} usually remained below 1000 ppm during the months of July and August 2008 (Figure 5.5a), every event where the Waitomo Stream and Glowworm Cave air P_{CO_2} displayed an anomalous pattern, the CO_2 in the Drum Passage increased above 1000 ppm. Aggressive Waterfall P_{CO_2} was typically lower and less responsive, seldom exceeding 650 ppm during non-rainfall, normal, stream discharge conditions. Each of the anomalous cave air P_{CO_2} events plotted, coincided with an increase in stream P_{CO_2}, rainfall and discharge (Figure 5.4 and Figure 5.5).

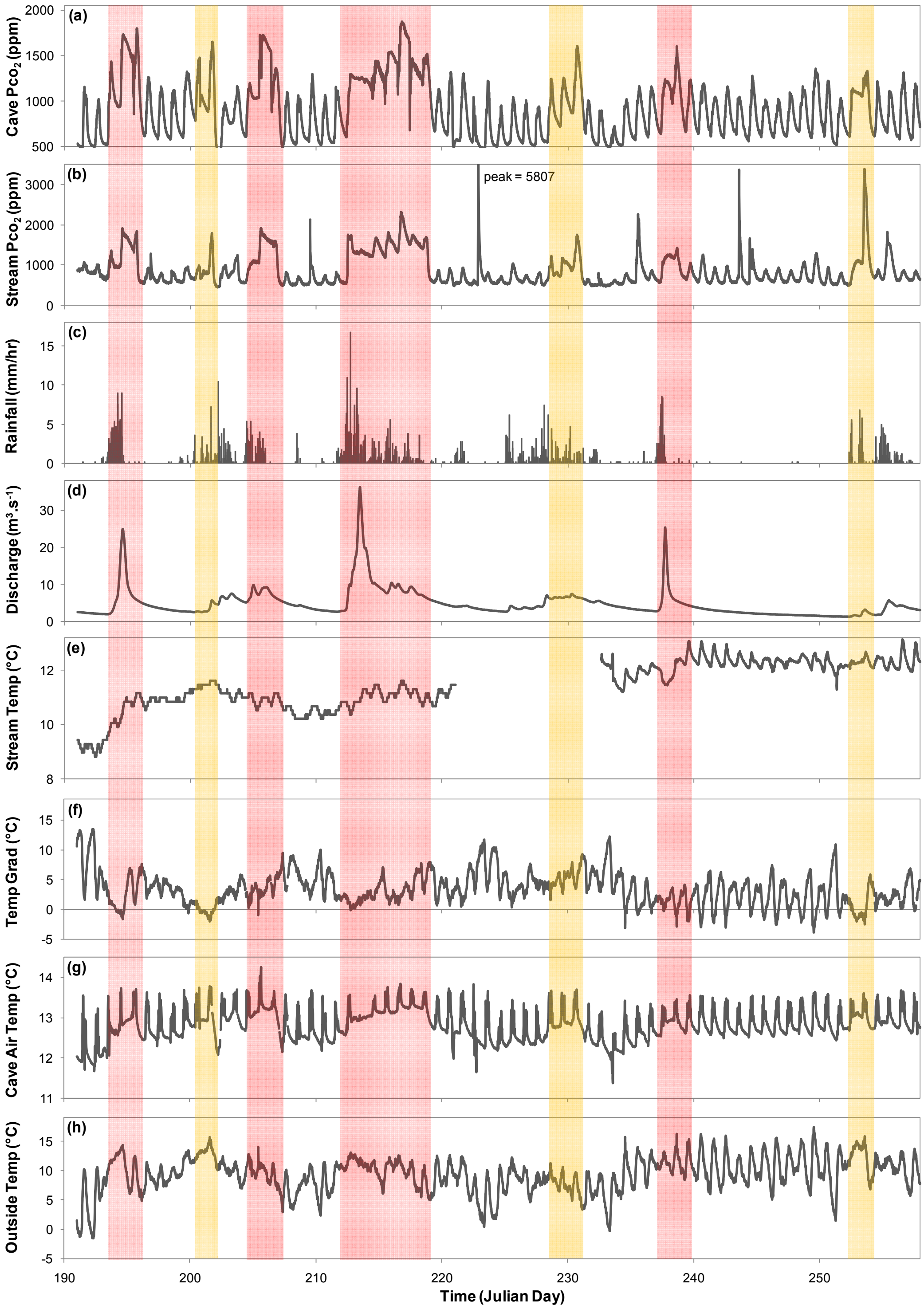

Figure 5.4. Glowworm Cave and Waitomo Stream monitoring data for days 191 – 257 (9th July – 13th September) 2008. (a) Cave air PCO_2; (b) stream PCO_2; (c) daily total rainfall; (d) discharge; (e) stream temperature; (f) temperature gradient between the Glowworm Cave and outside air temperature; (g) external air temperature; and (h) cave air temperature. The shaded regions highlight the periods where neither cave air nor stream CO_2 returned to base level. The shaded events indicate cave air PCO_2 anomalies. The "red" shaded events are presented in Figure 5.6, Figure 5.8, Figure 5.10, and Figure 5.12 .

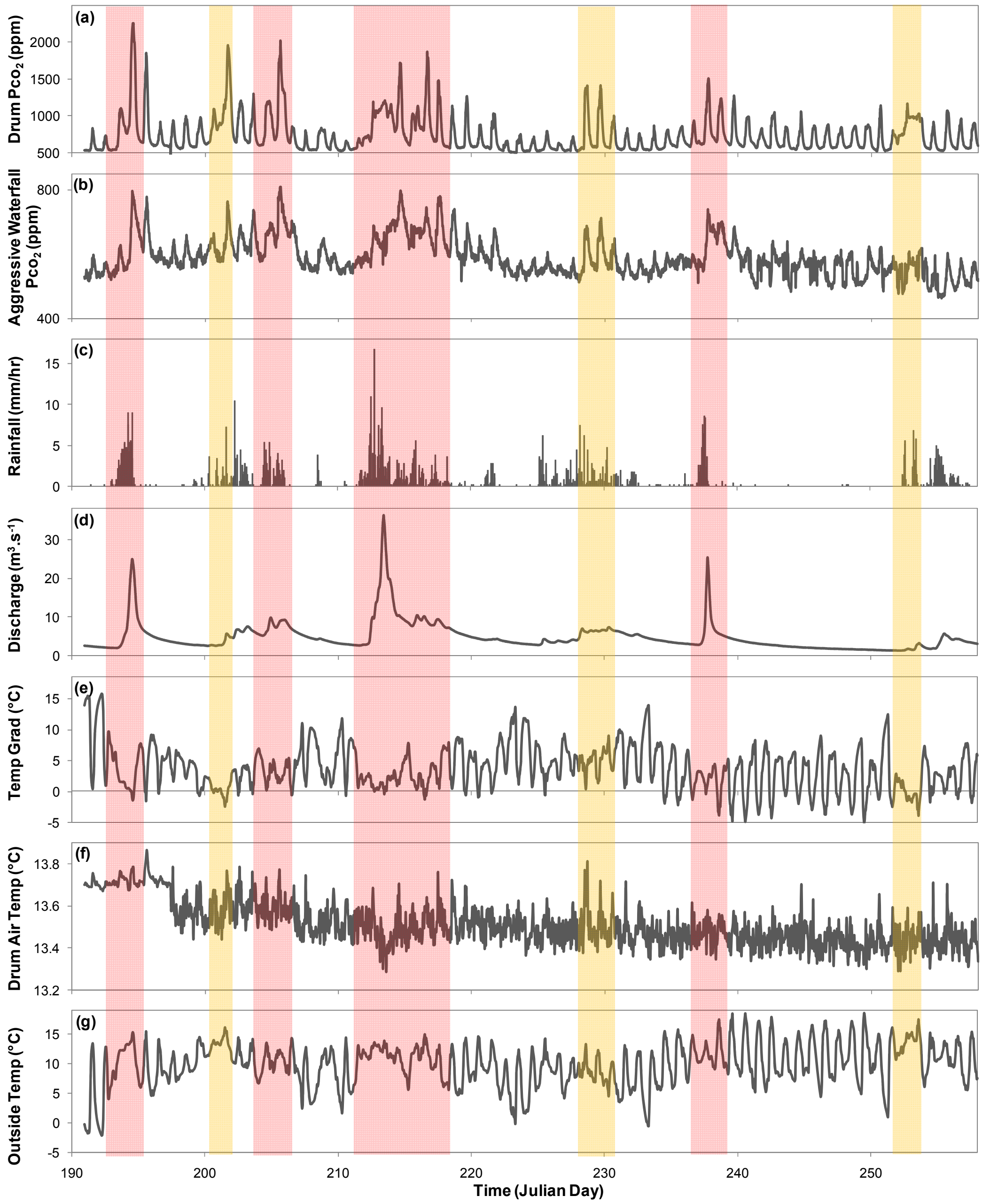

Figure 5.5. Ruakuri Cave and stream monitoring data for days 191 – 257 (9th July – 13th September) 2008. (a) Cave air PCO_2 recorded in the Drum Passage; (b) cave air PCO_2 recorded at the Aggressive Waterfall; (c) daily total rainfall; (d) discharge; (e) temperature gradient between the Ruakuri Cave (data recorded in the Drum Passage) and outside air temperature; (f) cave air temperature (data recorded in the Drum Passage); (g) external air temperature (data recorded at the Waitomo weather station). The shaded events indicate cave air PCO_2 anomalies. The "red" shaded events are presented in Figure 5.7, Figure 5.9, Figure 5.11, and Figure 5.13.

Temperature, both inside and outside the cave, as well as in the Waitomo Stream, usually increased during the anomalous stream P_{CO_2} events, however, at times, the temperature increase was small. Diurnal temperature variations almost always decreased during anomalous events. Similarly, temperature gradient mostly decreased, mainly due to the warmer, milder outside winter air temperature, as did the degree of diurnal variation in the temperature gradient. Ruakuri Cave air temperature did not show any variation during the anomalous events.

A good example of a cave air CO_2 anomaly occurred between days 211 and 219 (29^{th} July – 6^{th} August 2008) in the Glowworm Cave (Figure 5.10 and Figure 5.11). Day 211 exemplifies the typical diurnal pattern of cave air P_{CO_2} and stream P_{CO_2} where cave air P_{CO_2} is higher than stream P_{CO_2} (Figure 5.10a). During the afternoon of day 211, 9.6 mm of rain fell, followed by heavier rainfall on day 212. The heavy rainfall prompted an increase in stream discharge (Figure 5.10c). Stream P_{CO_2} responded during the evening of day 212 by reaching and maintaining a level of about 1400 ppm, well above the typical base level for July/August (approximately 500 ppm). From day 212 the stream maintained a higher P_{CO_2} than the cave for six and a half days, which is unusual given that the stream P_{CO_2} is typically lower than that of the cave.

Day 213 (1^{st} August) was particularly notable. The cave was closed due to flooding and thus it is highly likely that the lack of the typical diurnal peak in cave air and stream CO_2, as well as cave air temperature, can be attributed to the absence of tourists in the cave (Figure 5.10a, g, and h). Despite the lack of tourists, the CO_2 was considerably higher than normal in both the cave air and the stream. The rain continued, with 67 mm falling over the course of the day. The Waitomo Stream discharge peaked at approximately 39 $m^3.s^{-1}$ (considerably higher than the mean flow of 1.7 $m^3.s^{-1}$).

Over the following five days (214 – 218; 2^{nd} – 6^{th} August) tours resumed in the Glowworm Cave and accordingly, the daily peak in cave air and stream P_{CO_2} returned. The rain continued throughout this time, and finally, by day 219 (7^{th} August), the pattern of cave air and stream CO_2 had returned to normal. By day 219 the rainfall in Waitomo had also virtually stopped (daily total < 2 mm).

Cave air PCO_2 in both the Drum Passage (Figure 5.11a) and Aggressive Waterfall site (Figure 5.11b) of the Ruakuri Cave showed trends similar to the PCO_2 trend observed in the Glowworm Cave between days 211 – 219 (29^{th} July – 6^{th} August). Cave air PCO_2 at the Aggressive Waterfall showed an increase, with base level CO_2 (which was usually consistent at about 500 ppm (Figure 5.5)) rising to and maintaining a level of about 630 ppm for the evenings of days 213 – 216.

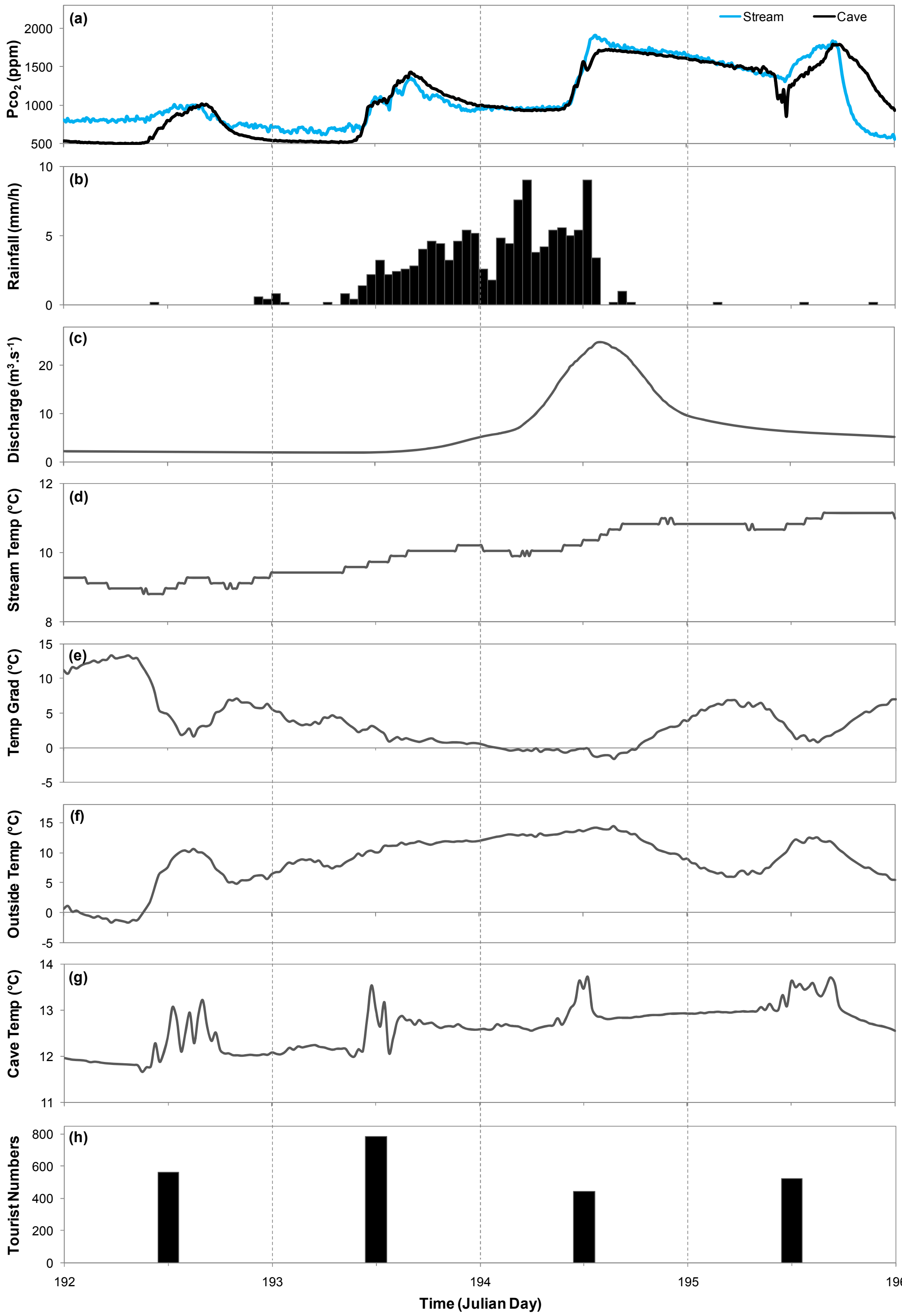

Figure 5.6. Glowworm Cave and Waitomo Stream monitoring data for days 192 – 195 (10th – 13th July) 2008. (a) Cave air and stream PCO_2; (b) rainfall; (c) Waitomo Stream discharge; (d) stream temperature; (e) temperature gradient between the Glowworm Cave and external air temperature; (f) outside air temperature; (g) Glowworm Cave temperature; and (h) tourist numbers. Dotted lines indicate midnight for each 24-hour period.

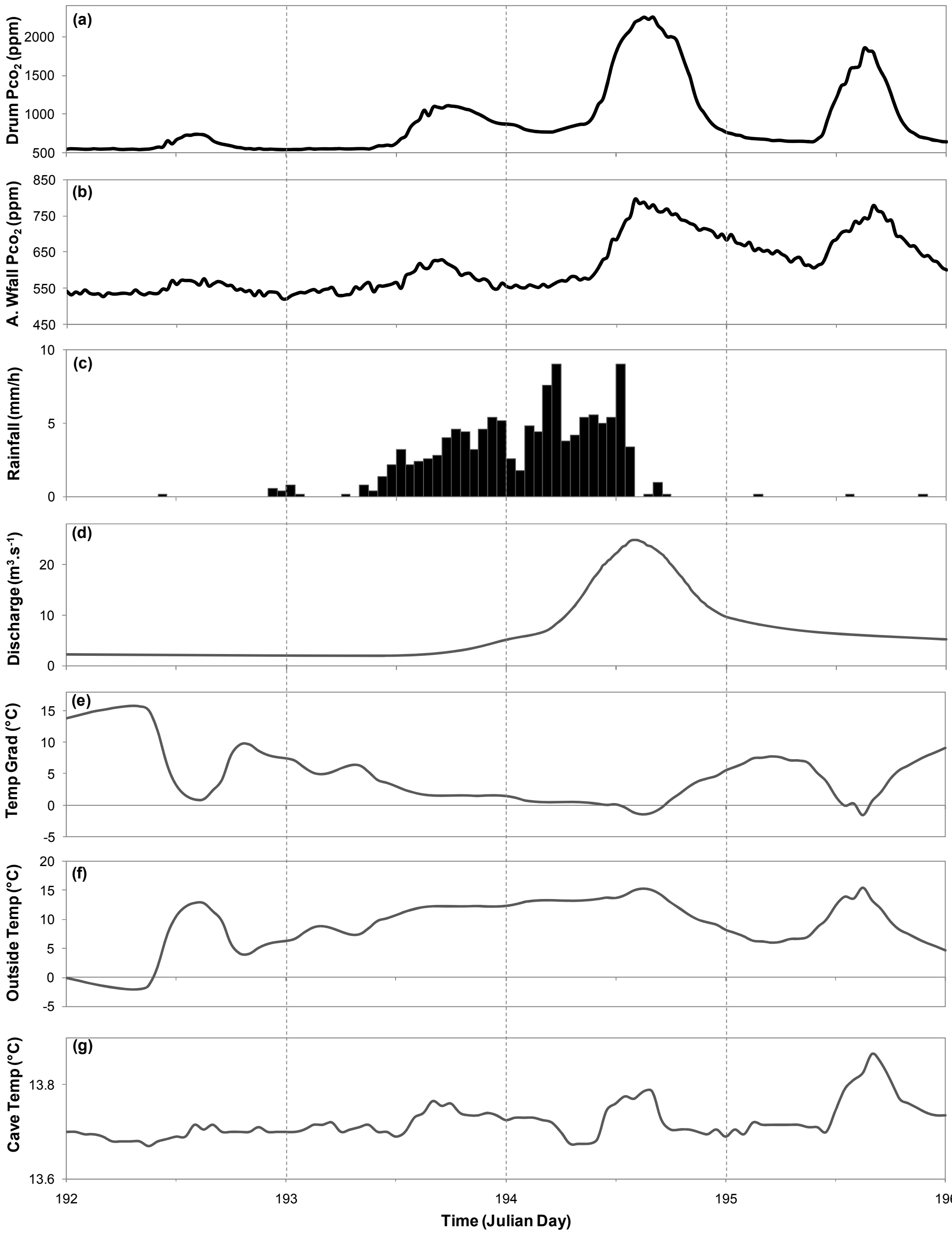

Figure 5.7. Ruakuri Cave and stream monitoring data for days 192 – 195 (10th – 13th July) 2008. (a) Cave air PCO_2 (recorded in the Drum Passage); (b) cave air PCO_2 (recorded at the Aggressive Waterfall); (c) rainfall; (d) Waitomo Stream discharge; (e) temperature gradient between the Ruakuri Cave (recorded in the Drum Passage) and external air temperature; (f) outside air temperature (recorded at the Waitomo weather station); and (g) Ruakuri Cave temperature (recorded in the Drum Passage). Dotted lines indicate midnight for each 24-hour period.

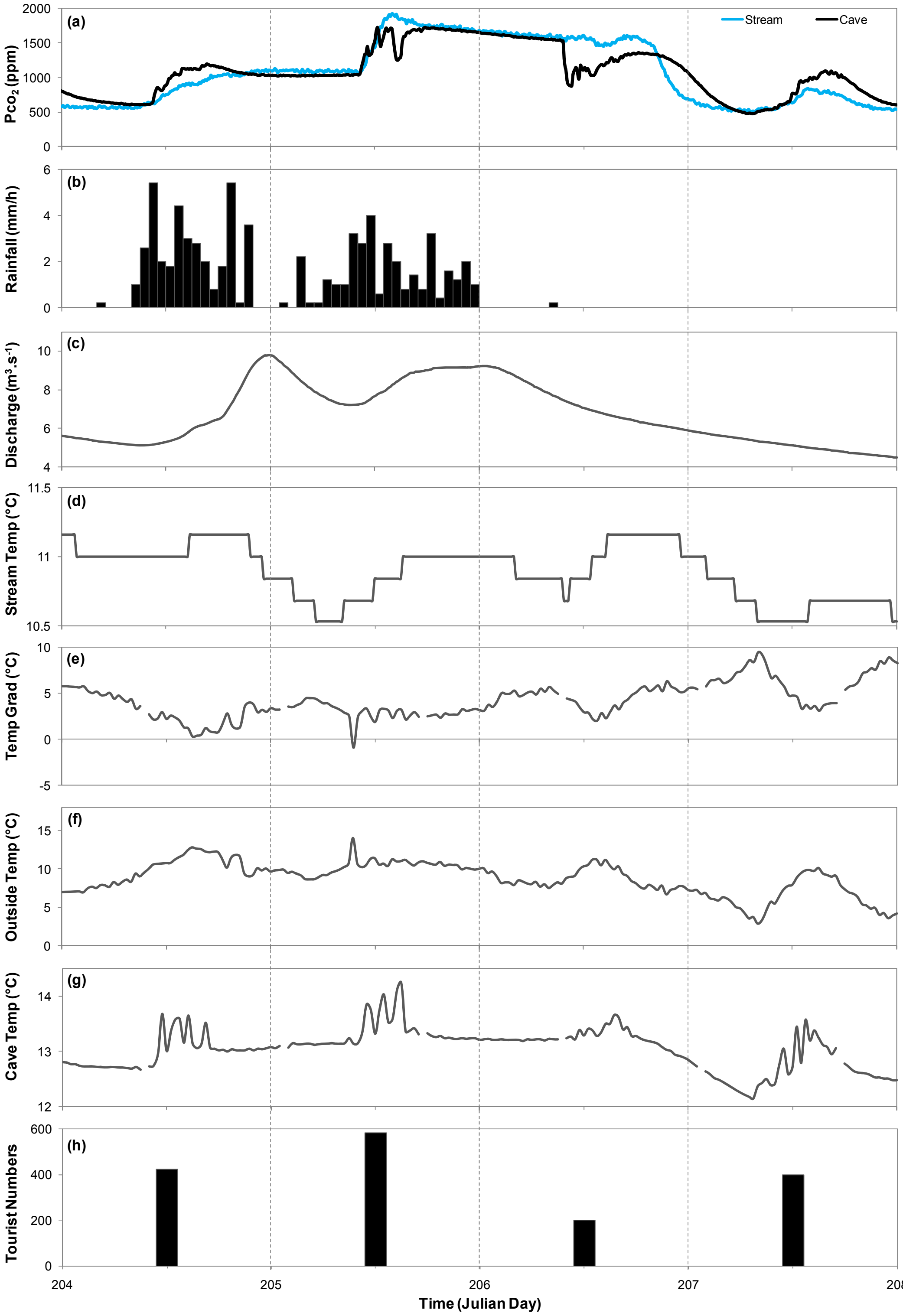

Figure 5.8. Glowworm Cave and Waitomo Stream monitoring data for days 204 – 207 (22nd – 25th July) 2008. (a) Cave air and stream P_{CO_2}; (b) rainfall; (c) Waitomo Stream discharge; (d) stream temperature; (e) temperature gradient between the Glowworm Cave and external air temperature; (f) outside air temperature; (g) Glowworm Cave temperature; and (h) tourist numbers. Dotted lines indicate midnight for each 24-hour period.

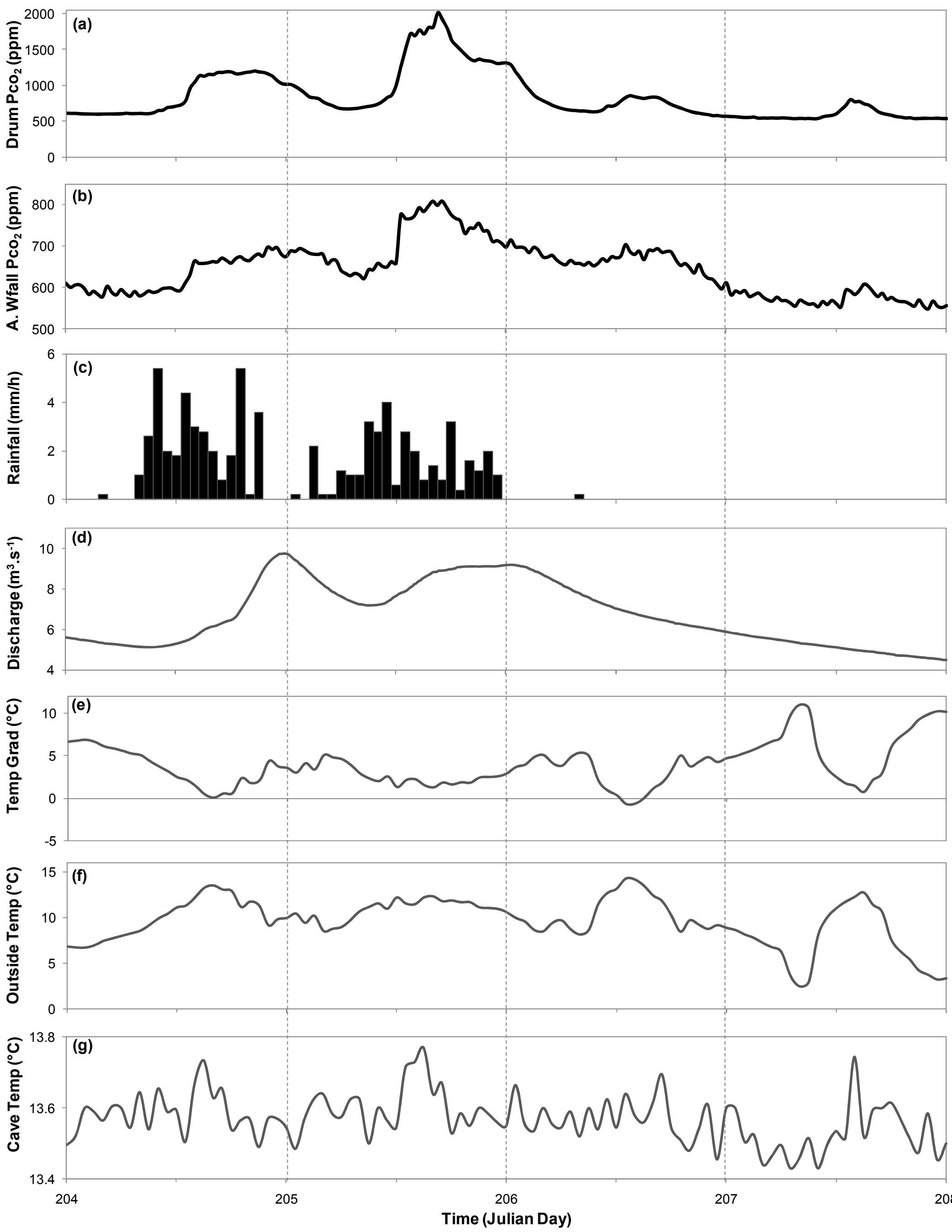

Figure 5.9. Ruakuri Cave and stream monitoring data for days 204 – 207 (22nd – 25th July) 2008. (a) Cave air P_{CO_2} (recorded in the Drum Passage); (b) cave air P_{CO_2} (recorded at the Aggressive Waterfall); (c) rainfall; (d) Waitomo Stream discharge; (e) temperature gradient between the Ruakuri Cave (recorded in the Drum Passage) and external air temperature; (f) outside air temperature (recorded at the Waitomo weather station); and (g) Ruakuri Cave temperature (recorded in the Drum Passage). Dotted lines indicate midnight for each 24-hour period.

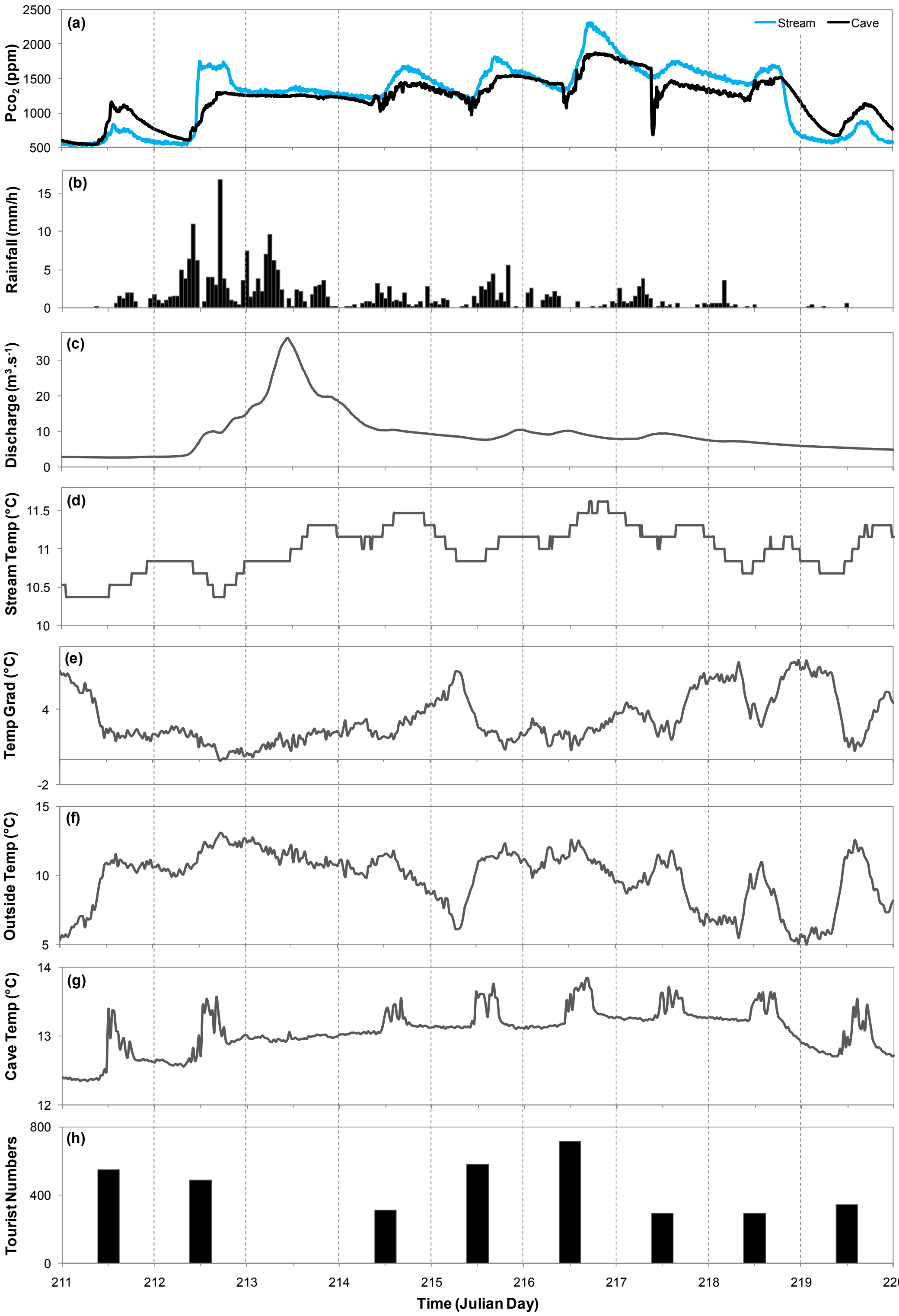

Figure 5.10. Glowworm Cave and Waitomo Stream monitoring data for days 211 – 219 (29th July – 6th August) 2008. (a) Cave air and stream PCO_2; (b) rainfall; (c) Waitomo Stream discharge; (d) stream temperature; (e) temperature gradient between the Glowworm Cave and external air temperature; (f) outside air temperature; (g) Glowworm Cave temperature; and (h) tourist numbers. Dotted lines indicate midnight for each 24-hour period.

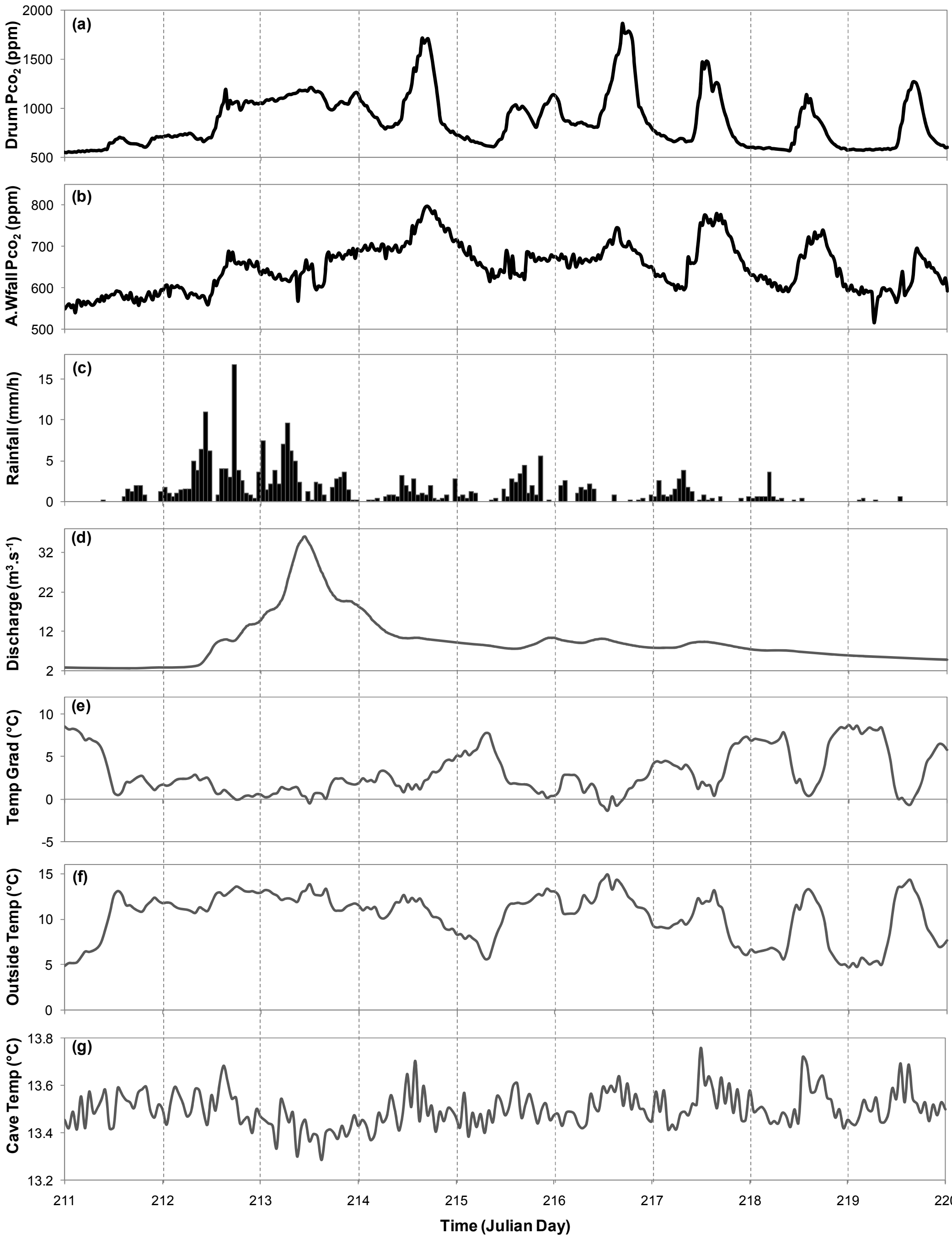

Figure 5.11. Ruakuri Cave and stream monitoring data for days 211 – 219 (29th July – 6th August) 2008. (a) Cave air PCO_2 (recorded in the Drum Passage); (b) cave air PCO_2 (recorded at the Aggressive Waterfall); (c) rainfall; (d) Waitomo Stream discharge; (e) temperature gradient between the Ruakuri Cave (recorded in the Drum Passage) and external air temperature; (f) outside air temperature (recorded at the Waitomo weather station); and (g) Ruakuri Cave temperature (recorded in the Drum Passage). Dotted lines indicate midnight for each 24-hour period.

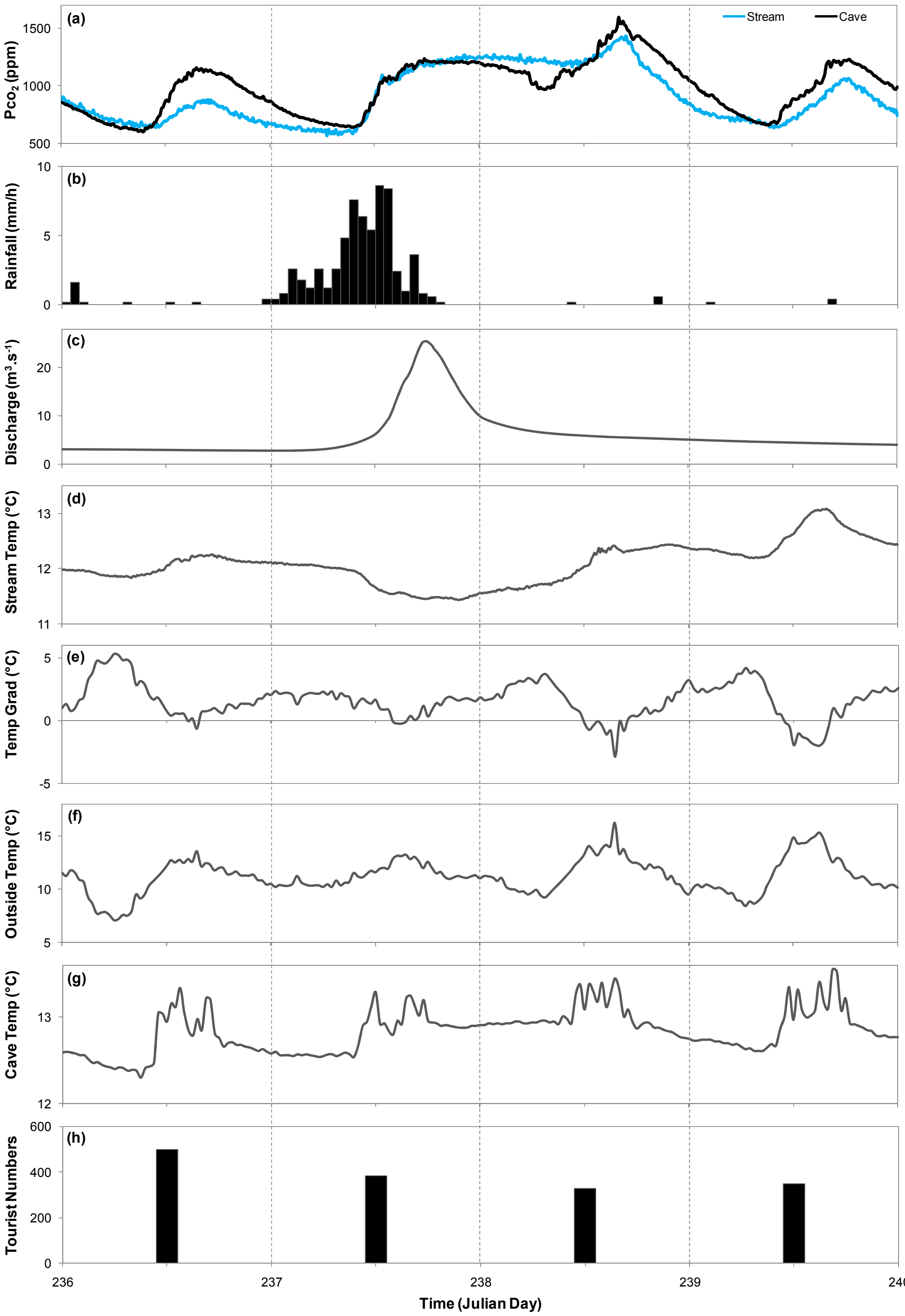

Figure 5.12. Glowworm Cave and Waitomo Stream monitoring data for days 236 – 239 (23rd – 26th August) 2008. (a) Cave air and stream P_{CO_2}; (b) rainfall; (c) Waitomo Stream discharge; (d) stream temperature; (e) temperature gradient between the Glowworm Cave and external air temperature; (f) outside air temperature; (g) Glowworm Cave temperature; and (h) tourist numbers. Dotted lines indicate midnight for each 24-hour period.

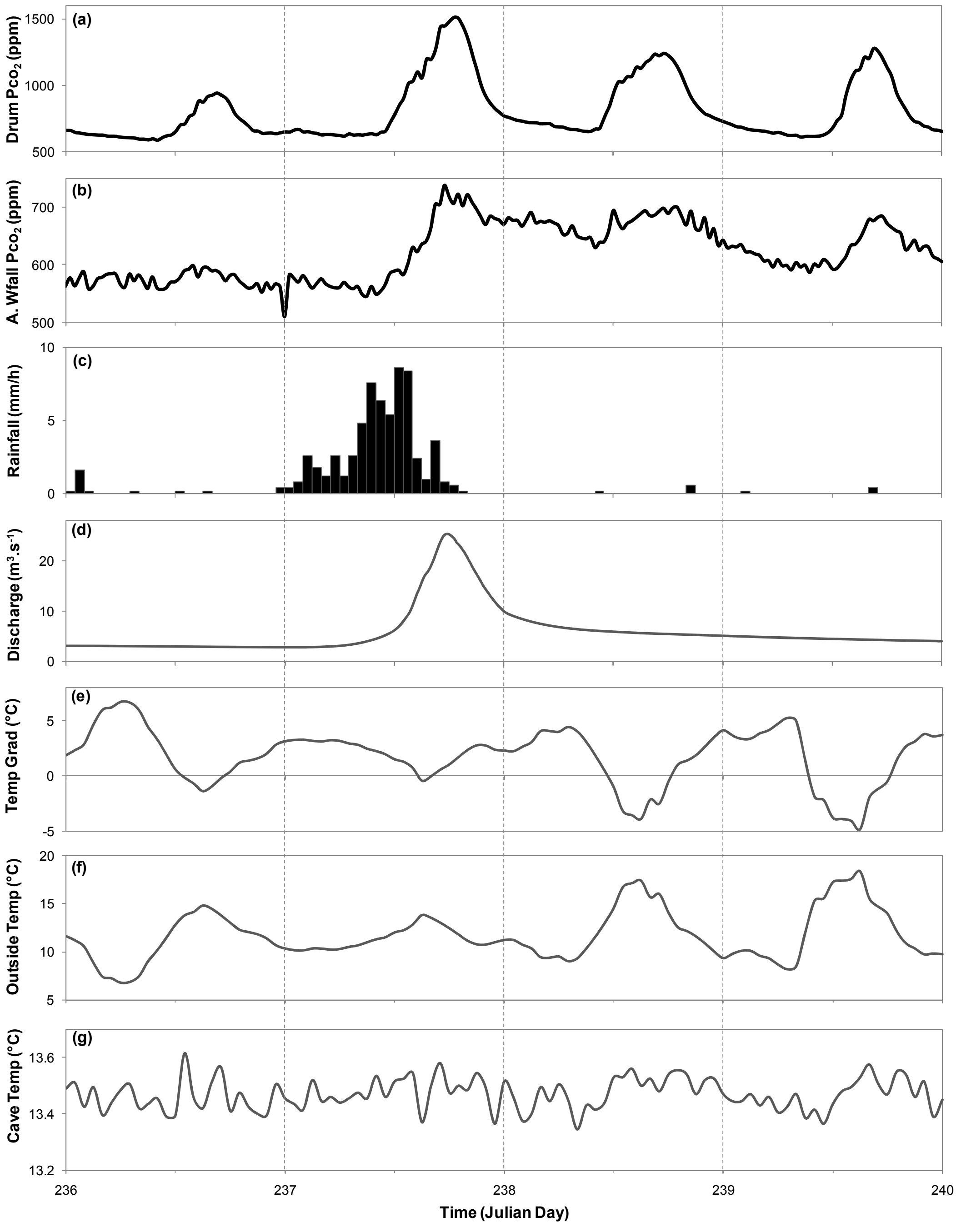

Figure 5.13. Ruakuri Cave and stream monitoring data for days 236 – 239 (23rd – 26th August) 2008. (a) Cave air PCO_2 (recorded in the Drum Passage); (b) cave air PCO_2 (recorded at the Aggressive Waterfall); (c) rainfall; (d) Waitomo Stream discharge; (e) temperature gradient between the Ruakuri Cave (recorded in the Drum Passage) and external air temperature; (f) outside air temperature (recorded at the Waitomo weather station); and (g) Ruakuri Cave temperature (recorded in the Drum Passage). Dotted lines indicate midnight for each 24-hour period.

5.6 Discussion

5.6.1 Seasonal trends in Waitomo Stream P_{CO_2}

The P_{CO_2} of the Waitomo Stream was higher during the summer months (with a base level of approximately 1000 ppm) than the winter months (base level of 500 ppm). Higher stream P_{CO_2} in the summer than in the winter may seem counterintuitive as the solubility of CO_2 decreases with increasing temperatures (Langmuir, 1997). The difference in average P_{CO_2} between summer and winter infer that an origin outside of the cave is responsible, however such an origin can only be speculated. One possible cause could be that the stream is constantly being recharged by groundwater that passes through the soil and karst aquifers, emerging into the stream at a relatively constant temperature and with relatively constant CO_2 concentrations (irrespective of season). In summer the stream warms this water and lowers the CO_2 solubility forcing the P_{CO_2} to increase. In winter the reverse would occur with the temperature of the groundwater dropping once in the stream, and thus the solubility of CO_2 in the stream rise, resulting in a decrease in the P_{CO_2}.

An alternative explanation as to why the stream P_{CO_2} is higher in the summer than in the winter may be that soil respiration (and thus soil CO_2) is higher during the warmer summer months. Water enriched with CO_2 from the soil, slowly percolates downwards to groundwater aquifers. As surface waters are supplied primarily by groundwater, and because groundwaters are highly enriched with CO_2 derived from the soil (Neal *et al.*, 2002), an increase in activity within the soil during the summer is a possible explanation for the observed seasonal differences in the Waitomo Stream P_{CO_2}. This has been termed the 'soil CO_2 effect' (Liu *et al.*, 2007). Research specific to Waitomo has also shown that biological activity within the soil increases during the spring and summer as temperatures increase (Gunn & Trudgill, 1982).

For the soil CO_2 effect to influence the stream P_{CO_2}, water must percolate through the soil. Even though sporadic rainfall, and thus some through-soil percolation, does occur throughout the summer at Waitomo, the relatively dry conditions mean that a proportion of the rainfall will remain within the soil as soil moisture recharge. Therefore, a discharge response, and thus an increase in the stream P_{CO_2} following the rainfall event, will not occur.

Other factors that can influence in-stream P_{CO_2} are physical processes (Rebsdorf *et al*., 1991). P_{CO_2} degassing is promoted by physical characteristics of streams including steeper bed gradient, increased turbulence, channel depth, flow velocities, etc. (Herman & Lorah, 1987; Rebsdorf *et al*., 1991). Whilst the stream bed gradient remains constant, the channel depth, flow velocities and degree of turbulence tend to increase during the winter in association with flood events. The increased physical turbulence of the water probably results in enhanced degassing of CO_2 from the Waitomo Stream.

The relationship between high summer and low winter CO_2 in streams is not a recent discovery, and considerable evidence exists in support of these trends. However the data provided here must be regarded with caution due to the limited period (six months, from July – December 2008) for which stream P_{CO_2} data was obtained.

5.6.2 Anomalous cave air P_{CO_2} and stream P_{CO_2}

Whilst it was reported that cave air CO_2 concentrations would be reduced during flooding or periods of steady rainfall (James, 1994), the Glowworm Cave air P_{CO_2} data does not support this. A clear relationship exists between Glowworm Cave air P_{CO_2} and Waitomo Stream P_{CO_2} (see Figure 5.6a, Figure 5.8a, Figure 5.10a and Figure 5.12a). 'Normal' patterns in Glowworm Cave air P_{CO_2} showed that during the day time the CO_2 of the Glowworm Cave air was higher than the Waitomo Stream. Typically streams have a P_{CO_2} that exceeds that of the surrounding atmosphere (Rebsdorf *et al*., 1991). However when the atmosphere above the stream already features elevated CO_2 concentrations (e.g. a cave), higher stream P_{CO_2} concentrations, with respect to the surrounding (cave) atmosphere, are less likely (e.g. this study). Cave air P_{CO_2} in the Glowworm Cave was elevated during the day as a result of anthropogenic CO_2 respired by daily tour groups within the cave. As the exchange of CO_2 across the air and water interface is rapid (Hoover & Berkshire, 1969), it is thought that when CO_2 in the cave air is higher than that of the stream, the stream will act as a CO_2 sink, as the cave air is constantly attempting to achieve an equilibrium with the stream. Equilibrium was usually reached just before the caves were due to open to tourists, with the cave air and stream P_{CO_2} both attaining a CO_2 concentration of approximately 400 – 500 ppm. During most anomalous cave air P_{CO_2} events, the pattern of higher cave air than stream P_{CO_2} was reversed, with the stream P_{CO_2} exceeding the cave air P_{CO_2}. When stream CO_2 exceeds atmospheric CO_2, streams will degas to achieve equilibrium, thus releasing CO_2 to the atmosphere (Neal *et al*., 2002). As degassing takes place within the Glowworm Cave the stream releases CO_2 into the cave, and thus acts as a CO_2 source. In systems such as caves, where air movement is usually limited, the P_{CO_2} would accumulate, resulting in increased cave atmosphere CO_2 levels. The consistent closely interacting relationship between cave air and stream P_{CO_2} is reasonable evidence that the Waitomo Stream alternates between acting as a source, or a sink, of CO_2 to the Glowworm Cave atmosphere.

Thus the hypothesis that anomalous increases in Glowworm Cave air P_{CO_2} were associated with increases in the Waitomo Stream P_{CO_2} (see section 5.1), is accepted, as supported by the evidence in this chapter.

5.6.3 Origin of anomalous stream P_{CO_2}

Streams are primarily groundwater fed (Neal *et al*., 2002). Groundwater contains high concentrations of CO_2 as a result of percolation through CO_2 enriched soils (Neal *et al*., 2002). Carbon dioxide in soils is produced in the O and A horizons (the top-most horizons of the soil) by microbial and plant root respiration, with soil moisture, temperature and plant activity controlling the rate of CO_2 production (White, 1988).

Soil CO_2 can be lost upwards to the atmosphere, and downwards into the groundwater, by dissolving in percolation waters. The percolation waters filter down through the unsaturated zone, and ultimately recharge the groundwater. Groundwater constantly enters nearby stream systems via flow paths which occur in the saturated zone. With rainfall, the soil surface becomes wet, restricting the loss of soil CO_2 to the atmosphere. The restriction of the CO_2 loss results in a rise of CO_2 in the soil, and thus soil water CO_2 levels also increase. The additional loading pressure of the rain at the surface results in CO_2 rich seepage being 'pushed' out of aquifers and into local stream systems. A relationship between rainfall and stream PCO_2 can, therefore, be expected.

The hypothesis which stated that the PCO_2 of the Waitomo Stream will respond to rainfall events was tested by comparing stream PCO_2 with rainfall and stream discharge data. Cave air PCO_2, temperature within and outside of the cave as well as the temperature gradient between the cave and outside air temperatures, were also plotted, to determine their possible contribution to cave air PCO_2 levels (Figure 5.4 to Figure 5.13). The temperature gradient decreased with each cave air PCO_2 anomaly. As the anomalous cave air PCO_2 events were also associated with rainfall events, the decrease in temperature gradient was likely to be a 'spin-off' effect from the associated low pressure system responsible for delivering the rain.

Rainfall and discharge were clearly associated with anomalous cave air PCO_2 events, with every anomalous event (i.e. elevated PCO_2 levels, and a failure to return to base level) coinciding with a period of increased stream discharge. Where rainfall events were too small to trigger a response in discharge there was generally no increase in stream and cave air PCO_2, thus suggesting that discharge was a better indicator of PCO_2 pulses into cave systems than rainfall. Discharge-induced responses in stream PCO_2 also supported the idea that the PCO_2 in the stream (which in turn contributes to the cave air PCO_2) originated from the soil, emphasising that rainfall events need to be significant enough to trigger a percolation event in the soil and a subsequent response in stream discharge for a change in stream and cave air PCO_2 to occur.

5.6.4 Flood events and Waitomo Stream PCO_2

Anomalous cave air PCO_2 and corresponding stream PCO_2 coincided with discharge-induced rainfall (or 'flood' events). Karst hydrological systems are characterised by widened joints, dolines and stream-sinks which enable rapid drainage of surface waters into large underground conduits (Ford & Williams, 2007). Observations of rapidly rising water levels within karst systems following rainfall highlight the responsive nature of conduit systems (as opposed to diffuse systems) (Groves & Meiman, 2005). Because rapid drainage is an inherent feature of karst landscapes (Groves & Meiman, 2005), including Waitomo (Gillieson, 1996), 'flood events' are common. The Waitomo Stream responds quickly to rainfall events. The hilly countryside of the upstream catchment, which, at the Glowworm Cave, is 43.2 km^2 (D. Stewart, pers. comm., 2008), as well as the conduit flow characteristic of the Waitomo karst hydrologic system, contribute to the responsive flow regime of the Waitomo Stream.

Hydrochemical responses of karst springs to storm-scale events have been increasingly studied over recent years. Liu *et al*. (2004) analysed the chemistry of fracture water and conduit water during flood periods in peak cluster karst in China. They found that the fracture water had higher PCO_2 whilst the conduit water had lower PCO_2 compared to lower flows. The contrasting trends highlighted that two key processes were occurring: dilution by precipitation (conduit waters) and water-rock-gas interactions (fracture waters). Further investigation into the relationship between flood events and the PCO_2 of karst conduit waters (at the spring emergence) (Liu *et al*., 2007) identified that rainfall intensity was also an important factor. During high intensity rainfall the PCO_2 of the water decreased, thus the dilution factor dominated. During lower intensity rainfall the PCO_2 of the water increased, thus the soil effect dominated (Liu *et al*., 2007). The Waitomo Stream PCO_2 data presented in this chapter (Figure 5.4) has not shown evidence of dilution with rainfall events, regardless of rainfall intensity, at least at the storm-scale.

Waitomo differs from most other karst systems due to the presence of thick tephric soils. The soils act as a barrier between the active soil root zone, where most of the CO_2 is generated, and the rock interaction zone, where the CO_2 is consumed. With no rainfall, soil moisture slowly drains into the limestone, taking CO_2 from the ventilated soil above. Upon contact with the limestone, the $CO_{2(aq)}$ in the soil moisture equilibrates with the calcite. Due to equilibrium being achieved, the PCO_2 of the percolated soil moisture is low. After moderate rainfall, ventilation from the root zone is impeded. The PCO_2 of the percolation water passing down from the root zone is raised, and the calcite solubility enhanced. With high rainfall, soil water is forced quickly through the soil and underlying limestone, with insufficient time for equilibrium to be reached. As a result, waters low in calcium, but much higher in P_{CO_2}, are discharged.

With respect to the hypothesis that increases in the Glowworm Cave air P_{CO_2} were associated with increased Waitomo Stream P_{CO_2}, it must be mentioned that rainfall results in a rapid rise of the Waitomo Stream level. As the stream comprises a boundary of the lower entrance of the Glowworm Cave, when the stream rises the size of the entrance is reduced. This is likely to obstruct air movement, restricting air flushing of the cave and thus may also influence the cave air P_{CO_2} levels.

5.7 Conclusion

- The Waitomo Stream P_{CO_2} is seasonally variable, with higher P_{CO_2} levels during the summer (approximately 1000 – 1200 ppm) than the winter (600 – 1000). Higher summer P_{CO_2} concentrations are probably the result of several factors, including:
    - warmer temperatures enhancing microbial and root respiration thus resulting in more soil CO_2 entering streams via percolation waters;
    - decreased flow rates and thus agitation of the stream due to lower summer flows; and
    - a greater concentration gradient between the Glowworm Cave air and the Waitomo Stream due to higher tourist numbers during the summer months.
- The hypothesis that anomalous increases in the Glowworm Cave air P_{CO_2} were associated with increased Waitomo Stream P_{CO_2}, could be accepted. Disequilibrium in the P_{CO_2} levels between the Glowworm Cave air and the Waitomo Stream P_{CO_2} promoted the movement of CO_2 between the streamwater and cave air. When the Waitomo Stream had a higher P_{CO_2}

than the Glowworm Cave air, the disequilibrium resulted in the stream degassing, thus acting as a source of CO_2 to the cave air. Conversely, when the Glowworm Cave PCO_2 was higher than the Waitomo Stream PCO_2, the relationship between the cave and the stream is reversed, resulting in the stream acting as a CO_2 sink.

- The Waitomo Stream PCO_2 did increase with rainfall events, but only when the rainfall event was large enough to induce a discharge response in the Waitomo Stream. Therefore, the hypothesis that the PCO_2 of the Waitomo Stream increased following rainfall events can be accepted in part. An alternative hypothesis, which the data supports, is that the Waitomo Stream PCO_2 increased when the discharge of the Waitomo Stream increased.

6.0 Chapter Six: Origin of stream P_{CO_2} – examining dripwater and stream geochemistry

6.1 Introduction

The P_{CO_2} of the Waitomo Stream increases during storm events where rainfall is substantial enough to induce a discharge response in the Waitomo Stream (Chapter Five). A possible source of stream CO_2 induced by storm events is the soil. Rainfall saturates the soil surface essentially forming a seal that temporarily restricts the loss of CO_2 to the atmosphere (McLaren & Cameron, 1996). Continued plant and microbial respiration contributes CO_2 to the soil atmosphere, which accumulates due to the limited movement of air within the soil pores. The CO_2 in the soil atmosphere is then dissolved by the percolating waters. Under-saturated conditions the water moves relatively rapidly down through the soil to the water table and into the stream as recharge, transporting dissolved CO_2 in the process. If the increase in the Waitomo Stream P_{CO_2} is a result of CO_2 being flushed from the soil during storm events, then it is possible that dripwaters would show a similar response.

Chapter Six investigates dripwater P_{CO_2} to identify if a correlation existed between dripwater and Waitomo Stream P_{CO_2}. In addition, the geochemistry of the Waitomo Stream and the Glowworm Cave dripwaters was analysed. Streamwater samples were collected daily from the Waitomo Stream and the Ruakuri (or Okohua) Stream. Dripwater samples were collected intermittently, and are indicative of the mean dripwater chemistry between sampling periods. Additionally a series of dripwater samples were collected using an autosampler, enabling a detailed record of dripwater chemistry to be obtained over a 48-hour period. All samples were analysed for sodium (Na) and calcium (Ca). All samples (except those collected using the autosampler), were also analysed for bicarbonate (HCO_3^-) and $\delta^{13}C$. It was anticipated that the chemistry data would help to determine the origin of the additional Waitomo Stream P_{CO_2} which enters the system during storm events.

6.2 Hypothesis and chapter objective

The objective of this chapter was to test the hypothesis that;

- **the additional P_{CO_2} in the Waitomo Stream, during times of increased discharge, was derived from relatively rapid throughflow from the soil.**

6.3 Dripwater P_{CO_2}

A straw stalactite in the Blanket Chamber of the Glowworm Cave was monitored to determine if the dripwater P_{CO_2} changed during rainfall events. The collection of P_{CO_2} data began in July 2008 using a Vaisala GMP222 sensor that could measure CO_2 within the range of 0 – 5000 ppm. The dripwater had a substantially higher CO_2 content than the Waitomo Stream or the Glowworm Cave air, (mean P_{CO_2} of 3484 ppm, and range of 6336 ppm for days 322 – 377, 17th November

2008 – 11th January 2009), thus it became apparent that the 0 – 5000 ppm CO_2 sensor range was inadequate for obtaining dripwater P_{CO_2} data (Figure 6.1). A new sensor (also a Vaisala GMP222) capable of measuring CO_2 up to 10000 ppm was installed in November, with data recorded until the 10th January 2009 (Figure 6.2). Gaps in the data indicated periods when the dripwater monitoring system was modified to some degree, resulting in human induced fluctuations in the data (Figure 6.1).

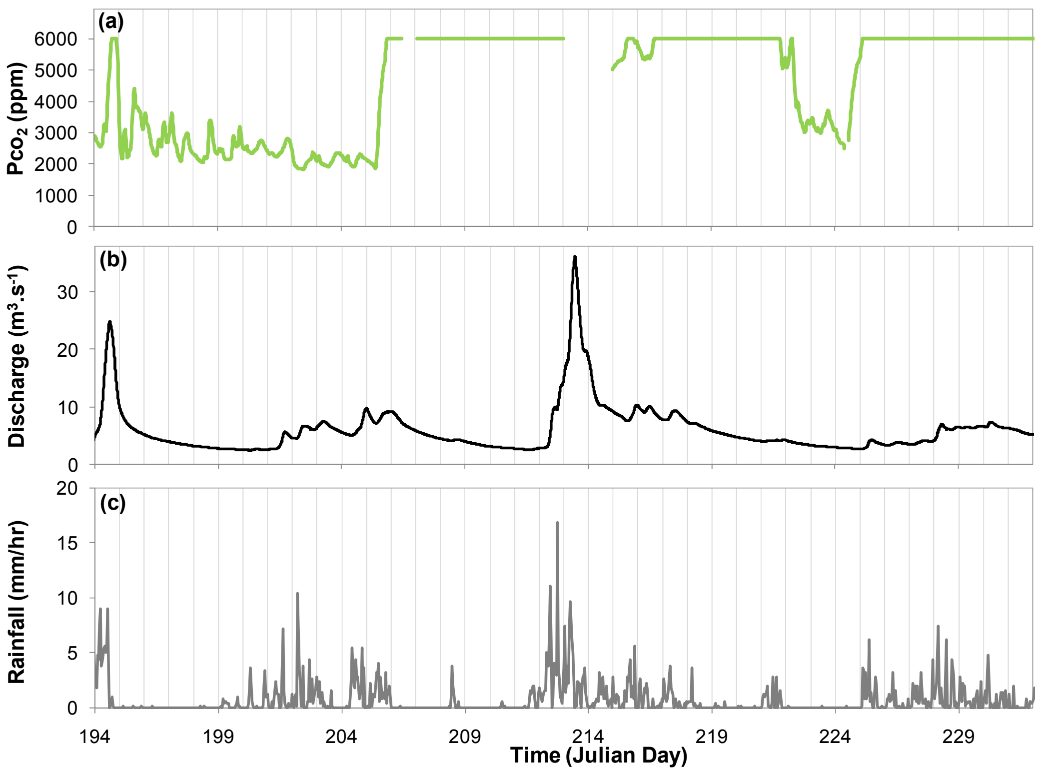

Figure 6.1. Dripwater P_{CO_2}, rainfall and Waitomo Stream discharge for the period 12th July – 18th August 2008. (a) Dripwater P_{CO_2} (two-hourly running mean) from a straw stalactite in the Blanket Chamber, Glowworm Cave; (b) Waitomo Stream discharge and (c) rainfall data. Flat-line data at 6000 ppm indicated periods when the P_{CO_2} of the dripwater reached levels outside of the range measured by the sensor.

Generally the P_{CO_2} of the dripwater increased when discharge in the Waitomo Stream increased (day 194 of 2008, Figure 6.1; day 323 of 2008, Figure 6.2; and days 360, 365 of 2008, 367 and 370 (1st and 4th January 2009), Figure 6.3). However, at times the inverse occurred (days 330 – 331 2008), with decreased dripwater P_{CO_2} as the Waitomo Stream discharge increased.

Variability in the P_{CO_2} of the dripwaters changed substantially over the course of the monitoring (July – August 2008, November – December 2008, and January 2009). In July and August (Figure 6.1), and November through to the beginning of December (days 322 – 336 of 2008; Figure 6.2) the P_{CO_2} of the dripwater varied between 1500 and > 6000 ppm. For the remainder of the sampling period (6th December – 11th January) the variation in the P_{CO_2} of the dripwater decreased to a range of 2500 – 4500 ppm. The differences observed in the dripwater P_{CO_2} between July and August ('winter', Figure 6.1) compared to November, December and January ('summer', Figure 6.2 and Figure 6.3) may be associated with the differences in magnitude of the discharge events between summer and winter. The faster rate of water transmission through the soil (due to the ground being saturated, Gillieson, 1996) and the associated rapid increase in stream discharge may be a contributing factor to the variability in dripwater P_{CO_2}. During periods of low (days 341 – 358 of 2008) or subsiding (days 196 – 205 of 2008) discharge, the dripwater P_{CO_2} fluctuated between 2900 and 3600 ppm, regardless of season.

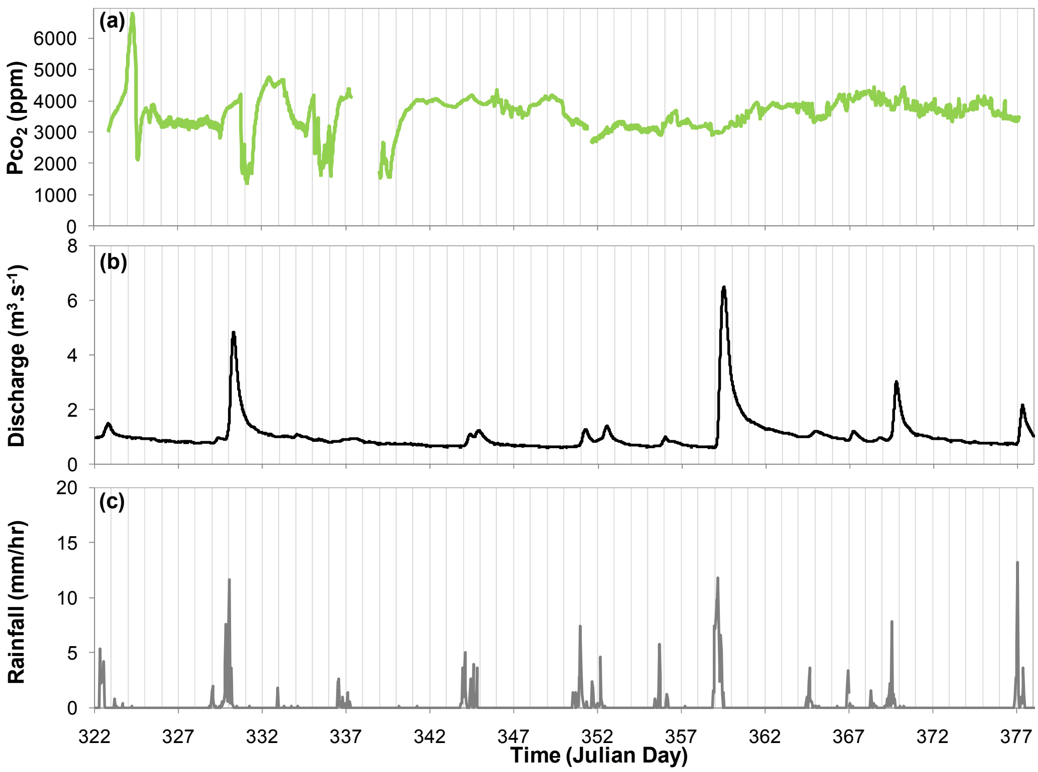

Figure 6.2. Dripwater P_{CO_2}, rainfall and Waitomo Stream discharge for the period 17th November 2008 – 11th January 2009. (a) Dripwater P_{CO_2} (two-hourly running mean) from a straw stalactite in the Blanket Chamber, Glowworm Cave; (b) Waitomo Stream discharge and (c) rainfall data.

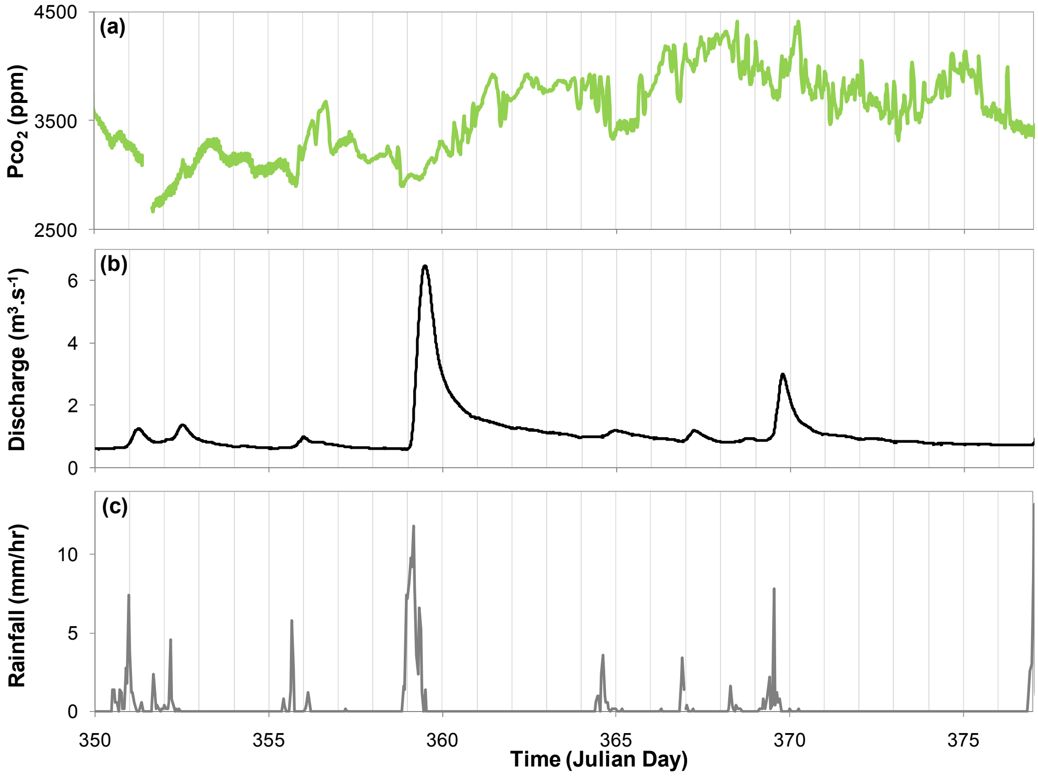

Figure 6.3. Dripwater P_{CO_2}, rainfall and Waitomo Stream discharge for the period 15th December 2008 – 11th January 2009, an enlargement of Figure 6.2. (a) Dripwater P_{CO_2} (two-hourly running mean) from a straw stalactite in the Blanket Chamber, Glowworm Cave; (b) Waitomo Stream discharge and (c) rainfall data.

6.4 Geochemistry of stream and dripwaters

The stream and dripwater chemistry was analysed for HCO_3^-, Ca^{2+}, Na^+, Mg^{2+} and K^+. Like the trends in the P_{CO_2} of the Waitomo and Ruakuri Streams (Chapter Five, and briefly summarised in Table 6.1), the ion concentrations for the Waitomo and Ruakuri Streams were, on average, higher in summer than winter (Table 6.1). Concurrently, summer months corresponded with lower rainfall, discharge, and water levels. The concurrence of lower rainfall and higher ion concentrations in the streamwater in summer than winter highlighted the influence of dilution during wetter periods.

Table 6.1. General chemical and physical properties of the Waitomo and Ruakuri Streams and dripwater from a straw stalactite in the Blanket Chamber of the Glowworm Cave for 2008. The summer and winter total mean of daily means are given for each site. Sample size for each parameter is given italicised and in parentheses.

	Mean daily rainfall (mm)	Mean daily discharge ($m^3.s^{-1}$)	Mean water level (m)	P_{CO_2} (ppm)	HCO_3^- (ppm)	Ca^{2+} (ppb)	Na^+ (ppb)	Mg^{2+} (ppb)	K^+ (ppb)	Water temp (°C)
Waitomo Stream										
Summer	4.64 *(182)*	0.800 *(182)*	0.413 *(145)*	1161 *(62)*	120 *(92)*	21079 *(90)*	6439 *(90)*	2069 *(90)*	856 *(90)*	13.60 *(67)*
Winter	9.2 *(184)*	3.121 *(184)*	0.621 *(184)*	901 *(117)*	80 *(114)*	17816 *(114)*	6005 *(114)*	1310 *(114)*	948 *(114)*	10.64 *(99)*
Ruakuri Stream										
Summer	4.64 *(182)*		0.328 *(61)*		115 *(44)*	22232 *(44)*	6632 *(44)*	1840 *(44)*	1139 *(44)*	13.67 *(61)*
Winter	9.2 *(184)*		0.407 *(18)*		86 *(123)*	18626 *(123)*	6032 *(123)*	1392 *(122)*	936 *(122)*	12.44 *(68)*
Dripwater in the Blanket Chamber, Glowworm Cave										
Summer	4.64 *(182)*			3407 *(45)*						
Winter	9.2 *(184)*				238 *(11)*	56500 *(11)*	9063 *(11)*	3616 *(11)*	397 *(11)*	

The sporadic nature of the dripwater sampling in conjunction with the discontinuous P_{CO_2} record means that robust seasonal comparisons cannot be made, however it is clear from the data available that the chemistry of dripwater (for the P_{CO_2} and all measured ions, except for K^+) is more concentrated than streamwaters. Dripwaters contain more than double the concentration of HCO_3^-, Ca^{2+}, and Mg^{2+} than the Waitomo and Ruakuri Streams. The higher ion concentrations are due to the longer residence time of the dripwater within the limestone.

A comparison of the Waitomo and Ruakuri Stream chemistries for days with, and days without, rain emphasised the dilution response of the streamwater to rainfall events (Appendix A.4). Whilst P_{CO_2}, HCO_3^-, Ca^{2+}, Na^+ and Mg^{2+} in the Waitomo and Ruakuri Streams were lowest during the winter and on rainy days (i.e. dilution effect), K^+ showed the opposite trend. This was unusual and suggests that K^+ (which is likely to be derived from fertilisers) may be being displaced by Ca^{2+} in the soil, and leached from the soils by the rainwater.

6.4.1 Bicarbonate

The bicarbonate (HCO_3^-) within the Waitomo and Ruakuri Streams decreased as discharge increased (Figure 6.4). During the first 100 days of the year (the summer months of January – April), the HCO_3^- in the streamwater fluctuated between 100 and 140 ppm. The flow of the Waitomo Stream had been particularly low between January and April 2008, due to the drought in the Waikato region. The mean daily flows between 1st January and 8th April were less than 0.28 $m^3.s^{-1}$ for 28 days. The discharge value of 0.28 $m^3.s^{-1}$, represents the 99th percentile of low flow for the Waitomo Stream, calculated from 21 years of data between 1986 and 2007 (i.e. 99% of the time the Waitomo Stream discharge will be above 0.28 $m^3.s^{-1}$, with discharge falling below 0.28 $m^3.s^{-1}$ for roughly four days each year).

A large rainfall event occurred over days 105 and 106 (14th and 15th April 2008). The rainfall triggered a rapid rise in the Waitomo Stream discharge and an immediate decrease in HCO_3^- from 130 – 46 ppm in the Waitomo Stream and 120 – 59 ppm in the Ruakuri Stream. In a dry period, between days 131 and 160 (10th May – 8th June), the HCO_3^- steadily increased. Between June and October, rain frequented the Waitomo and Ruakuri Stream catchments. The rainfall events coincided with decreased HCO_3^- concentrations. The negative relationship between HCO_3^- and rainfall highlighted the dilution response of HCO_3^- to rainfall events (Figure 6.5).

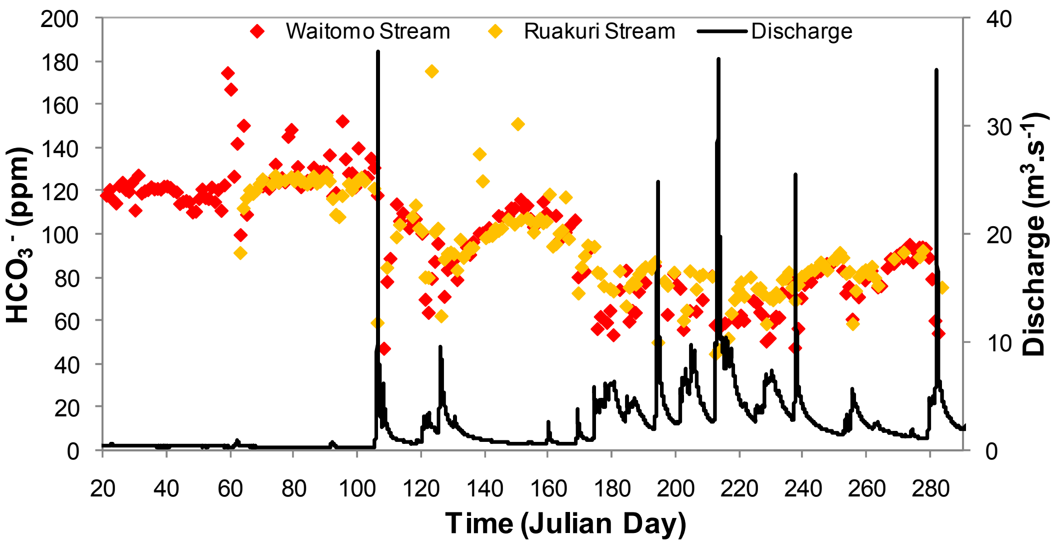

Figure 6.4. Daily bicarbonate concentrations in the Waitomo and Ruakuri Streams, and Waitomo Stream discharge plotted against time in Julian Days of 2008 (21st January – 9th October).

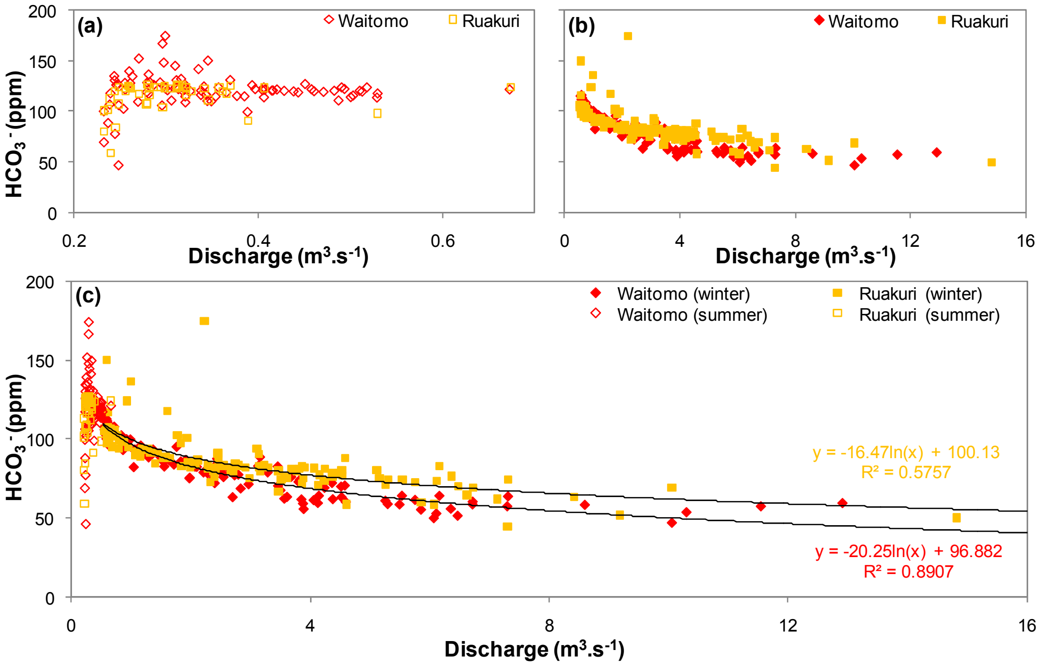

Figure 6.5. Relationship between HCO_3^- and discharge for the Waitomo and Ruakuri Stream waters. (a) HCO_3^- and discharge for the Waitomo and Ruakuri Stream waters during the summer months of January – April 2008; (b) HCO_3^- and discharge for the Waitomo and Ruakuri Stream waters during the winter months of May – October 2008; and (c) relationship between HCO_3^- and discharge for the combined summer and winter data for the Waitomo and Ruakuri Stream waters. A logarithmic trend line has been applied to the winter data for the Waitomo and Ruakuri Streams.

There is a clear trend of increasing HCO_3^- during dry periods (due to streamwater dominated by concentrated groundwater recharge), and decreasing HCO_3^- during rainfall events (due to dilution of streamwater from overland flow and rapid throughflow) (Figure 6.6). In May and June (Figure 6.6a) the HCO_3^- in both the Waitomo and Ruakuri Streams fluctuated around 110 ppm. During September the HCO_3^- was lower, fluctuating between 80 – 100 ppm (Figure 6.6b). Stream discharge was higher in September compared to the May – June period (Figure 6.6a and b). This provided evidence that HCO_3^- concentrations in the Waitomo and Ruakuri Streams increased in response to low water levels and concentrated groundwater inputs, and decreased (by dilution) with rising water levels.

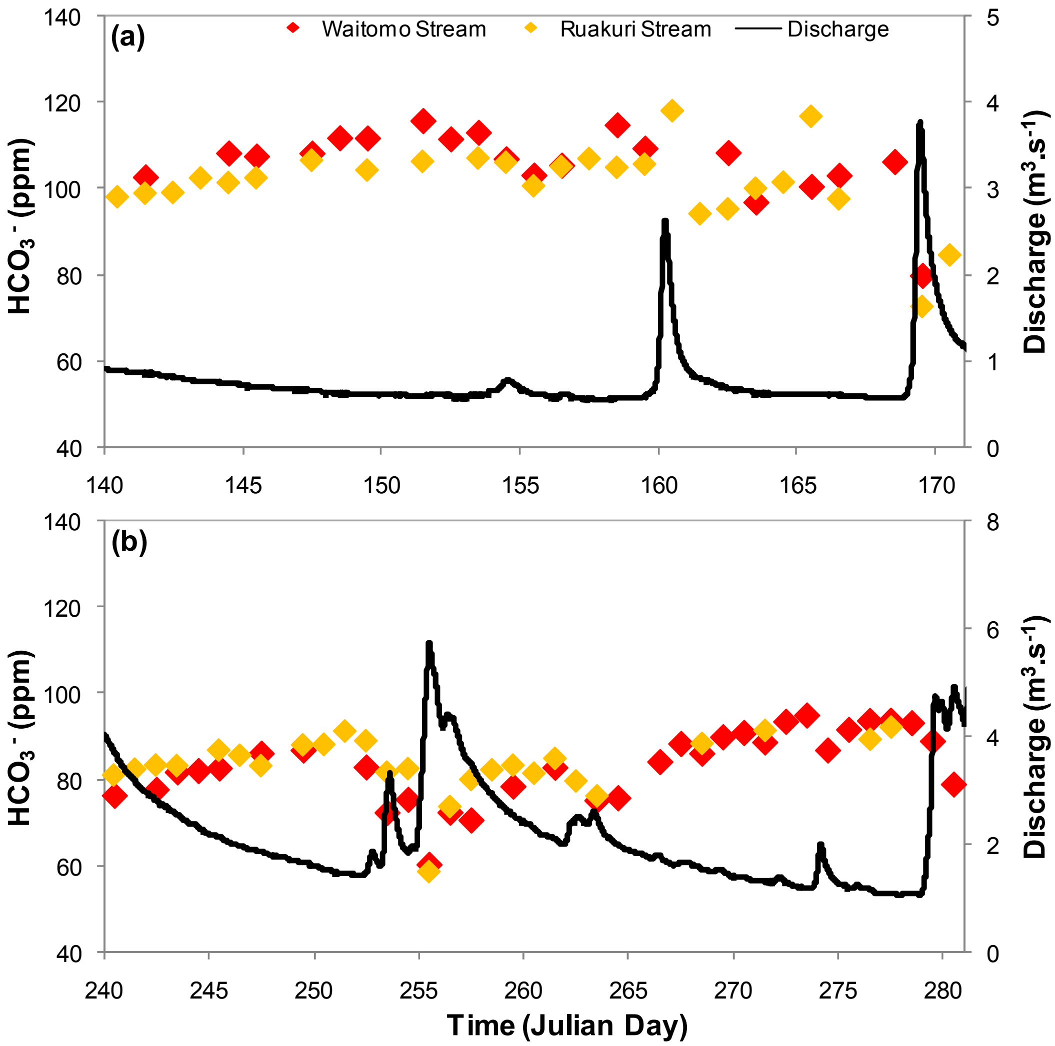

Figure 6.6. Two events highlighting the relationship between increased discharge and HCO_3^- concentrations within the Waitomo and Ruakuri Streams; (a) 19th May – 18th June 2008, and (b) 27th August – 6th of October 2008.

6.4.2 Calcium and sodium

During normal flow, the Waitomo and Ruakuri Streams showed similar Ca^{2+} concentrations. The Ca^{2+} concentrations for both streams were highest during the summer and lowest during the winter (Figure 6.7a), following the seasonal pattern of HCO_3^- and P_{CO_2} in the Waitomo Stream. During periods of increased stream discharge the Ca^{2+} concentration in the Waitomo and Ruakuri Streams almost always decreased (e.g. Figure 6.7a and Figure 6.8a and c), however occasionally the Ca^{2+} concentration increased with rainfall when the discharge increased (Figure 6.9). The Na^+ concentration also decreased as stream discharge increased (Figure 6.7b and Figure 6.8b). However, the trend was absent between day 20 and day 100 (20th January – 9th April 2008) in the Na^+ chemistry of the Waitomo Stream (Figure 6.7b). Prior to day 100, the Na^+ concentration decreased (from approximately 7000 ppb to 6000 ppb). This coincided with the dry weather that caused the 2008 drought in the Waikato. On day 61, 27 mm of rain fell and, in concordance with the rain event, the Na^+ concentration of the Waitomo Stream increased for about 15 days, after which the Na^+ in the Waitomo Stream decreased substantially. This was opposite to the increasing trend with rainfall observed in the Waitomo and Ruakuri Streams for the Ca^{2+} data, as well as for the Na^+ data collected during the winter of 2008.

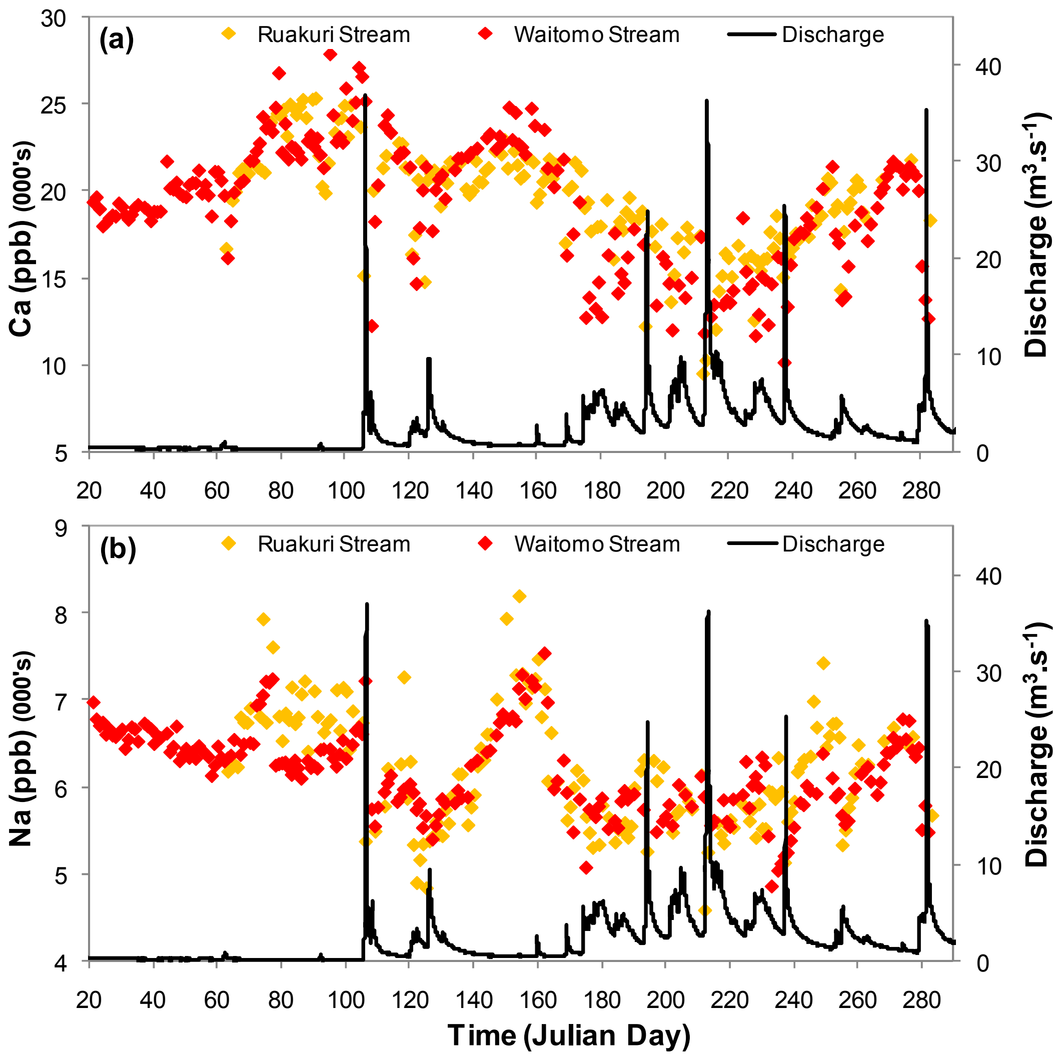

Figure 6.7. The concentrations of Ca^{2+} and Na^+ in the Waitomo and Ruakuri Streams and Waitomo Stream discharge plotted against time. (a) Ca^{2+} and (b) Na^+, with discharge plotted on each figure. Data range from the 21st January – 16th October 2008.

An intense rainfall event occurred on days 212 and 213 (30th and 31st July), which resulted in a considerable increase in Waitomo Stream discharge, as well as anomalous cave air and stream P_{CO_2} which lasted until day 220 (7th August) (see Figure 5.10, Chapter Five). The Ca^{2+} and Na^{+} chemistry of the Waitomo and Ruakuri Streams, for this same anomalous period (day 210 – 221, 29th July – 7th August) both show a decrease in Ca^{2+} and Na^{+} concentrations corresponding to the discharge increase (Figure 6.8). Water samples collected at 2-hour intervals from a stalactite drip in the Blanket Chamber (6th – 8th October) during a substantial rainfall event, also showed decreased Ca^{2+} and Na^{+} concentrations with increased stream discharge (Figure 6.10).

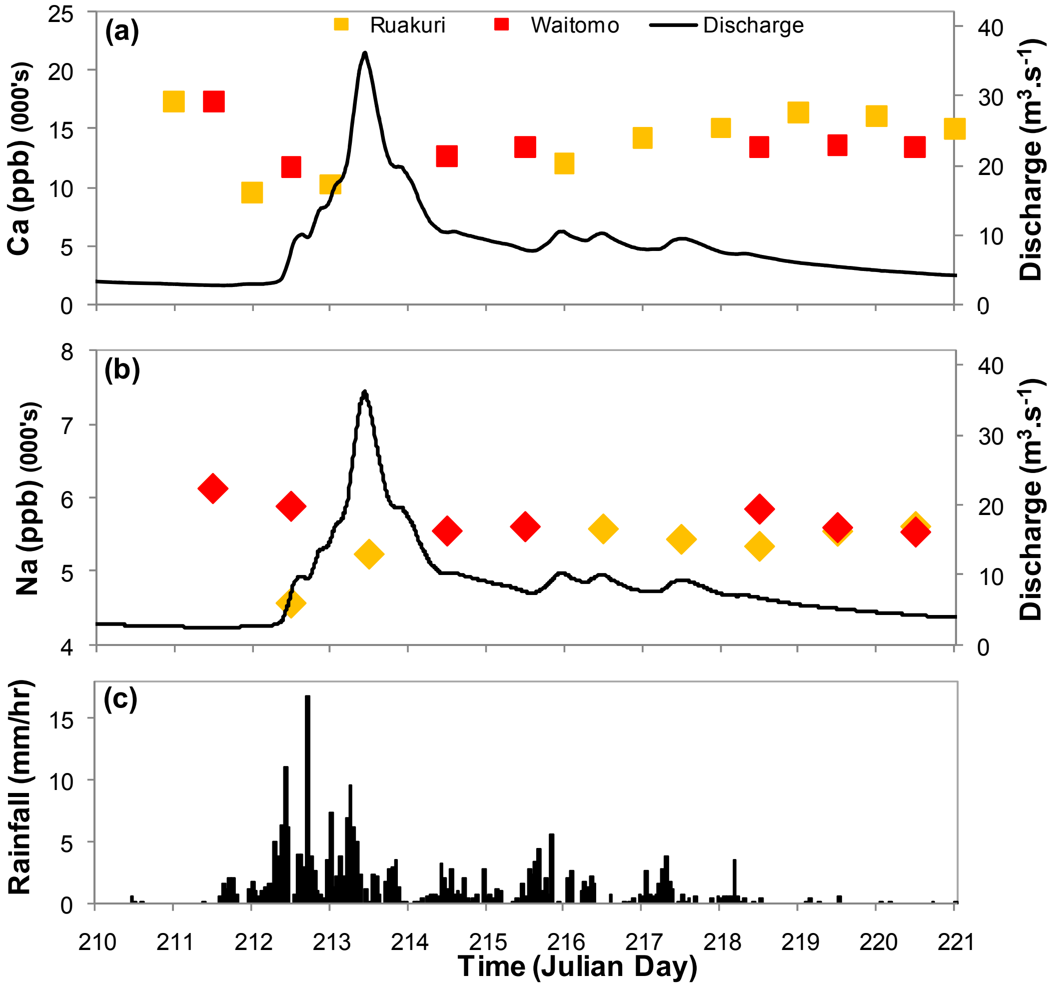

Figure 6.8. The concentrations of Ca^{2+} and Na^{+} in the Waitomo and Ruakuri Streams and Waitomo Stream discharge plotted against time. (a) Ca^{2+} and (b) Na^{+}, with discharge plotted on each figure. (c) Hourly rainfall data for the 29th July – 7th August 2008. Data presented are for the anomalous event which occurred from the 29th July – 7th August 2008, as described in Figure 5.10, Chapter Five.

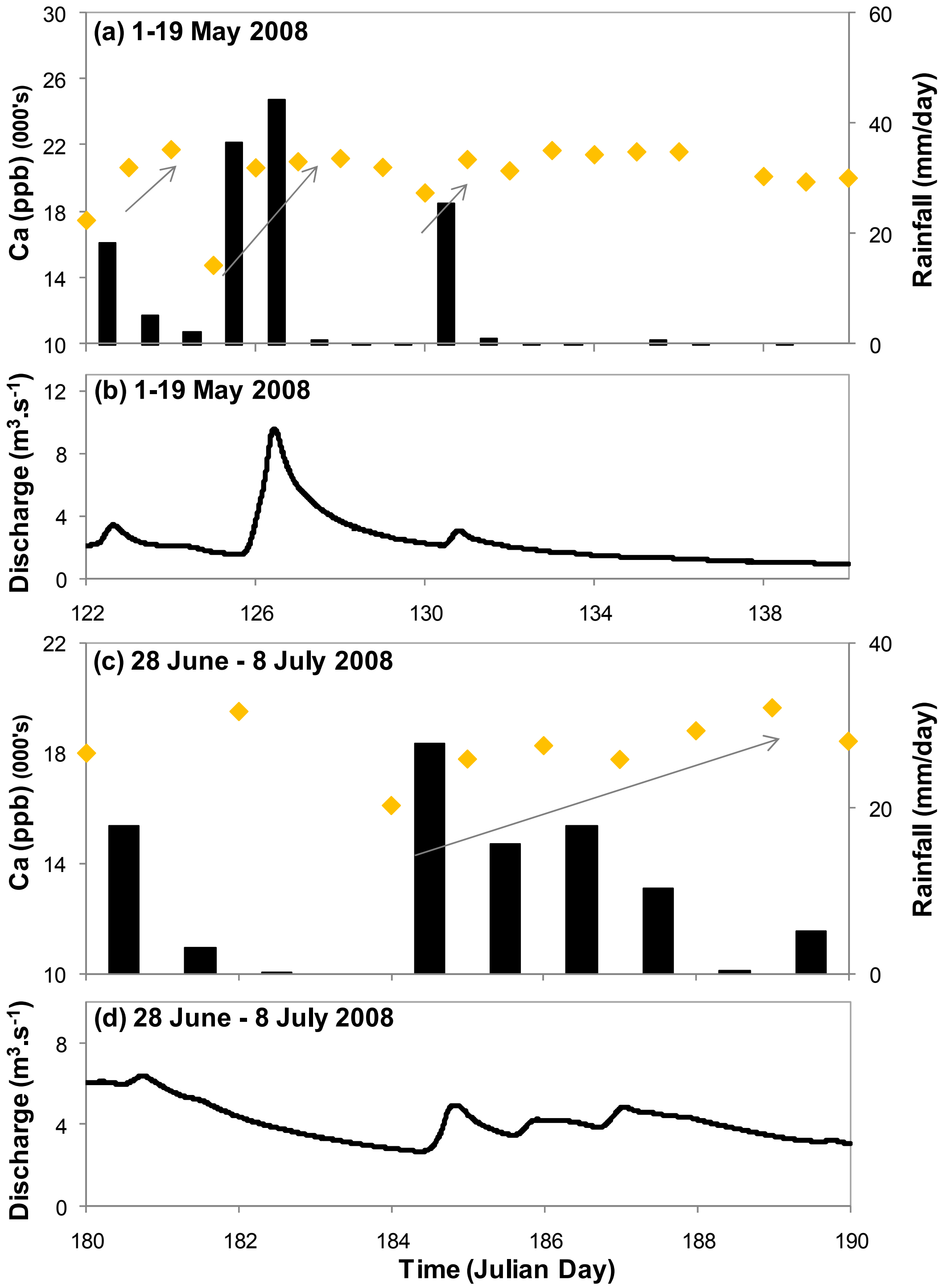

Figure 6.9. The concentration of Ca^{2+} in the Ruakuri Stream with (a) rainfall and (b) discharge for the 1st – 19th May 2008; and (c) rainfall and (d) discharge for the period 28th June – 8th July 2008. Grey arrows indicate periods where the Ca^{2+} concentration increased with rainfall and increased discharge.

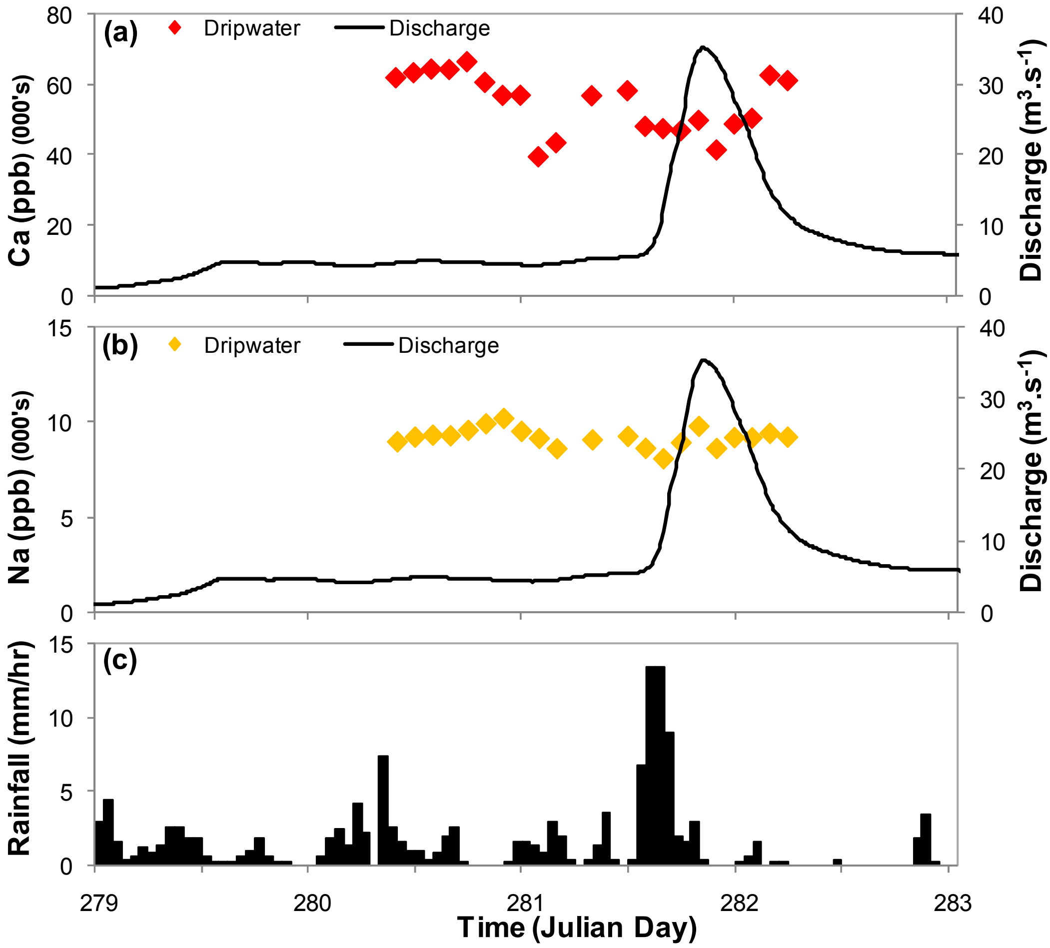

Figure 6.10. The concentrations of Ca^{2+} and Na^{+} in the dripwater of a straw stalactite in the Blanket Chamber, Glowworm Cave, plotted with Waitomo Stream discharge data. (a) Ca^{2+} and (b) Na^{+} concentrations from the dripwater collected over a 46-hour period between 10.00 a.m. on the 6th and 6.00 a.m. on the 8th of October 2008. (c) Hourly rainfall data for the period 6th – 8th October 2008.

6.5 $\delta^{13}C$ measurements

6.5.1 Background

Carbon (C) naturally occurs as two stable isotopes ^{12}C and ^{13}C. ^{12}C has an atomic weight (by definition) of exactly 12 atomic mass units (amu) and is by far the most abundant, making up about 98.9% of all C. ^{13}C has an atomic weight of 13 amu and accounts for about 1.1% of all C. Together ^{12}C and ^{13}C make up natural carbon which has an atomic weight of 12.011 amu (Langmuir, 1997).

A variety of natural processes can lead to small changes in the proportions of ^{12}C to ^{13}C, and this is known as isotopic fractionation (Craig, 1953). Such changes are normally expressed in terms of carbon isotopic composition ($\delta^{13}C$) where:

$$\delta^{13}C(‰) = \left[\frac{^{13}C/^{12}C(sample) - ^{13}C/^{12}C(standard)}{^{13}C/^{12}C(standard)}\right] \times 10^3 \quad \text{(Equation 6.1)}$$

The standard is known as PDB which is a calcite-PDB belemnite, a marine carbonate fossil, for which, by definition $\delta^{13}C = 0$ ‰ (zero per mil) (Craig, 1957). Negative $\delta^{13}C$ values reflect enrichment in ^{12}C, whilst positive (or less negative $\delta^{13}C$) values indicate ^{13}C enrichment. Typical $\delta^{13}C$ values for various materials are illustrated in Figure 6.11.

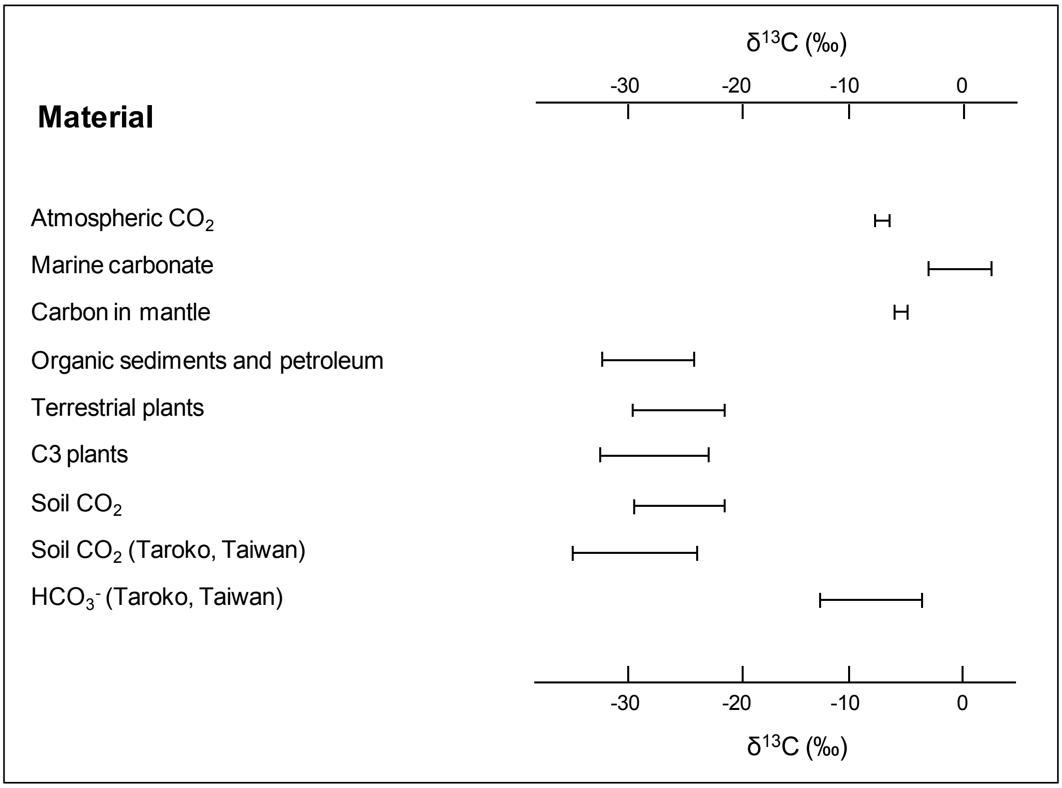

Figure 6.11. The carbon isotope composition of natural materials (adapted from Yoshimura *et al.*, 2001 after Sakai and Matsuhisa, 1996).

Inorganic C within the Waitomo and Ruakuri Stream systems comes from three main sources: atmospheric CO_2, soil air CO_2 and HCO_3^- derived from limestone (through the dissolution process). Atmospheric CO_2 has a carbon isotopic composition of approximately -7 ‰ (Craig, 1953; Yoshimura *et al.*, 2001). The soil air $\delta^{13}C$ is about -24 ‰ (-22 – -29 ‰, Langmuir, 1997) and is more negative than the atmosphere due to plant (and microbial) respiration (microbially respired CO_2 has a $\delta^{13}C$ very similar to that of vegetation, Clark & Fritz, 1997). $HCO_3^-{}_{(aq)}$ sourced from the limestone, has a $\delta^{13}C$ of approximately 0 ‰. When soil air CO_2 is hydrated and subsequently dissociated to HCO_3^-, the $\delta^{13}C$ increases to roughly -15.1 ‰ due to enrichment (ε) (ε values during hydration and dissociation for various C species are given in Figure 6.12). Although there are three species of dissolved inorganic carbon present in karst waters, $CO_{2(aq)}$, HCO_3^- and CO_3^{2-}, virtually all the C is in the form of HCO_3^-, therefore the $\delta^{13}C$ is often referred to as $\delta^{13}C_{HCO_3}$ (Yoshimura *et al.*, 2001). Soil air (plant) and limestone derived CO_2 are the primary contributors forming HCO_3^- in karst waters. Soil derived C makes up approximately 60% of the HCO_3^- in the stream, whilst the remaining 40% is derived from the limestone (C. Hendy, pers. comm., 2008). Thus, the Waitomo Stream would be expected to have a $\delta^{13}C$ of ~ -15 ‰.

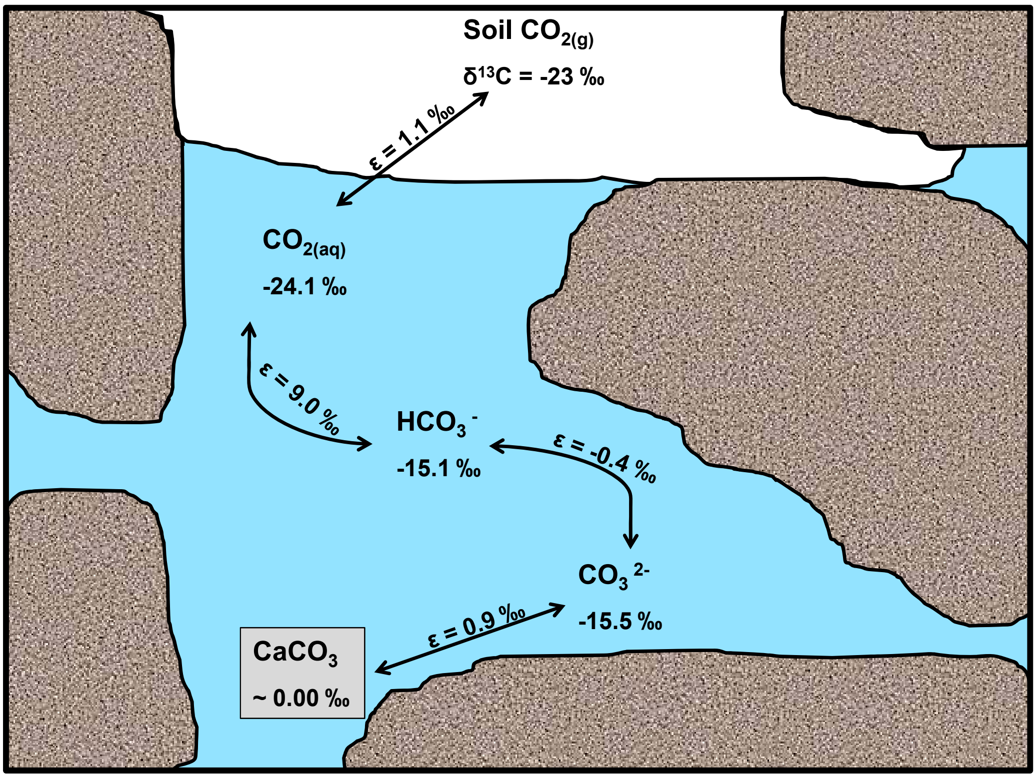

Figure 6.12. Schematic of ^{13}C isotope fractionation during equilibrium exchange of C between CO_2, dissolved inorganic C and $CaCO_3$ (at 25 °C, with the assumptions of geochemical equilibrium conditions and calcite saturation) and the ready exchange between soil air CO_2 and the reaction solution (open system) (Hendy, 1971) (adapted from Clark & Fritz, 1997).

6.5.2 *$\delta^{13}C$ isotope results*

The mean $\delta^{13}C$ was -11.55 ‰ for the Waitomo Stream and -11.57 ‰ for the Ruakuri Stream. The Waitomo Stream is in contact with the atmosphere ($\delta^{13}C$ = -8 ‰) and is interconnected with the limestone bedrock ($\delta^{13}C$ = 0 ‰) and the soil (and thus vegetation within the catchment) ($\delta^{13}C$ = -24 ‰) (Hendy, 1971). The $\delta^{13}C$ values are therefore reflective of the interactions between the stream and the environment. With respect to karst development (Chapter Two, Section 2.1.2), the Waitomo Karst is a "closed" system (due to the thick overlying tephra soils). The calcite dissolution processes therefore occur in isolation from the atmosphere. This results in a $\delta^{13}C$ level that reflects a greater contribution from the limestone. Both streams had a mean range of 3.82 ‰, with maximum $\delta^{13}C$ in the order of -10.4 ‰ and minimum values of about -14.2 ‰ (Figure 6.13).

Data for both the Waitomo and Ruakuri Streams showed systematic decreases in $\delta^{13}C$ values coinciding with increased discharge (Figure 6.14). The degree of decline in the $\delta^{13}C$ value in the event of rainfall differed, but was usually between 1 – 2 ‰. Large events of increased discharge typically resulted in relatively large decreases in the $\delta^{13}C$, e.g. day 106 when discharge exceeded 35 $m^3.s^{-1}$ the $\delta^{13}C$ value decreased by 2.06 ‰ (from -10.74 – -12.8 ‰ in one day). However, on occasions, substantially smaller rainfall events yielded a drop in the $\delta^{13}C$ value of a similar magnitude to that of large flood events, e.g. day 171, discharge was approximately 5 $m^3.s^{-1}$ (elevated above the mean level of 1.7 $m^3.s^{-1}$) and the $\delta^{13}C$ value decreased by 2.19 ‰ (from -10.3 – -12.49 ‰ in three days). Conversely, some large discharge events yielded little change in the $\delta^{13}C$ value (e.g. days 240 – 244, $\delta^{13}C$ value decreased by 0.61 ‰, from -11.75 – -12.36 ‰, during which time the maximum discharge was 25.4 $m^3.s^{-1}$), whilst other, smaller discharge events yielded relatively large decreases in the $\delta^{13}C$ value (e.g. maximum discharge of 0.9 $m^3.s^{-1}$ between days 59 – 65, when the $\delta^{13}C$ value decreased by 1.82 ‰, from -11.5 – -13.32 ‰).

Seasonal variability was clearly evident in the $\delta^{13}C$ of the Waitomo and Ruakuri Stream waters. The summer mean for both sets of data was -11.32 ‰ whilst the winter average was -11.74 ‰ (Figure 6.13 and Figure 6.14). The lower summer

$\delta^{13}C$ value reflected that groundwater was the main source of recharge to the stream, during the summer, with limited dilution occurring. Also, as the rate of throughflow was reduced due to low soil moisture contents and less water in the aquifer, the groundwater remained in contact with the $\delta^{13}C$ = 0 ‰ limestone for longer, compared to groundwater recharge in the winter, and thus became more $\delta^{13}C$ enriched.

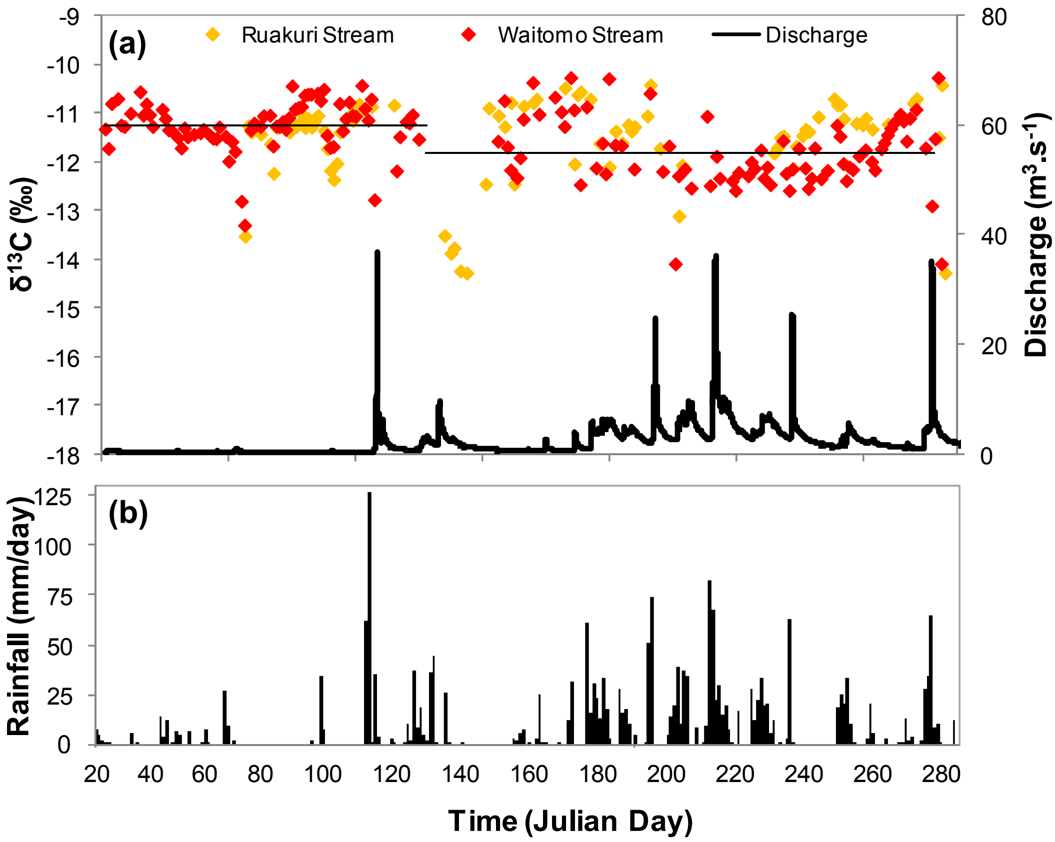

Figure 6.13. $\delta^{13}C$ for the Waitomo and Ruakuri Streams from 21st January – 9th October 2008. (a) Daily $\delta^{13}C$ values and hourly discharge plotted against time; and (b) daily rainfall. The horizontal black lines indicate the mean $\delta^{13}C$ values for summer (day 21 – 121, January – April) and winter (day 122 – 284, May – October).

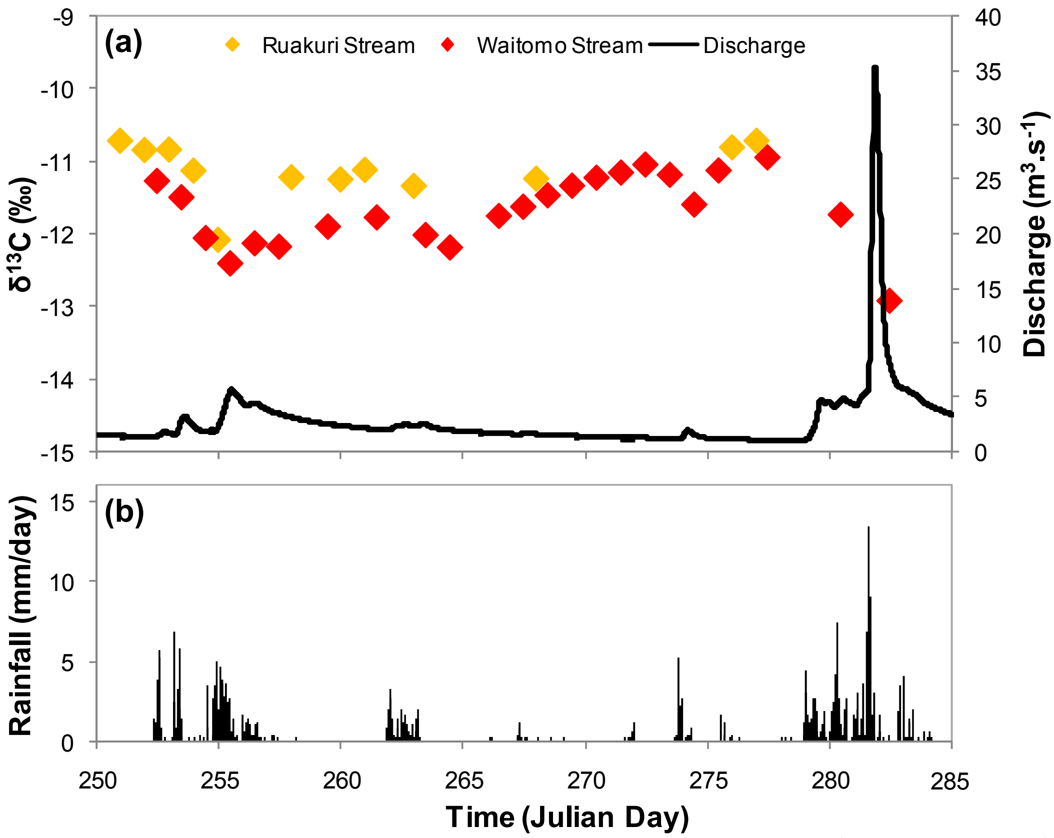

Figure 6.14. $\delta^{13}C$ values for the Waitomo and Ruakuri Streams for the 6th September – 10th October 2008, and Waitomo Stream discharge. (a) Daily $\delta^{13}C$ values and hourly discharge against time; and (b) hourly rainfall.

6.6 Discussion

6.6.1 Dripwater PCO_2

Dripwater PCO_2 from a straw stalactite in the Glowworm Cave was about 3500 ppm CO_2, and exceeded 5000 ppm on occasions. The findings of this study were within the range (1000 – 13000 ppm CO_2) reported by McCabe (1977) from dripwaters within the Waipuna Cave in Waitomo. The PCO_2 was typically higher than the stream (600 – 1200 ppm) and cave air (1000 ppm) PCO_2 under both 'normal' and high discharge conditions. The higher CO_2 levels are a direct result of the relationship between overlying soils and the dripwater. A delay of between one and four days between the rainfall-induced discharge response and the increase in dripwater PCO_2 generally occurred. The delay was likely related to the moisture content of the soil prior to the rainfall event, which alters the flow path of the percolating waters (Tooth & Fairchild, 2003).

Dripwater P_{CO_2} (3500 – 5000 ppm) was relatively low compared to typical soil P_{CO_2}, (10000 – 30000 ppm for New Zealand volcanic ash soils; Gunn & Trudgill, 1982), thus the dripwater entering the Glowworm Cave is characteristic of a 'closed system' (Hendy, 1971, McCabe, 1977). This means that once the CO_2 enriched percolation waters have left the soil, limestone dissolution will occur until the dissolved CO_2 is completely consumed (Baldini *et al*., 2006), thus the amount of CO_2 available for limestone dissolution is finite in closed systems.

On occasions dripwater P_{CO_2} increased, in relation to rainfall events that were large enough to induce increased stream discharge, while at times the P_{CO_2} decreased when rainfall produced a stream discharge response. Dripwater was directly connected to the soil system through the diffuse hydrologic flow paths which enable the water to percolate. Two dominant throughflow processes have been identified in karst systems: soil matrix flow, which dominants within karst systems during dry periods; and preferential flow through soil macropores, which dominates during recharge (Tooth & Fairchild, 2003). When the soil is dry, and percolation down through the overlying soil and limestone layers is slow, it is likely that the P_{CO_2} of the dripwater will be reduced, as sufficient time will have lapsed during the percolation process for the seepage waters to dissolve limestone.

One peculiarity within the dripwater P_{CO_2} data was the change in variability that occurred part way through December. Whilst the mean dripwater P_{CO_2} did not change, the range in the data decreased markedly (from 6336 ppm to approximately 1500 ppm). The high degree of variability that occurred throughout July, August and November may be associated with substantial rainfall events on already wet soils, triggering rapid flow through macropores in the soil (i.e. a flushing event). By December (summer) the soil moisture was beginning to be depleted, and the magnitude and frequency of rainfall events was reduced. Consequently, during the summer/dry period, the dripwater consisted of lower P_{CO_2} water that had been stored in and, hence, was at equilibrium with the limestone aquifer.

6.6.2 Stream and dripwater chemistry

Groundwater geochemistry is generally determined by water-rock interactions that occur within the aquifer (Vesper & White, 2004). The trends of HCO_3^-, Ca^{2+}, Na^+, Mg^{2+} and K^+ through time, and in relation to increases in stream discharge, were similar for the Waitomo and Ruakuri Streams, therefore proving to be reliable and reproducible.

The geochemistry of karst waters involves the interaction of various species of carbon, including $CO_{2(aq)}$, CO_3^{2-}, and HCO_3^-, as well as the interaction with the limestone (primarily Ca^{2+} in Waitomo). During a rainfall event, the amount of H_2O in the system rapidly increases and the H_2O forms an aqueous solution with CO_2 as it becomes equilibrated with the soil air. The water percolates downwards, with the rate of percolation strongly influenced by the flow path within the system (e.g. diffuse or conduit) and/or the soil moisture content (e.g. soil matrix flow occurring when conditions are dry, or macropore preferential flow occurring under-saturated conditions (Tooth & Fairchild, 2003)). The $CaCO_3$ is slow to react to the influx of CO_2 and therefore the existing dissolved Ca is diluted by increased H_2O within the system. This is known as the dilution factor or dilution response (Liu *et al*., 2004). As there is not enough $CaCO_3$ to drive the forward reaction (because the reaction rate of limestone dissolution is slow compared to the rate at which H_2O increases with a rainfall event), the Ca and the HCO_3 decrease during rainfall events (Liu *et al*., 2004). The trend was evident within the Glowworm and Ruakuri Cave systems with the HCO_3^- always decreasing with events of increased discharge, and the Ca almost always decreasing with increased discharge. Occasionally, however, the Ca did increase with rainfall/increased discharge. This indicates that at times the discharged water was predominantly sourced from the phreatic zone, with the discharging waters having had sufficient time to equilibrate with the limestone, before the rainwater entered the stream, and diluted the streamwater.

Concentrations of HCO_3^-, Ca^{2+}, and Na^+ in the Waitomo and Ruakuri Streams were higher in the summer compared to the winter. Concentrations for the same three ions (HCO_3^-, Ca^{2+} and Na^+) also typically decreased as stream discharge increased (independent of season). During summer and low discharge periods, the higher ion concentrations occurred due to the longer residence time of the groundwater within the limestone aquifer. Conversely, during the winter and high discharge periods, the lower ion concentrations were the result of dilution.

Compared to stream chemistry, dripwaters had higher concentrations of HCO_3^-, Ca^{2+} and Na^+. Dripwaters were more concentrated than streams, as the water remained in contact with the soil and limestone for longer, resulting in the higher ion concentrations observed. Furthermore, Ca^{2+} is abundant in karst waters as it is a product of limestone ($CaCO_3$) dissolution. When the P_{CO_2} of water increases, the water becomes more "aggressive" towards carbonates increasing the rate of dissolution, and therefore the Ca concentration should increase.

It has previously been shown that rainfall events can result in pulses of P_{CO_2} into the stream, regardless of season (refer to Chapter Five). Given that:

$$CaCO_3 + H_2O + CO_{2(aq)} \leftrightarrow Ca^{2+}_{(aq)} + 2HCO_3^-{}_{(aq)}$$

If the P_{CO_2} of the system increases, the forward reaction will proceed and the amount of Ca^{2+} in the system will then increase. It is, therefore, expected that rainfall events (large enough to induce increased stream discharge), result in an increase in the P_{CO_2} of seepage, and thus streamwaters. The P_{CO_2} enriched waters will therefore lead to increased Ca^{2+} concentrations (via limestone dissolution). Despite the increase in P_{CO_2} in both the Waitomo Stream and dripwaters with rainfall events, the concentration of Ca^{2+} in the waters clearly decreased with the same events (Figure 6.8a and Figure 6.10a) (input of rainwater results in a decrease of Ca^{2+} via dilution). The results suggest that, at Waitomo, dilution is a more instantaneous and prominent process than the chemical reaction of calcite dissolution. It was initially thought that whilst the immediate event of the rain diluting the Ca^{2+} and Na^{2+} concentrations within the system was clearly evident, perhaps the increase in Ca^{2+} over time (e.g. Figure 6.8a) was an indicator that there was a delay in the reaction of calcite dissolution. To test this, the relationship between the Ca:Na ratio against the Ca concentration was plotted (Figure 6.15). As both the Ca^{2+} and Na^{2+} concentrations track each other, the possibility that Ca^{2+} concentrations changed with response to increased PCO_2 brought into the system with the onset of rainfall is eliminated, resulting in clear evidence that dilution is a major influence.

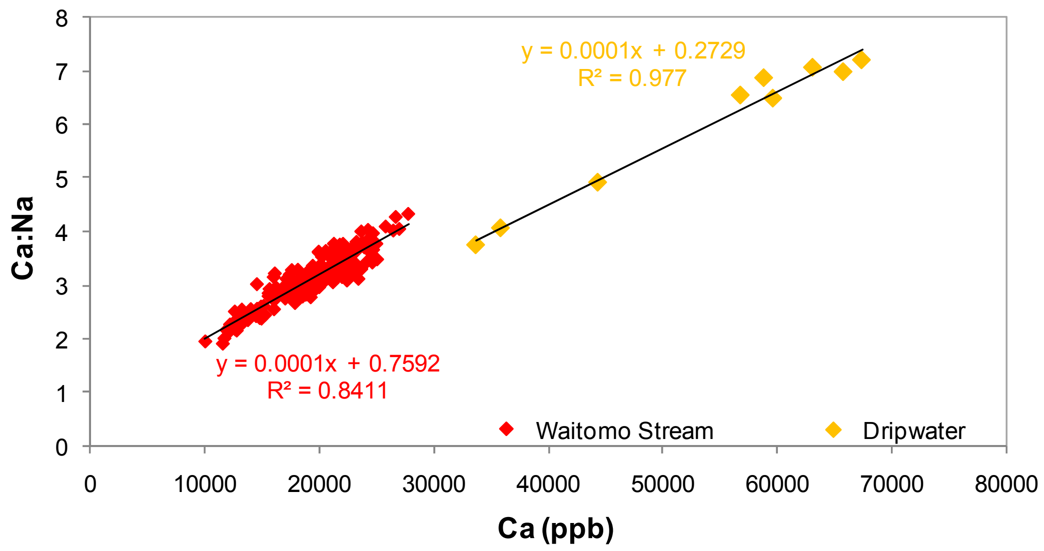

Figure 6.15. Ca:Na ratio against Ca^{2+} concentration for Waitomo Stream and Blanket Chamber dripwaters collected from the Glowworm Cave throughout 2008.

6.6.3 $\delta^{13}C$ isotope

$\delta^{13}C$ isotope of the Waitomo and Ruakuri Stream waters was analysed in a final attempt to determine whether the increased PCO_2 was derived from the soil. Results showed that $\delta^{13}C$ of the Waitomo and Ruakuri Streams decreased (became more negative) during increased discharge. The decrease in the $\delta^{13}C$ values varied, with a decrease of about 1 – 2 ‰ commonly occurring (Figure 6.13 and Figure 6.14).

An explanation for the decreasing $\delta^{13}C$ values with increased discharge was that CO_2 rapidly entered the system as a pulse during the displacement of percolation waters. Soil CO_2, with a $\delta^{13}C$ characterised by plant respiration, was more negative (~ -24 ‰) than the $\delta^{13}C$ of water that had been in contact with $CaCO_3$ (~ 0 ‰). In closed systems (e.g. Waitomo), where the $CaCO_3$-water interaction occurred in the absence of atmospheric CO_2, the $\delta^{13}C$ of the water reflected the dissolution interaction between the $CaCO_3$ (~ 0 ‰) and the soil derived $CO_{2(aq)}$ (~ -24 ‰). As the Waitomo and Ruakuri Stream water $\delta^{13}C$ values following increased discharge were about -12 ‰ – -14 ‰, it is evident that the streamwater is comprised of approximately equal contributions from the limestone (~ 0 ‰) and CO_2 enriched soil water (~ -24 ‰) sources during times of increased discharge.

Isotopic records captured by speleothems have been used in the reconstruction of palaeoclimate records (Bar-Matthews *et al*., 1996; Williams *et al*., 1999b). Understanding the processes that alter the $\delta^{13}C$ of karst waters (i.e. rainfall events that induce an increase in discharge) is, therefore, important for the accurate interpretation of speleothem-derived palaeoclimate records.

6.7 Conclusion

The major findings of the stream geochemistry analyses were that:

- increased negativity in $\delta^{13}C$ isotope coincided with increased discharge events, which supports the contention that additional CO_2 in the system, following discharge-inducing rainfall events, was soil derived. The $\delta^{13}C$ of limestone is about 0 ‰, while the $\delta^{13}C$ of the soil atmosphere is about -24 ‰. During summer low flow, the mean $\delta^{13}C$ of Waitomo Stream waters was -11.3 ‰, but during high stream discharge events the $\delta^{13}C$ dropped to -12 – -14 ‰. The decrease in the $\delta^{13}C$ value with increased discharge supports the idea that the additional CO_2 entering the stream during high flow events is being sourced from the lower $\delta^{13}C$ soil atmosphere.

- HCO_3, Ca, and Na concentrations were higher in the dripwater than the stream, indicating that the stream included water derived from sources other than immediate local groundwater; and/or that the flow paths carrying seepage waters to the stream enabled a much faster transmission, and thus less time for the water to react with the $CaCO_3$.

- HCO_3 and Na concentrations decreased with increased stream discharge, which reflects a dilution response. The water-rock interactions appeared to be less important than dilution in the Waitomo system when rainfall induced an increase in stream discharge.

- Ca in the stream showed both an increase and a decrease with rainfall/increased discharge. Decreased Ca with increased discharge indicated that rapid percolation and throughflow of the rainwater was occurring, whilst increased Ca with increased discharge implied that the water was coming from the phreatic zone, as sufficient time had passed for the waters to equilibrate with the limestone.
- dripwater P_{CO_2} showed a weak positive relationship with discharge. The dripwater had a mean P_{CO_2} of 3500 ppm and occasionally the P_{CO_2} exceeded 5000 ppm during periods when rainfall resulted in increased discharge. However, the pattern was not consistent as the dripwater P_{CO_2} response to rainfall/increased discharge events was also, at times, delayed. This was presumably due to the diffuse nature of the hydrological system, as well as variable soil moisture levels prior to rainfall events.
- the evidence presented here supports the hypothesis that additional P_{CO_2} in the Waitomo Stream, during times of increased discharge, was derived from relatively rapid throughflow from the soil.

7.0 Chapter Seven: Applying new knowledge to ten years of Glowworm Cave records

7.1 Introduction

Cave air P_{CO_2} and stream P_{CO_2} data collected from the Glowworm Cave throughout 2008 (Chapter Five), as well as streamwater geochemistry data from the Waitomo and Ruakuri Streams and dripwater geochemistry data from the Glowworm Cave (Chapter Six), have provided evidence for the hypothesis that P_{CO_2} anomalies in the Glowworm Cave air are influenced by events of increased stream discharge. This evidence was that:

- anomalous patterns in cave air P_{CO_2} often coincided with increased stream P_{CO_2}, which, in turn, coincided with increased discharge events;

- increases in dripwater P_{CO_2} within the Glowworm Cave were, at times, related to increased Waitomo Stream discharge, although the pattern was not consistent and thus the relationship was weak; and
- the isotopic signature ($\delta^{13}C$) of the Waitomo and Ruakuri Stream waters changed with rainfall events, reflecting an increase in soil derived CO_2.

7.2 Hypothesis and objectives

In Chapter Four, P_{CO_2} limit exceedences were identified within the ten year dataset (1998 – 2007). A number of the P_{CO_2} limit exceedences were unexplained by tourist numbers. In light of the findings presented in Chapters Five and Six (where measurements of the Waitomo Stream P_{CO_2} increased with increased discharge and the $\delta^{13}C$ of the water decreased, reflecting soil derived C), the unexplained P_{CO_2} limit exceedences were revisited to determine if the events could be explained by increased stream discharge. Thus, the hypothesis addressed in this chapter was that:

- **historic P_{CO_2} limit exceedences within the Glowworm Cave air that could not be explained by tourist numbers, could be related to events of increased Waitomo Stream discharge.**

The objectives of this chapter were therefore:

- to establish whether the P_{CO_2} limit exceedences presented in Chapter Four coincided with high stream discharge, to test the possibility that high Glowworm Cave air P_{CO_2} could be related to increased Waitomo Stream discharge; and,
- to present a rudimentary prediction model for daily P_{CO_2} maxima, using mean P_{CO_2} from the previous day, as well as ambient conditions and tourist numbers for the predicted day.

7.3 Correlations of P_{CO_2} limit exceedences with stream discharge

Between 1998 and 2007 the P_{CO_2} of the Glowworm Cave exceeded 2400 ppm 48 times (see Chapter Four, and Table 7.1). The P_{CO_2} limit exceedence events were investigated and categorised based on tourist numbers, stream level class, increased discharge (or the presence of a discharge peak) and the appearance of the diurnal P_{CO_2} pattern.

Events identified as 'tourist driven' (T) were when tourist numbers were high (> 1000), the P_{CO_2} followed the typical diurnal pattern (with base level being attained), while streamflow was normal (e.g. Figure 7.1). 'Anomalous' (A) (or discharge dominated) events were characterised by periods when the P_{CO_2} pattern differed from the normal diurnal day time-high, night time-low (to base level) cycle, generally had < 1000 tourists, and the water level was above normal (> 2.9 $m^3.s^{-1}$) (e.g. Figure 7.2). The 'combination' (C) category indicated events when streamflow increased above normal, and the typical diurnal P_{CO_2} pattern occurred (indicating the influence of tourists), but night time base level was reached (e.g. Figure 7.3). When events were classified as 'anomalous/combination' (A/C) P_{CO_2} deviated from the usual diurnal pattern (e.g. night time base level was not achieved), the flow class was normal, but there was a peak in discharge, and tourist numbers were > 1000. 'Unexplainable anomalous' events (A/U) could not be classed under any of the previous categories, as these events had normal flow and relatively normal tourist numbers yet the P_{CO_2} pattern was anomalous, failing to return to base level at night (Figure 7.4).

Of the 48 P_{CO_2} limit exceedences that occurred between 1998 and 2007, 31% (15) of the events were largely driven by high tourist numbers, whilst 27% were mainly driven by non-anthropogenic factors (e.g. increased discharge, rainfall, low temperature gradient between the cave and outside air). A combination of tourists and non-anthropogenic factors were responsible for 29% of the P_{CO_2} limit exceedences (Table 7.1). The remaining 13% of exceedences were unexplained by tourists or non-anthropogenic factors. It was speculated that the unexplained exceedences were due to the night time closure of the cave door, restricting air exchange; however no data was available to confirm the cause.

Table 7.1. P_{CO_2} limit exceedences that occurred in the Glowworm Cave between 1998 – 2007 (identified in Chapter Four), with a summary of the rainfall and discharge conditions that coincided with each event, as well as an interpretation of the event appearance. For descriptions of the peak appearance anomaly key, refer to Section 7.3; (*indicates events when the P_{CO_2} did not recover over night (e.g. anomalous) but the lack of recovery was a tourist effect).

Event	Date	Time[1]	Event duration (h)	Max. CO_2 (ppm)	Mean discharge[2] ($m^3.s^{-1}$)	Water level class[3]	Rainfall (mm/day)	Tourist numbers	Mean T.grad (°C)	Peak appearance (anomaly)
5	17/02/1999	13:00	0.5	2438	0.41	norm	0	1455	-6.56	T
7	3/01/2000	14:00	5	2689	1.01	norm	12.2	1684	-0.21	T
8	21/04/2000	14:00	10	2802	0.69	norm	0	1704	0.26	T*
9	22/04/2000	0:00	6.5	2864	0.62	norm	0	1699	-0.11	T*
15	2/01/2001	17:00	0.5	2439	2.44	norm	0	1937	-0.02	T
21	28/12/2001	14:30	1.5	2606	1.36	norm	6.7	1919	-3.41	T
25	11/11/2002	16:00	2	2470	2	norm	0	1365	-1.29	T
28	27/12/2002	14:00	6.5	2982	1.51	norm	0	2387	-1.77	T
34	3/01/2005	12:30	3.5	2911	2.45	norm	0	2086	-3.6	T
35	4/01/2005	13:00	3.5	2799	2.1	norm	0	1940	-3.4	T
39	21/01/2007	13:00	0.5	2401	0.54	norm	0	1406	-6.22	T
44	8/04/2007	14:00	0.5	2488	0.41	norm	0	1624	-4.25	T
45	29/09/2007	16:00	2	2517	1.13	norm	0	1002	-1.17	T
46	30/09/2007	13:30	2.5	2709	1.09	norm	0	1181	-2.22	T
48	7/11/2007	12:30	1.5	3358	2.41	norm	0	1281	-2.8	T
1	27/09/1998	15:00	1	2428	3.62	high	27	1097	-0.46	A
3	10/10/1998	12:00	2	2591	4.08	high	6	913	-0.65	A
4	14/10/1998	15:30	6	2549	5.69	flood	13.4	1271	2.71	A
6	11/11/1999	14:00	4	2525	6.13	flood	59.5	1228	-1.94	A
10	2/10/2000	14:00	10	2841	30.11	extreme	46.3	801	1.02	A
11	3/10/2000	0:00	23	2945	14.3	flood	56.8	663	3.26	A
12	4/10/2000	0:00	2.5	2782	7.81	flood	6.2	804	3.56	A
13	29/12/2000	13:30	10.5	2954	9.28	flood	46.2	1287	-1.94	A
14	30/12/2000	0:00	4.5	2628	5.13	flood	27.4	1822	-0.12	A
17	7/12/2001	20:30	3.5	3043	8.2	flood	15.3	773	-3.04	A
18	8/12/2001	0:00	10.5	2846	7.09	flood	34.4	1195	-2.09	A
19	9/12/2001	15:30	8.5	2586	11.13	flood	64.3	677	-3.59	A
20	10/12/2001	12:30	3	2815	6.39	flood	3.8	952	-3.06	A
16	23/02/2001	13:00	3	3250	4.96	high	44.2	1204	0.7	C
23	29/09/2002	15:30	6.5	2718	4.04	high	4.6	1650	-2.61	C
27	26/12/2002	14:30	3.5	2982	3.03	high	25.6	1999	-0.55	C
29	23/11/2003	12:00	8.5	3946	4.52	high	2.4	1831	0.58	C
30	29/12/2003	12:30	0.5	2424	3.3	high	21.3	1072	1.27	C
31	15/11/2004	13:30	1.5	2809	3.6	high	41.7	1536	1.11	C
32	1/01/2005	15:00	4.5	2893	3.74	high	8.5	1588	-0.71	C
33	2/01/2005	13:00	2.5	2844	3.02	high	9.4	1588	-2.49	C
36	7/01/2005	13:30	1	2492	4.15	high	6.3	1585	-2.37	C
47	5/11/2007	15:30	6.5	2658	6.3	flood	43.5	775	0.11	C
22	18/03/2002	14:00	3.5	2754	1.7	norm	29.5	1259	-1.02	A/C
24	9/11/2002	17:30	0.5	2410	1.69	norm	0	1425	-2.88	A/C
26	13/12/2002	20:30	0.5	2403	1.81	norm	31.5	1131	0.62	A/C
38	20/12/2006	15:30	5.5	2484	1.27	norm	20.5	1173	0.29	A/C
2	3/10/1998	15:00	3	2551	1.38	norm	1	948	-0.9	A/U
37	18/12/2006	13:30	4.5	2603	0.95	norm	3.3	1017	-3.4	A/U
40	4/02/2007	15:00	1	2429	0.45	norm	0	1122	-3.12	A/U
41	5/02/2007	11:00	5	2567	0.48	norm	3.1	936	-6.21	A/U
42	11/02/2007	12:30	1.5	2506	0.41	norm	0	1253	-8.03	A/U
43	12/02/2007	11:30	2	2582	0.41	norm	0	1014	-3.07	A/U

[1] Time of first instance that P_{CO_2} exceeded 2400 ppm on the given day.
[2] Mean discharge for the period duration of the event.
[3] Extreme ≥ 27 $m^3.s^{-1}$ (mean annual flood flow), flood ≥ 4.972 $m^3.s^{-1}$ (exceeded 5% of the time), high ≥ 2.886 $m^3.s^{-1}$ (exceeded 15% of the time), normal ≥ 0.396 $m^3.s^{-1}$ (exceeded 95% of the time), low < 0.396 $m^3.s^{-1}$ (5% of the time flow is less than 0.396 $m^3.s^{-1}$) Values have been derived from 21 years of Waitomo Stream flow data provided by Environment Waikato.

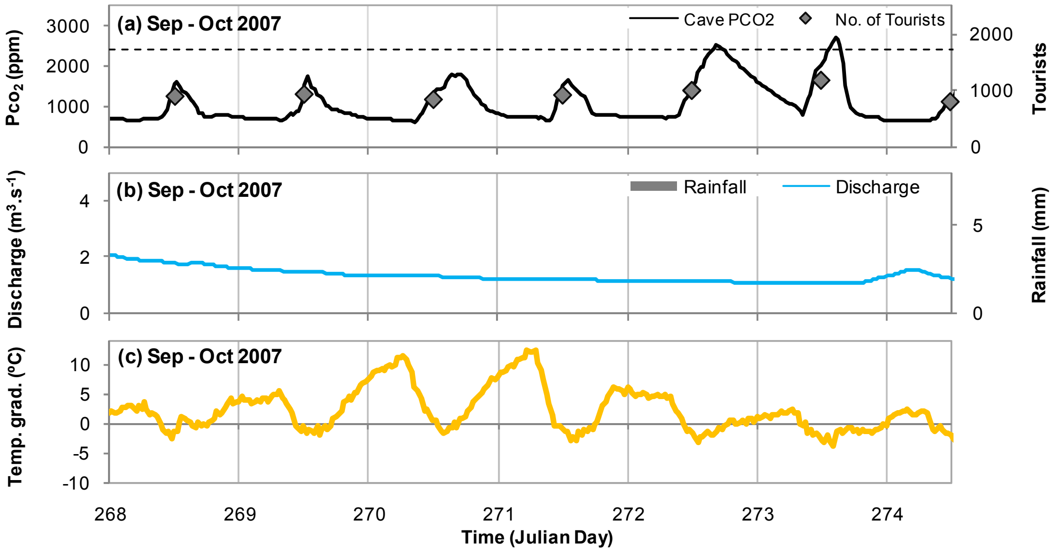

Figure 7.1. A 'tourist driven' (T) PCO_2 limit exceedence that occurred between days 272 and 273 of 2007 (29th and 30th September) in the Glowworm Cave. (a) Cave air PCO_2 and daily tourist numbers; (b) discharge and rainfall; and (c) temperature gradient between the cave air and outside air.

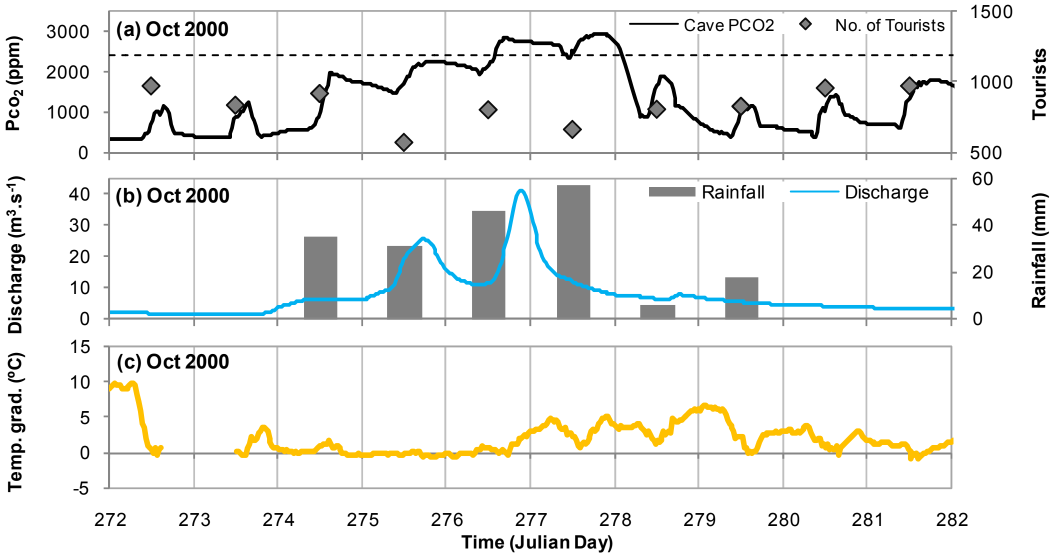

Figure 7.2. An 'anomalous' (A) PCO_2 limit exceedence that occurred on days 276, 277 and 278, 2000 (2nd – 4th October) in the Glowworm Cave. (a) Cave air PCO_2 and daily tourist numbers; (b) discharge and rainfall; and (c) temperature gradient between the cave air and outside air.

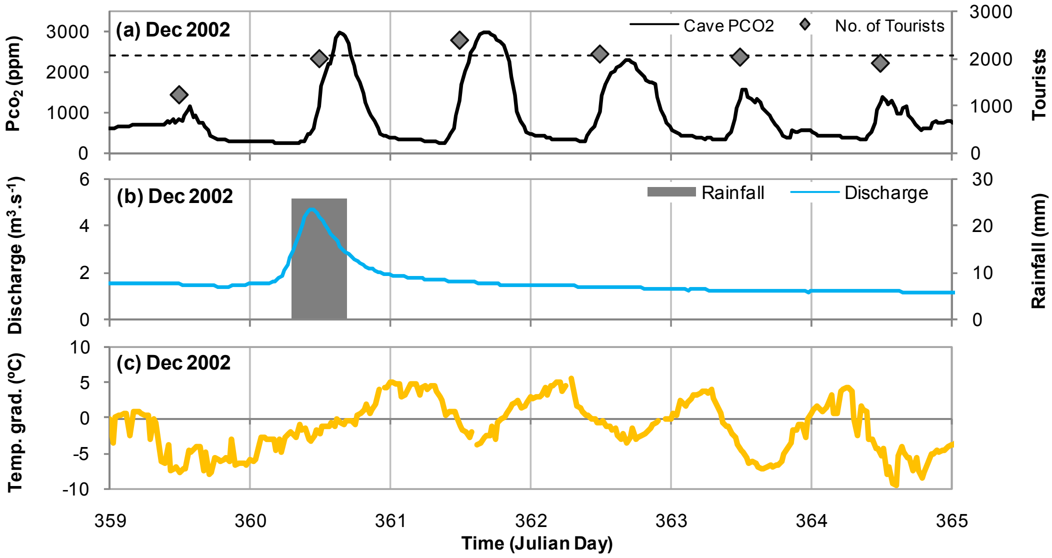

Figure 7.3. A 'combination' (C) PCO_2 limit exceedence that occurred between day 359 – 364 2002 (25th – 30th December), in the Glowworm Cave. (a) Cave air PCO_2 and daily tourist numbers; (b) discharge and rainfall; and (c) temperature gradient between the cave air and outside air.

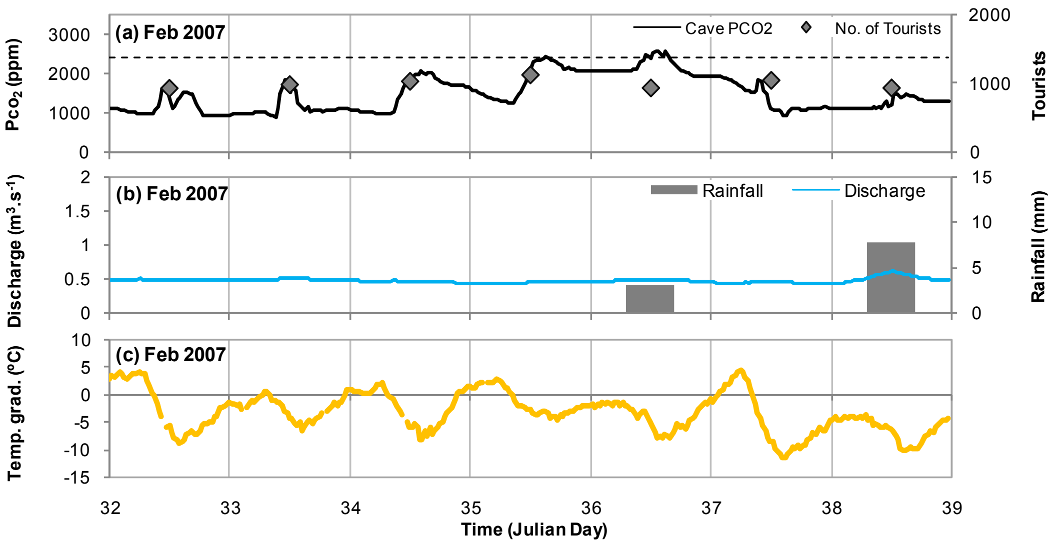

Figure 7.4. An 'unexplainable anomalous' (A/U) PCO_2 limit exceedence that occurred between day 32 – 38 2007 (1st and 7th February), in the Glowworm Cave. (a) Cave air PCO_2 and daily tourist numbers; (b) discharge and rainfall; and (c) temperature gradient between the cave air and outside air.

High-frequency data analysed over a short period is well known to show a strong correlation between tourists and increased cave air PCO_2 (Cigna, 1993; Pulido-Bosch *et al.*, 1997; De Freitas & Banbury, 1999). However, often when larger datasets are analysed, a different trend emerges. A poor correlation was found between daily total number of tourists and mean daily cave air PCO_2 for ten years of Waitomo data ($R^2 < 0.1$) (Figure 7.5a). Tourists had a slightly better correlation with daily maximum PCO_2 ($R^2 = 0.2$) (Figure 4.8). The large spread in the data (and thus poor correlation) is likely to be associated with seasonal variations in both CO_2 levels and tourist numbers, as well as temperature, microbial activity and probably inputs of CO_2 from the cave stream. The most interesting feature of Figure 7.5a was that on many of the days where tourist numbers were low and mean daily P_{CO_2} was high, rainfall was occurring.

When classifying days based on discharge and water level, a similar pattern to that observed in Figure 7.5a was seen. On most days that had low tourist numbers but high P_{CO_2} levels, a coincidence occurred with days that had high water levels (Figure 7.5b).

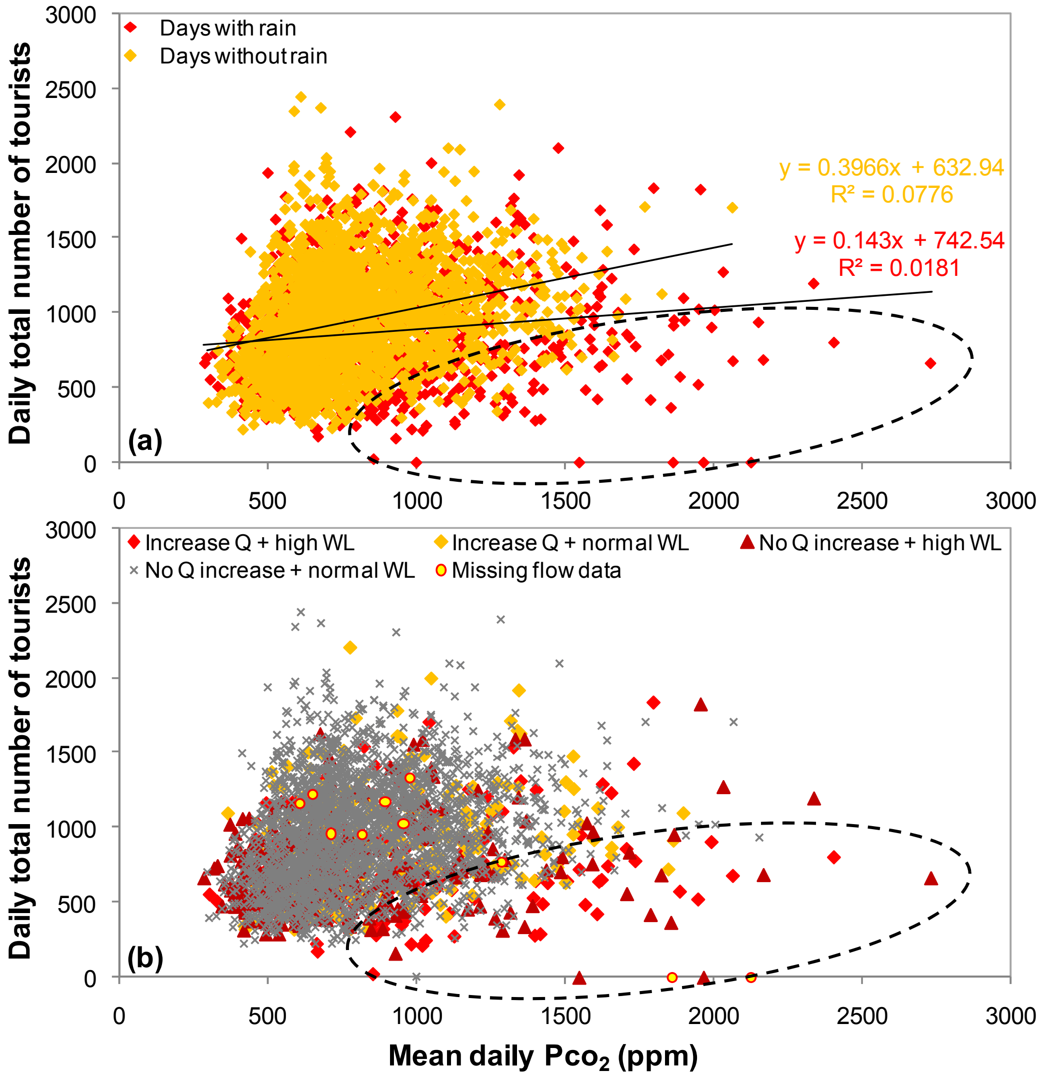

Figure 7.5. The relationship between mean daily P_{CO_2} and total daily number of tourists from 1998 – 2007. (a) Days with rain, compared to days without rain. (b) Days with increased discharge versus no increased discharge compared to previous day, and classed based on water level (high water level > 2.9 $m^3.s^{-1}$; normal < 2.9 $m^3.s^{-1}$). Circled data highlights the events where CO_2 was high whilst tourist numbers were low.

7.4 Seasonal trends

Cave air P_{CO_2} peaked annually around day 270 – 290 (27th September – 17th October) (Figure 7.6a). In Chapter Four it was noted that between 1998 and 2007, the spring period (September – October) coincided with an increase in tourist numbers. However, although tourist numbers peaked in the summer, P_{CO_2} frequently reached a daily mean maximum during the spring. It is evident that there are factors additional to tourist numbers that influence the CO_2 levels within the Glowworm Cave.

Measurements of stream P_{CO_2} (Chapter Five) have shown that times of increased discharge often result in times of increased P_{CO_2} within the stream. The high stream P_{CO_2} coincided with increased cave air P_{CO_2} (Figure 5.4 – Figure 5.13). A comparison of seven-day running means of daily mean discharge for the Waitomo Stream for each year between 1998 – 2007 (Figure 7.6b) has also shown that discharge increased during the spring period. The peak in discharge was typically lower in spring than in winter (days 150 – 225). The CO_2 concentrations within the Glowworm Cave air, however, were typically lowest during the winter. This pattern was probably due to less people touring through the caves each day in winter than in summer, as well as reduced concentrations of CO_2 soil during late autumn and winter. Peak soil CO_2 concentrations generally occurred during late spring or early summer (Gunn & Trudgill, 1982). It is also possible that the cooler water temperatures of the Waitomo Stream will contribute to the lower P_{co_2} levels of the streamwater. As CO_2 is more soluble at lower temperatures, the cooler Waitomo Stream temperature during the winter, may also explain the P_{CO_2} reduction.

Temperature gradient data were investigated, noting that the spring period was a transitional time, during which the external air was warming after the winter. As the spring warming took place, mean external air and cave temperatures were similar, and thus the temperature gradient was minimal (Figure 7.6c). As temperature gradient can be used as a surrogate for air density differences between the Glowworm Cave air and external air (de Freitas *et al*., 1982), temperature gradient can also be used as a proxy for air flow.

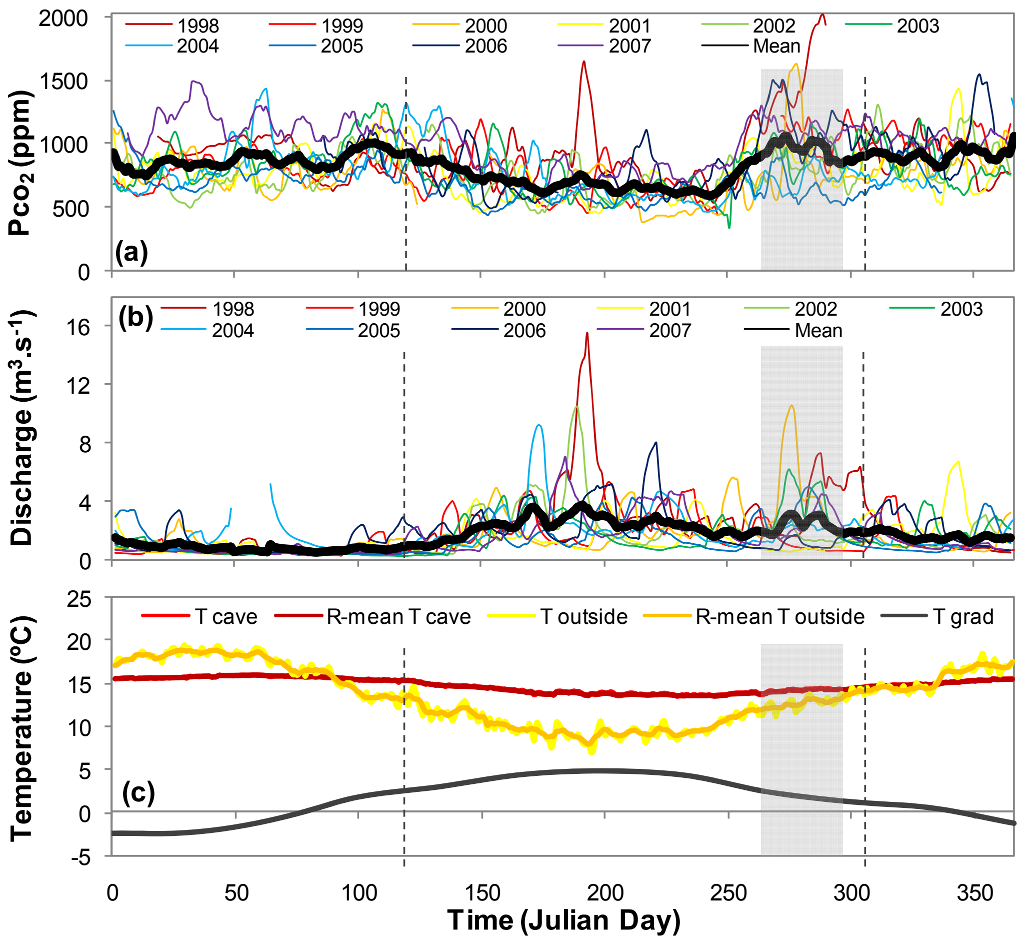

Figure 7.6. Annual variation of Glowworm Cave air PCO_2, Waitomo Stream discharge, and temperature gradient from 1998 – 2007. Seven-day running means of (a) PCO_2, (b) Waitomo Stream discharge, and (c) temperature gradient for each year between 1998 – 2007 (coloured lines), with the mean across the ten years plotted in black. The shaded area highlights the period where the annual peak in Glowworm Cave air PCO_2 coincides with an annual peak in discharge in the Waitomo Stream, as well as low daily temperature gradients.

7.5 Predictive model

For cave tourism operators it is important to know daily maximum PCO_2, as often operating guidelines prohibit CO_2 exceeding a given level (e.g. the Glowworm Cave must close if the CO_2 rises above 2400 ppm). A predictive tool that forecasts the daily maximum PCO_2, based on available information, would be useful for tourist cave managers so that exceedences of the 2400 ppm limit can be anticipated. Such a tool would enable managers to prevent, rather than mitigate, high CO_2 events.

It is clear that there are a number of factors that contribute to the P_{CO_2} of the Glowworm Cave air. The factors that have been identified are: tourist numbers, temperature gradient (and thus air flow), rainfall, and Waitomo Stream discharge. Multiple linear regression uses simple linear weightings for independent variables to generate a relationship with a dependent variable. Using the general linear regression function in Statistica (a product of StatSoft), a multiple linear regression was carried out.

The first aim was to determine which of the independent variables were most meaningful in predicting the daily maximum P_{CO_2} (dependent variable). The available independent variables were: previous day daily mean P_{CO_2}, previous day daily maximum P_{CO_2}, daily number of tourists, daily mean outside air temperature, daily mean cave air temperature, daily mean temperature gradient (difference between cave air and outside air temperature), daily mean stream discharge, daily maximum stream discharge, and daily rainfall. Firstly, a general linear regression was performed using all nine independent variables. The 'best subsets' function was selected, which enabled the stepwise elimination of the variables that were the least influential. The 'best subset' function showed that previous day mean P_{CO_2}, daily number of tourists, daily mean outside temperature, daily mean cave air temperature, daily mean temperature gradient, and daily maximum stream discharge were the most useful independent variables. These independent variables were included in the predictive model of daily maximum P_{CO_2}.

Using daily Glowworm Cave data for the years 1998 – 2005 a linear predictive model was created. The resulting equation for predicting daily maximum P_{CO_2} was:

$$Predicted\ daily\ max. Pco_2 = 0.522 \times P_c + 0.576 \times N - 42.020 \times T_o + 70.844 \times T_c + 92.656 \times T_g + 20.559 \times Q_{max} + 145.126 \quad \text{(Equation 7.1)}$$

where:

P_c = previous day mean PCO_2 (β = 0.34)

N = daily number of tourists (β = 0.49)

T_o = mean outside temp (β = -0.40)

T_c = mean cave temp (β = 0.18)

T_g = mean temp gradient (β = -0.40)

Q_{max} = maximum stream discharge (β = 0.14)

The standard error of the estimate = 275.54 ppm

The predictive model was developed using 1999 – 2005 data, and then validated using data from 2006 – 2008. A strong seasonal trend existed in the Glowworm Cave daily maximum PCO_2 data. The model was accurate in predicting the general seasonal trend for the calibration period, however it acted poorly in predicting extreme highs and lows (Figure 7.7). The daily maximums for the validation period (2006 – 2008) however were almost always under-predicted, and the typical seasonal trend evident in the observed data was also 'lost' by the model (Figure 7.7). Figure 7.8 shows the difference in the relationship between the observed and predicted daily maximum PCO_2 values between the calibration and validation datasets.

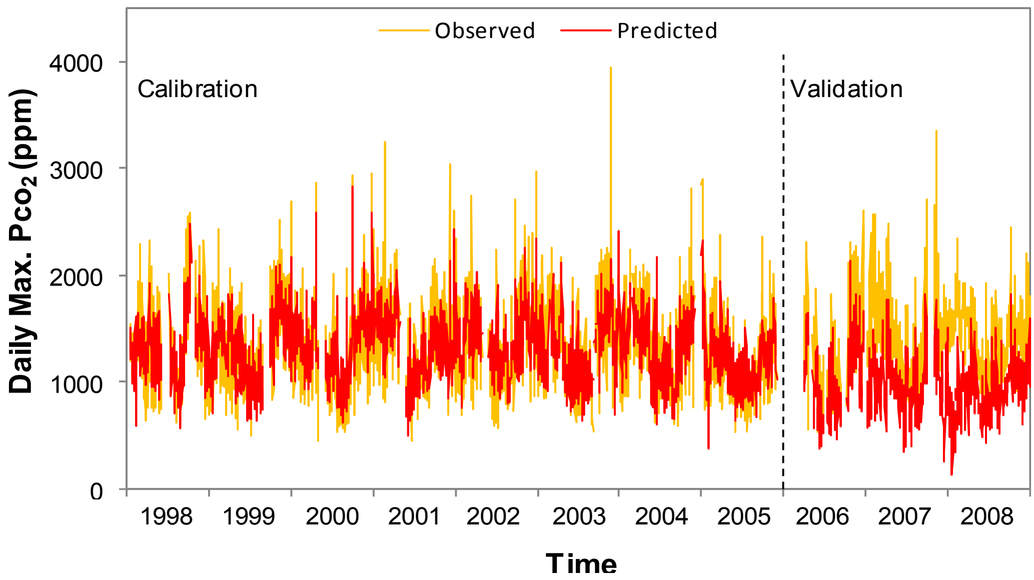

Figure 7.7. Relationship between predicted and observed daily maximum PCO_2 levels in the Glowworm Cave for the calibration period 1998 – 2005 (R^2 = 0.56) and the validation period 2006 – 2008 (R^2 = 0.35).

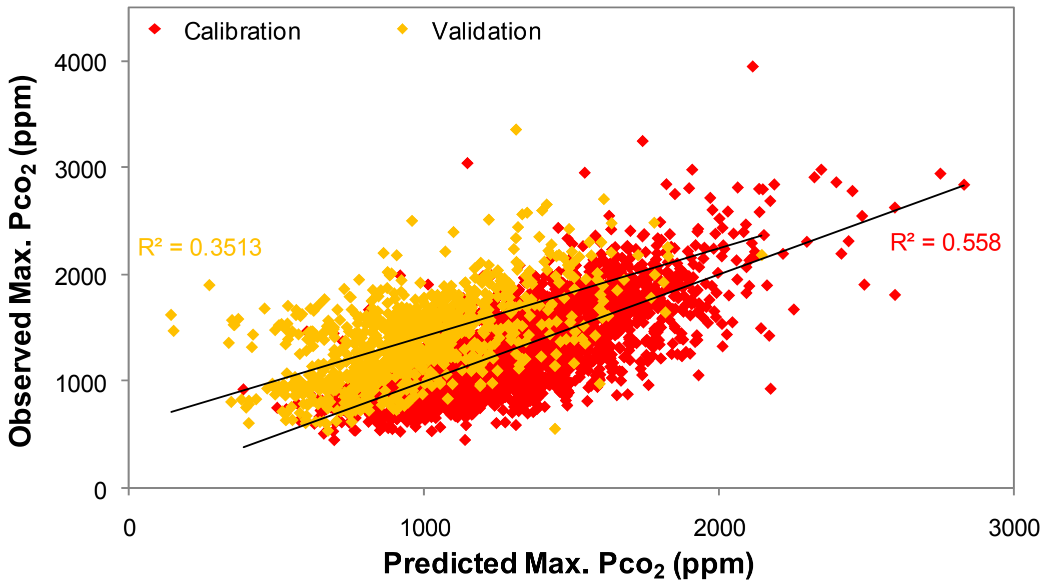

Figure 7.8. Correlation between predicted and observed daily maximum PCO_2 values for the calibration dataset (1998 – 2005); and the validation dataset (2006 – 2008) and the relationship between the calibration and validation datasets.

The model was recalibrated using Glowworm Cave data for 2006 and 2007 to give the equation:

$$Predicted\ daily\ max. Pco_2 = 0.655 \times P_c + 0.522 \times N - 22.858 \times T_o + 26.315 \times T_c + 69.692 \times T_g + 14.382 \times Q_{max} + 449.266 \qquad \text{(Equation 7.2)}$$

where:

P_c = previous day mean PCO_2 (β = 0.43)

N = daily number of tourists (β = 0.44)

T_o = mean outside temp (β = -0.22)

T_c = mean cave temp (β = 0.07)

T_g = mean temp gradient (β = -0.03)

Q_{max} = maximum stream discharge (β = 0.10)

The standard error of the estimate = 285.22 ppm

The addition of data from 2006 and 2007 in the calibration of the predictive model, enabled a better fit to be achieved between the predicted and observed maximum cave air PCO_2 values within the validation period (2008) (Figure 7.9

and Figure 7.10). While there was a visual improvement in the predicting power of the model after the 2006 and 2007 data were added to the calibration phase and the R^2 value for the validation improved from 0.35 to 0.37, the standard error of estimate increased from 275 to 285 ppm. Whilst the model shows some promise, it is clear that the model is not particularly accurate in predicting extreme maximum P_{CO_2} values.

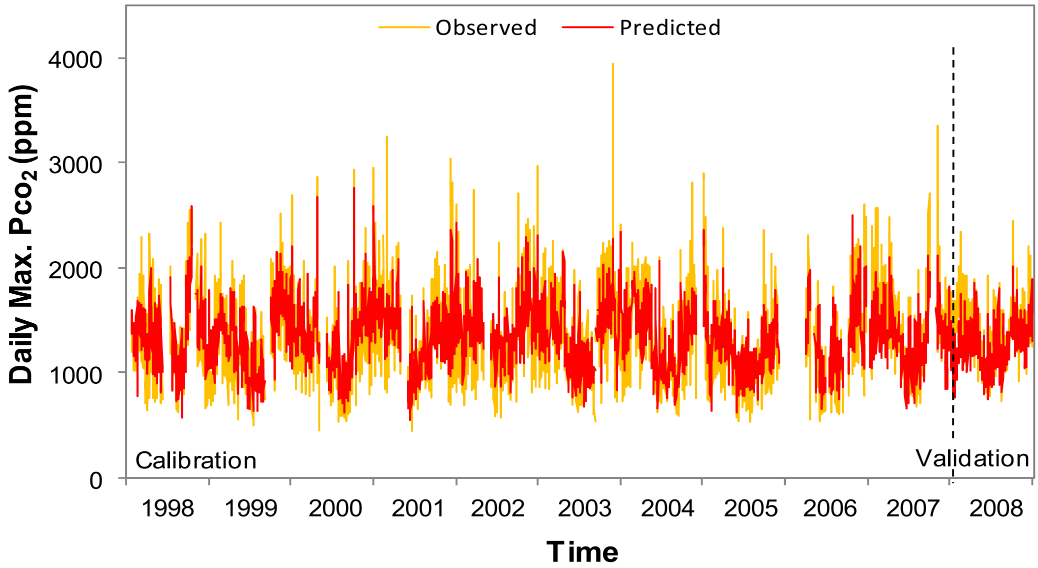

Figure 7.9. Relationship between predicted and observed daily maximum P_{CO_2} levels in the Glowworm Cave for the calibration period 1998 – 2007 ($R^2 = 0.54$) and the validation period 2008 ($R^2 = 0.37$).

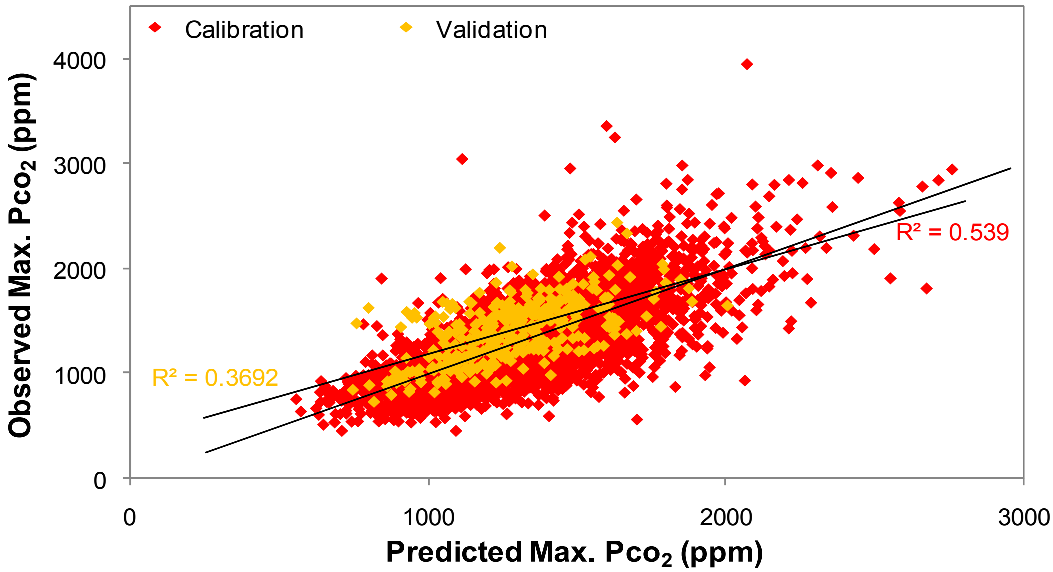

Figure 7.10. Correlation between predicted and observed daily maximum P_{CO_2} values for the calibration dataset (1998 – 2007); and the validation dataset (2008) and the relationship between the calibration and validation datasets.

7.6 Discussion

7.6.1 Integration of 2008-gained knowledge with historic data

P_{CO_2} limit exceedences in the historic Glowworm Cave air record, which were unexplainable by tourist numbers, generally showed a correlation with increased Waitomo Stream discharge. Of the 48 P_{CO_2} limit exceedences that were identified from the ten year dataset, most events (87%) could either be associated with high tourist numbers (> 1000), increased discharge or rainfall, elevated stream levels, low temperature gradient, or a combination of these factors.

Measurements of the P_{CO_2} of the Waitomo Stream, Chapter Five, have shown that P_{CO_2} increased when Waitomo Stream discharge increased. Chapter Six investigated the geochemistry of the Waitomo Stream and found that during storm events, when the stream discharge increased, the $\delta^{13}C$ of the water decreased (i.e. became more negative) suggesting that, at the time of sampling, a larger proportion of the C in the water was soil-derived, and insufficient time had lapsed for the CO_2 enriched (aggressive) water to interact with the higher $\delta^{13}C$ limestone.

The ten year dataset highlighted that an increase in both cave air P_{CO_2} and stream discharge occurred during the winter and/or spring each year (Figure 7.6). Gunn & Trudgill (1982) found that soil CO_2 concentrations at Waitomo were highest during the late spring. Ghani *et al*. (2007) analysed dissolved organic nitrogen and carbon in soils across New Zealand and found that the risk of leaching was exacerbated during spring. As CO_2 in Waitomo soils was reported to be highest in the spring, and leaching maxima also occur in the spring, it is probable that spring time leaching of CO_2 from the soil will result in higher P_{CO_2} levels within waterways (e.g. Waitomo Stream). The leaching was likely to contribute to the spring peak in the cave air P_{CO_2}. The spring period was characterised by a low temperature gradient between the cave and outside air, and high water levels. The low temperature gradient, as well as high water levels, reduced the amount of air flow through the cave, and thus the flushing of the cave.

7.6.2 Model limitations

Although predictive models can be useful tools for management, models need to be used with caution. Whilst the predictive model presented in this chapter did show some promise, it is clearly ineffective at accurately forecasting the daily maximum CO_2. The model over-predicted low, and under-predicted high daily P_{CO_2} maxima. A linear model is clearly inappropriate for the prediction of daily P_{CO_2} maxima, and perhaps a polynomial based model would be better.

The inclusion of two extra years (2006 and 2007) of data in the calibration phase of the model (Figure 7.7 and Figure 7.8, compared with Figure 7.9 and Figure 7.10) gave limited improvement in validation. It seems likely that there are other factors also influencing the cave CO_2 that are not accounted for in the model. For example, in light of the findings of Chapters Five and Six, the inclusion of stream P_{CO_2} as an independent variable within the model, is likely to account for some of the variability within the model.

7.7 Conclusions

- Increased Waitomo Stream discharge could, at least in part, explain 56% of the P_{CO_2} limit exceedences previously unexplained in the historic Glowworm Cave air data.
- The spring peak in Glowworm Cave air P_{CO_2} coincided with spring peaks in discharge, soil CO_2 maxima and annual leaching maxima. Data showed a sharp increase in the P_{CO_2} of the Waitomo Stream at the beginning of summer (Chapter Five) (Figure 5.2b). It is likely that, between 1998 and 2007, the Waitomo Stream P_{CO_2} would have also increased.
- An accurate predictive model would be a useful management tool, however the model presented in this chapter requires revision before it can be implemented (i.e. $R^2 = 0.37$). As there is a substantial dataset (eleven years including 2008 data), there is potential to use other modelling approaches, or include further variables (e.g. stream P_{CO_2}) to improve the predictive capability of the model.

8.0 Chapter Eight: Conclusions and future recommendations

8.1 Summary

The primary goal of this research was to identify whether a correlation existed between the P_{CO_2} of the Waitomo Stream and that of the Glowworm Cave. A preliminary investigation of ten years of Glowworm Cave data illustrated typical patterns of cave air P_{CO_2}, temperature and tourist number trends within the Glowworm Cave. The analysis of the ten year historic dataset showed that several times each year the cave air P_{CO_2} increased above the 2400 ppm limit; the limit imposed on the Glowworm Cave tourism operators to protect the cave and its speleothems. Previously, when the P_{CO_2} in the Glowworm Cave attained a level > 2400 ppm, tourists were thought to be the source. However, this research has shown that tourists were not the sole CO_2 source during anomalous events (i.e. abnormal P_{CO_2} cycle, usually where base level was not attained), or during P_{CO_2} limit exceedence events. It was hypothesised that the Waitomo Stream may be contributing to unusual and/or high cave air P_{CO_2} events.

The partial pressure of carbon dioxide (P_{CO_2}) in the Glowworm Cave air was typically higher during the summer and in the day time. Mean annual minima occurred during the winter and daily minima occurred just before tours commenced each day (i.e. 9.00 a.m.). Patterns in Glowworm Cave air P_{CO_2} are consistent with trends in tourist number data and with reported findings from other tourist caves around the world.

Temperature differences between the cave air and external atmosphere (i.e. temperature gradient) are fundamental in the circulation and exchange of air, and thus flushing of cave CO_2. When the temperature gradient is greatest, airflow through the cave is enhanced, however when the temperature gradient is small, there is restricted airflow, and flushing of the cave air is limited. For temperature gradient to facilitate air circulation it is necessary that the two entrances (the Upper and the Lower Entrance) are open. The Upper Entrance is contained by a door which is manually opened and closed, and thus used as a management tool to 'control' air exchange between the Glowworm Cave and the outside air. The Lower Entrance is bounded by the Waitomo Stream, therefore, when discharge increases and stream level subsequently rises, air circulation is restricted.

Higher summer stream P_{CO_2} concentrations are probably linked to three main factors: (i) a greater concentration gradient between the Glowworm Cave air and the Waitomo Stream, due to higher tourist numbers during the summer months; (ii) warmer temperatures increasing soil CO_2 (due to increased root respiration and microbial activity); and (iii) decreased stream discharge and thus reduced agitation of the stream due to summer low flows.

Waitomo and Ruakuri Stream samples were obtained throughout the 2008 measurement period and analysed for Na^+, Ca^{2+}, and HCO_3^-. Na and HCO_3 concentrations in the Waitomo and Ruakuri Streams decreased with increased stream discharge showing that dilution, compared to short-term rock-water interactions, was a dominant effect within the Waitomo karst hydrological system. In general, the concentration of Ca also decreased with increasing discharge, lending further evidence that the streamwaters were being diluted. On occasions, however, the Ca concentration increased when discharge increased, suggesting that the waters percolating into the stream were coming from the phreatic zone, where sufficient time had lapsed for the CO_2 in the groundwaters to react with and dissolve the limestone.

The P_{CO_2} of dripwater within the Glowworm cave was also measured. At times, the dripwater P_{CO_2} showed a positive relationship with discharge, when the P_{CO_2} increased from a mean of 3500 ppm to sometimes > 5000 ppm. However, the pattern of dripwater P_{CO_2} in relation to discharge events was not consistent.

8.2 Summary of thesis hypotheses

The four hypotheses of this thesis were that:

1. **anomalous increases in Glowworm Cave air P_{CO_2} were associated with increased Waitomo Stream P_{CO_2};**
2. **the P_{CO_2} of the Waitomo Stream increased with rainfall events;**
3. **the additional P_{CO_2} in the Waitomo Stream during events of elevated discharge was derived from relatively rapid throughflow from the soil; and**
4. **historic P_{CO_2} limit exceedences within Glowworm Cave air data, which could not be explained by tourist numbers, could be related to events of increased Waitomo Stream discharge.**

8.3 Conclusions

- Glowworm Cave air P_{CO_2} anomalies were associated with increased Waitomo Stream P_{CO_2}, therefore hypothesis one can be accepted. Disequilibrium in the P_{CO_2} between the Glowworm Cave air and the Waitomo Stream promoted the movement of CO_2 between the stream and the cave air. When the Waitomo Stream had a higher P_{CO_2} than the Glowworm Cave air, the disequilibrium presumably resulted in degassing of CO_2 from the stream, thus the stream was a source of CO_2 to the cave air. Conversely, when the Glowworm Cave P_{CO_2} was higher than the Waitomo Stream, the stream was presumed to become a CO_2 sink.

- The Waitomo Stream P_{CO_2} did increase with rainfall events, but only when the rainfall event was large enough to induce a discharge response, therefore, hypothesis two can be accepted in part. An alternative hypothesis, which the data supports, is that the Waitomo Stream P_{CO_2} increased when the discharge of the Waitomo Stream increased. Measurements of the partial pressure of CO_2 within the Waitomo Stream were obtained by equilibrating air with the streamwater within a closed loop, and the air was subsequently passed through an infrared gas analyser (IRGA). The stream P_{CO_2} was typically between 600 – 1000 ppm during the winter, and between 1000 – 1200 ppm during the summer. The Waitomo Stream P_{CO_2} showed typical diurnal and seasonal patterns consistent with cave air P_{CO_2} (i.e. day time and summer maxima/night time and winter minima). During periods of increased stream discharge the Waitomo Stream P_{CO_2} increased, at times exceeding 2000 ppm. With almost every increased discharge event that occurred between July and September 2008, the Waitomo Stream P_{CO_2} increased during the day and remained anomalously high (i.e. did not return to base level) at night.

- The additional P_{CO_2} in the Waitomo Stream during events of elevated discharge was derived from relatively rapid throughflow from the soil. Increased negativity in $\delta^{13}C$ isotope in the Waitomo and Ruakuri Streams coincided with increased discharge events. These findings were consistent with hypothesis three, that additional CO_2 in the system, following an increase in discharge, is derived from the soil atmosphere. The Waitomo Stream had a mean $\delta^{13}C$ value of -11.3 ‰ during summer low flow conditions. During periods of elevated stream discharge the $\delta^{13}C$ value of the Waitomo Stream waters decreased to between -12 and -14 ‰. As the $\delta^{13}C$ value of limestone is 0 ‰, and that of the soil atmosphere is -24 ‰, a reduction in the $\delta^{13}C$ of the streamwater during periods of increased discharge supports the hypothesis that the additional CO_2 in the stream is derived from the soil.

- High P_{CO_2} anomalies within the historic Glowworm Cave data that could not be explained by tourist numbers, can be related to events of increased Waitomo Stream discharge. The 2400 ppm P_{CO_2} limit was exceeded 48 times between 1998 and 2007. High tourist numbers were primarily responsible for 31% of events. A further 13 % of events could not be explained by high tourist numbers, elevated discharge, or a low temperature gradient. Increased discharge, rainfall, and/or a low temperature gradient between the cave and outside air (e.g. non-anthropogenic factors) were responsible for 27% of P_{CO_2} limit exceedence events, whilst the remaining 29% appeared to be influenced by a combination of factors, including an increase in discharge. Therefore, given that over three quarters (81%) of the events were unexplained by tourists alone and were, at least in part, related to increased discharge, I accept hypothesis four that historic P_{CO_2} limit exceedences within Glowworm Cave air data, which cannot be explained by tourist numbers, can be related to events of increased Waitomo Stream discharge.

- A predictive model was created to predict daily maximum P_{CO_2} in the Glowworm Cave using the independent variables: previous day mean P_{CO_2}, daily number of tourists, daily mean outside temperature, daily mean cave air temperature, daily mean temperature gradient, and daily maximum stream discharge. The model showed some promise in predicting the diurnal and seasonal P_{CO_2} patterns. A predictive model could potentially be an effective management tool if the accuracy in predicting daily P_{CO_2} maxima can be improved.

8.4 Recommendations for future work

- In the collection of my stream and dripwater P_{CO_2} data I used a combination of silicon and stainless steel tubing. For future studies attempting to undertake continuous stream P_{CO_2} measurements I would recommend using nylon tubing in place of silicon tubing as this will ensure a CO_2 tight system. Investigation of eliminating the saturated air component from the system would overcome problems of saturated air condensing on the CO_2 sensor. This could be achieved by using a water-tight gas-pervious material such as PVC tubing weighted down under water and connected to nylon (or stainless steel tubing) to complete the above-air components of the system. Using a technique where gas-pervious tubing within the stream was involved for the exchange of CO_2 would also increase the area and thus opportunity for CO_2 exchange between the stream and the analysed air to occur.

- Obtaining stream P_{CO_2} data for at least 12 months, from both the Glowworm and Ruakuri streams would improve the 'robustness' of the data and enable stronger seasonal conclusions to be made.

- A detailed balance of sources and sinks of CO_2 could be calculated using high frequency P_{CO_2} measurements over various temporal scales, and using $\delta^{13}C$ isotope to identify the source of the CO_2 entering the system. Analysis of the $\delta^{13}C$ of rainwater and of the cave air, particularly before and during a storm event, would potentially provide the evidence necessary to ascertain that the increased CO_2 within the cave air during periods of increased discharge is originating from the stream, and thus the soil.

- The predictive model should be refined, possibly using a polynomial model. An increased measurement database, e.g. including parameters such as the P_{CO_2} of the stream, may also increase the power of the model to predict daily maximum cave P_{CO_2}.

- It is highly likely that there are sources of CO_2 within the Glowworm Cave other than the ones currently known/reported e.g. perhaps the contribution from microorganisms is more significant than was originally thought. Further, more rigorous sampling of the air at various locations and times within the Glowworm Cave may prove useful in improving the current knowledge on P_{CO_2} sources within the Glowworm Cave.

References

Adams, C. S. & Swinnerton, A. C. (1937). Solubility of limestone. *Transactions of the American Geophysical Union*, *18*(Part II), 504-508.

Amar, A. (2004). *Microclimate of a mid-latitude, single entrance tourist cave*. Unpublished master's thesis, University of Auckland, Auckland, New Zealand.

Atkinson, T. C. (1977). Carbon dioxide in the atmosphere of the unsaturated zone: An important control of groundwater hardness in limestones. *Journal of Hydrology*, *35*, 111-123.

Baldini, J. U. L., Baldini, L. M., McDermott, F. & Clipson, N. (2006). Carbon dioxide sources, sinks, and spatial variability in shallow temperate zone caves: Evidence from Ballynamintra Cave, Ireland. *Journal of Cave and Karst Studies*, *68*(1), 4-11.

Bar-Matthews, M., Ayalon, A., Matthews, A., Sass, E., & Halicz, L. (1996). Carbon and oxygen isotope study of the active water-carbonate system in a karstic Mediterranean cave: Implications for paleoclimate research in semiarid regions. *Geochimica et Cosmochimica Acta*, *60*(2), 337-347.

Batiot-Guilhe, C., Seidel, J-L., Jourde, H., Hébrard, O. & Bailly-Comte, V. (2007). Seasonal variations of CO_2 and ^{222}Rn in a mediterranean sinkhole – spring (Causse d'Aumelas, SE France). *International Journal of Speleology*, *36*(1), 51-56.

Bourges, F., d'Hults, D. & Mangin, A. (1998). *Étude de l'Aven d'Orgnac* (Rapport final). Moulis, France: Laboratoire Souterrain de Moulis, C.N.R.S Géologie Environment Conseil.

Bourges, F., Mangin, A. & d'Hulst, D. (2001). Le gaz carbonique dans la dynamique de l'atmosphère des cavités karstiques: L'exemple de l'Aven d'Orgnac (Ardèche). *Earth and Planetary Sciences*, *333*, 685-692.

Campbell Scientific. (2008a). *Instruction Manual: Model 107 temperature probe*. Logan, Utah: Campbell Scientific Inc.

Campbell Scientific. (2008b). *Instruction Manual: CSI model TB4 rain gage*. Logan, Utah: Campbell Scientific Inc.

Cigna, A. A. (1993). Environmental management of tourist caves. *Environmental Geology*, *21*, 173-180.

Cigna, A. A. (2005). Show caves. In D. C. Culver & W. B. White (Eds.), *Encyclopedia of caves* (pp. 495-500). London, England: Elsevier Academic Press.

Cigna, A. A. & Burri, E. (2000). Development, management and economy of show caves. *International Journal of Speleology*, *29 B* (1/4), 1-27.

Clark, I. D. & Fritz, P. (1997). *Environmental isotopes in hydrogeology*. New York, USA: Lewis Publishers.

Craig, H. (1953). The geochemistry of the stable carbon isotope. *Geochimica et Cosmochimica Acta*, *3*, 53-92.

Craig, H. (1957). Isotopic standards for carbon and oxygen and correction factors for mass-spectrometric analysis of carbon dioxide. *Geochimica et Cosmochimica Acta*, *12*, 133-149.

Crossley, P. C. (1998). *The New Zealand cave atlas North Island.* Christchurch, New Zealand: New Zealand Speleological Society.

Culver, D. C. & White, W. B. (2005). *Encycopedia of caves*. London, UK: Elsevier Academic Press.

de Freitas, C. R. (1998). Cave monitoring and management: The Glowworm Cave, New Zealand. In *Cave and Karst Management in Australasia XII: Proceedings of the Twelfth Australasian Conference on Cave and Karst Management*, *1998* (pp. 55-66). Carlton South, Victoria, Australia: Australasian Cave and Karst Management Association.

de Freitas, C. R. & Banbury, K. (1999). Build up and diffusion of carbon dioxide in cave air in relation to visitor numbers at the Glowworm Cave, New Zealand. In *Cave and Karst Management in Australasia XII: Proceedings of the Thirteenth Australasian Conference on Cave and Karst Management*, *1999* (pp. 84-91). Carlton South, Victoria, Australia: Australasian Cave and Karst Management Association.

de Freitas, C. R. & Littlejohn, R. N. (1987). Cave climate: Assessment of heat and moisture exchange. *Journal of Climatology*, *7*, 553-569.

de Freitas, C. R., Littlejohn, R. N., Clarkson, T. S. & Kristament, I. S. (1982). Cave climate: Assessment of airflow and ventilation. *Journal of Climatology*, *2*, 383-397.

de Freitas, C. R. & Schmekal, A. (2003). Condensation as a microclimate process: Measurement, numerical simulation and prediction in the Glowworm Cave, New Zealand. *International Journal of Climatology*, *23*, 557-575.

de Freitas, C. R. & Schmekal, A. (2006). Studies of condensation/evaporation processes in the Glowworm Cave, New Zealand. *International Journal of Speleology*, *35*(2), 75-81.

Department of Conservation. (1999). *Karst management guidelines: Policies and actions*. Wellington, New Zealand: Department of Conservation.

Doorne, S. (1999). *Visitor experience at the Waitomo Glowworm Cave* (Science for Conservation 95). Wellington, New Zealand: Department of Conservation.

Dragoni, W. V. U. & Verdacchi, A. (1993). First results from the monitoring system of the karstic complex "Grotte di Frasassi-Grotta Grande del Vento" (Ventral Apennines, Italy). In *Hydrological Processes in Karst Terranes: Proceedings of the Atlanta Symposium and Field Seminar, October 1990* (pp. 107-117). Italy: IAHS.

Dragovich, D. & Grose, J. (1990). Impact of tourists on carbon dioxide levels at Jenolan Caves, Australia: An examination of microclimatic constraints on tourist cave management. *Geoforum*, *21*(1), 111-120.

Dublyansky, V. N. & Dublyansky, Y. V. (1998). The problem of condensation in karst studies. *Journal of Cave and Karst Studies*, *60*(1), 3-17.

Duckeck, D. (2008). *Ruakuri Cave: Cave of the dogs – den of the dogs*. Retrieved July 27, 2008, from http://www.showcaves.com/english/index.html.

Ek, C. & Gewelt, M. (1985). Carbon dioxide in cave atmospheres. New results in Belgium and comparison with some other countries. *Earth Surface Processes and Landforms*, *10*, 173-187.

Faimon, J., Štelcl, J & Sas, D. (2006). Anthropogenic CO_2 – flux into cave atmosphere and its environmental impact: A case study in the Císařskà Cave (Moravian Karst, Czech Republic). *Science of the Total Environment*, *369*, 213-245.

Fairbridge, R. W. (1968). Condensation corrosion. In R. W. Fairbridge (Ed.), *Encyclopedia of geomorphology* (pp. 204-205). New York, USA: Reinhold.

Fernandez-Cortes, A., Calaforra, J. M. & Sanchez-Martos, F. (2006). Spatiotemporal analysis of air conditions as a tool for the environmental management of a show cave (Cueva del Agua, Spain). *Atmospheric Environment*, *40*, 7378-7394.

Ford, D. & Williams, P. (1989). *Karst geomorphology and hydrology*. London, England: Unwin Hyman.

Ford, D. & Williams, P. (2007). *Karst hydrogeology and geomorphology*. Chichester, England: John Wiley & Sons Ltd.

Forti, P. (1980). Formazione di aragonite nella Grotta di Castellana: Un esempio della modificazione indotta dalla turisticizzazione. *Grotte d'Italia*, *4*(8), 1-10.

Garrels, R. M. & Christ, C. L. (1965). *Solutions, minerals, and equilibria*. New York, USA: Harper & Row.

Ghani, A., Dexter, M., Carran, R. A. & Theobald, P. W. (2007). Dissolved organic nitrogen and carbon in pastoral soils: The New Zealand experience. *European Journal of Soil Science*, *58*, 832-843.

Gillieson, D. (1996). *Caves: Processes, development and management.* Oxford, UK: Blackwell Publishers Ltd.

Groves, C. & Meiman, J. (2005). Flooding. In D. C. Culver & W. B. White (Eds.), *Encyclopedia of caves* (pp. 495-500). London, England: Elsevier Academic Press.

Guasch, H., Armengol, J., Marti, E. & Sabater, S. (1998). Diurnal variation in dissolved oxygen and carbon dioxide in two low-order streams. *Water Resources*, *32*(4), 1067-1074.

Gunn, J. & Trudgill, S. T. (1982). Carbon dioxide production and concentrations in the soil atmosphere: A case study from New Zealand volcanic ash soils. *CATENA*, *9*(1-2), 81-94.

Hendy, C. H. (1971). The isotopic geochemistry of speloethems – I. The calculation of the effects of different modes of formation on the isotopic composition of speleothems and their applicability as palaeoclimatic indicators. *Geochemica et Cosmochimica Acta*, *35*, 801-824.

Herman, J. S. & Lorah, M. M. (1987). CO_2 outgassing and calcite precipitation in Falling Spring Creek, Virginia, USA. *Chemical Geology*, *62*, 251-262.

Hill, C. & Forti, P. (1997). *Cave minerals of the world* (2^{nd} ed.). Alabama, USA: National Speleological Society.

Hoffer-Frence, K. J. & Herman, J. S. (1989). Evaluation of hydrological and biological influences on CO_2 fluxes from a karst stream. *Journal of Hydrology*, *108*, 189-212.

Hoover, T. E. & Berkshire, D. C. (1969). Effects of hydration on carbon dioxide exchange across an air-water interface. *Journal of Geophysical Research*, *74*, 456-464.

Hope, D., Dawson, J. J. C., Cresser, M. S. & Billett, M. F. (1995). A method for measuring free CO2 in upland streamwater using headspace analysis. *Journal of Hydrology*, *166*, 1-14.

James, J. M. (1977). Carbon dioxide in the cave atmosphere. *Transactions of the British Cave Research Association*, *4*(4), 417-429.

James, J. M. (1994). Carbon dioxide in tourist cave air. *Comptes Rendus du Colloque International de Karstologie a Luxembourg*, 27, 187-195.

James, J. M. (2004a). Condensation corrosion. In J. Gunn (Ed.), *Encyclopedia of caves and karst science* (pp. 240-241). New York, USA: Fitzroy Dearborne.

James, J. M. (2004b). Tourist caves: Air quality. In J. Gunn (Ed.), *Encyclopedia of caves and karst science* (pp. 730-731). New York, USA: Fitzroy Dearborne.

James, J. M. & Dyson, J. (1981, October 13). Cave science topics: CO_2 in caves. *Caving International Magazine*, 54-59.

Jennings, J. N. (1985). *Karst geomorphology*. Oxford, UK: Basil Blackwell Ltd.

Jones, J. B. & Mulholland, P. J. (1998). Carbon dioxide variation in a hardwood forest stream: An integrative measure of whole catchment soil respiration. *Ecosystems*, *1*, 183-196.

Keeling, C. D. & T. P. Whorf. (2005). Atmospheric CO_2 records from sites in the SIO air sampling network. In *Trends: A Compendium of Data on Global Change*. Tennessee, USA: Department of Energy.

Kermode, L. O. (1974). Geological setting of Glowworm Cave, Waitomo. *New Zealand Speleological Bulletin*, *5*(92), 361-369.

Kermode, L. O. (1978). *Cave visitors and calcite corrosion: Excess carbon dioxide in Waitomo Caves*. New Zealand Geological Survey. Otara, New Zealand: DSIR.

Langmuir, D. (1997). *Aqueous environmental geochemistry*. New Jersey, USA: Prentice-Hall Inc.

Liu, Z., Groves, C., Yuan, D., Meiman, J., Jiang, G., He, S. & Li, Q. (2004). Hydrochemical variations during flood pulses in the south-west China peak cluster karst: Impacts of $CaCO_3$ – H_2O – CO_2 interactions. *Hydrological Processes*, *18*, 2423-2437.

Liu, Z., Li, Q., Sun, H. & Wang, J. (2007). Seasonal, diurnal and storm-scale hydrochemical variations of typical epikarst springs in subtropical karst areas of SW China: Soil CO_2 and dilution effects. *Journal of Hydrology*, *337*, 207-233.

Marion, J. B. (1979). *General physics with bioscience essays.* New York, USA: Wiley.

Mayer, J. (1999). Spatial and temporal variation of groundwater chemistry in Pettyjohns Cave, Northwest Georgia, USA. *Journal of Cave and Karst Studies*, *61*(3), 131-138.

McCabe, B. (1977). *The geochemistry of groundwater solutions entering limestone caverns*. Unpublished master's thesis, University of Waikato, Hamilton, New Zealand.

McLaren, R. G. & Cameron, K. C. (1996). *Soil science: Sustainable production and environmental protection* (2nd ed.). Auckland, New Zealand: Oxford University Press.

Michie, N. A. (1999). An instrument and method for measurement of dust fall in caves. In *National Cave and Karst Management Symposium*, *1999* (pp. 123-128). Albuquerque, New Mexico, USA: Speleobooks.

Ministry of Tourism Research. (2008). *Tourist activity: Nature based tourism*. Retrieved July 22, 2008, from http://www.tourismresearch.govt.nz/Documents/Tourism%20Sector%20Profiles/NatureBasedTourismApril2000.pdf

Miotke, F. D. (1974). Carbon dioxide and the soil atmosphere. *Abhandlungen zur Karst-und Höhlenkunde, Reihe A, Speläologie*, *9*, 1-49.

Moore, G. W. (1952). Speleothem – a new cave term. *National Speleological Society News*, *10*(6), 2.

Neal, C. & Thomas, A. G. (1985). Field and laboratory measurement of pH in low conductivity natural waters. *Journal of Hydrology*, 79, 319-322.

Neal, C., Watts, C., Williams, R. J., Neal, M., Hill, L. & Wickham, H. (2002). Diurnal and longer term patterns in carbon dioxide and calcite saturation for the River Kennet, south-eastern England. *The Science of the Total Environment*, *282-283*, 205-231.

Nelson, C. S. (1973). Stratigraphy and sedimentology of the Te Kuiti group in Waitomo County, South Auckland. Unpublished doctoral dissertation, University of Auckland, Auckland, New Zealand.

New Zealand Department of Labour. (1994). *Workplace exposure standards effective from 1994*. Wellington, New Zealand: Occupational Safety and Health Service.

Parfitt, R. L., Percival, H. J., Dahlgren, R. A. & Hill, L. F. (1997). Soil and solution chemistry under pasture and radiate pine in New Zealand. *Plant and Soil*, *191*, 279-290.

Pentecost, A. (1992). Carbonate chemistry of surface waters in a temperate karst region: The southern Yorkshire Dales, UK. *Journal of Hydrology*, *139*, 211-232.

Plummer, L. N. & Wigley, T. M. (1976). The dissolution of calcite in CO_2-saturated solutions at 25 °C and 1 atm. total pressure. *Geochemica et Cosmochimica Acta*, *40*, 141-202.

Pulido-Bosch, A., Martin-Rosales, W., Lopez-Chicano, M., Rodriguez-Navarro, C. M. & Vallejos, A. (1997). Human impact in a tourist karstic cave (Arcena, Spain). *Environmental Geology*, *31*(3/4), 142-149.

Rebsodrf, A., Thyssen, N. & Erlandsen, M. (1991). Regional and temporal variation in pH, alkalinity, and carbon dioxide in Danish streams, related to soil type and land use. *Freshwater Biology*, *25*, 419-435.

Roques, H. (1969). A review of the present-day problems in the physical chemistry of carbonates in solution. *Transactions of the Cave Research Group of Great Britain*, *11*(3), 139-163.

Russell, M. J. & MacLean, V. L. (2008). Management issues in a Tasmanian tourist cave: Potential microclimatic impacts of cave modifications. *Journal of Environmental Management*, *87*, 474-483.

Schmekal, A. A. & de Freitas, C. R. (2001). Condensation in Glowworm Cave, Waitomo, New Zealand. *Department of Conservation Science Internal Series*, *15*, 5-12.

Showcaves. (2008). *General information*. Retrieved September 2, 2008, from http://www.showcaves.com/english/explain/index.html.

Smith F. B. & Brown, P. E. (1933). The concentration of carbon dioxide in the soil air under various crops and in fallow soils. *Iowa State College Journal*, *8*, 1-16.

Song, L., Xiaoning, W. & Fuyuan, L. (2000). The influence of cave tourism on CO_2 and temperature in Baiyun Cave, Hebei, China. *International Journal of Speleology*, *29B*(1/4), 77-87.

Tarhule-Lips, R. F. A. & Ford, D. C. (1998). Condensation corrosion in caves on Cayman Brac and Isla de Mona. *Journal of Cave and Karst Studies*, *60*(2), 84-95.

Thrailkill, J. & Robl, T. L. (1981). Carbonate geochemistry of vadose water recharging limestone aquifers. *Journal of Cave Hydrology*, *54*, 195-208.

Tooth, A. F. & Fairchild, I. J. (2003). Soil and karst aquifer hydrological controls on the geochemical evolution of speleothem-forming drip waters, Crag Cave, southwest Ireland. *Journal of Hydrology*, *273*, 51-68.

Troester, J. W. & White, W. B. (1984). Seasonal fluctuations in the carbon dioxide partial pressure in a cave atmosphere. *Water Resources Research*, *20*(1), 153-156.

Vaisala. (2004). *Vaisala product catalogue: GMM220 carbon dioxide modules for harsh and demanding OEM applications*. Helsinki, Finland: Vaisala. (http://www.hoskin.qc.ca/uploadpdf/Instrumentation/Vaisala/hoskin_GMM220 40bf88bfb54bd.pdf).

Vesper D. J. & White, W. B. (2004). Storm pulse chemographs of saturated index and carbon dioxide pressure: Implications for shifting recharge sources during storm events in the karst aquifer at Fort Campbell, Kentucky/Tennessee, USA. *Hydrogeology Journal*, *12*, 135-143.

Villar, E., Bonet, A., Diaz-Caneja, B., Fernandez, P. L., Gutierrez, I., Quindos, L. S., Solana, J. R. & Soto, J. (1984). Ambient temperature variations in the hall of paintings of Altamira Cave due to the presence of visitors. *Cave Science, Transactions British Research Association*, *11*(2), 99-104.

White, P. J. & Waterhouse, B. C. (1993). Lithostratigraphy of the Te Kuiti Group: A revision. *New Zealand Journal of Geology and Geophysics*, *36*, 255-266.

White, W. B. (1984). Rate processes: Chemical kinetics and karst landform development. In R. G. La Fleur (Ed.), *Groundwater as a geomorphic agent* (pp. 227-48). Boston, USA: Allen & Unwin.

White, W. B. (1988). *Geomorphology and hydrology of karst terrains*. New York, USA: Oxford University Press.

White, W. B. (2005). Springs. In D. C. Culver & W. B. White (Eds.), *Encyclopedia of caves* (pp. 495-500). London, England: Elsevier Academic Press.

White, W. B. & Culver, D. C. (2005). Cave, definition of. In D. C. Culver & W. B. White (Eds.), *Encyclopedia of caves* (pp. 81-85). London, England: Elsevier Academic Press.

Wilde, K. A. (1986). An historical review of cave and karst conservation and management in New Zealand 1889-1985. In *Proceedings of the Sixth Australasian Conference on Cave Tourism and Management*, *1986*. Waitomo, New Zealand: Australasian Cave and Karst Management Association.

Williams, P. (2004). Karst systems. In J. Harding, P. Mosley, C. Pearson & B. Sorrell (Eds.), *Freshwaters of New Zealand* (pp. 31.1-31.20). Christchurch, New Zealand: New Zealand Hydrological Society INC and New Zealand Liminological Society INC.

Williams, P., de Freitas, C., Millar, I., Worthy, T., Hurst, B. & Crossley, P. (1999a). The current state of the Ruakui Cave environment. Unpublished report. A Consultants Report for New Zealand Glowworm Caves Ltd.

Williams, P. W., Marshall, A., Ford, D. C. & Jenkinson, A. V. (1999b). Palaeoclimatic interpretation of stable isotope data from Holocene speleothems of the Waitomo district, North Island, New Zealand. *The Holocene*, *9*(6), 649-657.

Yoshimura, K., Nakao, S., Noto, M., Inokura, Y., Urata, K., Chen, M. & Lin, P. -W. (2001). Geochemical and stable isotope studies on natural water in the Taroko Gorge karst area, Taiwan – chemical weathering of carbonate rocks by deep source CO_2 and sulfuric acid. *Chemical Geology*, *177*, 415-430.

Yuan, D. (2001). *Guidebook for ecosystems of semiarid karst of North China and subtropical karst in Southwest China*. Guilin, China: Karst Dynamics Laboratory.

Zhang, S. & Jin, Y. (1996). Tourism resources on karst and caves in China. In *Actas II Congress ISCA*, *29 October-1 November 1994* (pp. 111-119). Malaga, Spain.

Appendices

A.1 Water Chemistry

Table A.1.1. Raw HCO_3^- data for the Waitomo and Ruakuri Streams for the 2008 sampling period.

Date	Julian Day	WAITOMO STREAM HCO_3^- Concentration (ppm) Sample (a)	(b)	(c)	*Mean*	RUAKURI STREAM HCO_3^- Concentration (ppm) Sample (a)	(b)	(c)	(d)	(e)	*Mean*
21/01/08	21	117.36			*117.36*						
22/01/08	22	119.99			*119.99*						
23/01/08	23	115.25			*115.25*						
24/01/08	24	113.71			*113.71*						
25/01/08	25	121.77			*121.77*						
26/01/08	26	123.31			*123.31*						
27/01/08	27	119.97			*119.97*						
28/01/08	28	119.15			*119.15*						
29/01/08	29	123.25			*123.25*						
30/01/08	30	110.46			*110.46*						
31/01/08	31	126.67			*126.67*						
1/02/08	32	118.35			*118.35*						
2/02/08	33	119.38			*119.38*						
3/02/08	34	119.92			*119.92*						
4/02/08	35	121.22			*121.22*						
5/02/08	36	120.28			*120.28*						
6/02/08	37	120.45			*120.45*						
7/02/08	38	120.16			*120.16*						
8/02/08	39	121.47			*121.47*						
9/02/08	40	121.59			*121.59*						
10/02/08	41	120.96			*120.96*						
11/02/08	42	119.55			*119.55*						
12/02/08	43	118.90			*118.90*						
13/02/08	44	113.49			*113.49*						
14/02/08	45	114.46			*114.46*						
15/02/08	46	114.89			*114.89*						
16/02/08	47	114.32			*114.32*						
17/02/08	48	109.57			*109.57*						
18/02/08	49	109.95			*109.95*						
19/02/08	50	115.81			*115.81*						
20/02/08	51	120.21			*120.21*						
21/02/08	52	116.24			*116.24*						
22/02/08	53	115.83			*115.83*						
23/02/08	54	121.08			*121.08*						
24/02/08	55	114.38			*114.38*						
25/02/08	56	119.92			*119.92*						
26/02/08	57	110.34			*110.34*						
27/02/08	58	122.14			*122.14*						
28/02/08	59	174.06			*174.06*						
29/02/08	60	166.43			*166.43*						
1/03/08	61	126.12			*126.12*						
2/03/08	62	141.35			*141.35*						
3/03/08	63	99.11			*99.11*	91.12					*91.12*
4/03/08	64	149.69			*149.69*	111.61					*111.61*

Date	Julian Day	WAITOMO STREAM HCO_3^- Concentration (ppm)				RUAKURI STREAM HCO_3^- Concentration (ppm)					
		Sample				Sample					
		(a)	(b)	(c)	*Mean*	(a)	(b)	(c)	(d)	(e)	*Mean*
5/03/08	65	108.50			*108.50*	116.29					*116.29*
6/03/08	66					119.93					*119.93*
7/03/08	67	118.31			*118.31*	118.34					*118.34*
8/03/08	68	119.72			*119.72*	119.84					*119.84*
9/03/08	69					122.69					*122.69*
10/03/08	70	121.65			*121.65*	125.00					*125.00*
11/03/08	71	123.40			*123.40*						
12/03/08	72	120.53			*120.53*						
13/03/08	73	124.53			*124.53*	122.62					*122.62*
14/03/08	74	131.71			*131.71*	126.67					*126.67*
15/03/08	75	123.30			*123.30*	123.53					*123.53*
16/03/08	76	125.50			*125.50*						
17/03/08	77	123.50			*123.50*	124.39					*124.39*
18/03/08	78	144.55			*144.55*						
19/03/08	79	147.76			*147.76*	125.94					*125.94*
20/03/08	80	125.85			*125.85*	124.11					*124.11*
21/03/08	81	130.60			*130.60*	126.07					*126.07*
22/03/08	82	121.28			*121.28*	124.03					*124.03*
23/03/08	83	123.24			*123.24*	123.57					*123.57*
24/03/08	84	124.24			*124.24*	122.62					*122.62*
25/03/08	85	122.80			*122.80*	124.05					*124.05*
26/03/08	86	130.33			*130.33*	126.29					*126.29*
27/03/08	87					123.05					*123.05*
28/03/08	88	128.26			*128.26*	123.95					*123.95*
29/03/08	89	128.48			*128.48*						
30/03/08	90	128.00			*128.00*	126.81					*126.81*
31/03/08	91	136.04			*136.04*	124.15					*124.15*
1/04/08	92	117.00			*117.00*	118.33	116.71	112.95			*116.00*
2/04/08	93	118.57			*118.57*	108.67					*108.67*
3/04/08	94					107.66					*107.66*
4/04/08	95	151.74			*151.74*	117.38					*117.38*
5/04/08	96	134.17			*134.17*						
6/04/08	97	127.57			*127.57*	122.85					*122.85*
7/04/08	98	127.67			*127.67*	120.11					*120.11*
8/04/08	99	121.12			*121.12*	122.53					*122.53*
9/04/08	100	139.24			*139.24*	124.76					*124.76*
10/04/08	101					125.74					*125.74*
11/04/08	102	126.27			*126.27*	124.04					*124.04*
12/04/08	103	125.65			*125.65*						
13/04/08	104	134.49			*134.49*						
14/04/08	105	130.19			*130.19*	120.75					*120.75*
15/04/08	106	117.41			*117.41*	58.93					*58.93*
16/04/08	107										
17/04/08	108	46.53			*46.53*						
18/04/08	109	77.44			*77.44*	84.27					*84.27*
19/04/08	110	88.13			*88.13*						
20/04/08	111										
21/04/08	112	113.29			*113.29*	98.34					*98.34*
22/04/08	113	105.48			*105.48*	104.03					*104.03*
23/04/08	114	109.14			*109.14*						
24/04/08	115										
25/04/08	116	102.26			*102.26*						
26/04/08	117	105.84			*105.84*	107.67					*107.67*
27/04/08	118	106.47			*106.47*	113.01					*113.01*
28/04/08	119					102.36					102.36
29/04/08	120	99.75			*99.75*	100.93					*100.93*

Date	Julian Day	WAITOMO STREAM HCO_3^- Concentration (ppm) Sample (a)	(b)	(c)	Mean	RUAKURI STREAM HCO_3^- Concentration (ppm) Sample (a)	(b)	(c)	(d)	(e)	Mean
30/04/08	121	69.20			*69.20*	79.86					*79.86*
1/05/08	122	63.13			*63.13*	85.14	75.84	78.23			*79.73*
2/05/08	123	78.84			*78.84*	174.72					*174.72*
3/05/08	124	86.73			*86.73*	100.73					*100.73*
4/05/08	125	95.07			*95.07*	102.32					*102.32*
5/05/08	126					62.04					*62.04*
6/05/08	127	70.53			*70.53*	88.11					*88.11*
7/05/08	128	82.94			*82.94*	90.67					*90.67*
8/05/08	129	84.09			*84.09*	91.33					*91.33*
9/05/08	130	87.55			*87.55*	90.55					*90.55*
10/05/08	131	78.27			*78.27*	83.12					*83.12*
11/05/08	132					97.23					*97.23*
12/05/08	133					88.90					*88.90*
13/05/08	134	93.38			*93.38*	91.08					*91.08*
14/05/08	135	89.93			*89.93*	93.34					*93.34*
15/05/08	136	95.86			*95.86*	93.52					*93.52*
16/05/08	137										
17/05/08	138	99.82			*99.82*	98.45					*136.58*
18/05/08	139	99.93			*99.93*	97.82					*124.12*
19/05/08	140					98.01					*98.01*
20/05/08	141	103.29	101.47		*102.38*	98.84					*98.84*
21/05/08	142					99.02					*99.02*
22/05/08	143					102.39					*102.39*
23/05/08	144	107.92			*107.92*	101.31					*101.31*
24/05/08	145	107.20			*107.20*	102.43					*102.43*
25/05/08	146										
26/05/08	147	107.90			*107.90*	106.50					*106.50*
27/05/08	148	111.46			*111.46*						
28/05/08	149	111.41			*111.41*	104.22					*104.22*
29/05/08	150					150.42					*150.42*
30/05/08	151	115.44			*115.44*	106.24					*106.24*
31/05/08	152	111.20			*111.20*						
1/06/08	153	112.71			*112.71*	107.02					*107.02*
2/06/08	154	106.58			*106.58*	106.03					*106.03*
3/06/08	155	102.81			*102.81*	100.57					*100.57*
4/06/08	156	105.09			*105.09*	105.04					*105.04*
5/06/08	157					106.88					*106.88*
6/06/08	158	114.46			*114.46*	104.85					*104.85*
7/06/08	159	109.04			*109.04*	105.60					*105.60*
8/06/08	160					118.00					*118.00*
9/06/08	161					94.09					*94.09*
10/06/08	162	108.03			*108.03*	95.18					*95.18*
11/06/08	163	96.56			*96.56*	100.00					*100.00*
12/06/08	164					101.41					*101.41*
13/06/08	165	100.19			*100.19*	116.71					*116.71*
14/06/08	166	102.75			*102.75*	97.54					*97.54*
15/06/08	167										
16/06/08	168	105.95			*105.95*						
17/06/08	169	79.54			*79.54*	72.53					*72.53*
18/06/08	170					84.49					*84.49*
19/06/08	171	82.22			*82.22*	89.63					*89.63*
20/06/08	172					94.59					*94.59*
21/06/08	173	93.09			*93.09*						
22/06/08	174					93.97					*93.97*
23/06/08	175	55.61			*55.61*	82.11					*82.11*
24/06/08	176	61.23			*61.23*	81.46					*81.46*

Date	Julian Day	WAITOMO STREAM HCO_3^- Concentration (ppm)				RUAKURI STREAM HCO_3^- Concentration (ppm)					
		Sample				Sample					
		(a)	(b)	(c)	*Mean*	(a)	(b)	(c)	(d)	(e)	*Mean*
25/06/08	177					75.84					*75.84*
26/06/08	178	58.48			*58.48*						
27/06/08	179	64.02			*64.02*	74.53					*74.53*
28/06/08	180	52.78			*52.78*	73.44					*73.44*
29/06/08	181										
30/06/08	182	73.69			*73.69*	82.73					*82.73*
1/07/08	183										
2/07/08	184	82.62			*82.62*	66.57					*66.57*
3/07/08	185	59.03			*59.03*	75.21					*75.21*
4/07/08	186	64.02			*64.02*	77.29					*77.29*
5/07/08	187	63.12			*63.12*	76.63					*76.63*
6/07/08	188	72.81			*72.81*	81.22					*81.22*
7/07/08	189					83.31					*83.31*
8/07/08	190	76.98			*76.98*	84.57					*84.57*
9/07/08	191										
10/07/08	192					83.82					*83.82*
11/07/08	193	84.79			*84.79*	86.89					*86.89*
12/07/08	194					49.87					*49.87*
13/07/08	195										
14/07/08	196					78.03					*78.03*
15/07/08	197	62.21			*62.21*	76.03					*76.03*
16/07/08	198										
17/07/08	199	81.10			*81.10*	82.07					*82.07*
18/07/08	200	75.87			*75.87*						
19/07/08	201	74.25			*74.25*						
20/07/08	202	55.21			*55.21*	59.92					*59.92*
21/07/08	203					64.61					*64.61*
22/07/08	204	63.98			*63.98*	82.69					*82.69*
23/07/08	205										
24/07/08	206	63.64			*63.64*	74.28					*74.28*
25/07/08	207					80.32					*80.32*
26/07/08	208	69.05			*69.05*	81.11					*81.11*
27/07/08	209										
28/07/08	210										
29/07/08	211	80.04			*80.04*	80.23					*80.23*
30/07/08	212	55.77	58.08	58.08	*57.31*	44.58					*44.58*
31/07/08	213					46.51					*46.51*
1/08/08	214	57.29	57.28	57.28	*57.28*						
2/08/08	215	59.73	57.24	57.79	*58.25*						
3/08/08	216					51.71					*51.71*
4/08/08	217					63.17					*63.17*
5/08/08	218	60.32	59.91	60.66	*60.29*	69.45					*69.45*
6/08/08	219	58.72			*58.72*	73.64	74.44	75.44			*74.51*
7/08/08	220	55.79	61.82	67.94	*61.85*	77.65					*77.65*
8/08/08	221	59.05	59.74	59.38	*59.39*	71.03					*71.03*
9/08/08	222										
10/08/08	223					79.85					*79.85*
11/08/08	224	46.58	79.45	79.86	*68.63*						
12/08/08	225	67.49			*67.49*	74.53					*74.53*
13/08/08	226	64.27	62.61	62.97	*63.28*	75.47	73.26	76.12			*74.95*
14/08/08	227	61.71			*61.71*	71.98					*71.98*
15/08/08	228	49.60	49.60	50.22	*49.81*	56.73	59.53	58.92			*58.39*
16/08/08	229	51.30			*51.30*	70.14					*70.14*
17/08/08	230	58.52			*58.52*	69.40					*69.40*
18/08/08	231	61.85	60.93		*61.39*	73.54	70.83	73.74	74.32		*72.70*
19/08/08	232	60.90			*60.90*	73.24	68.76				*71.00*

Date	Julian Day	WAITOMO STREAM HCO_3^- Concentration (ppm)				RUAKURI STREAM HCO_3^- Concentration (ppm)					
		Sample				Sample					
		(a)	(b)	(c)	*Mean*	(a)	(b)	(c)	(d)	(e)	*Mean*
20/08/08	233	72.52	71.12	72.86	*72.17*	77.40	76.55	82.20			*78.72*
21/08/08	234					79.28					*79.28*
22/08/08	235	77.39	81.06	78.00	*78.82*	81.77	81.47	83.28			*82.18*
23/08/08	236	71.29			*71.29*	69.45	80.73				*75.09*
24/08/08	237	46.88			*46.88*	68.98					*68.98*
25/08/08	238	56.52	54.80	55.92	*55.74*	78.10	76.60	74.52	83.64	80.11	*76.41*
26/08/08	239	69.86			*69.86*	80.22					*80.22*
27/08/08	240	76.66	75.71	75.71	*76.03*	83.00	80.90	78.83			*80.91*
28/08/08	241					82.27					*82.27*
29/08/08	242	79.24	76.29	76.67	*77.40*	82.14	84.27	83.29			*83.23*
30/08/08	243	81.44			*81.44*	83.09					*83.09*
31/08/08	244	81.75			*81.75*						
1/09/08	245	81.84	83.14	82.07	*82.35*	87.59	84.23	88.33			*86.71*
2/09/08	246					85.52					*85.52*
3/09/08	247	84.42	89.31	83.52	*85.75*	83.08	83.64	82.54			*83.09*
4/09/08	248										
5/09/08	249	84.89	87.87	86.75	*86.50*	87.92					*87.92*
6/09/08	250					88.02					*88.02*
7/09/08	251					91.91	90.36				*91.14*
8/09/08	252	89.24	84.45	74.06	*82.58*	89.35	88.60	88.69			*88.88*
9/09/08	253	72.06			*72.06*	81.57					*81.57*
10/09/08	254	71.22	76.09	77.99	*75.10*	82.83	81.79	82.61			*82.41*
11/09/08	255	60.05			*60.05*	58.47					*58.47*
12/09/08	256	59.53	96.18	60.62	*72.11*	73.59					*73.59*
13/09/08	257	70.32			*70.32*	79.89					*79.89*
14/09/08	258					82.14					*82.14*
15/09/08	259	79.58	78.73	76.12	*78.14*	83.26	82.42	83.93			*83.20*
16/09/08	260					81.34					*81.34*
17/09/08	261	83.34	81.37	82.82	*82.51*	85.29	84.33	84.72			*84.78*
18/09/08	262					79.53					*79.53*
19/09/08	263	76.28	75.84	72.59	*74.90*	77.11	73.90	77.15			*76.05*
20/09/08	264	75.46			*75.46*						
21/09/08	265										
22/09/08	266	82.66	83.15	85.68	*83.83*						
23/09/08	267	88.01			*88.01*						
24/09/08	268	87.48	86.19	83.65	*85.77*	88.73	88.94	87.09			*88.25*
25/09/08	269	89.56			*89.56*						
26/09/08	270	92.00	88.56	91.12	*90.56*						
27/09/08	271	88.36			*88.36*	90.32	92.08	91.45			*91.29*
28/09/08	272	93.14			*93.14*						
29/09/08	273	94.72	94.18	94.92	*94.61*						
30/09/08	274	86.51			*86.51*						
1/10/08	275	89.48	93.26	91.12	*91.28*						
2/10/08	276	93.34			*93.34*	89.22					*89.22*
3/10/08	277	93.61	92.49	94.10	*93.40*	91.18	92.03	92.97			*92.06*
4/10/08	278	92.83			*92.83*						
5/10/08	279	88.61			*88.61*						
6/10/08	280	102.34	67.00	66.54	*78.62*						
7/10/08	281	59.98	56.98	61.19	*59.39*						
8/10/08	282	54.24	53.99	52.44	*53.56*						
9/10/08	283					73.46	76.59	75.58			*75.21*

Table A.1.2. Concentrations of Na, Ca, Mg and K in the Waitomo and Ruakuri Stream waters for the 2008 sampling period. (On days when more than one streamwater sample was collected (e.g. days where data exists for samples a, b, and c, Table A.1.1) the concentration is the daily mean).

Date	Julian Day	WAITOMO STREAM				RUAKURI STREAM			
		Na (ppb)	Ca (ppb)	Mg (ppb)	K (ppb)	Na (ppb)	Ca (ppb)	Mg (ppb)	K (ppb)
21/01/08	21	6980	19293	2201	944				
22/01/08	22	6784	19577	2206	852				
23/01/08	23	6709	18901	2092	820				
24/01/08	24	6747	17917	2089	782				
25/01/08	25	6607	18095	2106	764				
26/01/08	26	6671	18367	2117	774				
27/01/08	27	6597	18539	2144	714				
28/01/08	28	6580	18477	2134	697				
29/01/08	29	6620	19228	2172	735				
30/01/08	30	6666	19031	2214	683				
31/01/08	31	6443	18549	2119	665				
1/02/08	32	6547	18297	2120	669				
2/02/08	33	6693	18587	2160	784				
3/02/08	34	6669	18971	2197	710				
4/02/08	35	6527	19142	2152	688				
5/02/08	36								
6/02/08	37	6735	18989	2200	695				
7/02/08	38	6703	18842	2206	646				
8/02/08	39	6673	18216	2164	738				
9/02/08	40	6500	18750	2135	651				
10/02/08	41	6595	18729	2180	788				
11/02/08	42	6568	18765	2191	647				
12/02/08	43								
13/02/08	44	6620	21633	2326	874				
14/02/08	45	6404	20091	2170	938				
15/02/08	46	6467	20027	2205	1051				
16/02/08	47	6701	20426	2263	918				
17/02/08	48	6301	19787	2169	858				
18/02/08	49	6370	19651	2178	831				
19/02/08	50	6444	19593	2187	823				
20/02/08	51	6339	20283	2220	777				
21/02/08	52	6408	20407	2278	761				
22/02/08	53	6328	20387	2268	750				
23/02/08	54	6474	21117	2309	760				
24/02/08	55	6424	19790	2229	829				
25/02/08	56	6387	20289	2257					
26/02/08	57	6347	19691	2121	837				
27/02/08	58	6130	18483	1864	772				
28/02/08	59	6247	21039	2075	793				
29/02/08	60	6471	21023	2044	763				
1/03/08	61	6342	20535	1962	735				
2/03/08	62	6298	19673	1956	1238				
3/03/08	63	6334	16089	1746	1140	6174	16680	1624	1224
4/03/08	64	6364	18213	1935	987	6291	19606	1896	1146
5/03/08	65	6546	19845	2042	940	6250	19460	1849	851
6/03/08	66					6225	19949	1865	778
7/03/08	67	6373	20387	2060	806	6798	21034	1975	983
8/03/08	68	6495	20530	2078	822	6741	21255	2037	890
9/03/08	69					6735	21329	1979	800
10/03/08	70	6512	21674	2108	837	6904	21001	2000	971
11/03/08	71	6497	21660	1967	746				
12/03/08	72	6943	22210	2092	766				
13/03/08	73	6961	22673	2094	775	6807	21339	2019	894

Date	Julian Day	WAITOMO STREAM				RUAKURI STREAM			
		Na (ppb)	Ca (ppb)	Mg (ppb)	K (ppb)	Na (ppb)	Ca (ppb)	Mg (ppb)	K (ppb)
14/03/08	74	*7061*	*24190*	2285	*815*	*7931*	*21189*	*2048*	*2035*
15/03/08	75	*7220*	*23529*	2281	*807*	*6738*	*21052*	*2027*	*730*
16/03/08	76	*7209*	*23699*	2196	*819*				
17/03/08	77	*7248*	*23328*	2173	*799*	*7607*	*23948*	*1933*	*1724*
18/03/08	78	*6249*	*24720*	2075	*799*				
19/03/08	79	*6266*	*26703*	2161	*767*	*6809*	*24445*	*1854*	*723*
20/03/08	80	*6277*	*22146*	1953	*638*	*6527*	*24304*	*1802*	*721*
21/03/08	81	*6286*	*23798*	2052	*677*	*6844*	*24666*	*1822*	*1111*
22/03/08	82	*6226*	*21756*	1952	*668*	*6769*	*23147*	*1727*	*1450*
23/03/08	83	*6143*	*22480*	1908	*657*	*7146*	*24969*	*1889*	*1370*
24/03/08	84	*6308*	*22395*	1971	*650*	*6723*	*24781*	*1829*	*837*
25/03/08	85	*6220*	*22150*	1951	*638*	*6798*	*24370*	*1884*	*771*
26/03/08	86	*6098*	*21750*	1919	*625*	*7066*	*24824*	*1871*	*954*
27/03/08	87					*7215*	*25237*	*1890*	*1625*
28/03/08	88	*6304*	*22791*	2042	*678*	*6404*	*24194*	*1830*	*728*
29/03/08	89	*6223*	*23140*	2037	*678*				
30/03/08	90	*6243*	*22472*	1989	*676*	*7101*	*25249*	*1941*	*1175*
31/03/08	91	*6215*	*22960*	2030	*679*	*6806*	*25320*	*1919*	*849*
1/04/08	92	*6427*	*22003*	1948	*1108*	*6427*	*22003*	*1746*	*1131*
2/04/08	93	*6438*	*21258*	2098	*1067*	*6624*	*20250*	*1779*	*1207*
3/04/08	94					*6727*	*19867*	*1809*	*1157*
4/04/08	95	*6437*	*27793*	2417	*969*	*6768*	*21590*	*1885*	*1308*
5/04/08	96	*6331*	*24290*	2149	*955*				
6/04/08	97	*6238*	*22746*	2047	*810*	*7113*	*23338*	*1878*	*1589*
7/04/08	98	*6379*	*23023*	2098	*813*	*6646*	*24126*	*1911*	*869*
8/04/08	99	*6540*	*22712*	1912	*786*	*7140*	*24199*	*1918*	*1391*
9/04/08	100	*6328*	*25823*	2017	*806*	*7096*	*24897*	*1933*	*1342*
10/04/08	101					*6426*	*23108*	*1771*	*1249*
11/04/08	102	*6490*	*23970*	1878	*764*	*6870*	*24923*	*1959*	*809*
12/04/08	103	*6652*	*25019*	2145	*769*				
13/04/08	104	*6692*	*27010*	2265	*833*				
14/04/08	105	*6612*	*26496*	2209	*793*	*6734*	*23666*	*1981*	*1199*
15/04/08	106	*7226*	*25079*	2725	*1748*	*5368*	*15126*	*1479*	*1961*
16/04/08	107								
17/04/08	108	*5744*	*12194*	1408	*1832*				
18/04/08	109	*5547*	*18171*	1460	*1391*	*5483*	*20019*	*1579*	*1164*
19/04/08	110	*5764*	*20273*	1596	*1338*				
20/04/08	111								
21/04/08	112	*5940*	*23707*	1781	*1291*	*5774*	*21311*	*1675*	*933*
22/04/08	113	*6042*	*24289*	1806	*1256*	*6206*	*22022*	*1714*	*1314*
23/04/08	114	*6134*	*23279*	1871	*1066*				
24/04/08	115								
25/04/08	116	*5829*	*21832*	1782	*959*				
26/04/08	117	*5882*	*22117*	1809	*961*	*6260*	*22753*	*1785*	*872*
27/04/08	118	*5972*	*22156*	1823	*933*	*7261*	*22697*	*1739*	*1885*
28/04/08	119					*5862*	*21353*	*1707*	*995*
29/04/08	120	*6034*	*21299*	1815	*1076*	*6288*	*21252*	*1753*	*1268*
30/04/08	121	*5934*	*16077*	1699	*1304*	*5329*	*16359*	*1441*	*1151*
1/05/08	122	*5736*	*14614*	1374	*1395*	*4891*	*17471*	*1563*	*1052*
2/05/08	123	*5808*	*17815*	1526	*1221*	*5155*	*20641*	*1302*	*1295*
3/05/08	124	*5529*	*19982*	1376	*1326*	*5337*	*21715*	*1242*	*1077*
4/05/08	125	*5667*	*21314*	1448	*1256*	*4830*	*14771*	*1314*	*1091*
5/05/08	126					*5371*	*20627*	*1159*	*1689*
6/05/08	127	*5396*	*17642*	1149	*1532*	*5421*	*20989*	*1281*	*1266*
7/05/08	128	*5554*	*19991*	1228	*1362*	*5595*	*21184*	*1295*	*1004*
8/05/08	129	*5681*	*20607*	1267	*1418*	*5446*	*20649*	*1329*	*1029*
9/05/08	130	*5861*	*20860*	1329	*1351*	*5431*	*19120*	*1282*	*1042*

Date	Julian Day	WAITOMO STREAM				RUAKURI STREAM			
		Na (ppb)	*Ca (ppb)*	*Mg (ppb)*	*K (ppb)*	*Na (ppb)*	*Ca (ppb)*	*Mg (ppb)*	*K (ppb)*
10/05/08	131	*5811*	*19477*	1335	*1229*	*5731*	*21120*	*1295*	*1053*
11/05/08	132					*5574*	*20447*	*1358*	*1028*
12/05/08	133					*5891*	*21663*	*1353*	*929*
13/05/08	134	*5814*	*21140*	1449	*1051*	*5870*	*21412*	*1420*	*1196*
14/05/08	135	*5962*	*21804*	1386	*1182*	*6144*	*21583*	*1445*	*934*
15/05/08	136	*5872*	*21819*	1398	*1113*	*6144*	*21583*	*1493*	*950*
16/05/08	137								
17/05/08	138	*5881*	*21892*	1502	*980*	*5557*	*20104*	*1535*	*736*
18/05/08	139	*6248*	*22129*	1626	*1064*	*5761*	*19779*	*1558*	*809*
19/05/08	140					*5904*	*20009*	*1618*	*804*
20/05/08	141	*6308*	*22381*	1745	*825*	*6234*	*21723*	*1757*	*760*
21/05/08	142					*6442*	*20531*	*1736*	*762*
22/05/08	143					*6307*	*20482*	*1728*	*797*
23/05/08	144	*6403*	*22978*	1762	*821*	*6603*	*21154*	*1825*	*973*
24/05/08	145	*6424*	*23207*	1739	*865*	*6601*	*21326*	*1851*	*819*
25/05/08	146								
26/05/08	147	*6600*	*22342*	1839	*793*	*7006*	*22302*	*1944*	*1055*
27/05/08	148	*6744*	*23067*	1858	*822*				
28/05/08	149	*6843*	*22709*	1893	*914*	*6816*	*22104*	*1933*	*716*
29/05/08	150					*7937*	*22929*	*2018*	*1512*
30/05/08	151	*6777*	*24730*	1895	*864*	*6779*	*21291*	*1943*	*754*
31/05/08	152	*6817*	*22867*	1875	*829*				
1/06/08	153	*6761*	*24424*	1902	*914*	*7285*	*22294*	*1992*	*776*
2/06/08	154	*7138*	*22619*	1952	*912*	*8197*	*21475*	*1994*	*1673*
3/06/08	155	*7297*	*22453*	1988	*991*	*7302*	*20717*	*2027*	*819*
4/06/08	156	*7020*	*22031*	1940	*838*	*6961*	*20867*	*1995*	*748*
5/06/08	157					*7200*	*21878*	*2084*	*747*
6/06/08	158	*7232*	*24668*	2024	*881*	*7140*	*21820*	*2096*	*736*
7/06/08	159	*7162*	*23679*	2004	*930*	*7243*	*21643*	*2034*	*839*
8/06/08	160					*7468*	*19333*	*2058*	*1675*
9/06/08	161					*6803*	*19803*	*1982*	*819*
10/06/08	162	*7547*	*23450*	2102	*1011*	*7124*	*20527*	*1999*	*861*
11/06/08	163	*6977*	*21228*	1930	*863*	*6061*	*21144*	*1618*	*787*
12/06/08	164					*6620*	*21830*	*1662*	*1815*
13/06/08	165	*5975*	*20163*	1361	*776*	*6023*	*20724*	*1512*	*727*
14/06/08	166	*6070*	*21120*	1378	*873*	*6059*	*21519*	*1551*	*738*
15/06/08	167								
16/06/08	168	*6309*	*21749*	1480	*795*				
17/06/08	169	*5933*	*16237*	1332	*1286*	*5611*	*17001*	*1337*	*1073*
18/06/08	170					*5765*	*20059*	*1474*	*892*
19/06/08	171	*5478*	*17458*	1152	*1015*	*5986*	*20244*	*1437*	*804*
20/06/08	172					*6185*	*21638*	*1533*	*800*
21/06/08	173	*5858*	*19293*	1336	*811*				
22/06/08	174					*6074*	*21166*	*1467*	*1230*
23/06/08	175	*5069*	*12667*	979	*1136*	*5654*	*19026*	*1386*	*1240*
24/06/08	176	*5740*	*13826*	1063	*1019*	*5467*	*19353*	*1336*	*1123*
25/06/08	177					*5296*	*17683*	*1261*	*858*
26/06/08	178	*5654*	*13178*	1042	*970*				
27/06/08	179	*5776*	*14696*	1067	*959*	*5330*	*17934*	*1241*	*1001*
28/06/08	180	*5870*	*12705*	1033	*1028*	*5783*	*17970*	*1301*	*972*
29/06/08	181								
30/06/08	182	*5515*	*16256*	1055	*885*	*5643*	*19481*	*1295*	*1103*
1/07/08	183								
2/07/08	184	*5610*	*17514*	1088	*866*	*5357*	*16072*	*1217*	*934*
3/07/08	185	*5528*	*14062*	1010	*966*	*5504*	*17756*	*1286*	*885*
4/07/08	186	*5836*	*15183*	1094	*900*	*5499*	*18242*	*1285*	*804*
5/07/08	187	*5956*	*14671*	1103	*917*	*5583*	*17742*	*1289*	*812*

Date	Julian Day	WAITOMO STREAM				RUAKURI STREAM			
		Na (ppb)	Ca (ppb)	Mg (ppb)	K (ppb)	Na (ppb)	Ca (ppb)	Mg (ppb)	K (ppb)
6/07/08	188	5856	16131	1097	900	5413	18782	1286	730
7/07/08	189					5542	19615	1318	723
8/07/08	190	5919	17740	1145	926	5986	18402	1373	844
9/07/08	191								
10/07/08	192					6184	18412	1390	760
11/07/08	193	5738	16860	1180	689	6307	18827	1389	959
12/07/08	194					5250	12220	1116	1157
13/07/08	195								
14/07/08	196					6299	17685	1269	1462
15/07/08	197	5480	13369	1008	1005	6065	16798	1294	808
16/07/08	198								
17/07/08	199	5602	16159	1065	808	6225	18092	1339	796
18/07/08	200	5660	15768	1082	823				
19/07/08	201	5796	14630	1098	822				
20/07/08	202	5553	11947	1047	913	5469	13621	1126	975
21/07/08	203					5680	15190	1168	1063
22/07/08	204	6025	14525	1088	863	5723	17297	1211	797
23/07/08	205								
24/07/08	206	5910	13812	1050	901	5925	16481	1157	1338
25/07/08	207					5831	17904	1194	779
26/07/08	208	5774	14960	1057	832	5740	17276	1180	805
27/07/08	209								
28/07/08	210								
29/07/08	211	6126	17303	1248	762	6133	17418	1256	821
30/07/08	212	5887	11764	1095	1042	4575	9507	842	1024
31/07/08	213					5240	10264	1025	1099
1/08/08	214	5555	12697	1022	1196				
2/08/08	215	5613	13409	1030	1081				
3/08/08	216					5583	12032	938	1476
4/08/08	217					5441	14237	1136	953
5/08/08	218	5850	13398	1086	1089	5346	15121	1131	797
6/08/08	219	5600	13658	1068	1078	5550	16412	1199	765
7/08/08	220	5541	13524	1084	1086	5615	16149	1202	775
8/08/08	221	5858	14219	1164	1224	5526	15062	1197	748
9/08/08	222								
10/08/08	223					5826	16866	1275	736
11/08/08	224	5909	18386	1232	938				
12/08/08	225	6293	15301	1242	1017	5752	16069	1312	790
13/08/08	226	5758	14332	1070	943	5603	15489	1234	768
14/08/08	227	6018	14587	1128	957	5743	16271	1288	763
15/08/08	228	6120	11624	1079	951	5410	12564	1148	891
16/08/08	229	5992	12839	1040	953	5798	15974	1238	851
17/08/08	230	6343	15006	1115	964	5513	15414	1181	814
18/08/08	231	6251	14850	1094	953	5512	16066	1185	756
19/08/08	232	5432	12252	1058	774	5948	16126	1299	886
20/08/08	233	4853	14592	988	873	5933	17637	1261	886
21/08/08	234					5859	16712	1218	843
22/08/08	235	5034	16153	1068	877	6332	18576	1305	900
23/08/08	236	5113	16057	1045	906	5940	17280	1289	901
24/08/08	237	5201	10090	1011	955	5123	15040	1118	1022
25/08/08	238	5241	13287	1011	1086	5593	17103	1180	910
26/08/08	239	5379	15694	1041	955	5706	16214	1151	815
27/08/08	240	5531	17181	1145	904	5827	16724	1171	816
28/08/08	241					6167	17565	1243	868
29/08/08	242	5818	17568	1190	912	6234	17227	1239	848
30/08/08	243	5793	17493	1188	890	6311	17448	1295	818
31/08/08	244	6017	18387	1247	874				

Date	Julian Day	WAITOMO STREAM				RUAKURI STREAM			
		Na (ppb)	Ca (ppb)	Mg (ppb)	K (ppb)	Na (ppb)	Ca (ppb)	Mg (ppb)	K (ppb)
1/09/08	245	5956	17976	1283	826	6348	17368	1278	810
2/09/08	246					6982	19191	1432	862
3/09/08	247	5923	18994	1303	874	6681	18111	1363	840
4/09/08	248								
5/09/08	249	6386	20069	1443	933	7425	18592	1497	992
6/09/08	250					6455	20095	1250	776
7/09/08	251					6583	20714	1298	782
8/09/08	252	6103	21331	1343	879	6723	20478	1335	763
9/09/08	253	5883	17448	1270	900	6728	18824	1343	841
10/09/08	254	5925	16944	1282	879	6568	19193	1296	1013
11/09/08	255	5672	13677	1187	978	5326	14317	1021	1093
12/09/08	256	5568	13878	1100	934	5498	17654	1087	855
13/09/08	257	5608	15608	1136	847	5755	18990	1140	821
14/09/08	258					5872	19341		
15/09/08	259	5982	17960	1266	803	6156	20046	1222	824
16/09/08	260					6480	20615	1268	1103
17/09/08	261	6150	18722	1322	786	6265	20246	1242	973
18/09/08	262					6222	18755	1235	791
19/09/08	263	6232	17069	1326	836	6253	18387	1241	801
20/09/08	264	6064	18028	1328	775				
21/09/08	265								
22/09/08	266	5909	18971	1223	774				
23/09/08	267	6053	19827	1280	798				
24/09/08	268	6260	20146	1327	823	6525	20641	1342	752
25/09/08	269	6397	20755	1379	789				
26/09/08	270	6396	21179	1377	804				
27/09/08	271	6570	21626	1435	807	6680	21338	1354	948
28/09/08	272	6458	21406	1436	759				
29/09/08	273	6516	21290	1453	751				
30/09/08	274	6784	20024	1485	799				
1/10/08	275	6553	20811	1448	789				
2/10/08	276	6766	21310	1492	791	6454	21218	1328	944
3/10/08	277	6424	21061	1386	779	6573	21776	1362	866
4/10/08	278	6351	20803	1342	781				
5/10/08	279	6453	19947	1351	817				
6/10/08	280	5504	15618	1103	924				
7/10/08	281	5785	13690	1104	1033				
8/10/08	282	5477	12607	1001	1327				
9/10/08	283					5667	18310	1154	1026

Table A.1.3. $\delta^{13}C$ of the Waitomo and Ruakuri Streams for the 2008 sampling period.

Date	Julian Day	WAITOMO STREAM Isotope $\delta^{13}C$ (‰) Sample (a)	(b)	(c)	*Mean*	RUAKURI STREAM Isotope $\delta^{13}C$ (‰) Sample (a)	(b)	(c)	*Mean*
21/01/08	21	-11.35			*-11.35*				
22/01/08	22	-11.75			*-11.75*				
23/01/08	23	-10.83			*-10.83*				
24/01/08	24								
25/01/08	25	-10.73			*-10.73*				
26/01/08	26	-11.27			*-11.27*				
27/01/08	27	-11.30			*-11.30*				
28/01/08	28								
29/01/08	29	-11.03			*-11.03*				
30/01/08	30								
31/01/08	31								
1/02/08	32	-10.59			*-10.59*				
2/02/08	33	-11.07			*-11.07*				
3/02/08	34	-10.84			*-10.84*				
4/02/08	35	-11.06			*-11.06*				
5/02/08	36	-11.30			*-11.30*				
6/02/08	37								
7/02/08	38								
8/02/08	39	-10.95			*-10.95*				
9/02/08	40	-11.14			*-11.14*				
10/02/08	41	-11.37			*-11.37*				
11/02/08	42	-11.39			*-11.39*				
12/02/08	43								
13/02/08	44	-11.53			*-11.53*				
14/02/08	45	-11.74			*-11.74*				
15/02/08	46	-11.33			*-11.33*				
16/02/08	47	-11.51			*-11.51*				
17/02/08	48								
18/02/08	49	-11.46			*-11.46*				
19/02/08	50								
20/02/08	51	-11.43			*-11.43*				
21/02/08	52	-11.36			*-11.36*				
22/02/08	53								
23/02/08	54	-11.48			*-11.48*				
24/02/08	55	-11.54			*-11.54*				
25/02/08	56	-11.55			*-11.55*				
26/02/08	57	-11.31			*-11.31*				
27/02/08	58								
28/02/08	59	-11.50			*-11.50*				
29/02/08	60	-12.01			*-12.01*				
1/03/08	61	-11.61			*-11.61*				
2/03/08	62	-11.81			*-11.81*				
3/03/08	63								
4/03/08	64	-12.83			*-12.83*				
5/03/08	65	-13.32			*-13.32*	-13.53			*-13.53*
6/03/08	66					-11.28			*-11.28*
7/03/08	67	-11.37			*-11.37*	-11.41			*-11.41*
8/03/08	68	-11.23			*-11.23*	-11.32			*-11.32*
9/03/08	69					-11.26			*-11.26*
10/03/08	70	-11.30			*-11.30*	-11.45			*-11.45*
11/03/08	71	-11.08			*-11.08*				
12/03/08	72								
13/03/08	73	-11.07			*-11.07*	-11.65			*-11.65*
14/03/08	74	-11.70			*-11.70*	-12.25			*-12.25*
15/03/08	75	-11.29			*-11.29*	-11.32			*-11.32*
16/03/08	76	-11.30			*-11.30*				

Date	Julian Day	WAITOMO STREAM Isotope δ13C (‰) Sample (a)	(b)	(c)	Mean	RUAKURI STREAM Isotope δ13C (‰) Sample (a)	(b)	(c)	Mean
17/03/08	77	-11.20			*-11.20*	-11.30			*-11.30*
18/03/08	78	-11.36			*-11.36*				
19/03/08	79	-11.12			*-11.12*	-11.41			*-11.41*
20/03/08	80	-10.47			*-10.47*	-11.26			*-11.26*
21/03/08	81	-10.94			*-10.94*	-11.30			*-11.30*
22/03/08	82	-10.91			*-10.91*	-11.24			*-11.24*
23/03/08	83	-10.89			*-10.89*	-11.04			*-11.04*
24/03/08	84	-10.66			*-10.66*	-11.32			*-11.32*
25/03/08	85	-10.64			*-10.64*	-11.14			*-11.14*
26/03/08	86	-10.64			*-10.64*	-11.31			*-11.31*
27/03/08	87					-11.18			*-11.18*
28/03/08	88	-10.62			*-10.62*	-11.07			*-11.07*
29/03/08	89	-10.77			*-10.77*				
30/03/08	90	-10.54			*-10.54*	-11.38			*-11.38*
31/03/08	91	-11.48			*-11.48*	-11.75			*-11.75*
1/04/08	92	-11.73			*-11.73*	-12.28	-12.21	-12.09	*-12.19*
2/04/08	93	-11.71			*-11.71*	-12.38			*-12.38*
3/04/08	94					-12.05			*-12.05*
4/04/08	95	-10.83			*-10.83*	-11.41			*-11.41*
5/04/08	96	-11.39			*-11.39*				
6/04/08	97	-11.14			*-11.14*	-11.17			*-11.17*
7/04/08	98	-10.80			*-10.80*	-11.07			*-11.07*
8/04/08	99	-11.07			*-11.07*	-11.18			*-11.18*
9/04/08	100	-11.09			*-11.09*	-10.89			*-10.89*
10/04/08	101					-10.84			*-10.84*
11/04/08	102	-10.46			*-10.46*	-10.97			*-10.97*
12/04/08	103	-10.93			*-10.93*				
13/04/08	104	-11.17			*-11.17*				
14/04/08	105	-10.74			*-10.74*	-10.89			*-10.89*
15/04/08	106	-12.80			*-12.80*				
16/04/08	107								
17/04/08	108								
18/04/08	109								
19/04/08	110								
20/04/08	111								
21/04/08	112					-10.86			*-10.86*
22/04/08	113	-12.21			*-12.21*				
23/04/08	114	-11.51			*-11.51*				
24/04/08	115								
25/04/08	116	-11.20			*-11.20*				
26/04/08	117	-11.23			*-11.23*				
27/04/08	118	-11.06			*-11.06*				
28/04/08	119								
29/04/08	120	-11.56			*-11.56*				
30/04/08	121								
1/05/08	122								
2/05/08	123								
3/05/08	124								
4/05/08	125								
5/05/08	126								
6/05/08	127								
7/05/08	128					-13.52			*-13.52*
8/05/08	129								
9/05/08	130					-13.88			*-13.88*
10/05/08	131					-13.77			*-13.77*
11/05/08	132								
12/05/08	133					-14.24			*-14.24*
13/05/08	134								

Date	Julian Day	WAITOMO STREAM Isotope δ13C (‰)				RUAKURI STREAM Isotope δ13C (‰)			
		Sample				Sample			
		(a)	(b)	(c)	*Mean*	(a)	(b)	(c)	*Mean*
14/05/08	135					-14.28			*-14.28*
15/05/08	136								
16/05/08	137								
17/05/08	138								
18/05/08	139								
19/05/08	140								
20/05/08	141					-12.47			*-12.47*
21/05/08	142					-10.92			*-10.92*
22/05/08	143								
23/05/08	144								
24/05/08	145	-11.60			*-11.60*	-11.07			*-11.07*
25/05/08	146								
26/05/08	147	-10.77			*-10.77*	-11.30			*-11.30*
27/05/08	148	-11.72			*-11.72*				
28/05/08	149	-12.19			*-12.19*	-10.81			*-10.81*
29/05/08	150					-12.47			*-12.47*
30/05/08	151	-12.35			*-12.35*				
31/05/08	152	-11.94			*-11.94*				
1/06/08	153	-11.15			*-11.15*	-10.88			*-10.88*
2/06/08	154								
3/06/08	155								
4/06/08	156	-10.40			*-10.40*	-10.81			*-10.81*
5/06/08	157					-10.74			*-10.74*
6/06/08	158	-11.05			*-11.05*				
7/06/08	159								
8/06/08	160								
9/06/08	161								
10/06/08	162								
11/06/08	163	-10.70			*-10.70*				
12/06/08	164								
13/06/08	165	-11.00			*-11.00*				
14/06/08	166	-11.30			*-11.30*	-10.51			*-10.51*
15/06/08	167								
16/06/08	168	-10.30			*-10.30*				
17/06/08	169	-10.96			*-10.96*	-12.06			*-12.06*
18/06/08	170					-10.65			*-10.65*
19/06/08	171	-12.49			*-12.49*	-10.59			*-10.59*
20/06/08	172								
21/06/08	173	-10.90			*-10.90*				
22/06/08	174					-10.74			*-10.74*
23/06/08	175								
24/06/08	176	-12.15			*-12.15*				
25/06/08	177					-11.64			*-11.64*
26/06/08	178	-11.64			*-11.64*				
27/06/08	179	-12.27			*-12.27*				
28/06/08	180	-10.32			*-10.32*	-12.12			*-12.12*
29/06/08	181								
30/06/08	182	-11.68			*-11.68*	-11.39			*-11.39*
1/07/08	183								
2/07/08	184	-11.69			*-11.69*	-11.63			*-11.63*
3/07/08	185								
4/07/08	186					-11.26			*-11.26*
5/07/08	187					-11.39			*-11.39*
6/07/08	188	-12.17			*-12.17*	-11.30			*-11.30*
7/07/08	189								
8/07/08	190								
9/07/08	191								
10/07/08	192					-11.08			*-11.08*

Date	Julian Day	WAITOMO STREAM Isotope $\delta^{13}C$ (‰) Sample (a)	(b)	(c)	*Mean*	RUAKURI STREAM Isotope $\delta^{13}C$ (‰) Sample (a)	(b)	(c)	*Mean*
11/07/08	193	-10.62			*-10.62*	-10.45			*-10.45*
12/07/08	194								
13/07/08	195								
14/07/08	196					-11.74			*-11.74*
15/07/08	197	-12.22			*-12.22*				
16/07/08	198								
17/07/08	199	-11.70			*-11.70*				
18/07/08	200								
19/07/08	201	-14.11			*-14.11*				
20/07/08	202	-12.31			*-12.31*	-13.12			*-13.12*
21/07/08	203					-12.08			*-12.08*
22/07/08	204	-12.17			*-12.17*				
23/07/08	205								
24/07/08	206	-12.56			*-12.56*	-12.42			*-12.42*
25/07/08	207					-11.36			*-11.36*
26/07/08	208					-11.92			*-11.92*
27/07/08	209								
28/07/08	210								
29/07/08	211	-11.09			*-11.09*	-11.45			*-11.45*
30/07/08	212	-12.47	-12.55		*-12.51*				
31/07/08	213					-12.99			*-12.99*
1/08/08	214	-11.91			*-11.91*				
2/08/08	215	-12.36			*-12.36*				
3/08/08	216					-12.78			*-12.78*
4/08/08	217					-12.43			*-12.43*
5/08/08	218					-12.08			*-12.08*
6/08/08	219			-12.41	*-12.41*	-11.96			*-11.96*
7/08/08	220	-12.61			*-12.61*				
8/08/08	221		-12.24		*-12.24*				
9/08/08	222								
10/08/08	223					-11.27			*-11.27*
11/08/08	224	-12.31			*-12.31*				
12/08/08	225	-12.03			*-12.03*	-11.56			*-11.56*
13/08/08	226	-12.16			*-12.16*	-11.31			*-11.31*
14/08/08	227								
15/08/08	228	-11.78			*-11.78*				
16/08/08	229	-12.36			*-12.36*				
17/08/08	230	-12.13			*-12.13*		-11.68		*-11.68*
18/08/08	231	-12.49			*-12.49*		-11.56	-11.61	*-11.59*
19/08/08	232					-11.84	-11.58		*-11.71*
20/08/08	233	-12.01			*-12.01*	-11.73			*-11.73*
21/08/08	234					-11.52			*-11.52*
22/08/08	235	-11.59			*-11.59*	-11.43	-11.55		*-11.49*
23/08/08	236	-12.26			*-12.26*				
24/08/08	237	-12.61			*-12.61*				
25/08/08	238	-12.17			*-12.17*	-12.34	-11.95		*-12.15*
26/08/08	239					-11.75	-11.65		*-11.70*
27/08/08	240	-11.75			*-11.75*				
28/08/08	241					-11.48			*-11.48*
29/08/08	242	-12.15			*-12.15*	-11.35			*-11.35*
30/08/08	243	-12.57			*-12.57*	-11.40			*-11.40*
31/08/08	244	-12.36			*-12.36*				
1/09/08	245	-11.74			*-11.74*	-11.04			
2/09/08	246					-11.10			*-11.10*
3/09/08	247	-12.37			*-12.37*				
4/09/08	248								
5/09/08	249	-12.20			*-12.20*				
6/09/08	250								

Date	Julian Day	WAITOMO STREAM Isotope δ13C (‰) Sample (a)	(b)	(c)	*Mean*	RUAKURI STREAM Isotope δ13C (‰) Sample (a)	(b)	(c)	*Mean*
7/09/08	251					-10.73			*-10.73*
8/09/08	252	-11.07	-11.48		*-11.28*	-11.20	-10.67	-10.70	*-10.86*
9/09/08	253	-11.50			*-11.50*	-10.85			*-10.85*
10/09/08	254	-11.91	-12.21		*-12.06*	-11.16	-11.18	-11.08	*-11.14*
11/09/08	255	-12.41			*-12.41*	-12.09			*-12.09*
12/09/08	256	-12.24	-12.00	-12.16	*-12.13*				
13/09/08	257	-12.18			*-12.18*				
14/09/08	258					-11.23			*-11.23*
15/09/08	259	-11.70	-12.05	-11.96	*-11.90*	-11.46			*-11.46*
16/09/08	260					-11.26			*-11.26*
17/09/08	261	-11.48	-12.06	-11.79	*-11.78*	-11.13			*-11.13*
18/09/08	262								
19/09/08	263	-11.94	-11.99	-12.13	*-12.02*	-11.35			*-11.35*
20/09/08	264	-12.19			*-12.19*				
21/09/08	265								
22/09/08	266	-11.91	-11.86	-11.50	*-11.76*				
23/09/08	267	-11.63			*-11.63*				
24/09/08	268	-11.42	-11.38	-11.62	*-11.47*	-11.25			*-11.25*
25/09/08	269	-11.34			*-11.34*				
26/09/08	270	-11.28	-11.16	-11.25	*-11.23*				
27/09/08	271	-11.16			*-11.16*	-10.95			*-10.95*
28/09/08	272	-11.05			*-11.05*				
29/09/08	273	-11.14	-11.21	-11.22	*-11.19*				
30/09/08	274	-11.60			*-11.60*				
1/10/08	275	-11.13			*-11.13*				
2/10/08	276					-10.82			*-10.82*
3/10/08	277	-10.95			*-10.95*	-10.73			*-10.73*
4/10/08	278								
5/10/08	279								
6/10/08	280	-11.25	-12.23		*-11.74*				
7/10/08	281								
8/10/08	282	-12.64	-13.21		*-12.93*				
9/10/08	283								

Table A.1.4. Chemistry of dripwater samples collected from a drip in the Blanket Chamber, Glowworm Cave, throughout 2008.

Date	Drip collection period (Julian day)	HCO_3 (ppm)	Na (ppb)	Ca (ppb)	Mg (ppb)	K (ppb)	δ 13C (‰)
17/05/08 - 17/06/08	138-169	162	8860	35845	3411	416	-9.88
17/06/08 - 26/06/08	169-178	161	9032	33676	3440	408	
26/06/08 - 8/07/08	178-190	214	9049	44344	3429	372	
8/07/08 - 11/07/08	190-193	142	9217	59654	3562	362	-13.48
11/07/08 - 24/07/08	193-206	305	8587	58864	3534	369	-13.08
24/07/08 - 1/08/08	206-214	285	8698	56813	3600	380	-12.14
1/08/08 - 11/08/08	214-224	324	8956	63134	3602	386	-13.31
11/08/08 - 19/08/08	224-232	333	9315	66404	3865	409	-13.82
19/08/08	232	336	9444	65810	3909	409	-13.88
19/08/08 - 5/09/08	232-249	177	9153	69544	3588	432	-13.65
5/09/08	249	180	9378	67411	3833	423	-13.56

Table A.1.5. Dripwater autosampler raw data (days 253 and 254, 9th and 10th September 2008).

Day:Time	Na	Ca	Na	Ca	Na	Ca	Mean Na	Mean Ca	Rainfall
	(a)	(a)	(b)	(b)	(c)	(c)			
253:0900	18302	38688	17719	34575	17818	33850	***17946***	***35704***	5.8
253:1000	10182	39500	10410	36731	10712	38500	***10434***	***38244***	2
253:1100	9543	40938	9451	39570	9654	39379	***9549***	***39962***	1.4
253:1200	9602	40266	9726	38791	9132	37576	***9487***	***38877***	0.4
253:1300	10257	35530	10563	34205	9858	34090	***10226***	***34608***	0
253:1400	12028	50497	12371	49811	11689	49428	***12030***	***49912***	0
									0
253:1600	9589	41232	10094	42274	9783	42083	***9822***	***41863***	0
253:1700	10194	42934	10127	41314	10059	41970	***10127***	***42073***	0
253:1800	9913	44284	9876	42991	9849	44577	***9879***	***43950***	0.2
253:1900	10133	40143	10089	39831	9643	40208	***9955***	***40060***	0
253:2000	9667	44818	9617	43722	9503	44187	***9596***	***44242***	0
253:2100	9934	41913	9920	41106	9453	40607	***9769***	***41209***	0
253:2200	10311	40096	10246	37230	9950	37926	***10169***	***38417***	0
									0
254:2400	10107	43824	9989	43153	9645	42712	***9914***	***43230***	0.2
254:0100	8956	41836	9909	41114	9788	41555	***9551***	***41501***	0
254:0200	9945	29255					***9945***	***29255***	0
254:0300	9414	25674					***9414***	***25674***	0
254:0400	12072	30763					***12072***	***30763***	0
									0
254:0600	9687	36428	10561	36523	10026	35353	***10091***	***36101***	0.4
									0
254:0800	9363	50831	10120	50505	9380	48782	***9621***	***50039***	0

Table A.1.6. Dripwater autosampler raw data (days 280 and 282, 6th – 8th October 2008).

Day:Time	Na	Ca	Na	Ca	Na	Ca	Mean Na	Mean Ca	Rainfall
	(a)	(a)	(b)	(b)	(c)	(c)			
280:1000	8851	62194	8955	62341	9053	60412	***8953***	***61649***	4.2
280:1200	9196	63392	9112	62798	9273	62972	***9194***	***63054***	2
280:1400	9110	63364	9422	65143	9345	63730	***9292***	***64079***	1.2
280:1600	9400	63116	8942	64044	9445	64730	***9262***	***63963***	4.6
280:1800	9502	64887	9582	67532	9540	66040	***9541***	***66153***	0.2
280:2000	9723	59630	9841	60648	10075	60752	***9880***	***60343***	0
281:2200	10002	55459	10179	56839	10283	57667	***10155***	***56655***	0.2
281:2400	9574	56479	9302	56309	9589	57319	***9488***	***56702***	3.2
281:0200	9123	39378					***9123***	***39378***	2.2
281:0400	8682	42275	8578	43431	8523	44303	***8594***	***43336***	5
									0.4
281:0800	9067	55707	9001	55583	9087	58390	***9052***	***56560***	1.8
									4
281:1200	9376	57686	9339	58130	8971	58150	***9228***	***57989***	0.4
281:1400	8978	48605	8447	46879	8419	48347	***8615***	***47943***	20.2
281:1600	7673	50715	8480	43854			***8077***	***47285***	22.4
281:1800	8650	44694	9151	48714			***8900***	***46704***	3.6
281:2000	9748	49639					***9748***	***49639***	3.4
281:2200	8605	41294					***8605***	***41294***	0
281:2400	9130	48006	9375	49178	8994	48648	***9166***	***48610***	0.2
282:0200	9003	49754	9515	51218	8955	49705	***9158***	***50226***	2.2
282:0400	9108	60250	9730	64125	9325	62656	***9388***	***62344***	0.2
282:0600	9083	60288	9504	61722	8988	60496	***9192***	***60836***	0.2

A.2 An example of a GRAN plot calibration curve in Excel

GRAN plots were used to accurately obtain the HCO_3 concentration of the sample. Using the Titrino titrator print-out, the volume of acid required to reduce the sample pH to 5.5 (V1c), and the pH values as they changed with the addition of acid, were attained.

The Gran function was calculated using the equation:

$$(V_o + V) \times 10^{-pH} \quad \text{Equation A.2.1}$$

where:
V_o is the volume of the sample
V is the volume of the acid added.

Table A.2.1. An example of a GRAN function table.

Sample	**Sample volume** (mls)	**Initial volume HCl** (mls)	**pH**	**Vol HCl added** (mls)		**Gran function**
	V_o	V_1c		V_2e	V (mls)	(Vo + V) × 10^{-pH}
GLO 200	10	0.13	4.79	0.00	0.130	0.00016
	10	0.13	4.37	0.01	0.140	0.00044
	10	0.13	4.18	0.02	0.150	0.00067
	10	0.13	4.01	0.03	0.160	0.00100
	10	0.13	3.89	0.04	0.170	0.00132
	10	0.13	3.79	0.05	0.180	0.00165
	10	0.13	3.72	0.06	0.190	0.00193
	10	0.13	3.65	0.07	0.200	0.00227
	10	0.13	3.61	0.08	0.210	0.00251
	10	0.13	3.55	0.09	0.220	0.00287
	10	0.13	3.52	0.10	0.230	0.00313
	10	0.13	3.49	0.11	0.240	0.00329

The Gran function was then plotted against the sample volume (V), producing a straight line, which crossed the x-axis at V_2 (the volume of acid required to 'neutralise' the bicarbonate) (Figure A.2).

$$Bicarbonate\ concentration = \frac{V_2 M\ (HCl)}{V_o}\ moles.\ l^{-1}$$ Equation A.2.2

where:

M is the concentration, in moles, of HCl used (e.g. 0.0987).

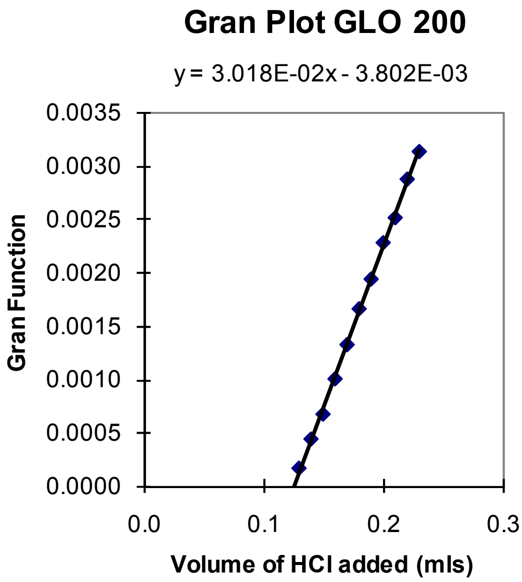

Figure A.2 1. Gran plot for the Waitomo Stream sample GLO 200.

Using the equation obtained from the Gran plot, the endpoint was determined:

$$Endpoint = \frac{3.802e^{-3}}{3.018e^{-2}}$$

(e.g. endpoint = 0.126 mls)

The calculation to determine the bicarbonate was completed via activated cells to give a data table as follows, e.g:

Table A.2.2. The active cells used to determine the bicarbonate concentration.

Sample Name	Sample Volume	Endpoint	Acid Conc.	HCO_3^- Concentration	
	V_o	V_2	M	$mMol.l^{-1}$	ppm
GLO 200	10.0	0.126	0.0987	***1.24***	***75.87***

A.3 Mean annual data

Table A.3. Summary table of the mean annual daily averages for cave microclimate, local external climatic and tourist associated parameters for the Glowworm Cave between 1998 and 2007. (Every day throughout the ten-year data period was evaluated to determine the daily average and/or maximum values for P_{CO_2}, internal and external temperatures, temperature gradient, number of tourists, stream discharge and rainfall. Numbers in brackets indicate the number of data points used to obtain each value.

	Mean P_{CO_2} (ppm)	Max. P_{CO_2} (ppm)	Tourist numbers	Mean Temp. out (°C)	Mean Temp. Cave (°C)	Avg. Temp. grad (°C)	Mean Temp. grad (°C)	Mean discharge ($m^3.s^{-1}$)	Max discharge ($m^3.s^{-1}$)	Rainfall (mm)
1998	904 *(328)*	1318 *(328)*	803 *(365)*	13.95 *(330)*	15.65 *(289)*	3.49 *(289)*	6.38 *(289)*	2.19 *(365)*	3.08 *(365)*	5.42 *(365)*
1999	829 *(335)*	1331 *(335)*	871 *(365)*	13.87 *(334)*	15.82 *(334)*	3.92 *(334)*	7.09 *(334)*	1.49 *(365)*	1.95 *(365)*	4.65 *(365)*
2000	759 *(336)*	1295 *(336)*	941 *(366)*	13.45 *(336)*	15.37 *(336)*	3.41 *(336)*	6.46 *(336)*	1.61 *(366)*	2.17 *(366)*	5.05 *(366)*
2001	771 *(365)*	1366 *(365)*	1009 *(365)*	13.68 *(334)*	15.17 *(330)*	3.53 *(330)*	6.34 *(330)*	1.48 *(365)*	1.86 *(365)*	5.10 *(365)*
2002	777 *(360)*	1369 *(360)*	1090 *(365)*	14.22 *(327)*	14.44 *(327)*	2.74 *(327)*	5.80 *(327)*	1.66 *(365)*	2.08 *(365)*	4.96 *(365)*
2003	817 *(360)*	1368 *(360)*	990 *(365)*	13.09 *(349)*	14.53 *(360)*	3.74 *(349)*	6.97 *(349)*	1.61 *(365)*	2.05 *(365)*	5.37 *(365)*
2004	764 *(336)*	1336 *(336)*	975 *(365)*	12.10 *(335)*	14.31 *(335)*	3.51 *(335)*	6.55 *(335)*	1.88 *(357)*	2.45 *(357)*	6.11 *(366)*
2005	687 *(335)*	1194 *(335)*	884 *(358)*	13.22 *(334)*	14.28 *(334)*	3.20 *(334)*	6.43 *(334)*	1.42 *(365)*	1.74 *(365)*	4.48 *(365)*
2006	889 *(233)*	1352 *(233)*	819 *(365)*	11.28 *(209)*	13.62 *(235)*	3.31 *(209)*	6.25 *(209)*	1.84 *(365)*	2.54 *(365)*	5.35 *(365)*
2007	1003 *(357)*	1481 *(357)*	812 *(365)*	13.93 *(357)*	14.12 *(357)*	3.74 *(357)*	7.56 *(357)*	1.56 *(365)*	2.02 *(365)*	4.53 *(334)*

A.4 Water chemistry data summarised

Table A.4. Summary of the general chemical and physical properties of the Waitomo and Ruakuri Streams and dripwater from a straw stalactite in the Blanket Chamber for 2008. A summer total and winter total for the mean of daily means are given for each site, followed by a further breakdown in the data where rain days and non-rain days are considered separately. Sample size for each parameter is given italicised and in parentheses.

	Rainfall (mm)	Discharge ($m^3.s^{-1}$)	Water Level (m)	P_{CO_2} (ppm)	HCO_3^- (ppm)	Ca^{2+} (ppb)	Na^{2+} (ppb)	Mg^{2+} (ppb)	K^+ (ppb)	Water Temp (°C)
WAITOMO STREAM										
Total	6.93 *(366)*	1.967 *(366)*	0.529 *(329)*	991 *(179)*	98 *(206)*	19256 *(204)*	6196 *(204)*	1645 *(204)*	907 *(204)*	11.83 *(166)*
Summer	4.64 *(182)*	0.800 *(182)*	0.413 *(145)*	1161 *(62)*	120 *(92)*	21079 *(90)*	6439 *(90)*	2069 *(90)*	856 *(90)*	13.60 *(67)*
No rain	0 *(102)*	0.549 *(101)*	0.408 *(76)*	1165 *(27)*	125 *(54)*	21667 *(53)*	6459 *(53)*	2078 *(53)*	786 *(53)*	13.56 *(42)*
Rain	10.57 *(80)*	1.11 *(81)*	0.419 *(69)*	1157 *(35)*	114 *(38)*	20237 *(37)*	6412 *(37)*	2057 *(37)*	957 *(37)*	13.66 *(25)*
Winter	9.2 *(184)*	3.121 *(184)*	0.621 *(184)*	901 *(117)*	80 *(114)*	17816 *(114)*	6005 *(114)*	1310 *(114)*	948 *(114)*	10.64 *(99)*
No rain	0 *(37)*	1.719 *(37)*	0.574 *(37)*	845 *(24)*	89 *(17)*	19852 *(17)*	6198 *(17)*	1451 *(17)*	896 *(17)*	10.45 *(16)*
Rain	11.5 *(147)*	3.474 *(147)*	0.633 *(147)*	915 *(93)*	78 *(97)*	17459 *(97)*	5971 *(97)*	1285 *(97)*	957 *(97)*	10.68 *(83)*
RUAKURI STREAM										
Summer	4.64 *(182)*		0.328 *(61)*	640 *(61)*	115 *(44)*	22232 *(44)*	6632 *(44)*	1840 *(44)*	1139 *(44)*	13.67 *(61)*
No rain	0 *(102)*		0.363 *(27)*	647 *(34)*	122 *(27)*	23111 *(27)*	6845 *(27)*	1894 *(27)*	1117 *(27)*	13.63 *(27)*
Rain	10.57 *(80)*		0.300 *(34)*	631 *(27)*	105 *(17)*	20836 *(17)*	6293 *(17)*	1753 *(17)*	1175 *(17)*	13.70 *(34)*
Winter	9.2 *(184)*		0.407 *(18)*	893 *(18)*	86 *(123)*	18626 *(123)*	6032 *(123)*	1392 *(122)*	936 *(122)*	12.44 *(68)*
No rain	0 *(37)*		0.381 *(6)*	923 *(12)*	92 *(21)*	20009 *(21)*	6376 *(21)*	1471 *(21)*	903 *(21)*	12.35 *(21)*
Rain	11.5 *(147)*		0.420 *(12)*	835 *(6)*	85 *(102)*	18341 *(102)*	5962 *(102)*	1375 *(101)*	943 *(101)*	12.48 *(47)*
DRIPWATER										
Summer	4.64 *(182)*			3407 *(45)*						
No rain	0 *(102)*			3404 *(18)*						
Rain	10.57 *(80)*			3408 *(27)*						
Winter	9.2 *(184)*				238 *(11)*	56500 *(11)*	9063 *(11)*	3616 *(11)*	397 *(11)*	
No rain	0 *(37)*				179 *(2)*	68478 *(2)*	9266 *(2)*	3710 *(2)*	427 *(2)*	
Rain	11.5 *(147)*				251 *(9)*	53838 *(9)*	9018 *(9)*	3595 *(9)*	390 *(9)*	